



**THE RELATIONSHIP BETWEEN REACTOR PERFORMANCE AND
FUNCTIONAL MICROBIAL COMMUNITIES IN THE ANAEROBIC
DIGESTION OF TANNERY WASTEWATER**

by

Victoria Alex KIBANGOU

214052710

Thesis submitted in fulfilment of the requirements for the degree of

Master of Engineering: Chemical Engineering

in the **Faculty of Engineering**

at the Cape Peninsula University of Technology

Supervisor: Dr Pamela Welz

Co-supervisors: Dr Mariska Lilly & Associate Prof Oluwaseun Oyekola

Bellville

December 2020

CPUT Copyright

The thesis may not be published either in part (in scholarly, scientific or technical journals), or as a whole (as a monograph), unless permission has been obtained from the university

DECLARATION

I, Victoria Alex KIBANGOU, declare that the contents of this dissertation represent my own unaided work, and that the dissertation has not previously been submitted for academic examination towards any qualification. Furthermore, it represents my own opinions and not necessarily those of the Cape Peninsula University of Technology.



09-02-2021

Signature

Date

ABSTRACT

Tannery wastewater poses severe environmental threats due to its characteristically high organic load and metal content. The remediation of this waste stream is often problematic. While anaerobic digestion (AD) has significant advantages, the process remains enigmatic due to a lack of data about the microbial communities responsible for the success of the process. There is a need for the simultaneous investigation of reactor performance and microbial consortia dynamics in response to changes in operational conditions.

This study aimed to quantify copy numbers of methyl coenzyme M reductase (*mcrA*) and dissimilatory sulfite reductase (*dsrB*) genes encoding the enzymes that catalyse the terminal processes in AD treatment of ostrich tannery wastewater. It also aimed to correlate these gene copy numbers respectively with the efficiency of methane (CH₄) generation and sulfate (SO₄²⁻) concentrations in anaerobic digesters treating ostrich tannery wastewater.

Biochemical methane potential (BMP) tests were conducted in 2 L glass bottles at 37°C. Thirteen reactors were set up based on central composite design at different inoculum to substrate ratios (ISR) of 2 to 5 and different SO₄²⁻ concentrations ranging from 665 to 2000 mg/L to assess the effect of ISR and SO₄²⁻ concentration on CH₄ generation and biodegradability of ostrich tannery wastewater. To try and maximize AD efficiency, two 20 L anaerobic sequencing batch reactors (ASBR) were operated under similar conditions to those suggested by the BMP results. However, ASBR1 operated at intermittent mixing (300 rpm for 5 to 10 min/day) while ASBR2 operated at continuous mixing at 300 rpm. The study was conducted for 50 days in two different operational runs. The first run at the start-up period of the ASBR operated for 30 days with a 5-day settling period before decanting. During the second run, the ASBRs operated for 20 days. Deoxyribonucleic acid (DNA) was extracted from (i) samples from the BMP tests collected at baseline, when the reactors started and stopped producing biogas, and at the end of the study and (ii) samples from the ASBRs collected at the beginning of the experiment and every week thereafter. Quantitative Real-Time PCR (qRT-PCR) was performed on all the DNA samples, and next generation sequencing (NGS) was conducted on selected DNA samples taken from the BMPs (based on SO₄²⁻ concentration) and biweekly samples taken from the ASBRs.

Based on response surface methodology (RSM), the optimum operating conditions for maximal gas (CH₄, biogas) and biodegradability were found to be 983.687 and 3.687 for SO₄²⁻ concentration and ISR respectively. Results showed that minimal CH₄ (<1 mLCH₄/gVS) was

produced at high SO_4^{2-} concentration (≥ 1960 mg/L) and ISR < 3.0 , suggesting that pre-treatment is required at high SO_4^{2-} concentration. In the ASBRs, continuous mixing in ASBR2 was shown to be more efficient than intermittent mixing in ASBR1 by producing high cumulative CH_4 in total (1149 and 106 mL CH_4 /gVS in ASBR2 and ASBR1, respectively). However, a large decrease in CH_4 production was observed between successive runs in both ASBRs. It was therefore assumed that biomass washout occurred during the decanting step.

From a microbial point of view, the NGS results revealed that SO_4^{2-} concentration and ISR did not have significant ($P > 0.05$) effects on the methanogenic and sulfidogenic community structure in the BMP tests. However, *Desulfofustis glycolicus*, known to reduce SO_4^{2-} to H_2S was found at high relative abundance (RA, 15.91%) in the BMP test operating at $SO_4^{2-} \geq 1960$ mg/L compared to the other BMP tests ($< 0.003\%$ RA). It was postulated that the H_2S may have inhibited some methanogens in the former. According to the analysis of similarity (ANOSIM), both methanogenic and sulfidogenic community structures were established once biogas generation commenced, and were responsible for ongoing physicochemical changes thereafter, as there was significant difference between the measured physicochemical parameters with factor 'time' (initial, start of biogas production and final). The changes in the sulfidogenic community structure were driven mainly by combinations of ammonia (NH_3), volatile organic acids (VOA), total organic carbon (TOC), and alkalinity concentrations, as well as VOA:alkalinity and *dsrB* copy numbers, while changes in the methanogenic structure was driven mainly by pH, NH_3 , VOA, TOC, alkalinity and nitrogen (N) concentrations. In ASBRs, continuous mixing promoted better survival and high abundance of *Methanosarcina mazei* in ASBR2 (14.7-31.6%) than in ASBR1 (4.3-6.8%).

Quantitative Real-Time PCR (qRT-PCR) results showed that in the BMP tests, the abundance of the *mcrA* gene ranged from 3.63×10^5 to 6.46×10^6 copy numbers/ng DNA and were 1 to 2 order of magnitude higher than the *dsrB* gene copy numbers (5.13×10^4 to 8.44×10^5 /ng DNA) indicating the dominance of the former. While in the ASBRs, although the copy numbers of *mcrA* were higher in ASBR2 (from 8.23×10^6 to 1.26×10^7 , and 9.32×10^6 to 1.32×10^7 in ASBR1 and ASBR2 respectively), the difference was not significant. The selection of *M. mazei* was therefore associated with the higher CH_4 yield in ASBR2. The *dsrB* gene copy numbers varied between 2.70×10^5 to 1.12×10^6 and 2.27×10^5 to 6.72×10^5 /ng DNA in ASBR1 and ASBR2 respectively, indicating that, in contrast to methanogenesis, sulfidogenesis was more favoured in ASBR1 than ASBR2, and may have contributed to the lower production CH_4 in this digester. Positive significant correlations ($P < 0.05$) were observed between *mcrA* gene copies and

specific CH₄ yield in the BMPs and the ASBRs, and also between *dsrB* gene copies and H₂S gas in the BMPs and S²⁻ concentration in ASBR1 but not with SO₄²⁻ (P >0.05).

Taken together, results from this study indicate that the knowledge about the selected functional microbial consortia in diverse anaerobic reactor systems is of practical interest in order to comprehensively understand and control the AD process, mitigate process disturbances, and maximize the CH₄ yield.

ACKNOWLEDGEMENTS

I wish to thank:

- My God who did not fail me, for the knowledge and strength He gave me to accomplish this work and for putting the right people in my way
- My supervisor Dr Pamela Welz, for being such an amazing supervisor. Her enthusiasm encouraged me. I thank you for your patience, your availability, your quick and pertinent feedback, your willingness to assist even in the lab and your continuous encouragement. Thanks for always going the extra mile for me and for always having my back. You made the completion of this thesis possible. I cannot thank you enough
- My co-supervisor Dr Mariska Lilly, for allowing me to work in her lab, for our everyday 5 min-chat and for always sharing her experience with me. Thank you for your advice, guidance and encouragement and for making me love microbiology at some points
- My second co-supervisor Associate prof Oluwaseun Oyekola, for his advice and encouragement but most of all for believing in me and bringing me into this project
- Our industrial partner, for sending tannery wastewater whenever needed
- Ashton Mpofu and Walu Kaira, for their precious time, the reactors setup and helping with the analysis of the reactors
- My dear friend Colombe Tchono for being a shoulder to cry on during this research, for always believing me and being my biggest fan after my family
- Dr Thandekile, Dr Mayowa and Calvin for their moral support and confidence
- The staff, postdoctoral fellows and postgraduate students of the Applied Microbial and Health Biotechnology Institute at Cape Peninsula University of Technology for the warm welcome. I will miss the drama
- The Department of Science and Innovation, the Water Research Commission of South Africa, and the Centre for Postgraduate Studies at the Cape Peninsula University of Technology for their financial support

DEDICATIONS

This thesis is dedicated to my dad, my inspiration, Joseph KIBANGOU, for all his sacrifices, support and love. I am so proud to say that I am an engineer like him

To my mum Jeanne KIBANGOU, for her prayers and blessings

And to my five sisters Armelle, Sandrine, Gwladys, Thérèse and Joëlle KIBANGOU and my cousin Ronny SOUZA, thanks be to God who always leads us to triumph in Christ

TABLE OF CONTENTS

DECLARATION	i
ABSTRACT.....	ii
ACKNOWLEDGEMENTS	v
DEDICATIONS	vi
LIST OF FIGURES	v
LIST OF TABLES.....	x
GLOSSARY	xii
LIST OF ABBREVIATIONS.....	xix
CHAPTER 1. INTRODUCTION.....	1
1.1. Background.....	1
1.2. Problem statement.....	2
1.3. Hypothesis and research questions	3
1.4. Aim and objectives of the research	3
1.5. Significance	3
1.6. Delineation.....	4
1.7. Thesis outline.....	4
CHAPTER 2. LITERATURE REVIEW	5
2.1. Introduction	5
2.2. Leather industry: An overview.....	5
2.3. Leather processing	6
2.1. Wastewater consumption and generation	8
2.2. Wastewater treatment.....	11
2.2.1. Physicochemical treatment	12
2.2.2. Biological treatment	13
2.3. Anaerobic digestion	21
2.3.1. Metabolic processes	21
2.3.2. Biochemical methane potential testing.....	26

2.3.3.	Biogas generation.....	27
2.3.4.	Factors affecting growth and function of methanogens and sulfate reducing bacteria 28	
2.4.	Species identification	30
2.4.1.	Next generation sequencing	31
2.4.2.	Quantitative real-time polymerase chain reaction.....	32
2.5.	Design of experiment.....	34
2.6.	Overview and conclusion	35
CHAPTER 3.	MATERIALS AND METHODS.....	36
3.1.	Introduction	36
3.2.	Substrate and inoculum	36
3.3.	Experimental set-up and operation	37
3.3.1.	Biochemical methane potential test.....	37
3.3.2.	Anaerobic sequencing batch reactor.....	39
3.4.	Analytical methods.....	42
3.5.	Biogas analysis.....	44
3.6.	Analysis of methanogenic and sulfidogenic microbial communities.....	45
3.6.1.	Sample collection.....	45
3.6.2.	DNA extraction.....	45
3.6.3.	Next generation sequencing	45
3.6.4.	Quantitative real-time polymerase chain reaction.....	47
3.6.1.	Standard curves.....	50
3.6.2.	Quantitative Real-Time PCR amplification of the target genes.....	51
3.7.	Statistical analysis.....	51
3.7.1.	Biochemical methane potential test reactors and anaerobic sequencing batch reactors 51	
3.7.2.	Next generation sequencing analysis.....	52
3.7.3.	Quantitative real-time polymerase chain reaction analysis	52
3.8.	Summary	52

CHAPTER 4. ANAEROBIC DIGESTION OF OSTRICH TANNERY WASTEWATER	54
4.1. Introduction	54
4.2. Sample collection and characterisation	54
4.3. Biochemical methane potential test.....	56
4.3.1. Specific methane production.....	56
4.3.2. Changes in pH, hydrolysis, acidogenesis and acetogenesis	58
4.3.3. Sulfidogenesis and sulfide oxidation	62
4.3.4. Methanogenesis	64
4.3.5. Other factors contributing to methanogenic inhibition.....	65
4.3.6. Statistical analysis	68
4.4. Anaerobic sequencing batch reactors	81
4.4.1. Process performance and stability	81
4.5. Summary	89
CHAPTER 5. INVESTIGATING THE DISTRIBUTION OF METHANOGENIC AND SULFIDOGENIC COMMUNITIES	90
5.1. Introduction	90
5.2. DNA extraction.....	90
5.3. Next generation sequencing	90
5.3.1. Overall taxonomic comparison between methanogenic and sulfidogenic communities.....	90
5.3.2. Selection of sulfidogenic and methanogenic microbial communities during anaerobic digestion of ostrich tannery wastewater	95
5.4. Quantitative real-time polymerase chain reaction.....	107
5.4.1. Optimisation of the PCR amplification of target genes	107
5.4.2. Standard curves.....	110
5.4.3. Biochemical Potential test.....	112
5.4.4. Anaerobic sequencing batch reactors	125
5.5. Summary	136
CHAPTER 6. CONCLUSION AND RECOMMENDATIONS	138

6.1. Conclusions	138
6.2. Recommendations	139
REFERENCES	140
APPENDICES.....	165
Appendix A: Biochemical methane potential tests setup.....	165
Appendix B: Analytical treatment methods	165
Appendix C: Genomic DNA samples concentration	169
Appendix D: Preparation of buffers and reagents	171
Appendix E: Univariate analysis indices	172
Appendix F: Standard curves	175
Appendix G: SIMPER.....	177

LIST OF FIGURES

Figure 2.1: Typical leather manufacturing process	7
Figure 2.2: Tannery wastewater treatment methods (adapted from Lofrano et al., 2013)	11
Figure 2.3: Anaerobic treatment systems	15
Figure 2.4: Upflow anaerobic sludge blanket reactor (Aziz et al., 2019)	16
Figure 2.5: Schematic diagram of anaerobic filters (Aziz et al., 2019)	18
Figure 2.6: Schematic diagram of an expanded granular sludge bed reactor (de Lemos Chernicharo, 2007)	19
Figure 2.7: Anaerobic sequencing batch reactor (Aziz et al., 2019).....	20
Figure 2.8: Metabolic process of anaerobic digestion (adapted from Meegoda et al., 2018) 21	
Figure 2.9: Methanogenesis pathways (Guo et al., 2015)	24
Figure 2.10: Schematic representation of sulphidogenesis	26
Figure 2.11: Distribution diagram of H ₂ S at 25°C (de Lemos Chernicharo, 2007).....	29
Figure 2.12: Accumulation of PCR product over time (Maddocks & Jenkins, 2016). RFU= relative florescent units. Green colour= SYBR, grey colour and red colour= amplified products	32
Figure 2.13: SYBR green detection in qRT-PCR (Smith & Osborn, 2009).....	33
Figure 3.1: Schematic diagram of wastewater treatment of ostrich tannery effluent at the study site (Swartz et al., 2017)	36
Figure 3.2: Biochemical methane potential test set-up	37
Figure 3.3: Experimental set-up	40
Figure 3.4: Schematic diagram of the 20 L bioreactors with the transmitter and the programmable logic controller	40
Figure 3.5: Schematic diagram of the 20 L reactors connected to control system	41
Figure 3.6: Biogas analyser.....	45
Figure 3.7: Schematic diagram of DNA extraction, quantitative PCR and cloning and isolating the amplicon standard.....	49
Figure 3.8: Serial dilution for standard curves from the original working solutions (A) <i>mcrA</i> gene (B) <i>dsrB</i> gene. PCR= polymerase chain reaction	50
Figure 4.1: Cumulative methane yields from biochemical methane potential test reactors operating at inoculum to substrate ratio ≥ 3 and sulfate concentration of 1335 mg/L. ISR= inoculum to substrate ratio	57

Figure 4.2: Cumulative methane yield from biochemical methane potential test reactors operating at sulfate concentration (A) ≤ 710 mg/L, (B) ≥ 1960 mg/L. ISR= inoculum to substrate ratio.....	58
Figure 4.3: pH values measured in samples from biochemical methane potential test reactors	59
Figure 4.4: Ammonia concentrations measured in samples from biochemical methane potential test reactors.....	59
Figure 4.5: Fat oil and grease concentrations measured in samples from biochemical methane potential test reactors.....	60
Figure 4.6: (A) Volatile organic acid concentrations, (B) Alkalinity concentrations, (C) Volatile fatty acid to alkalinity ratios measured in samples taken from biochemical methane potential test reactors	61
Figure 4.7: White layer forming at the bulk water – headspace interface of a biochemical methane potential test reactor (R4).....	63
Figure 4.8: Sulfate concentrations in samples taken from biochemical methane potential test reactors.....	63
Figure 4.9: Sulfite concentrations in samples taken from biochemical methane potential test reactors.....	64
Figure 4.10: Chemical oxygen demand to sulfate ratios in samples taken from biochemical methane potential test reactors	65
Figure 4.11: Carbon to nitrogen ratio in samples taken from the biochemical methane potential test reactors	65
Figure 4.12: Phosphate and phosphorus concentrations in samples taken from biochemical methane potential test reactors	66
Figure 4.13: Change in soluble metal concentrations in samples taken from the biochemical methane potential test reactors	67
Figure 4.14: Sulfate removal diagnostic plot.....	71
Figure 4.15: 2D contour plot (A) and 3D surface plot (B) of predicted model for sulfate removal. ISR= inoculum to substrate ratio	71
Figure 4.16: Diagnostic plot for chemical oxygen demand removal: Externally studentized residuals vs predicted	73
Figure 4.17: 2D contour plot (A) and 3D surface plot (B) of predicted model for chemical oxygen demand removal. ISR= inoculum to substrate ratio, COD= chemical oxygen demand	74
Figure 4.18: Diagnostic plot for cumulative methane: Externally studentized residuals vs predicted.....	76

Figure 4.19: 2D contour plot (A) and 3D surface plot (B) of predicted model for cumulative methane. ISR= inoculum to substrate ratio.....	77
Figure 4.20: Biogas yield diagnostic plot.....	79
Figure 4.21: 2D contour plot (A) and 3D surface plot (B) of predicted model for biogas yield. ISR= inoculum to substrate ratio	80
Figure 4.22: Anaerobic sequencing batch reactors 1 and 2 cumulative methane yield.....	82
Figure 4.23: Weekly chemical oxygen demand concentration and removal efficiency. ASBR= anaerobic sequencing batch reactor, COD= chemical oxygen demand.....	84
Figure 4.24: A=Volatile organic acid concentration, B= Alkalinity, C= Volatile fatty acid to Alkalinity ratio, D= Ammonia concentration, E= total organic carbon concentration F= carbon to nitrogen ratio in the anaerobic sequencing batch reactors.....	86
Figure 4.25: A= Sulfate concentration, B= sulfide concentration, C= chemical oxygen demand to sulfate ratio, D= chloride concentration, E= nitrate concentration, F= total solids and volatile solids in the anaerobic sequencing batch reactors. ASBR= anaerobic sequencing batch reactor	87
Figure 5.1: Methanogenic distribution in the study (A) class (B) family (C) genera. I= initial, S= start of gas production, E= end of gas production, F= final (end of study), WK = week, S= substrate, I= inoculum, ASBR= anaerobic sequencing batch reactor	92
Figure 5.2: Sulfidogenic community phylum distribution. I= initial, S= start of gas production, E= end of gas production, F= final (end of study), WK = week, S= substrate, I= inoculum, ASBR= anaerobic sequencing batch reactor.....	93
Figure 5.3: Sulfidogenic community distribution (A) class (B) family (C) genera. I= initial, S= start of gas production, E= end of gas production, F= final (end of study), WK = week, S= substrate, I= inoculum, ASBR= anaerobic sequencing batch reactor	94
Figure 5.4: Non-metric multidimensional scaling plots of dsr amplicon sequencing results: (A) all samples, and (B) all samples excluding substrates. I= initial, S= start of gas production, E= end of gas production, F= final (end of study), WK = week	96
Figure 5.5: Non-metric multidimensional scaling plots of dsr amplicon sequencing results: (A) all samples, and (B) all samples excluding substrates. I= initial, S= start of gas production, E= end of gas production, F= final (end of study), WK = week	97
Figure 5.6: Shade plot of square root transformed Bray-Curtis similarity data from dsr amplicon sequencing, with group average linkages between samples, and index of association of species standardised by total resemblance. Inclusive of all species >1% of population in any one sample (28 of 78 species).	99

Figure 5.7: Shade plot of square-root transformed data from <i>dsr</i> amplicon sequencing of samples from anaerobic sequencing batch reactors. Inclusive of all species >1% of population in any one sample (28 of 78 species). WK = week.....	100
Figure 5.8: Non-metric multidimensional scaling plots of <i>mcr</i> amplicon sequencing results. I= initial, S= start of gas production, E= end of gas production, F= final (end of study), WK= week	101
Figure 5.9: Non-metric multi-dimensional scaling plots overlaid with cluster plots (group average linkage) of <i>mcr</i> amplicon sequencing results of samples from (A) biochemical methane potential test reactors and inoculum, and (B) anaerobic sequencing batch reactors and inoculum. I = initial, S = start of gas production, E = end of gas production, F = final (end of study), WK = week	104
Figure 5.10: Shade plot of square root transformed data from <i>mcr</i> amplicon sequencing of samples from biochemical methane potential test reactors. Inclusive of all species >1% of population in any one sample (18 of 42 species).....	105
Figure 5.11: Shade plot of square root transformed data from <i>mcr</i> amplicon sequencing of samples from anaerobic sequencing batch reactors. Inclusive of all species >1% of population in any one sample (18 of 42 species).....	106
Figure 5.12: 1.5% agarose gel electrophoresis showing the amplification of the <i>mcrA</i> gene after conventional PCR, lane 1: gene ruler, lane 2 negative control, lanes 3-4: inoculum sample	107
Figure 5.13: 1.5% agarose gel electrophoresis showing the amplification of the <i>dsrB</i> gene after conventional PCR, lane 1: gene ruler, lane 2 negative control, lanes 3-5: inoculum sample	108
Figure 5.15: <i>mcrA</i> gene melt curve analysis.....	110
Figure 5.16: <i>dsrB</i> gene melt curve analysis.....	111
Figure 5.17: <i>mcrA</i> gene agarose gel electrophoresis after qPCR, lane 1: gene ruler, lane 2 negative control, lanes 3-5: standard 2, lanes 7-9: reactor sample, lanes 11-13: standard	111
Figure 5.18: <i>mcrA</i> gene copy numbers in the biochemical methane potential tests. All measurements were performed independently in triplicate and error bars represent standard deviations.....	113
Figure 5.19: Correlation between <i>mcrA</i> gene copy numbers and specific methane yield in the biochemical methane potential tests	114
Figure 5.20: <i>dsrB</i> gene copy numbers per ng DNA contained in the biochemical methane potential tests. All measurements were performed independently in triplicate and error bars represent standard deviations	115

Figure 5.21: correlation between <i>dsrB</i> gene copy numbers and hydrogen sulfide gas produced in the biochemical methane potential tests.....	116
Figure 5.22: Correlation between <i>mcrA</i> copy numbers and alkalinity concentration contained in the biochemical potential tests	117
Figure 5.23: Similarity plots at different time instances (see key) of: methanogenic archaeal community structures (A,B), measured parameters (C,D) and bubble overlay on plot A of measured parameters determined to be most significant for community selection by BEST analysis (E).....	120
Figure 5.24: Similarity plots at different time instances (see key) of: sulfate reducing bacterial community structures (A,B), measured parameters (C,D) and bubble overlay on plot A of measured parameters determined to be most significant for community selection by BEST analysis (E).....	121
Figure 5.25: Competition between <i>mcrA</i> and <i>dsrB</i> genes in the biochemical methane potential tests operating at (A) inoculum to substrate ratio ≥ 3 and sulfate concentration of 1335 mg/L, (B) sulfate concentration ≤ 710 mg/L and (C) sulfate concentration ≥ 1960 mg/L. ISR= inoculum to substrate ratio	123
Figure 5.26: <i>dsrB</i> gene copy competition (A) inoculum to substrate ratio ≥ 3 and sulfate concentration of 1335 mg/L, (B) sulfate concentration ≤ 710 mg/L and (C) sulfate concentration ≥ 1960 mg/L. ISR= inoculum to substrate ratio	124
Figure 5.27: <i>mcrA</i> copy numbers per ng DNA contained in the anaerobic sequencing batch reactors. Wk= week, ASBR= anaerobic sequencing batch reactor.....	126
Figure 5.28: Correlation between <i>mcrA</i> copy numbers and alkalinity concentration contained in the anaerobic sequencing batch reactors. ASBR= anaerobic sequencing batch reactor	127
Figure 5.29: <i>mcrA</i> gene copy numbers per gTS contained in the anaerobic sequencing batch reactors. Wk= week, ASBR= anaerobic sequencing batch reactor.....	128
Figure 5.30: <i>mcrA</i> gene copy numbers per gVS contained in the anaerobic sequencing batch reactors. Wk= week, ASBR= anaerobic sequencing batch reactor.....	128
Figure 5.31: Correlations between <i>mcrA</i> gene copy numbers and methane yield in the anaerobic sequencing batch reactors. ASBR= anaerobic sequencing batch reactor.....	130
Figure 5.32: <i>dsrB</i> gene copy numbers per ng DNA contained in the anaerobic sequencing batch reactors. Wk= week, ASBR= anaerobic sequencing batch reactor	131
Figure 5.33: Correlation analysis between sulfide concentrations contained in anaerobic sequencing batch reactor with <i>dsrB</i> gene copy numbers expressed in (A) ng DNA (B) gTS. ASBR= anaerobic sequencing batch reactor.....	132

LIST OF TABLES

Table 1.1: Effluent standards of municipalities for water quality parameters regulated for effluents from tanneries in South Africa (Swartz et al., 2017)	2
Table 2.1: Leather processing process, purposes and chemicals used in each step (adapted from IFC, 2007)	7
Table 2.2: Water consumption in a bovine tannery (Black et al., 2013)	8
Table 2.3: Characteristics of tannery wastewater based on studies from different countries	10
Table 2.4: Comparison between aerobic and anaerobic digestion (adapted from de Lemos Chernicharo, 2007)	14
Table 2.5: Reactions involved in methanogenic pathways (Wang et al., 2015).....	23
Table 2.6: Typical biogas composition (%)	28
Table 3.1: Factors on central composite design	37
Table 3.2: Central composite design experimental matrix	38
Table 3.3: Inoculum to substrate ratios and sulfate concentrations used in the biochemical methane potential tests	39
Table 3.4: Volume of samples extracted from the biochemical methane potential tests and the anaerobic sequencing batch reactor	42
Table 3.5: Physicochemical parameters measured in this study	43
Table 3.6: Analytical methods used in this study	44
Table 3.7: Primers sequences used for the amplification of the <i>mcrA</i> and <i>dsrB</i> genes.....	46
Table 3.8: Optimisation of conventional PCR for the <i>mcrA</i> gene	48
Table 4.1: Physicochemical characteristics of tannery wastewater batches collected in this study	55
Table 4.2: Design matrix of central composite design and their corresponding responses ..	68
Table 4.3: Results of analysis of variance for sulfate removal	69
Table 4.4: Results of analysis of variance for COD removal.....	72
Table 4.5: Results of analysis of variance for methane yield	75
Table 4.6: Biogas yield analysis of variance.....	78
Table 4.7: Criteria for optimization of anaerobic digestion of tannery effluent.....	80
Table 4.8: Optimized conditions in for methane generation and organic and solids removal in anaerobic digestion of ostrich tannery	81
Table 4.9: Comparison of the results of this study with literature results on anaerobic digestion of tannery wastewater	88
Table 5.1: <i>mcrA</i> and <i>dsrB</i> genes sequences identification	109
Table 5.2: Results of ANISOM with time factor (R values)	119

Table 5.3: Results of BEST analysis: rho values and 'best' correlated parameters	119
Table 5.4: <i>mcrA</i> and <i>dsrB</i> genes quantitative polymerase chain reaction critical parameters for the anaerobic sequencing batch reactors.....	125
Table 5.5: <i>mcrA</i> gene copy numbers correlation coefficient and level of significance with methane production. Statistically significant coefficients are printed in bold	129
Table 5.6: Correlations analysis between <i>dsrB</i> copy numbers and sulfate and sulfide concentrations in the reactors	133
Table 5.7: Comparison of the results of this study with literature results	134

GLOSSARY

Acetogenesis	Biological catalysed conversion (fermentation) of short-chain fatty acids to acetic acid
Acidogenesis	Biologically catalysed conversion (fermentation) of complex organic compounds to short-chain fatty acids
Anaerobic digestion	Biological process that converts organic matter to biogas in the absence of oxygen
Biochemical methane potential	Procedure developed to determine the methane production of a given organic substrate during its anaerobic decomposition
Hydrolysis	Solubilization of particulate and colloidal, polymeric material and its biotransformation to simple monomers by extracellular enzymes produced by hydrolytic and fermentative (acidogenic) bacteria
Inoculum	Microbial cells added to start a culture
Chemical oxygen demand	Method of estimating how much oxygen would be depleted from a body of receiving water as a result of bacterial action
Lag phase	Time from inoculation to active cell replication in a batch culture
Methanogenesis	Production of methane by methanogenic archaea (acetoclastic and hydrogenotrophic methanogens)
Sulfidogenesis	Reduction of sulfate to hydrogen sulfide via dissimilatory sulfate reduction by sulfate-reducing bacteria

LIST OF ABBREVIATIONS

Abbreviation

AD	Anaerobic digestion
AF	Anaerobic filters
ANOSIM	Analysis of similarity
ANOVA	Analyses of variance
APHA	American Public Health Association
ASBR	Anaerobic sequencing batch reactor
BMP	Biochemical methane potential
bp	Base pair
BOD	Biological organic demand
COD	Chemical oxygen demand
DNA	Deoxyribonucleic acid
EGSB	Expanded granular sludge bed
ISR	Inoculum to substrate ratio
NGS	Next generation sequencing
nMDS	Non-metric multidimensional scaling
OTU	Operational taxonomic unit
PCR	Polymerase chain reaction
qRT-PCR	Quantitative real-time polymerase chain reaction
RNA	Ribonucleic acid
RT	Retention time
SIMPER	Similarity percentage
SRB	Sulfate reducing bacteria
TAN	Total ammonium nitrogen
TN	Total nitrogen
TOC	Total organic carbon
TS	Total solids
UASB	Upflow anaerobic sludge blanket
VFA	Volatile fatty acids
VOA	Volatile organic acid
VS	Volatile solids

CHAPTER 1. INTRODUCTION

1.1. Background

Awareness of environmental problems has increased considerably during recent years and protecting the environment has become a global issue. Industrial wastewater is an important source of water pollution. There are various types of industrial wastewater, and each industrial sector produces different arrays of pollutants (Shi, 2009) that may not meet the effluent discharge standards of a particular country (Akpomie & Ejechi, 2016).

Tannery industries can be categorised among the most polluting industries producing large amounts of wastewater (Ros & Gantar, 1998; P. Sabumon, 2016; Mustapha et al., 2017; Polizzi et al., 2018). According to Swartz et al. (2017), these industries use approximately 170 to 550 L of water per raw skin or hide of which about 90% is discharged as effluent (Mustapha et al., 2017). Because of the series of chemical treatments carried out during the manufacturing process (Tunay et al., 1995; Mathuriya, 2014; P. Sabumon, 2016), these effluents are associated with high loads of organics, organic nitrogen, sulphur, chemicals, suspended solids (SS), and metals (Zupancic & Jemec, 2010). An adequate treatment is therefore needed before discharge.

Various approaches and technologies have been developed to solve this problem. For years now, considerable attention has been paid to biological treatment due to the advantages it offers (Lofrano et al., 2013). However, despite being widely established, aerobic digestion processes encounter some problems such as high cost, the generation of large amounts of sludge that requires special handling and further treatment for landfilling, and high energy consumption (Midha & Dey, 2008; Dargo & Ayalew, 2014; Abdallh et al., 2016). Anaerobic digestion (AD) is found to counteract many problems associated with the conventional activated sludge process. In addition, biogas, which may serve as an alternative source of energy to reduce the dependence on fossil fuels, is produced (de Mes et al., 2003; Durai & Rajasimman, 2011; Cioabla et al., 2012; Nasir et al., 2012; Shalu & Bishnoi, 2016; Świątczak et al., 2017). Several studies have focused on optimising various aspects such as the design of bio-digesters, treatment conditions and process kinetics (Kim et al., 2002; Marti-herrero, 2011; Mekonnen, Leta & Njau, 2017; Hobbs et al., 2018; Polizzi et al., 2018) and a few have linked those with the microorganisms responsible for the success of the process (Staley et al., 2011; Moestedt et al., 2013; Madden et al., 2014; Morris et al., 2013).

Methanogens play an important role in AD by producing biogas consisting mainly of methane (CH₄) (Staley et al., 2011). These microorganisms could be inhibited by sulfate-reducing bacteria (SRB) due to the high amounts of sulfate (SO₄²⁻) or sulfide (S²⁻), within the substrate. SO₄²⁻-rich wastewaters stimulate SRB growth, which can outcompete methanogens for carbon sources [hydrogen/carbon dioxide (H₂/CO₂) and acetate] (Kristjanson et al., 1982; Schonheit et al., 1982; Madden et al., 2014) resulting in the formation of hydrogen sulfide (H₂S), a toxic gas. The outcome of the competition is important, as it determines the relative concentrations of H₂S and CH₄ (Lens et al., 1998; Jing et al., 2013) therefore, a fundamental understanding of these two communities is essential to improve digestion efficiency and biogas production.

1.2. Problem statement

Tannery wastewater poses severe environmental threats due to its characteristically high organic load and metal content. Considering the legislated limits for the quality of wastewater in SA (Table 1.1), those pollutants must be removed or reduced prior to discharge. While AD has significant advantages, the process remains enigmatic due to a lack of data about the microbial communities responsible for the success of the process.

Table 1.1: Effluent standards of municipalities for water quality parameters regulated for effluents from tanneries in South Africa (Swartz et al., 2017)

Local authority	pH	COD (mg/L)	Phosphate (mg/L)	TSS (mg/L)	Electrical conductivity	Sulphate (mg/L)	Total chromium (mg/L)	Chloride (mg/L)
City of Tshwane	6-10	5 000	10	2 000	300	1 800	5	100
City of Cape Town	5.5-12	5 000	25	1 000	500	1 500	10	1 500
Nelson Mandela Bay Metro	6-12	10 000	-	1 000	500	1 500	20	1 000
Ekurhuleni	6-10	5 000	50	1 000	500	1 800	20	100
Oudtshoorn	6.5-10	4 000	10	1 000	500	250	5	500
Mossel Bay	6-11	3 000	-	1 000	500	500	10	1 000

1.3. Hypothesis and research questions

It can be hypothesised that the copy numbers of methyl coenzyme M reductase (*mcrA*) gene encoding methanogens positively correlate with methane yield and the copy numbers of dissimilatory sulfite reductase (*dsrB*) genes encoding also positively correlate with sulfate and/or sulfide concentration.

To validate this hypothesis, the following questions need to be answered:

- How many copy numbers of *mcrA* and *dsrB* genes are there in samples taken from different lab-scale anaerobic digesters treating tannery effluent?
- Is there a statistically significant correlation between *mcrA* and *dsrB* gene copy numbers and specific methane generation and sulfate/sulfide concentration?

1.4. Aim and objectives of the research

This research aims to quantify copy numbers of *mcrA* and *dsrB* genes and correlate these respectively with the efficiency of methane generation and sulfate/sulfide concentrations in anaerobic digesters treating ostrich tannery wastewater.

The specific objectives are to:

- To determine the physicochemical properties of ostrich tannery wastewater
- To extract genomic DNA from digester sludge
- To perform next generation sequencing (NGS) and quantitative polymerase chain reaction (qPCR) using primers for *mcrA* and *dsrB* genes
- To measure specific methane generation from the anaerobic digesters
- To correlate gene copy numbers with methane generation efficiency and sulfate/sulfide concentrations

1.5. Significance

This research was conducted to ascertain whether it may be possible to successfully treat ostrich tannery wastewater using an anaerobic sequencing batch reactor (ASBR) in order to meet the relevant legislated limits for the quality of wastewater, thus reducing environmental pollution and health risks. The results of this research provide a fundamental understanding of the process mediators, and consequently will aid in optimizing the overall process. The research bridged the gap in knowledge of how performance (and process) is related to microbial consortium dynamics in response to changes in operational conditions in ASBRs treating ostrich tannery effluent.

1.6. Delineation

The research was limited to the study of one type of tannery wastewater in SA i.e. an ostrich tannery. The following were included:

- Design and modelling of the ASBR system
- Isolation and study of other microbial communities other than the methanogens and SRB
- Heat generation potential

1.7. Thesis outline

In Chapter 2, the literature review of the different treatments used for tannery wastewater are presented. This is followed by Chapter 3, which describes the research methodology used in this study. Chapter 4 presents and discusses the findings of the biodegradation of ostrich tannery wastewater using lab-scale digesters while Chapter 5 investigates the methanogenic and sulfidogenic communities involve. Chapter 6 presents the conclusion and recommendations for future studies

CHAPTER 2. LITERATURE REVIEW

2.1. Introduction

This Chapter emphasizes the background to understand the reason of this research. It first introduces the leather industry and its manufacturing process in Sections 2.2 and 2.3, then highlights the quantity of water consumed and quality and quantity of wastewater generated by this industry in Section 2.1. In Section 2.2, the different wastewater treatment methods are described; the advantages and disadvantages of secondary aerobic and anaerobic treatment are presented and, prior studies relevant to anaerobic technologies for the treatment of tannery wastewater are reviewed. Section 2.3 focuses on the AD process: the microbial communities mediating AD are presented, with a focus on the methanogens and SRB; the production of biogas and its composition, and the factors affecting growth and function of microorganisms are elaborated on. Finally, in Section 2.4, current molecular techniques employed in microbial ecology are outlined, as well as the efficiency of qPCR as a technique for identification and quantification of methanogens and SRB during anaerobic treatment of tannery wastewater.

2.2. Leather industry: An overview

The leather industry is one of the oldest industries in human civilization that transforms hides or skins (the waste products of the food industry) into a non-putrescible and stable material called leather (Lofrano et al., 2013). According to the Food and Agriculture Organisation (FAO, 2010) about 1.67×10^9 m² of leather is produced annually in the world. In 2010, the annual global trade estimated about US \$100 billion in the leather sector (UNIDO, 2010), making it one of the leading economic sectors in many countries (Lofrano et al., 2013).

Tanneries are classified in four categories, according to the stages involves in skin processing (Black et al., 2013). These are 1) integrated or full-house tanneries, where all the operations are performed from raw skins or hides to finished leather; 2) wet-blue tanneries: where raw skins or hides are transformed into a leather called wet blue; (3) half-finishing tanneries, where the wet blue is used as raw material and transformed into half-finishing leather called crust and (4) finishing tanneries, where crust leather is transformed into finished leather. Tanneries that process wet-blue leather until the finished leather is achieved also belong to the latter category (Costa et al., 2008).

Currently in South Africa, there are 35 tanneries (Swartz et al., 2017) providing a wide range of finished leather and consumer goods such as shoes, automobile upholstery, bags, garments as well as wet blue and pickled skins and hides for export.

2.3. Leather processing

As illustrated in Figure 2.1, the manufacturing process of leather can be divided into four main stages including 1) the beamhouse operation, which aims to wash and clean the hides or skins to remove substances such as hair, blood and flesh (Streit et al., 2014); 2) the tanning, which is the stage where the pre-treated hides or skins are stabilized into wet blue leather by the use of tanning agents. This process can be either vegetable or chrome based, but chrome tanning is used in 80% of cases; 3) the re-tanning or post-tanning, which gives additional properties such as uniform colour, tensile strength, water resistance and softness to the leather. The leather obtained after this stage is referred to as crust; and 4) the finishing, which defines the final aspect and presentation of the leather.

Each of these stages includes different steps where a series of mechanical and chemical treatments are applied. A summary of the purposes of each step and the chemicals used is presented in Table 2.1.

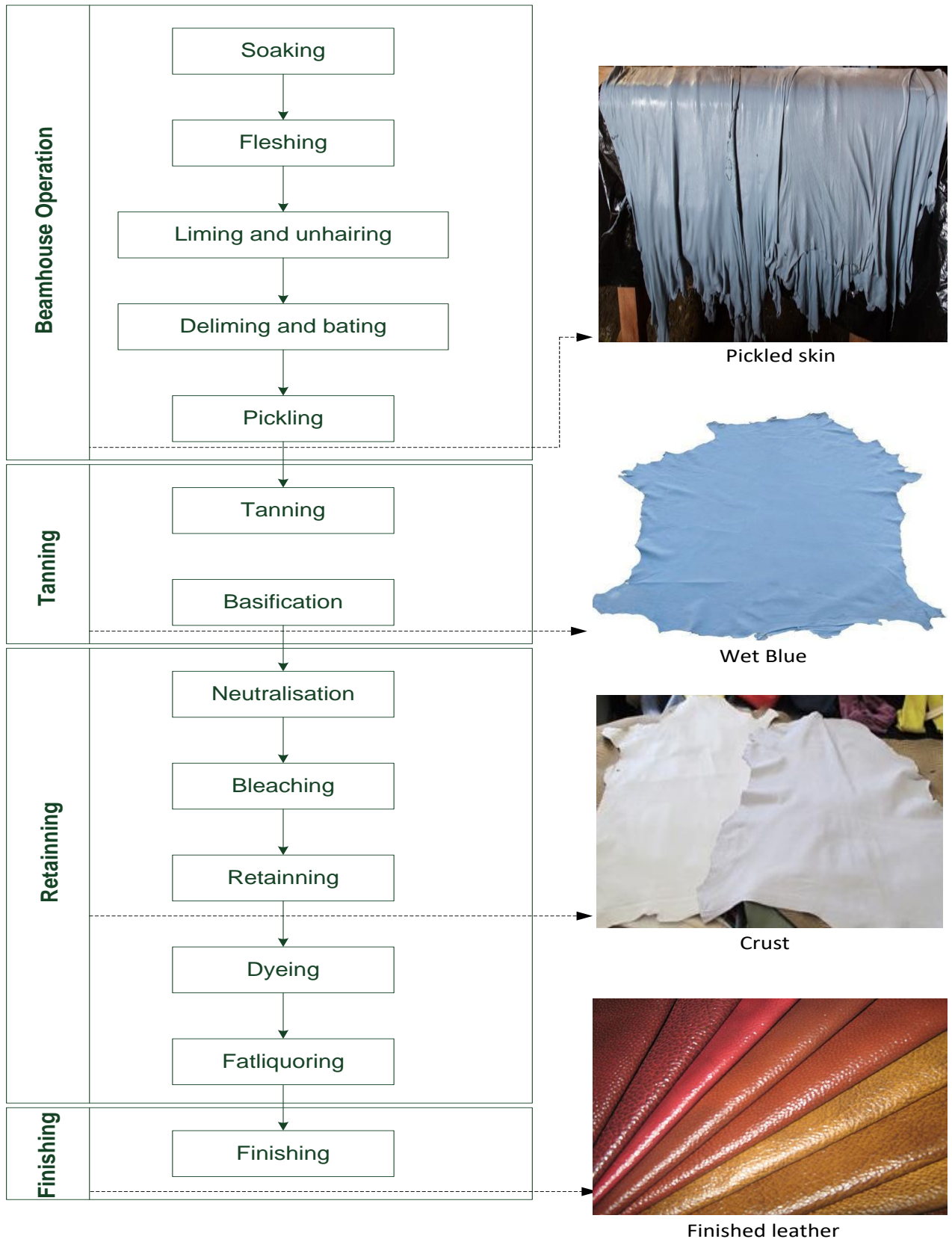


Figure 2.1: Typical leather manufacturing process

Table 2.1: Leather processing process, purposes and chemicals used in each step (adapted from IFC, 2007)

	Process	Purpose	Chemicals used
Beamhouse Operation	Soaking	Rehydrates the hides or skins and removes blood, salt, dung,	NaOH or Na ₂ CO ₃ , surfactants, biocides and enzymes
	Fleshing	Mechanically removes excess fat and tissues	None
	Liming and unhairing	Removes hair through chemical and mechanical treatment	NaHS and Na ₂ S and CaO
	Deliming	Removes lime and prepares the hides for the bating process	(NH ₄) ₂ SO ₄ , NH ₄ Cl, NaHSO ₃
	Bating	Cleans the grain of the hide by removing hair roots and other unwanted materials	Enzymes
	Pickling	Corrects the pH suitable to the tanning process and avoids dehydration of the leather	Salt, H ₂ SO ₄ or CH ₂ O or HCOONa
Tanning	Tanning	Gives the hide or skin mechanical properties of the leather such as abrasion resistance and flexibility to prevent them from decaying	Chrome tanning agent [Cr ₂ (SO ₄) ₃] or vegetable tanning agents or synthetic tanning agents (syntans)
	Basification	Ensures binding of chemical tanning to the hide	MgO, NaHCO ₃
Post-tanning	Neutralisation	Brings the tanned hide to a pH suitable for re-tanning, dyeing and fat liquoring	NaHCO ₃ or NH ₄ HCO ₃ , HCO ₂ ⁻ or C ₂ H ₃ O ₂
	Bleaching	Removes stains and reduces the colouring	Bleaching agents
	Re-tanning	Improves the leather characteristics to facilitate and optimise the dyeing process	Resins, mineral tanning agents, syntans, aldehydes
	Dyeing	Adjusts the dye to the desired colour	Natural or synthetic dyes and water-based acid dyes
	Fatliquoring	Lubricates the leather to achieve product-specific characteristics and to replace the oils and greases lost during processing	Animal or vegetable oils or synthetic products based on mineral oils
Finishing	Finishing	Enhances the appearance of the leather	Solvents, plasticizers, bindings, pigments

2.1. Wastewater consumption and generation

Among all the industries, the leather industry is one of the heaviest water users (Goswami & Mazumder, 2013). Water consumption is divided into 2 main components i.e. process water and technical water for energy generation, and water for sanitary purposes etc. According to the European Commission (2003), the latter is estimated to account about a fifth of the total consumed by tanneries. Process water varies from one tannery to another and it strongly depends on the type of skins or hides and leather processed, and the techniques applied (Sundar et al., 2001). The water consumption of tanneries manufacturing finished leather from intermediate products is low compared to that of full-house tanneries or those generating intermediate products due to less water usage in rinsing steps (European Commission, 2003). In full-house tanneries, high consumption is observed in the beamhouse operation. This is supported by Nacheva et al. (2004) who conducted a survey on different tanneries in Mexico. They found that more than 80% of water used in those tanneries was from the processing of raw hides to wet blue. Krishnamoorthi et al. (2009) estimated that tanneries in India use approximately 15 to 20 L per kg of raw skin while in SA, Swartz et al. (2017) estimated the use of water from a national survey around 170- 550 L per raw skin and hide. Table 2.2 shows typical water consumption in various stages for a conventional bovine tannery.

Table 2.2: Water consumption in a bovine tannery (Black et al., 2013)

Manufacturing process	Average water consumption (%)
Soaking	15- 25
Liming	23-27
Rinsing	
Deliming/Bating	10-15
Rinsing	
Total Beamhouse	50-65
Pickling/Tanning	10
Neutralisation	
Retaining, Dyeing, Fatliquoring, rinsing	
Total Post-tanning operations	30-40
Finishing	10

About 90% of water consumed by tanneries is converted into effluent (Mustapha et al., 2017) and with the variety of chemicals used, this effluent is very complex (Mandal et al., 2010). The potential environmental impacts of tanning are significant (Dixit et al., 2015). Their effluents are considered as high-strength wastewaters comprised of not only the classic pollutants, but also other chemicals such as biocides, surfactants and organic solvents

Tannery wastewater is generally characterised in terms of chemical oxygen demand (COD), biological oxygen demand (BOD), total dissolved solids (TDS), total SS (TSS), S^{2-} , SO_4^{2-} , total chrome (Cr), and salts. Wastewater from the soaking process is hyper-saline due to the amount of salt used to conserve the hides or skins and contains large amount of dissolved solids (World Bank Group, 2007). Fleshing wastewater contains dissolved solids, SS and biodegradable organics (Goswami & Mazumder, 2014), while wastewater obtained from the liming and unhairing processes is mostly biodegradable (Mazumder et al., 2008; Goswami & Mazumder, 2014). It contains large amounts of biodegradable organics, Total Kjeldahl Nitrogen (TKN) which is the total organic and inorganic nitrogen, ammonia (NH_3), S^{2-} , dissolved organic and inorganic salts (Mocanu & Balanescu, 2010).

Tanning wastewater is also highly toxic as it contains large amounts of chromium if chrome tanning is employed. According to Goswami & Mazumder (2013), about 25-30% of the total chrome used is present in the wastewater. Finishing wastewater is composed of solvents, colour pigments, lacquer polymers and coagulants (Mocanu & Balanescu, 2010).

Typical characteristics of tannery wastewater are shown in Table 2.3. It shows that COD is considerably high, ranging between 800 and 54000 mg/L, BOD is in the range 900-18000 mg/L, while higher amounts of TDS (400-187000 mg/L) are observed in comparison to TSS (70-16000 mg/L). Due to the amount of inorganic S^{2-} used in the unhairing process, tannery wastewater contains S^{2-} in the range of 40-860 mg/L. Small traces of phosphorus (P) and iron (Fe) are also found in the wastewater. Considering these characteristics, the development of holistic treatment methods for these effluents is extremely necessary.

Table 2.3: Characteristics of tannery wastewater based on studies from different countries

Parameters	Unit	Country									
		UK	India	China	Italy	Turkey	India	Ethiopia	Egypt	Pakistan	South Africa*
pH		7.5-9	7.2-9.2	8.1-8.5	6.6	7.2	7.8	8.38	10.5	7.3-10	3.46-12.7
Conductivity(EC)	mg/L	-	20 042		8600	19 950	-	-	-	-	-
COD	mg/L	5000-10 000	2533	8300-9250	6855	2810	8853	4546	19 628	1320-54 000	880-12 901
BOD ₅	mg/L	1500-2000	977	2230-2530	2700	910	3700	-	6721	840-18 620	-
TOC	mg/L	-	-	3310-3660	-	-	-	-	-	-	-
TSS	mg/L	-	1244	352-420	2865	1520	1728	-	15 824	220-1 610	78-8944
TS	mg/L	-	-	-	-	-	6450	-	-	-	-
SS	mg/L	1500-4000	-	-	-	-	-	-	-	-	-
TDS	mg/L	-	21 620	4310-5160	-	-	38 192	7800	-	-	483-187 470
Alk	mg/L	-			1010	-	-	-	-	-	-
Chloride	mg/L	-	6528	3240-3850	2835	6400	-	-	-	-	46-24 902
SO ₄ ²⁻	mg/L	-		334-428	745	-	-	440	-	800-6400	71-3707
S ²⁻	mg/L		860	42-65	-	89	-	264.4	1870	90	-
NH ₄ -N	mg/L		118	285-330	70.5	130	-	256		-	-
P	mg/L		62	7.25-8.53	-		-	25.6	31.8		-
Cr	mg/L	100	258	26-35	140	62	-	-	150.86	41-133	141.3
Fe	mg/L		2.56	-	-	0.62	-	-	-	-	
References		Song et al. (2000)	Mandal et al. (2010)	W.-H. Liu et al. (2017)	Lofrano et al. (2006)	Kurt et al. (2007)	Latha et al. (2016)	Mekonnen et al. (2016)	Abdallh et al. (2016)	Haydar et al. (2007)	Swartz et al. (2017)

* 35 tanneries tested COD= chemical oxygen demand BOD₅= 5 days biochemical oxygen demand TOC= total organic carbon TSS= total suspended solid SS= suspended solid TDS= total dissolved solid Alk= alkalinity

2.2. Wastewater treatment

Tannery wastewater is treated by a combination of primary treatment (also known as physicochemical treatment), secondary treatment (biological treatment) and tertiary treatment (Lofrano et al., 2013) as shown in Figure 2.2.

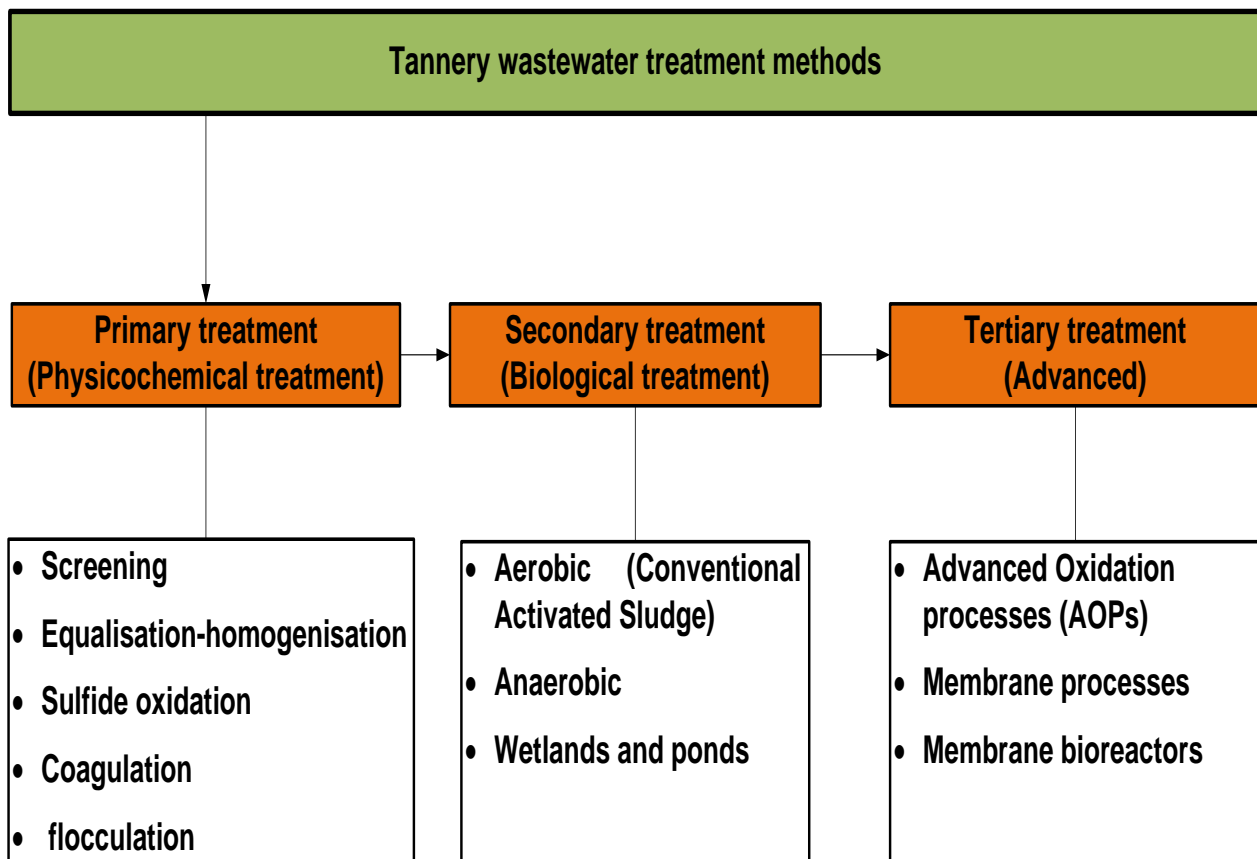


Figure 2.2: Tannery wastewater treatment methods (adapted from Lofrano et al., 2013)

The primary treatment involves screening, equalisation with pH correction, S^{2-} oxidation, coagulation and flocculation (UNIDO, 2011). It also involves the removal of SS, Cr, oil and grease (P. Sabumon, 2016). In this treatment, approximately 50-70% of TSS, 65% of the oil and grease, approximately 20-50% of BOD and almost all the Cr and S^{2-} are removed (UNIDO, 2011).

Primary treatment is followed by secondary treatment better known as biological treatment. This treatment aims to further reduce biodegradable solids, colloidal organic matter (COD and BOD) and other substances still present in the primary effluent to meet the standard discharge limits of a country (UNIDO, 2011). It can be done aerobically (in the presence of oxygen) through the conventional activated sludge (CAS) process or anaerobically (in the absence of oxygen) and sometimes using a combination of both (Porwal et al., 2015). Wetlands and ponds can also be used as alternatives to treat tannery wastewater, but they require large

land areas compared to conventional facilities and pose a risk to the surrounding environment (Goswami & Mazumder, 2013).

Tertiary treatment is applied when the quality of wastewater still does not meet the requirement standards of a country after physicochemical and biological treatments were applied (UNIDO, 2011). This treatment is required when colour, the recalcitrant COD and salts are to be removed (P. C. Sabumon, 2016) and it can be accomplished through various sophisticated techniques including advanced oxidation processes (AOPs) such as Fenton oxidation that uses H_2O_2 as an oxidising agent, photo oxidation through UV light, ozonation, photocatalytic oxidation and electrochemical treatment (Lofrano et al., 2013). Membrane processes and membrane bioreactors are also used for tertiary treatment of tannery wastewater (Lofrano et al., 2013). However, all those techniques are generally cost intensive (Midha & Dey, 2008).

Tanneries usually discharge their effluents to municipality treatment plants. Most tanneries discharging to sewer have some form of on-site effluent treatment installed, ranging from pre-treatment to biological treatment.

2.2.1. Physicochemical treatment

Physicochemical treatment of any types of water consists mainly of sedimentation, screening, aeration, filtration, flotation, degasification, chlorination, neutralization, coagulation, sorption, and ion exchange (Porwal et al., 2015). Numerous physicochemical techniques like coagulation, flocculation, ion exchange, activated carbon desorption, and membrane filtration, have been studied for their application for the treatment of tannery wastewater (Song et al., 2004; Elsheikh, 2009; Ayoub et al., 2011; Zouboulis et al., 2019). Among these techniques, coagulation and flocculation are by far the most widely used (Song et al., 2004). Coagulation is the addition and rapid mixing of coagulant with water to destabilise colloidal particles and form small flocs. This process can be achieved by chemical and electrical routes (Sahu & Chaudhari, 2013). Flocculation, on the other hand, involves the formation of aggregates from the destabilised colloids with the addition of a polymer (UNIDO, 2011). According to Lofrano et al. (2013), polymers with various ionic properties are available and consist of anionic polymers (with a positive charge), cationic polymers (with a negative charge) and non-ionic polymers (neutrally charged).

These two distinct processes are usually carried out in a sequence and often referred to using a single term being “coagulation” or “flocculation” or both as “coagulation-flocculation”. Inorganic coagulants such as aluminium sulfate (Al_2SO_4) also known as alum, ferric chloride ($FeCl_3$), ferrous sulfate ($FeSO_4$) and hydrated lime [$Ca(OH_2)$] have been applied to tannery wastewater (Lofrano et al., 2006). Each coagulant works effectively in a specific pH and aims

to reduce organic load and SS as well as to remove toxic substances such as chromium before biological treatment. In solution, aluminium and iron hydrolyse to form some ionic species like $Al_2(OH)_5^+$, $Al_2(OH)_2^{4+}$, and $Al(OH)_3$, $Fe(OH)_3$ or $Fe(OH)_2$ (Zongo et al., 2012). The contact of these species with the wastewater contaminants leads to the aggregation of colloidal particles that sediment later (Song et al., 2004; Costa et al., 2008).

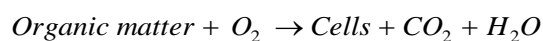
Song et al. (2004) reported 38-46% removal of SS, 30-37% of total COD and 74-99% removal of chromium from settled tannery wastewaters using Al_2SO_4 and $FeCl_3$ as coagulants at 7.5 pH. Kabdasli et al. (1999) also obtained a removal range of 40–70% of COD and >99% of total chromium from leather tanning wastewater using $FeSO_4$, $FeCl_3$ and alum. Haydar & Aziz (2009) conducted a study on the treatment of tannery wastewater through coagulation-flocculation-sedimentation using alum as a coagulant with cationic and anionic polymers as a coagulant aid. The results showed up to 99.7% removal of chromium, TSS removal up to 96.3% and total COD removal up to 48.3%.

On the other hand, Ayoub et al. (2011) combined coagulation with adsorption for the treatment of tannery wastewater. Lime and bittern (a rich source of magnesium derived from vaporized seawater or from brine rejects of seawater desalination systems) served as coagulant and activated carbon as adsorbent. This is reported to be more effective for the removal of COD than the conventional coagulation (Apaydin & Kurt, 2009).

2.2.2. Biological treatment

Biological treatment is widely used for the treatment of industrial and municipal wastewater due to the high degradation of organic matter and its economic advantages (Dargo & Ayalew, 2014). As previously mentioned, there are two major biological processes i.e. aerobic and AD (Ndon & Dague, 1997). The advantages and disadvantages of both processes are listed in Table 2.4.

Aerobic digestion is referred to as the direct oxidation of biodegradable organic matter, followed by degradation of microbial biomass when the readily biodegradable organic matter has been depleted by aerobic and/or facultative bacteria (Shammas & Wang, 2007). The end products are principally CO_2 , H_2O and large amount of sludge which has to be handled prior to disposal (de Lemos Chernicharo, 2007). This is illustrated by Equation 2.1 (Shammas & Wang, 2007):



Equation 2.1



Table 2.4: Comparison between aerobic and anaerobic digestion (adapted from de Lemos Chernicharo, 2007)

	Advantages	Disadvantages
Aerobic digestion	<ul style="list-style-type: none"> • Easy to operate • No generation of bad odours 	<ul style="list-style-type: none"> • Production of large quantity of sludge that needs to be handled before disposal or sent to landfill • High energy and operation costs • Limited production of useful products • No tolerance to high organic loads
Anaerobic digestion	<ul style="list-style-type: none"> • Low production of solids, about 3 to 5 times lower than in aerobic digestion • Tolerance to high organic loads • Low energy consumption • Low land requirements • Low construction costs • Production of biogas 	<ul style="list-style-type: none"> • Microorganisms susceptible to inhibition by a large number of compounds • Reliant on slow growing methanogenic archaea • Time consuming • Control of pH required • Slow process start-up in the absence of adapted seed sludge • Generation of bad odours due to the production of H₂S

In contrast, anaerobic digestion is considered as a sustainable waste management strategy as well as a source of renewable energy (Franke-whittle et al., 2014) compared to aerobic digestion. Shammass & Wang (2007) defines AD as the decomposition of organic matter to biogas (in the absence of air) which can be used for heat and for electricity, as a vehicle fuel, as well as a substitute for natural gas in a gas grid (Hagman et al., 2018). In addition, the process generates sludge of agricultural value (Lastella et al., 2002; Insam & Wett, 2008; Franke-whittle et al., 2014) as it is rich in nutrients (Alvarado et al., 2014). However, despite all these advantages, the process remains ineffective and enigmatic due to the lack of knowledge on the link between the process parameters and the microbial communities involved (Lee et al., 2009; Pycke et al., 2011; Franke-whittle et al., 2014).

2.2.2.1. Anaerobic technologies: overview

Anaerobic treatment has become the most frequently used method for the treatment of medium and high concentration effluents. Several anaerobic systems have been developed for the treatment of domestic and industrial wastewater. These are categorised into two main groups as illustrated in Figure 2.3: the conventional systems and the high-rate systems. According to de Lemos Chernicharo (2007), conventional systems categorize reactors that operate at low volumetric organic loads. High-rate systems have emerged as viable

technologies for the treatment of many industrial and municipal wastewaters due to their ability to separate hydraulic and solid retention times (SRT) effectively. They allow the presence of a large amount of high activity biomass, which can be maintained at low hydraulic retention time (HRT).

Those high-rate anaerobic processes include the upflow anaerobic sludge blanket (UASB), anaerobic filters (AF) mostly in the upflow configuration, the expanded granular sludge bed (EGSB), the fluidised bed, anaerobic baffled reactor (ABR), anaerobic hybrid reactor (AH) and the anaerobic sequencing batch reactor (ASBR) (Ndegwa et al., 2005).

Mannucci et al. (2010) reported that UASB reactors and AF are the anaerobic systems most used for the treatment of tannery wastewater. However, the application of EGSB and ASBR reactors has improved in recent years. These four systems are discussed below. However, several other high-rate anaerobic processes like upflow anaerobic fixed film reactor, hybrid upflow anaerobic sludge blanket reactor (Song & Williams, 2003; Banu & Kaliappan, 2007), sequencing batch biofilm reactor that are not covered in this Section, are reported in literature for the treatment of tannery wastewater.

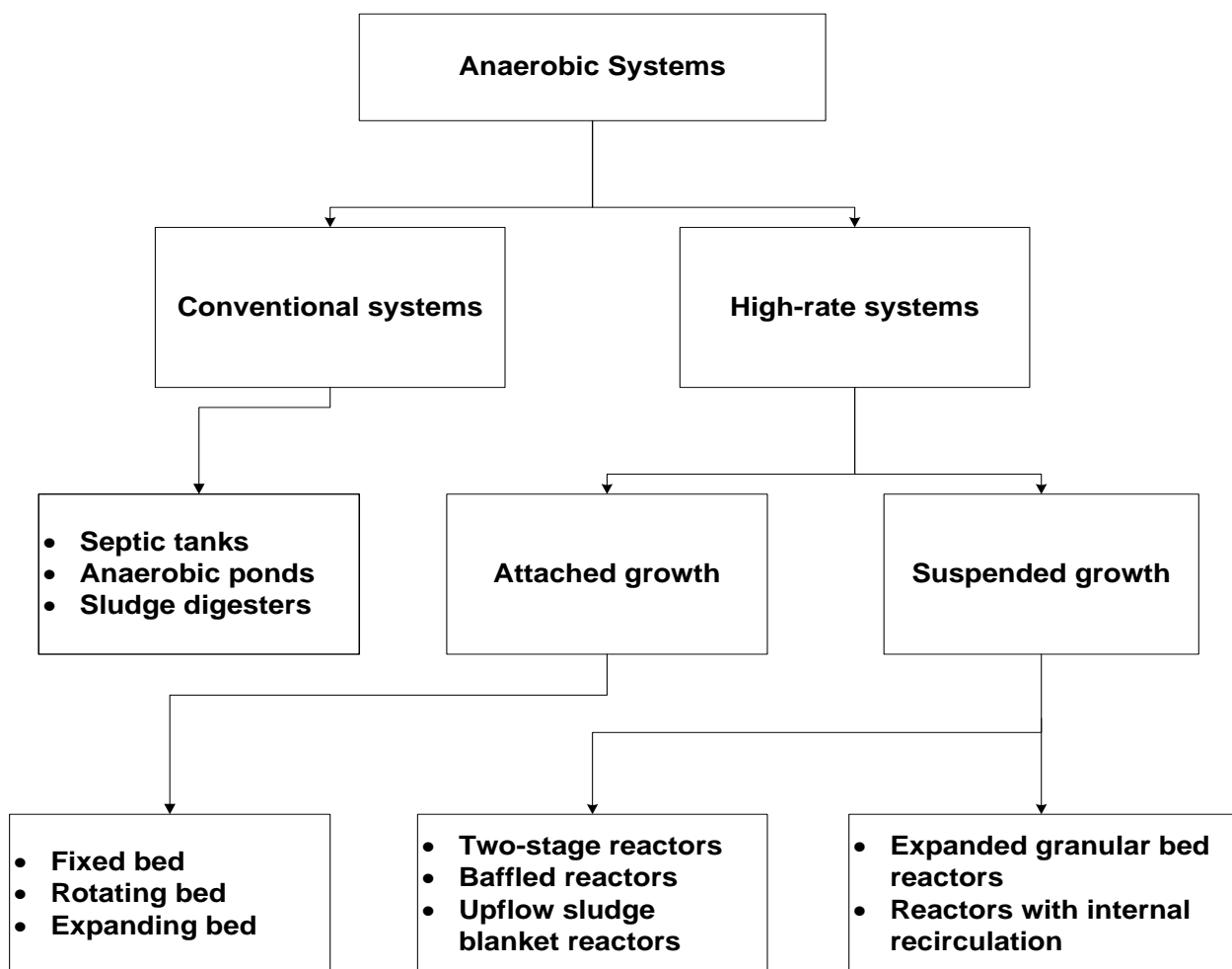


Figure 2.3: Anaerobic treatment systems

- **Upflow anaerobic sludge blanket**

Over the last three decades, UASB technology has been shown to be efficient for the treatment of tannery wastewater. The UASB reactor was invented by Lettinga and associates in the late 1970s (Tchobanoglous et al., 2003; Daud et al., 2018) with highly concentrated industrial wastewater and has successfully been used for the treatment of a variety of wastewaters including those with inhibitory characteristics (Latif et al., 2011). This reactor has positive characteristics such as high organic loading rates (OLRs), short HRT and a low energy demand (Borja & Banks, 1994; Tchobanoglous et al., 2003; Daud et al., 2018). Its success also depends on a dense sludge bed in the bottom of the reactor where all biological processes take place (Álvarez & Soto, 2012). The wastewater to be treated is fed from the bottom of the reactor and travels in an upward continuous mode through a blanket of biologically activated sludge, which is generally in the form of granular aggregates as shown in Figure 2.4 (Daud et al., 2018). The gas/liquid/solid separator at the top of the reactor helps to separate the gases contained in the liquid mixture and create a sedimentation zone that allows the solids to fall back to the sludge blanket (Hickey et al., 1991; Matangue & Campos, 2011).

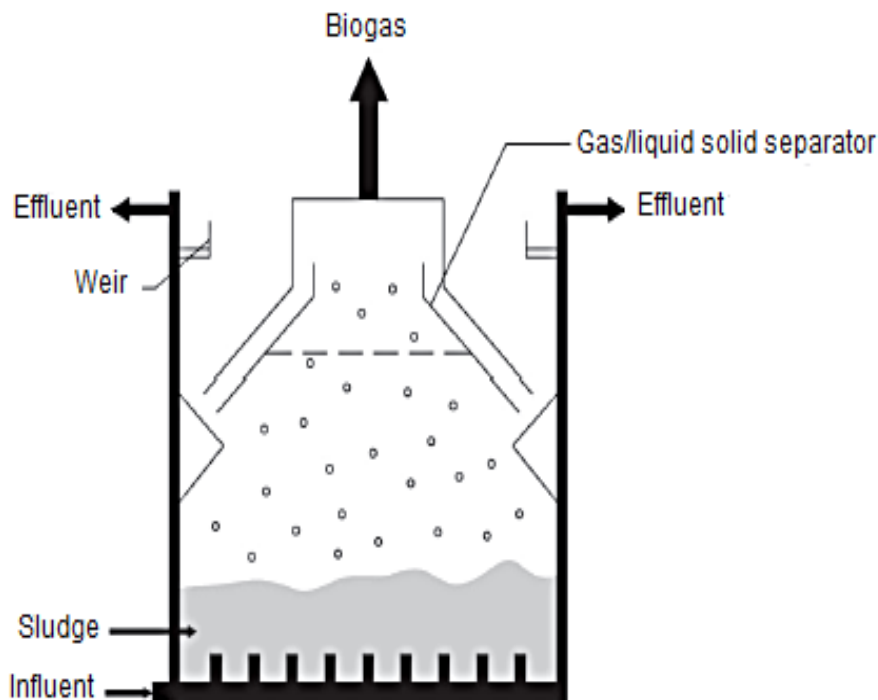


Figure 2.4: Upflow anaerobic sludge blanket reactor (Aziz et al., 2019)

Routh (2000) evaluated the performance of a UASB for the treatment of vegetable tannery wastewater. The wastewater was fed at different COD concentrations of 500, 1000, 4000 and 7000 mg/L and, COD and BOD removal efficiency of 85 to 92.6% and 86 to 94.7% were respectively achieved.

Lefebvre et al. (2006) focussed on treating tannery soak liquor generated by the soaking of hides and skins using a UASB. They achieved 78% COD removal at organic loading rate (OLR) of 0.5 kg COD/m³.day, HRT of 5 days and a TDS concentration of 71 g/L. El-sheikh et al. (2011), investigated the possibility of applying innovative low-cost biological treatment using two stages UASB reactors connected in series in the treatment for tannery wastewater at different HRT. They found that HRT of 12 h for each reactor resulted in the highest removal efficiency. COD removal efficiencies reached 75.9% and 82.4% after the two stage UASB reactors for sub-phase 1 and sub-phase 2 respectively.

The major disadvantages of UASBs are the long start-up period that is required to provide “a good balance among diverse microorganisms with respect to their optimal growth environment” (Liu et al., 2017), their effluent requires post-treatment to remove recalcitrant pathogens, they are not suitable in cold regions as temperatures in reactors need to be > 19°C, and granule formation and maintenance can be difficult (Kaviyarasan, 2014).

- **Anaerobic Filters**

Anaerobic filters (AF) or anaerobic fixed film reactors are contact units that consist of a column filled with packing material mainly used to retain high biomass concentration in the reactor (Manariotis & Grigoropoulos, 2006). According to de Lemos Chernicharo (2007) this biomass can be in three forms i.e. a thin biofilm layer attached to the surfaces of the packaging medium, dispersed biomass retained within the media matrix, and the flocs or granules retained in the bottom section, below the packing medium. The organic compounds in the wastewater get trapped on the surface of the filter media (stone/plastic media), and then removed by microorganisms attached to that filter (Young & McCarty, 1969; Aziz et al., 2019). They are then converted into biogas as shown in Figure 2.5. The AF can be operated in upflow, downflow, or horizontal modes with the upflow configuration being the most used to reduce washout of biomass (Manariotis & Grigoropoulos, 2006).

The effectiveness of anaerobic digestion of vegetable and chrome tannery wastewater (COD concentration ranging from 1500-16 500 mg/L) was studied by Vijayaraghavan & Murthy (1997) using an upflow AF at different HRT of 36, 48 and 60 hr. COD removal was in the range of 80-95% and 79-95% for pre-treated vegetable and chrome tannery wastewater, respectively, compared to 52-89% and 60-86% for untreated vegetable and chrome tannery wastewater, respectively. An upflow AF packed with two types of microcarriers achieved a COD removal range of 60-75%, up to 59% TSS removal and a CH₄ yield of 0.36 m³ CH₄/kg COD removed (Song & Williams (2003).

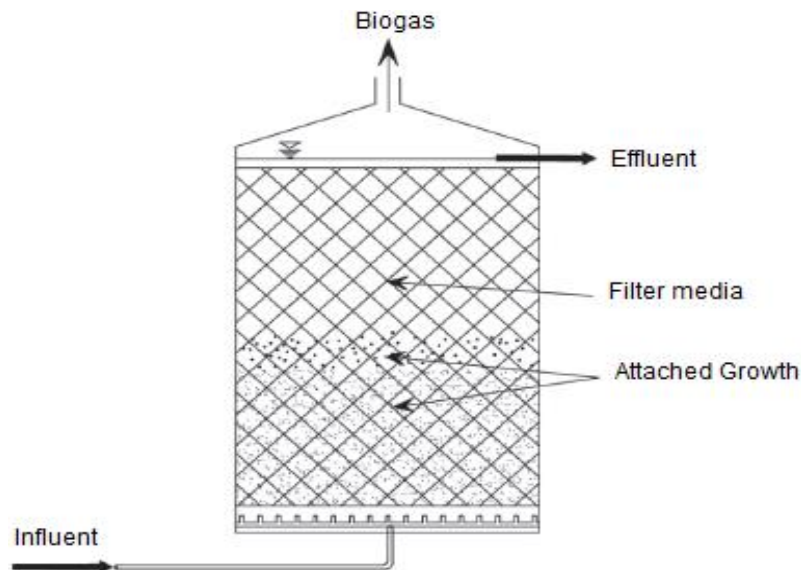


Figure 2.5: Schematic diagram of anaerobic filters (Aziz et al., 2019)

Long start-up period and clogging of the carriers due to the formation of inorganic precipitates, are some of the limitations for the application of anaerobic filters for tannery wastewaters. The clogged filters media need to be removed and cleaned occasionally (Ganesh & Ramanujam, 2009). In addition to that, channelling i.e. formation of preferential paths of liquid flow through the reactor may occur (Bodík et al., 2000).

- **Expanded granular sludge bed**

The expanded granular sludge bed (EGSB) bioreactor has several advantages like design simplicity, usage of unsophisticated equipment, low anaerobic granular, high treatment efficiency, low operating costs (Cruz-Salomón et al., 2019). The system is a modification of the UASB system (Vivekanandhan & Mohan, 2018). According to Álvarez & Soto (2012). EGSB reactors were developed to counteract problems such as preferential flows, hydraulic short cuts and dead zones that might occur in the UASB reactors. EGSB reactors are characterized by an improved hydraulic mixing, independent from the biogas production (Lier et al., 2015). Mixing is intensified by recycling a part of the effluent as illustrated in Figure 2.6 (Bhattacharyya & Singh, 2010). Therefore, all retained sludge is optimally mixed with the wastewater to be treated, while small inactive particles are washed-out from the system (Lier et al., 2015).

A study by Vivekanandhan & Mohan (2018) investigated the treatment of tannery wastewater the effectiveness of the EGSB reactor towards the treatment of the tannery industry complex wastewater and the start-up, performance of the EGSB reactor operating at different HRT and OLR, and the COD removal efficiency and biogas generation in different OLR. They achieved an optimum COD removal percentage of 85.52 % and 0.27 m³/kg COD biogas production at 1.512 kg COD/m³.days of OLR at 5.21 days of HRT.

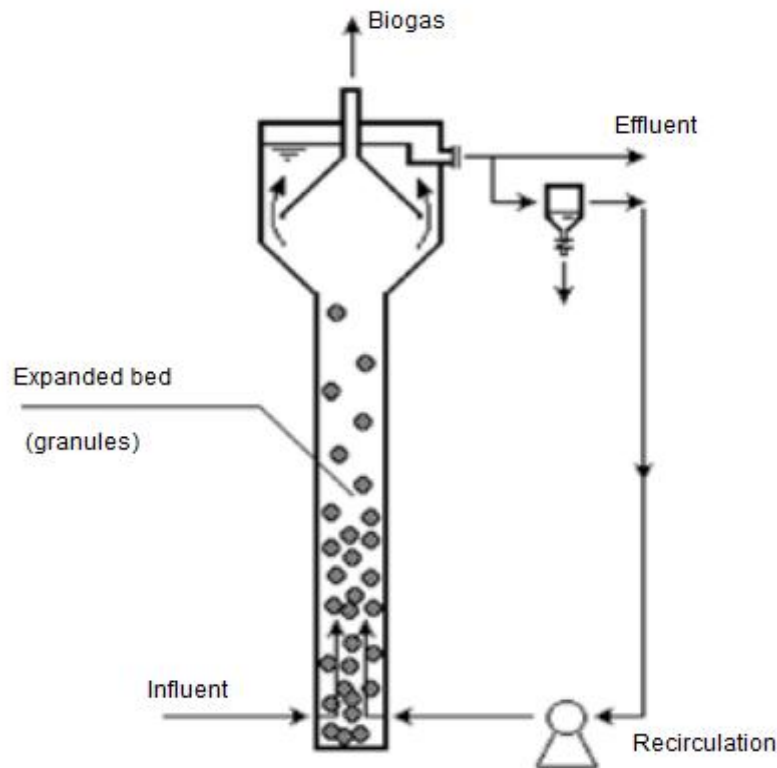


Figure 2.6: Schematic diagram of an expanded granular sludge bed reactor (de Lemos Chernicharo, 2007)

Like all reactors, EGSB reactors have shortcomings. According to Zheng et al. (2014), excessive effluent recirculation not only consumes energy, but may also wash out sludge granules and reduce sludge activities, therefore causing system failure.

- **Anaerobic sequencing batch reactor**

Anaerobic sequencing batch reactor (ASBR) was developed by Richard R. Dague and co-workers at Iowa State University (USA) in 1993 (Aziz et al., 2019) as a modification of anaerobic contact and anaerobic activated sludge processes (Tansengco et al., 2015). ASBRs have gained increasing attention for the treatment of high strength wastewater including slaughterhouse wastewater, municipal sludge, dairy wastewaters, and brewery wastewater (Xiangwen et al., 2008) due to their good COD removal efficiency and their ability to separate SRT from HRT in the same reactor chamber, to work in the absence of a secondary clarifier tank, and simple operation, thus resulting in capital savings (Ndegwa et al., 2005). In addition, ASBRs can treat more volume of substrate per unit time than conventional reactors, therefore reducing volume of the reactor (Mekonnen, Leta & Nicholas, 2017).

The ASBR process consists of five (5) discrete steps namely feed, react, settle, decant and idle that occur in a cyclic mode (Shi et al., 2017) (Figure 2.7). According to Massé & Masse (2000), the feed step can be performed in a batch, semi-continuous or intermittent mode, with the batch mode having a kinetic advantage over continuous systems such as UASBs (Sung

& Dague, 1995). Moreover, biomass retention is a key feature in ASBR (Aziz et al., 2019). The ASBR has alternating food to microorganism ratio (F:M): (i) from high F:M ratio during and immediately after feeding, providing good contact of substrate and microorganisms and high production of biogas, (ii) to low F:M ratio before settling, involving much lower biogas production (Mekonnen, Leta & Nicholas, 2017).

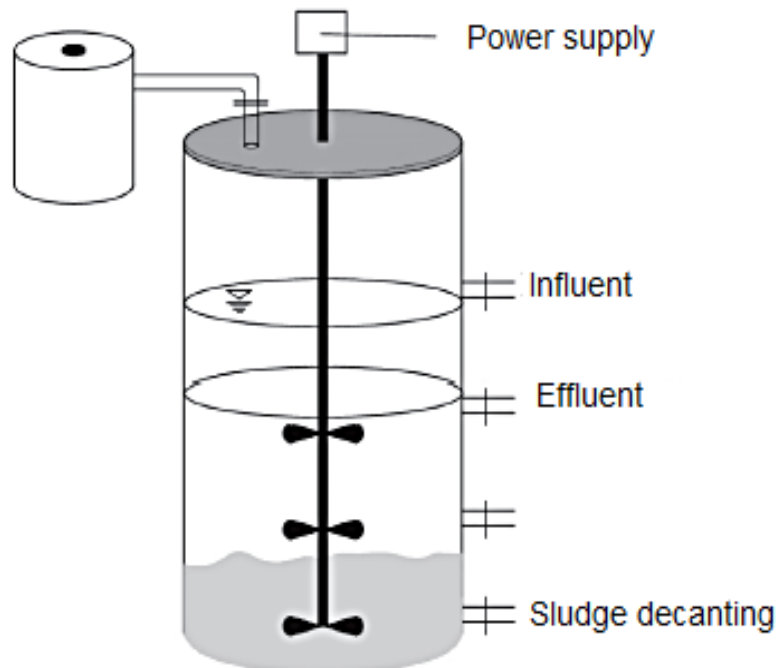


Figure 2.7: Anaerobic sequencing batch reactor (Aziz et al., 2019)

Similar to UASBs, the biomass in ASBR reactors is gradually converted into highly active granular biomass. Granule formation promotes good settling during the decanting step which is important because poorly settling flocs may be washed out during decanting (Sung & Dague, 1995).

However, the use of ASBRs is associated with some disadvantages such as the non-uniformity of biogas production through the process i.e. maximum biogas is produced at the beginning of the react step and minimum before the settling step (Massé & Masse, 2000) and the system operates at low OLR (Shizas & Bagley, 2002). Furthermore, there are a limited number of studies treating tannery wastewater using ASBRs; only 4 citations were found (Mekonnen et al., 2016; Mekonnen, Leta & Nicholas, 2017; Berhe & Leta, 2017; Emanu & Dawit, 2017) and none were full scale installations.

Extensive research was conducted by Mekonnen et al. (2016) in case of tannery wastewater. In their research, Mekonnen et al. (2016) investigated the treatment of tannery wastewater co-digested with cattle dung at five different mixing ratios. They achieved removal efficiencies of 75-82% for COD, 70-80% for TS and 81-89 for VS.

2.3. Anaerobic digestion

2.3.1. Metabolic processes

Anaerobic digestion is a complex process that can be divided into 4 principle steps namely hydrolysis, acidogenesis, acetogenesis and methanogenesis, which involve several microorganism groups (Zhang et al., 2014) such as fermentative bacteria, acidogenic bacteria and methanogenic archaea as illustrated in Figure 2.8.

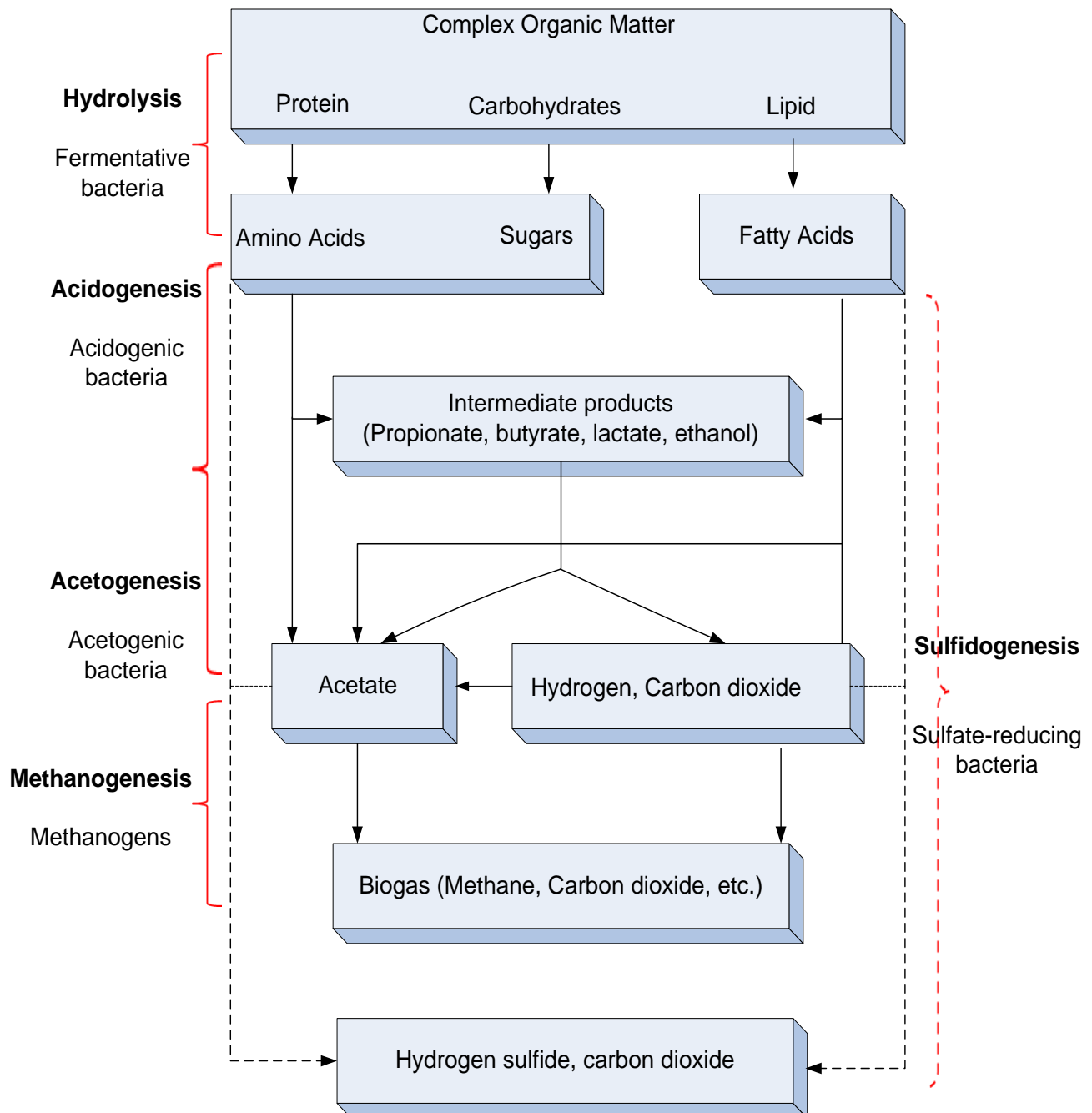


Figure 2.8: Metabolic process of anaerobic digestion (adapted from Meegoda et al., 2018)

In reactors treating wastewater like tannery effluent that contains SO_4^{2-} and S^{2-} , methanogens are inhibited (Midha & Dey, 2008), leading to the production of H_2S by SRB in a process called sulphidogenesis (refer to the dotted lines in Figure 2.8). SRB and methanogens compete for the same substrates i.e. acetate, H_2/CO_2 and soluble organic molecules (sugars, amino acids and fatty acid (Muyzer & Stams, 2008; Plugge et al., 2011). SRB often predominate in the competition due to several factors: (i) anaerobic respiration with SO_4^{2-} yields more energy for growth compared with CO_2 ; (ii) SRB possess higher affinity for both H_2 and acetate, enabling them to consume substrates below levels possible for use by methanogens; and (iii) methanogens have slow growth rates and are susceptible to environmental change and inhibitors (Moestedt et al., 2013). Therefore, enhancing methanogenesis together with sulphidogenesis is a promising mechanism for improving the performance of anaerobic reactors.

2.3.1.1. Hydrolysis

Hydrolysis is the first step of the anaerobic degradation of organic matter. In this process biopolymers such as proteins, carbohydrates and lipids are broken down to amino acids, sugars and fatty acids respectively, by fermentative bacteria (Anderson et al., 2003; Franke-whittle et al., 2014). Those fermentative bacteria include *Bacillus* spp., *Cellulomonas* spp. and *Eubacterium* spp., and the step is catalysed by enzymes like cellulase, amylase, protease and lipase (Franke-whittle et al., 2014).

2.3.1.2. Acidogenesis

Through this second step, the soluble organic molecules from hydrolysis are converted into alcohols, ketones, H_2 , CO_2 and volatile fatty acids by acidogenic bacteria (Franke-whittle et al., 2014).

2.3.1.3. Acetogenesis

This step consists of the oxidation of products resulting from acidogenesis into acetate, H_2 and CO_2 by acetogenic bacteria (de Lemos Chernicharo, 2007). These end products are essential substrates for the final step of AD. Acetogenic bacteria include the genera of *Syntrophomonas* and *Syntrophobacter* known to convert the acid products into H_2 and acetate (Anderson et al., 2003).

2.3.1.4. Methanogenesis

Methanogenesis is a critical step in the entire AD process as it is the slowest biochemical reaction (Jingura & Kamusoko, 2017). It is carried out by microorganisms called methanogens (Hook et al., 2010) which are strictly anaerobic (Fazli et al., 2013).

Methanogens are essential microorganisms found in a large variety of environments such as digesters, marine habitats, as well as the digestive tracts of animals, herbivores etc. (Zhu et al., 2004; Friedrich, 2005; Manyi-loh et al., 2013). They belong to the Archaea domain comprising of six (6) orders i.e. *Methanobacteriales*, *Methanococcales*, *Methanomicrobiales*, *Methanosarcinales*, *Methanocellales* and *Methanopyrales* (Friedrich, 2005; Ferry, 2010; Fazli et al., 2013; Manyi-loh et al., 2013). In the AD process, methanogens play a key role by producing CH₄ (Blaut, 1994).

According to Fazli et al. (2013), methanogenesis can occur through various metabolic pathways as illustrated in Figure 2.9: the hydrogenotrophic methanogenic pathway (the blue line), the acetoclastic methanogenic pathway (the red line) and the methylotrophic methanogenic pathway (the green line). However, only hydrogenotrophic and acetoclastic methanogenesis are quantitatively significant. Guo et al. (2015) investigated the three (3) pathways in the anaerobic digestion of wastewater and observed a major production of CH₄ in the acetoclastic pathway. The reactions occurring in each pathway are listed in Table 2.5.

Table 2.5: Reactions involved in methanogenic pathways (Wang et al., 2015)

Pathway	Reaction	ΔG° (kJ/mol)
Hydrogenotrophic	$4H_2 + CO_2 \rightarrow CH_4 + 2H_2O$	-135.6
Acetoclastic	$CH_3COOH \rightarrow CH_4 + CO_2$	-31
Methylotrophic	$4CH_3OH \rightarrow 3CH_4 + 2H_2O$	-112.5

Each of these pathways is catalysed by a series of enzymes and coenzymes that are exclusive to methanogens (Gargaud, 2015) and the scheme of these processes is illustrated in Figure 2.9.

Although all the pathways start differently, they all converge to a final step where methyl coenzyme M reductase (MCR) catalyses the reduction of the methyl group attached to coenzyme M (CH₃-CoM), releasing CH₄, making it the key enzyme of methanogenesis (Friedrich, 2005; Juottonen et al., 2006; Ma et al., 2012). According to Chistoserdova et al. (1998), Friedrich (2005) and Chaudhary et al. (2011), this enzyme is unique to methanogens, highly conserved and exists in two different forms designated as MCR I encoded by the *mcrBDCGA* operon which is found in all methanogens and MCR II encoded by *mrtBDGA* operon and only present in members of the *Methanococcales* and the *Methanomicrobiales* orders (Friedrich, 2005; Alvarado et al., 2014).

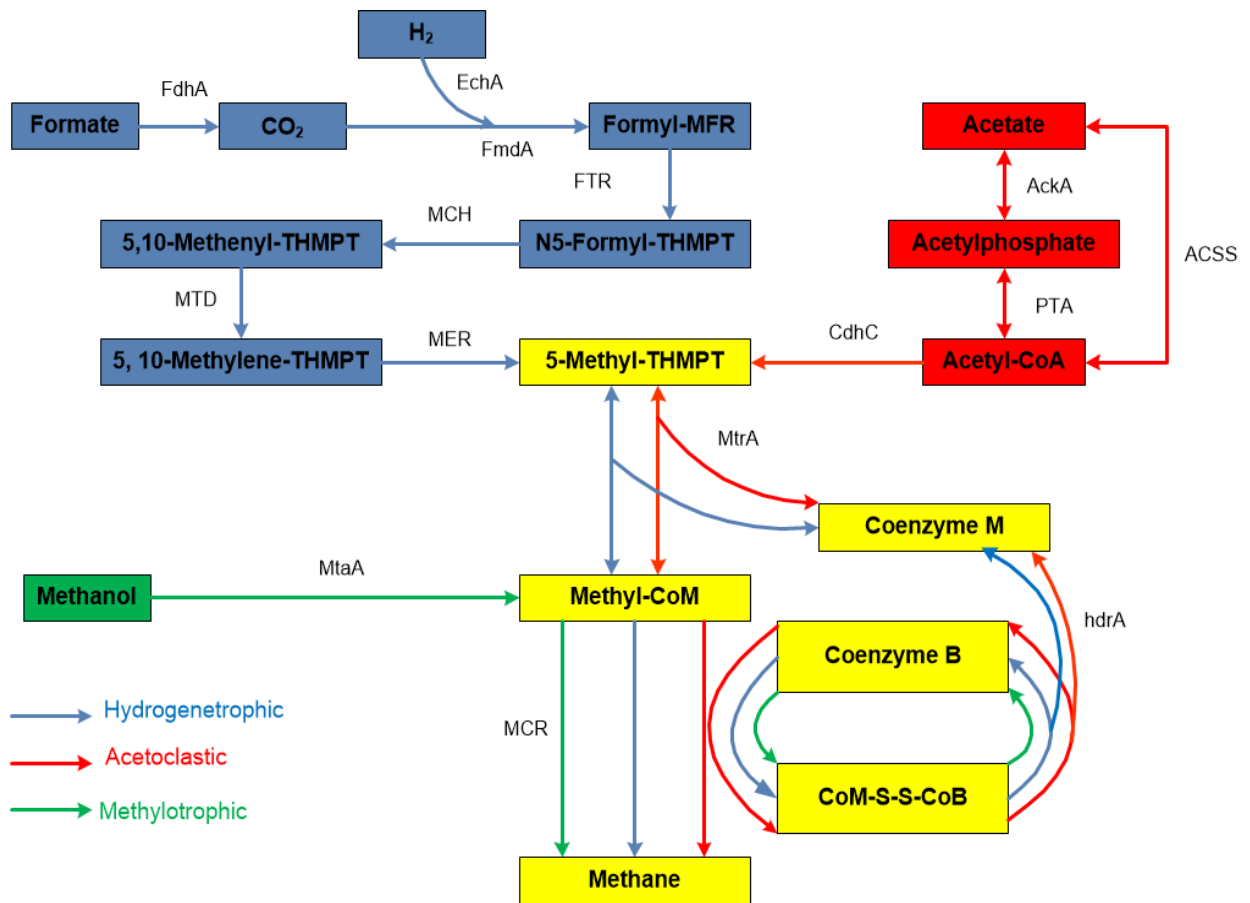


Figure 2.9: Methanogenesis pathways (Guo et al., 2015)

FdhA= glutathione-independent formaldehyde dehydrogenase EchA= hydrogenase subunit A; FmdA= formylmethanofuran dehydrogenase subunit A; FTR= formylmethanofuran-tetrahydromethanopterin N-formyltransferase; MCH= methenyltetrahydromethanopterin cyclohydrolase; MTD= methylenetetrahydromethanopterin dehydrogenase; MER= coenzyme F420-dependent N5= N10-methenyltetrahydromethanopterin reductase; MtrA, tetrahydromethanopterin S-methyltransferase; MtaA= [methyl-Co(III) methanol-specific corrinoid protein]:coenzyme M methyltransferase; AckA, acetate kinase; ACSS, acetyl-CoA synthetase; PTA= phosphate acetyltransferase; hdrA= heterodisulfide reductase subunit A; CdhC= acetyl-CoA decarbonylase/synthase complex subunit β .

Currently, the presence of the *mcrA* gene encoding the alpha subunit of MCR is a reliable marker of methanogenesis in various environments. Several researchers have studied this gene as a biomarker to detect the presence of methanogens and activity in paddy soil (Ma et al., 2012; Yuan et al., 2018), peat soil (Freitag & Prosser, 2009), rumen of bovines (Chaudhary et al., 2011) and anaerobic digesters (Rastogi et al., 2008). Chaudhary et al. (2011) investigated the diversity of methanogens in the rumen of Murrah buffaloes targeting this *mcrA* gene using 454-pyrosequencing and quantitative real-time polymerase chain reaction (qPCR), while Zeleke et al. (2013) used this gene to identify the types of methanogens inhabiting the Mudflat Sediments of Yangtze River Estuary in China. In anaerobic reactors, Cetecioglu et al. (2019) tested the effects of carbon sources and COD/SO_4^{2-} ratio on the diversity and

interactions of methanogens targeting the *mcrA* gene (further discussion can be found in CHAPTER 5).

2.3.1.5. Sulphidogenesis

According to Bijmans et al. (2011), sulphidogenesis or dissimilatory sulfate reduction (SR) is the conversion of SO_4^{2-} to sulfide coupled to the oxidation of an electron donor for energy conservation that is subsequently used for growth and maintenance. This metabolic feature is performed by sulfate-reducing bacteria (SRB).

Sulfate-reducing bacteria are important microbial community members with economic, environmental and biotechnological interest; they play an important role in the bioremediation of a variety of industrial effluents such as acid mine drainage (AMD) (Martins et al., 2009). However, in SO_4^{2-} -rich AD bioreactors, SRB use SO_4^{2-} as an electron acceptor to produce H_2S which has high toxicity and corrosion properties and eventually induce the failure of whole AD system (Jing et al., 2013). H_2S dissociates in water, in accordance with the following Equation 2.2:



Sulfate-reducing bacteria are included in a group of chemoorganotrophic and strictly anaerobic bacteria, which contains representatives of the genera *Desulfovibrio*, *Desulfomicrobium*, *Desulfobacter* and *Desulfotomaculum*, among others (Luptakova & Kusnierova, 2005). They are categorised in two major metabolic groups: (i) a group of species that is able to oxidise incompletely its substrates to acetate and (ii) a group which is able to oxidise its organic substrates, including acetate, to CO_2 .

Like methanogenesis, sulphidogenesis involves a series of enzymes. Two enzymes, adenosine 5'-phosphate sulfate reductase (APR) (Friedrich, 2002) encoded by the *AprAB* operon and dissimilatory sulfite reductase (DSR) (Klein et al., 2001) encoded by the *dsrABC* operon (Muller et al., 2015), catalyse this step (Madrid et al., 2006). As illustrated in Figure 2.10, SO_4^{2-} is first converted to adenosine 5 - phosphosulfate (APS) by ATP sulfurylase. APS is then reduced to sulfite by APR, and sulfite is then converted to S^{2-} by DSR (Duarte et al., 2016).

Both enzymes have been targeted for the studies of the diversity of SRB (Setya et al., 1996; Geets et al., 2006). However, genes for DSR are most commonly used (Wagner et al., 1998; Agrawal & Lal, 2009; Chang et al., 2001; Guan et al., 2013; Islamud-Din et al., 2014). According to Muller et al. (2015) these genes are required by all SO_4^{2-} reducers which are

distributed in four bacterial (*Proteobacteria*- class *Deltaproteobacteria*, *Nitrospirae*, *Firmicutes* and *Thermodesulfobacteria*) and two archaeal phyla (*Euryarchaeota* and *Crenarchaeota*), making it the key enzyme of the sulphidogenesis.

Currently, the presence of the *dsrB* gene encoding the β subunit of DSR is a functional marker of sulphidogenesis in diverse environments. For instance, Madden et al. (2014) used this gene to investigate the behaviour of SRB in low-temperature anaerobic expanded granular sludge bed-based bioreactors at different SO_4^{2-} concentrations. Agrawal & Lal (2009) quantified sulfate-reducing communities in oil field samples using *dsrB* gene. Moestedt et al. (2013) evaluated the effects of operational parameters and type of substrate on the abundance of SRB in 25 industrial biogas digesters using qPCR targeting the *dsrB* gene (results can be found in CHAPTER 5).

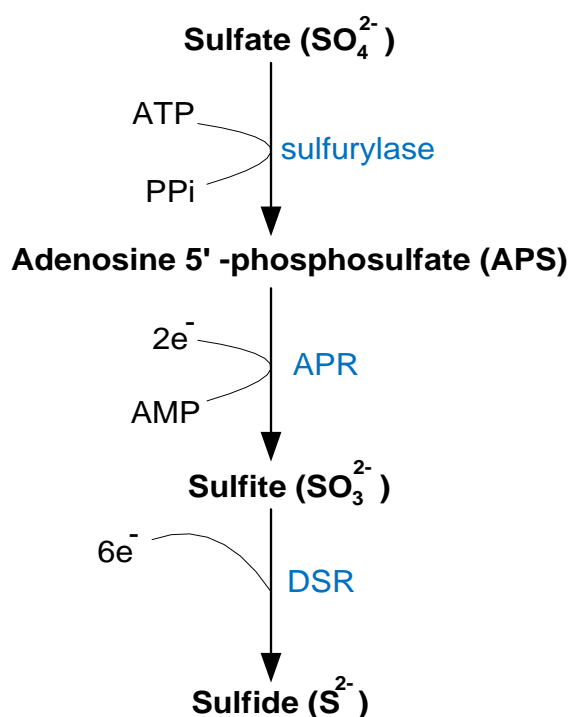


Figure 2.10: Schematic representation of sulphidogenesis

2.3.2. Biochemical methane potential testing

The biochemical methane potential (BMP) test is a key method that is used to assess the biodegradability of a substrate and its potential to produce CH_4 (Da Silva et al., 2018). Wang et al. (2016) defines the BMP test as a key parameter for the design, optimisation, economy and management in full-scale implementations of AD. These tests are conducted in batch conditions and at bench scale, measuring the maximum amount of biogas or CH_4/gVS contained in the organics used as substrates in the AD process (Esposito et al., 2012).

In recent years, many researchers have published the results of BMP tests using a wide variety of substrates such as municipal solid waste, food waste, primary sludge from a municipal wastewater treatment plant (WWTP), microcrystalline cellulose, and wheat straw (Boulanger et al., 2012; Elbeshbishy et al., 2012; Wang et al., 2016; S. R. Hobbs et al., 2018) and retention times (from 20 to >100 days). The results from these tests are variable and difficult to compare due to differences in both instrumentation and protocols, as well as different experimental conditions (Ebrahimi-nik et al., 2016). For example, the pH, head space, mixing intensity, inoculum to substrate ratio (ISR), inoculum dilutions but also initial substrate concentration can differ among different tests (Angelidaki et al., 2009).

One of the latest attempts to define a standard protocol for BMP testing with some basic guidelines for a common protocol is given by Holliger et al. (2016). They provided designated parameters and operational standards for the BMP. Of the many factors that can significantly influence the performance of BMP tests, ISR is considered as one of the most critical (Raposo et al., 2011; Ohemeng-ntiamoah & Datta, 2019). According to Holliger et al. (2016) ISR should be between 2 and 4 based on VS to minimise acidification and inhibition problems.

2.3.3. Biogas generation

Due to finiteness of fossil fuels such as oil, coal and natural gas and the environmental impact of producing and using them, there is a growing need to develop alternative fuels that are renewable and sustainable (Patil et al., 2012; Sahota et al., 2018). Among the many possible alternatives, biogas is one of the most promising forms of bioenergy for reducing our dependence on fossil fuels (Deng et al., 2017).

Biogas is a green and sustainable gaseous fuel produced through the anaerobic degradation of organic biomass such as animal manure, domestic waste, food industry waste, wastewater or sludge and agricultural residues or energy crops (Mutungwazi et al., 2018). It can be used for heat and for electricity, as a vehicle fuel, as well as a substitute for natural gas in a gas grid (Hagman et al., 2018). In addition, the digestate obtained at the end of the process may be used as a bio-fertilizer, allowing for nutrient recovery and subsequently, a potential increase in feedstock production in either agricultural or forest activities (Langeveld et al., 2010). Hence, producing biogas not only reduces the use of fossil fuels, but also contributes to waste reduction and environmental impacts such as global warming and pollution (Ohimain & Izah, 2017). Depending on the substrate and the operational conditions of the digester used, biogas is mainly comprised of CH₄, CO₂ and small traces of H₂S, Nitrogen (N₂), H₂ and Oxygen (O₂). The typical composition of biogas is listed in Table 2.6.

In South Africa, the first biogas digester was installed by John Firn who used pig manure as a substrate in 1957 (Mutungwazi et al., 2018). Today, there are around 700 digesters all over the country in which 40% treat wastewater and the rest for other purposes (SAIREC 2015).

Table 2.6: Typical biogas composition (%)

CH ₄	CO ₂	H ₂ S	N ₂	H ₂	O ₂	Substrate	References
55-75	30-45	1-2	0-1	0-1	-	Municipal solid waste	Igoni et al. (2008)
50-70	30-40	-	1-2	5-10	-	Food waste	Ohimain & Izah (2017)
66	34	<1	-	-	-	semi- solid organic waste	Lastella et al. (2002)
50-75	25-45	-	<2	-	<2	Municipal solid waste	World Bioenergy Association (2013)
50-75	25-50	0-3	0-10	0-1	0-0.5	Cattle waste	Bhardwaj & Payal (2017)
80-96	2-3	-	-	-	0.2-0.5	Municipal sludge	Sarker et al. (2018)
40-65	35-55	0.1-3	-	-	-	Energy crops	Sahota et al. (2018)
50-60	35-40	2	0-2	2-7	-	Slaughterhouse waste	Sawyer et al. (2019)

2.3.4. Factors affecting growth and function of methanogens and sulfate reducing bacteria

The activity of methanogens and SRB is influenced by different factors such as pH, temperature and mixing. These factors are discussed in the Sections 2.3.4.1 to 2.3.4.3.

2.3.4.1. pH

pH is a crucial factor that influences enzymatic activity as each enzyme shows maximum activity at an optimum pH or within a specific and narrow pH range (Lay et al., 1997). In anaerobic reactors, pH is extremely important for the activity of methanogenic archaea. According to Bitton (1994), van Haandel and Lettinga (1994), Lay et al. (1997) and Carotenuto et al. (2016), most methanogens are active in a pH range of 6.7-7.4 with optimum values of 7.0-7.2. They are inhibited at pH lower than 6.3 and higher than 7.8 due to the production of fatty acids (de Lemos Chernicharo, 2007) and increase of NH₃ concentration (Jha & Schmidt, 2017) respectively, leading to a significant decrease in CH₄ production (de Lemos Chernicharo, 2007).

Sivakumar et al. (2012) studied the effect of pH on cumulative biogas production in a reactor treating spoiled milk from milk processing industry at $32 \pm 3^\circ\text{C}$. They varied the pH from 5 to 8 and obtained maximum biogas production at pH ranging between 6.5 and 7.5 with an optimum at pH 7. Similar results were reported by Paramaguru et al. (2017) who investigated the effect of three different pH (6, 7 and 8) on biogas production through the AD of food waste at 50°C and 30 days HRT. They achieved high cumulative biogas of 3617 mL production at pH 7.

According to Pokorna & Zabranska (2015), SRB activity may be inhibited by sulfide generated during AD, if they occur in undissociated form, which is pH dependent (Figure 2.11). At the neutral pH required for anaerobic treatment, only the first dissociation of H_2S is important (Isa et al., 1986a; Koschorreck, 2008). The undissociated form of dissolved H_2S is toxic because it can diffuse through a cell membrane and inhibit cell activity inside. Around 50% of the sulfide is present in H_2S form at pH 7 (de Lemos Chernicharo, 2007).

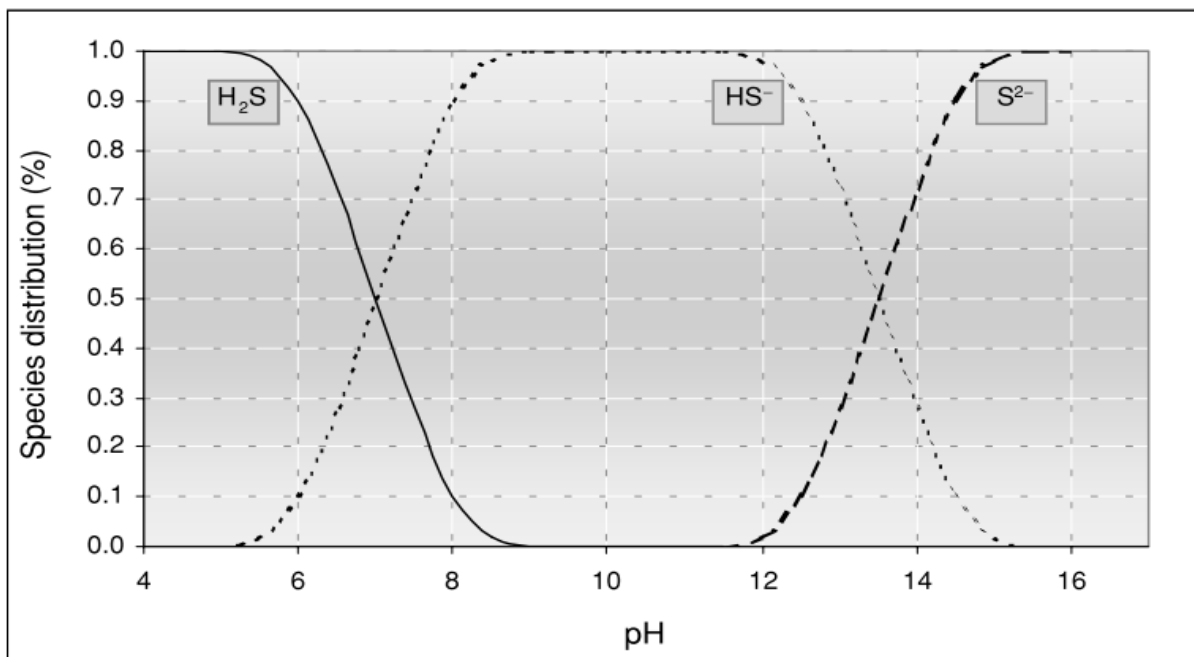


Figure 2.11: Distribution diagram of H_2S at 25°C (de Lemos Chernicharo, 2007)

2.3.4.2. Temperature

Temperature is one of the most important factors that affect microbial growth in biological processes. Three temperature ranges can be associated with microbial growth in most of the biological processes: the psychrophilic range (between 0 and approximately 15°C), the mesophilic range ($20\text{--}40^\circ\text{C}$) and the thermophilic range (between 45 and 70°C , and above) (de Lemos Chernicharo, 2007). In each of these ranges, three temperature values are usually used to characterise the growth of the microorganism species 1) minimum temperature, below

which growth is not possible; 2) optimum temperature, in which growth is maximum and 3) maximum temperature, above which growth is also not possible.

Methanogens are active within two temperature ranges: (i) the mesophilic range (20-40°C) (de Lemos Chernicharo, 2007) with most of the anaerobic reactors showing good performance between 35-37°C (Acharya et al., 2008; Méndez-Acosta et al., 2010) and (ii) the thermophilic range (50-60°C) (Kim et al., 2002). However, the thermophilic range is associated with some drawbacks such as poor supernatant quality and poor process stability due to high concentrations of propionate, making its use limited.

2.3.4.3. Mixing

The main purpose of mixing is to provide a homogeneous mixture, enhance contact between the microbial communities and the substrate (Mcmahon et al., 2001; Zhang et al., 2016; Kariyama et al., 2018) and ensure pH and temperature uniformity (Hoffmann et al., 2008), leading to high biogas production and better organic matter removal (Ghanimeh et al., 2018). However, a high mixing rate is reported to have a negative effect on syntrophic interactions between acetogens and methanogens (Kariyama et al., 2018). Methanogens are considered to be more sensitive to high mixing rates than the other bacteria involved in the anaerobic chain (Wang et al., 2015; Jha & Schmidt, 2017). Many researchers (e.g. McMahan et al., 2001; Karakashev et al., 2005; Hoffmann et al., 2008; Ziganshin et al., 2013) have observed an increase of *Methanosarcina* spp. and *Methanobacteria* at high mixing intensities due to high acetate and other volatile fatty acid (VFA) concentrations and, an increase in abundance of *Methanosaeta concilii* at low mixing intensities.

Hoffmann et al. (2008) examined the effect of four different mixing intensities (1500, 500, 250 and 50 rpm) on the performance, methanogenic community, and co-occurrence of syntrophic microbes in the treatment of cow manure at 34 ± 1 °C. No effect on the biogas production rates and yields was observed at steady state, but rather on the digester performance at 1500 rpm, leading to lower biogas production rates and high VFA concentration.

2.4. Species identification

As previously mentioned, knowledge of complex microbial communities is important for understanding and improving the performance of anaerobic reactors. According to Forster et al. (2003) and Khan et al. (2013), monitoring of the microbial communities in suspended growth secondary wastewater treatment systems can be instrumental in understanding and controlling bulking and foaming which are caused chiefly by filamentous bacterial communities.

Several molecular biological techniques, including polymerase chain reaction (PCR), denaturing gradient gel electrophoresis (DGGE), fluorescence *in situ* hybridisation (FISH) and restriction fragment length polymorphism (RFLP) have been used to study the abundance and diversity of methanogens and SRB in various environments such as anaerobic reactors (Montero et al., 2009; Shin et al., 2010), Nelson et al., 2011; Supaphol et al., 2011; Alvarado et al., 2014). Each of these techniques has some advantages and disadvantages and the choice of a given technique depends on the required resolution, flexibility, workload and cost (D'haene et al., 2010). PCR is the most useful tool for rapid detection of microbial communities.

Bailón-Salas et al. (2017) defined PCR as a molecular technique that simulates the process of deoxyribonucleic acid (DNA) replication *in vitro*, and involves the amplification of target DNA, generating millions of copies in the presence of synthetic oligonucleotide primers and a thermostable DNA polymerase (Farber 1996; Wang et al. 2000; Adzitey et al., 2013). It amplifies enough specific copies to be able to carry out other downstream molecular biology applications. This technique is highly sensitive, which makes it suitable for the detection of a range of microorganisms from a single water or wastewater sample. A further development of PCR has meant that not only can specific genes be detected, but they can be quantified as well. This technique is called quantitative PCR (qPCR) and is discussed in Section 2.4.2. However, qPCR is just a quantitative approach. To reveal the microbial structure of complex communities in wastewater treatment systems, next-generation sequencing (NGS) methods can be used as a cost-effective approach (Caporaso et al., 2012; Świątczak et al., 2017).

2.4.1. Next generation sequencing

The emergence of NGS has generated a huge number of sequences available at low cost to explore microbial structure with higher resolution (Liu et al. 2012). In contrast with the previous sequencing techniques, NGS technology, also known as massively parallel sequencing, is highly scalable, allowing sequencing of the entire metagenome of interest at once in an automated process. It gives a cross-section of the entire microbiota, including microorganisms minimally represented in the sample (Karamperis et al., 2020). During the course of 2000, numerous NGS systems were released.

In recent years, the sequencing industry has been dominated by Illumina, who adopts a sequencing by synthesis (SBS) technology, using fluorescently labelled reversible-terminator nucleotides, on clonally amplified DNA templates immobilized to an acrylamide coating on the surface of a glass flow cell (Quail et al., 2012). The Illumina Genome Analyzer and the HiSeq 2000 have set the standard for high throughput massively parallel sequencing, but in 2011 a lower throughput fast turnover called Illumina MiSeq was launched by Illumina. It is small in

size and targets smaller laboratories and clinical applications. The MiSeq integrates the cluster generation functions, SBS and data analysis in a single instrument and can go from sample to analysed data within a single day (as few as 8 hrs), making it suitable for this study.

Currently, Illumina MiSeq sequencing techniques have been widely applied to study the phylogenetic composition of bacterial communities in engineered ecosystems (Zhang et al., 2019), such as WWTPs. However, there is currently no NGS data available on the microorganisms involved in the treatment of ostrich tannery wastewater.

2.4.2. Quantitative real-time polymerase chain reaction

In recent years, qRT-PCR has become the dominant technique for quantification of methanogenic genes (McCartney et al., 2013). The advantages of this technique are the relatively low consumable and instrumentation costs, fast turnaround and assay development time, high sensitivity and open format (Morris et al., 2013). It is an advanced form of PCR that allows one to determine the starting template copy number with accuracy and high sensitivity over a wide range (Bio-Rad, 2006). qRT-PCR works in the same manner as the conventional PCR, i.e. DNA is initially denatured, followed by annealing of oligonucleotide primers targeting specific sequences, followed by extension of a complementary strand from each annealed primer by a DNA polymerase, resulting in an exponential increase in amplicon numbers (Smith & Osborn, 2009). However, the amplification process is monitored in real-time and the results are presented with a graphical representation of accumulation of amplified product against the number of PCR cycles (see Figure 2.12) (Maddocks & Jenkins, 2016), unlike in the conventional PCR where the amplicons are harvested for further studies at the end of the fixed number of cycles (Marilynn et al., 2010).

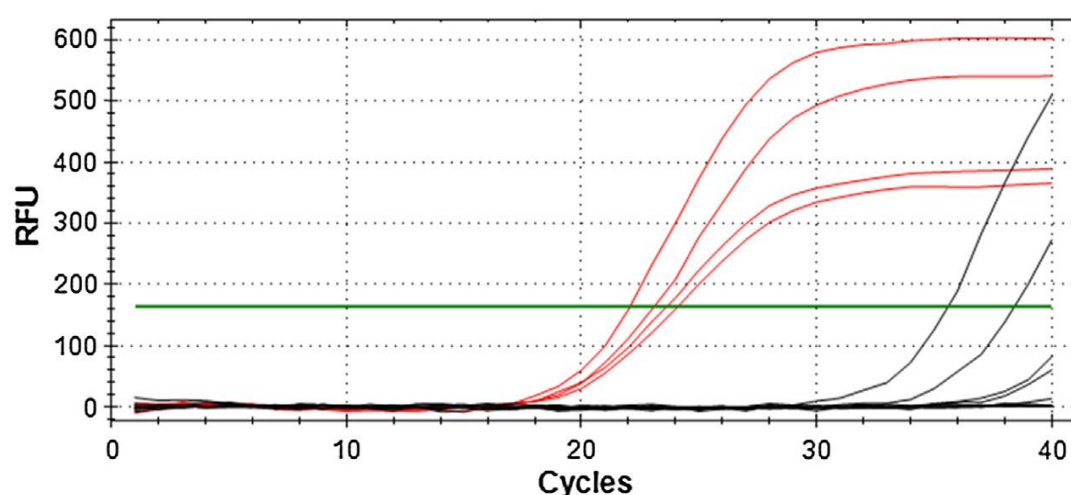


Figure 2.12: Accumulation of PCR product over time (Maddocks & Jenkins, 2016). RFU= relative florescent units. Green colour= SYBR, grey colour and red colour= amplified products

This accumulation of amplicons is recorded via detection of a fluorescent reporter (Smith & Osborn, 2009). According to Bailón-Salas et al. (2017), two types of fluorescents are mostly used. These are SYBR green and TaqMan. SYBR green binds to all double-stranded DNA (dsDNA) by intercalating adjacent base pairs (Figure 2.13) and emits a fluorescent signal that increases as amplicon numbers accumulate after each PCR cycle. To ensure reaction specificity, a melt curve analysis is generated by increasing the temperature in small increments and monitoring the fluorescent signal at each step (Bio-Rad, 2006). The dsDNA denatures or melts into a single-stranded DNA (ssDNA) as fluorescence decreases (Life Technologies, 2012). An optimised qRT-PCR should have a single peak (Bio-Rad, 2006) i.e. the fluorescence signal is generated only from target templates and not from the formation of nonspecific PCR products (Smith & Osborn, 2009).

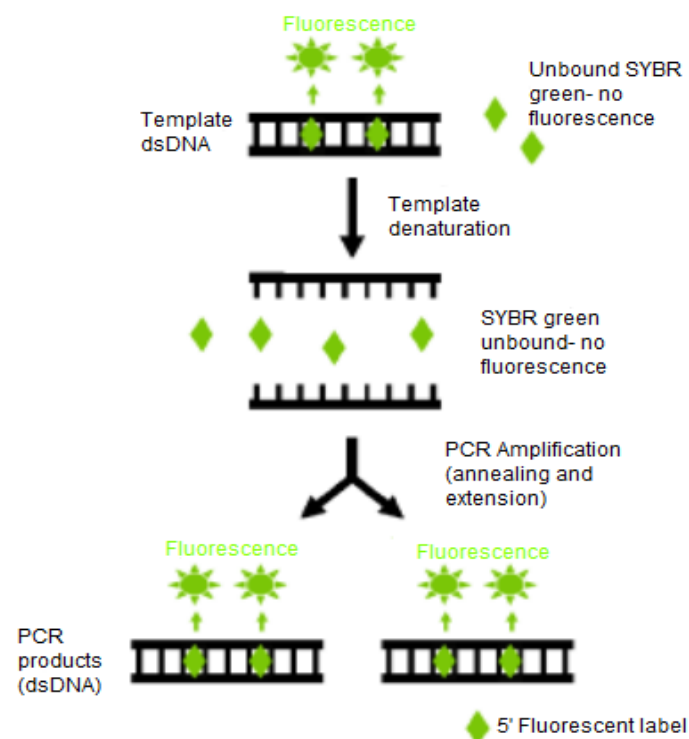


Figure 2.13: SYBR green detection in qRT-PCR (Smith & Osborn, 2009)

Two qRT-PCR methods can be performed: (i) absolute quantification that transmits the PCR signal to input copy number using a standard curve and (ii) relative quantification that measures the relative amount of a target nucleic acid (Pfaffl, 2004), which is used in gene expression studies. The former is frequently used in environmental microbiology (Brankatschk et al., 2012). A template such as recombinant plasmid DNA with a known concentration is used to construct a standard curve by making serial dilutions (see Pfaffl, 2004). This standard curve is then used to determine the copy number in samples (Bio-Rad, 2006).

2.5. Design of experiment

When comparing different factors on process efficiencies, conventional experimental protocols have high material costs and are time consuming because a large number of replicates are required in order for the results to be statistically valid (Pavani et al., 2016). To overcome this, widely accepted approach is the use of response surface method (RSM) which aims to (i) develop a regression model that is closest to the actual regression model, (ii) minimise the number of experiments and (iii) investigate the effects of process variables and their interactions (Qui et al., 2014). Pavani et al. (2016) defines RSM as a collection of statistical and mathematical techniques useful for modelling and analysing the problems in which a target response is influenced by several variables and the objective is to optimize this response. There are two major classes of RSM i.e. central composite design (CCD) and Box–Behnken design (BBD). Central composite design is a very efficient approach for fitting experimental data in the second order model. In this method variables are coded at three equally spaced levels -1, 0, +1 for low, medium and high values respectively (Dhawane et al., 2015).

A second order polynomial regression model equation is developed to fit experimental data and expressed by the Equation below

$$Y = b_o + \sum_{i=1}^k b_i X_i + \sum_{i=1}^k b_{ii} X_i^2 + \sum_{i=1}^{k-1} \sum_{j=2}^k b_{ij} X_i X_j$$

Where, Y is the response variable (dependent variable), b_o is the constant term, b_i is the coefficient that determines the influence of variable i in the response, b_{ii} is the parameter that determines the quadratic effect, and b_{ij} is the coefficient that determines the effect of interaction between the variables i and j. X_i and X_j are the independent factors.

The analysis of variance (ANOVA) is used to evaluate the statistical significance of the model. The quality and model terms are evaluated using F-test and probability values (p-values). According to Qiu et al. (2014) a p-value lower than 0.05 indicates that the model is statistically significant at 95% level of confidence. Two-dimensional (2D) contour and three-dimensional (3D) surface are constructed to study the interactive effect of variables on response. A multiple response method called desirability is used thereafter. For Morero et al. (2016), this method aims to optimise a combination of the factors that simultaneously satisfy the requirements placed on each of the responses and factors. The method makes use of an objective function (desirability function) which ranges for each response from 0 (least desirable) to 1 (most desirable). Each response can be assigned an importance relative to the other responses.

Importance varies from the least important (+) a value of 1, to the most important (+++++) a value of 5. If varying degrees of importance are assigned to the different responses

2.6. Overview and conclusion

This chapter provided an introduction to tannery wastewater and the various treatment options, with a focus on AD. The basic principles of AD and its application on wastewater were presented. However, no previous work has been done to understand the microorganisms involved in the AD process when treating ostrich tannery effluent. Therefore, with the aid of CCD, experiments were conducted, and culture independent microbial techniques were used to quantify copy numbers of *mcrA* and *dsrB* genes and correlate these respectively with the efficiency of methane generation and sulfate/sulfide concentrations in anaerobic digesters treating ostrich tannery wastewater. In addition, microbial community structure dynamics under different physiological conditions were analysed.

CHAPTER 3. MATERIALS AND METHODS

3.1. Introduction

This chapter provides a comprehensive description of experimental set-up and procedures and materials used to meet the study objectives (refer to Section 1.4). The experimental procedure is divided into 3 sections. These include the BMP tests, up-scaling using 20 L ASBRs, and the microbial community structure and dynamics inside both the BMPs and the 20 L reactors.

3.2. Substrate and inoculum

Tannery wastewater was obtained with permission from an ostrich tannery in South Africa. The wastewater was taken in six batches after the primary physicochemical treatment from April to August 2018. The tannery and ostrich slaughterhouse are on the same site, and the general wastewater also contains effluent from the slaughterhouse. The wastewater batches were taken from the balancing tank, and consisted of tanyard liquor after chrome removal, beamhouse liquor after S^{2-} oxidation, and general wastewater (Figure 3.1), and stored at -15°C until utilisation. All the batches were blended at equal volumes to keep the influent consistent and allow comparison between experimental runs (total 300 L). This blended effluent served as the substrate in this study.

An active inoculum was collected from a mesophilic anaerobic reactor that treated tannery sludge. It was randomly acclimatized with tannery wastewater and incubated at 37°C until utilisation.

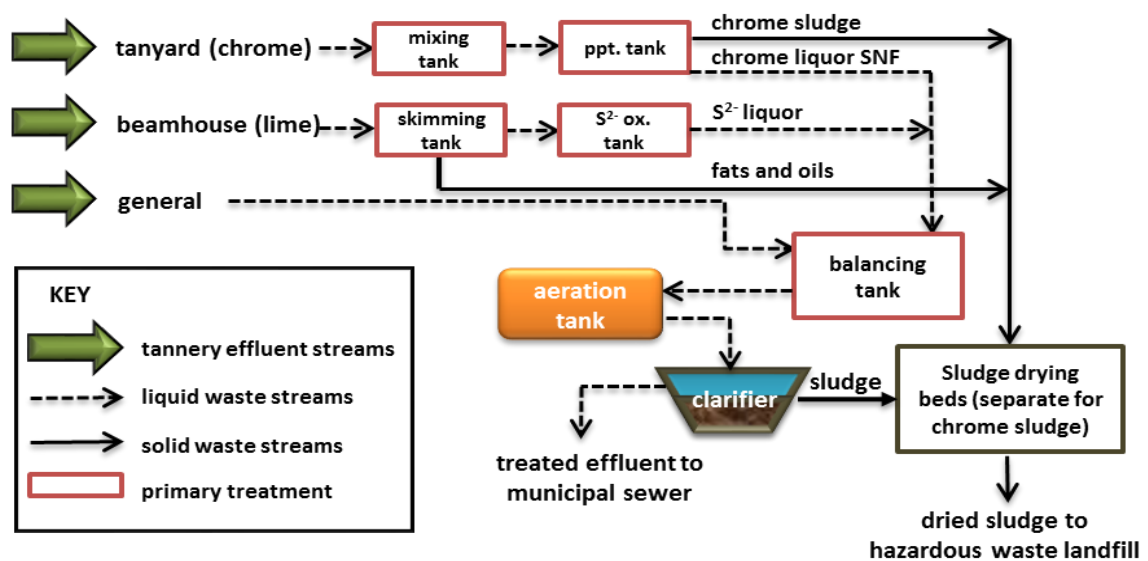


Figure 3.1: Schematic diagram of wastewater treatment of ostrich tannery effluent at the study site (Swartz et al., 2017)

3.3. Experimental set-up and operation

3.3.1. Biochemical methane potential test

Biochemical methane potential tests were conducted in 2 L screw-capped glass bottles (Schott Duran, Germany) that represented the bioreactors according to the method described by Holliger et al. (2016). Each bottle was equipped with a modified lid fitted with an O-ring containing stainless steel inserts with gas-tight ports and tubing to allow sampling and biogas collection as shown in Figure 3.2.



Figure 3.2: Biochemical methane potential test set-up

In this study, a two-factor three level CCD was used to statistically analyse the effect of operating parameters and their interactions on the BMP performance using Stat-Ease Design Expert version 11 (Stat-Ease, Inc., Minneapolis, USA). The studied parameters were (i) SO_4^{2-} concentration and (ii) ISR because the SO_4^{2-} concentration (665 mg/L) of the chosen tannery was lower than expected for tannery effluents (Swartz et al., 2017) and ISR is considered as one of the most critical factors that significantly influence the performance of BMP tests (Ohemeng-ntiamoah & Datta, 2019). The factors required being run at only three levels i.e. low, medium and high that were represented by codes -1, 0 and +1 respectively as shown in Table 3.1.

Table 3.1: Factors on central composite design

Factor	Name	Units	Level used		
			Low	Medium	High
A	Sulfate concentration	mg/L	665 (-1)	1335 (0)	2000 (+1)
B	ISR	-	2 (-1)	3 (0)	5 (+1)

ISR= inoculum to substrate ratio

After selection of process operating variables and their ranges, experiments were established based on a CCD which consisted of 13 experiments with five centre points. Design Expert® Software designed the experiment in a random pattern. Table 3.2 shows the experimental setup of CCD matrix of each factor and their actual values. In summary, 13 reactors were set up at different ISR of 2, 2.5, 3, 4 and 5 and sulfate (SO_4^{2-}) concentrations ranging from 665-2000 mg/L (mid-upper range expected in tannery effluent). Two control reactors were also set up, one with inoculum only and the other with substrate only.

To calculate the ISR, the amount of VS in the final inoculum and the substrate were determined as described in Section 3.4 and the final volume was made up to 2.3 L with distilled water as described by (Holliger et al., 2016). The concentration of SO_4^{2-} was increased by adding magnesium sulfate ($MgSO_4$) and potassium sulfate (K_2SO_4) salts (Appendix A).

Table 3.2: Central composite design experimental matrix

		Factor 1	Factor 2
Std	Run	A: Sulfate concentration (mg/L)	B: ISR
3	1	1960	2.5
13	2	1335	2.0
8	3	710	2.5
5	4	1335	3.0
4	5	710	4.0
1	6	1335	5.0
7	7	1960	4.0
6	8	1335	3.0
2	9	1335	3.0
11	10	1335	3.0
9	11	1335	3.0
12	12	2000	3.0
10	13	665	3.0

ISR= inoculum to substrate ratio, Std= Standard

After the reactors were filled with a constant amount of inoculum (176 mL) and appropriate amounts of SO_4^{2-} , substrate and distilled water (dH_2O) as shown in Table 3.3, the pH was measured and when necessary adjusted to 7.0 with 1 M of NaOH or 32% of HCl solution. The bioreactors were bubbled with N_2 gas to expel the oxygen, immediately sealed and incubated at 37°C until end of biogas production.

The bottles were shaken manually by gentle swirling twice a day to homogenise the contents, free trapped gas, and to assist in preventing accumulation of intermediates such as fatty acids.

Table 3.3: Inoculum to substrate ratios and sulfate concentrations used in the biochemical methane potential tests

	ISR	Inoculum		Substrate		dH ₂ O		Final	
		Vol. (L)	VS (mg/L)	Vol. (L)	VS (mg/L)	Vol. (L)	Vol. (L)	VS (mg/L)	[SO ₄ ²⁻] _t
RI	-	0,176	50.3	0	0	2.12	2.30	3.85	574
RS	-	0	50.3	2.3	2.08	0	2.30	2.08	680
R1	2.5	0.176	50.3	1.70	2.08	0.424	2.30	5.39	1960
R2	2	0.176	50.3	2.12	2.08	0.004	2.30	5.77	1335
R3	2.5	0.176	50.3	1.70	2.08	0.424	2.30	5.39	710
R4	3	0.176	50.3	1.42	2.08	0.704	2.30	5.14	1335
R5	4	0.176	50.3	1.04	2.08	1 084	2.30	4.79	710
R6	5	0.176	50.3	0.85	2.08	1 274	2.30	4.62	1335
R7	4	0.176	50.3	1.04	2.08	1 084	2.30	4.79	1960
R8	3	0.176	50.3	1.42	2.08	0.704	2.30	5.14	1335
R9	3	0.176	50.3	1.42	2.08	0.704	2.30	5.14	1335
R10	3	0.176	50.3	1.42	2.08	0.704	2.30	5.14	1335
R11	3	0.176	50.3	1.42	2.08	0.704	2.30	5.14	1335
R12	3	0.176	50.3	1.42	2.08	0.704	2.30	5.14	2000
R13	3	0.176	50.3	1.42	2.08	0.704	2.30	5.14	665

RI = inoculum only RS = substrate only ISR = inoculum to substrate ratio VS = volatile solids

3.3.2. Anaerobic sequencing batch reactor

Two polyethylene ASBRs were used in this study with experimental set-up as illustrated in Figure 3.3. The bioreactors had a total working volume of 20 L each with an inner diameter of 173 mm and a height of 554 mm. They were equipped with the Hei-torque Value 100 overhead stirrer (Heidolph Instruments GmbH & Co. KG, Schwabach, Germany) connected to a shaft and an impeller.

The lid of the bioreactors consisted of an O-ring and ports i.e. a port connected to a 2 L gas sampling bag for gas collection, a port for the pH and redox probe and inlet and outlet ports for the heat exchangers that were connected to a custom-made water bath.



Figure 3.3: Experimental set-up

InPro 325Xi pH and redox probes (Mettler Toledo, Columbus, USA) connected to a Mettler Toledo M200 transmitter were used. The transmitter acted as a local interface for the display of process values, as well as an integrator to a Mettler Toledo programmable logic controller (PLC). The PLC was used to monitor and log 7 parameters (pH, redox, temperature from each bioreactor and in the water bath) that were displayed on a human machine interface (HMI) (Figure 3.4).

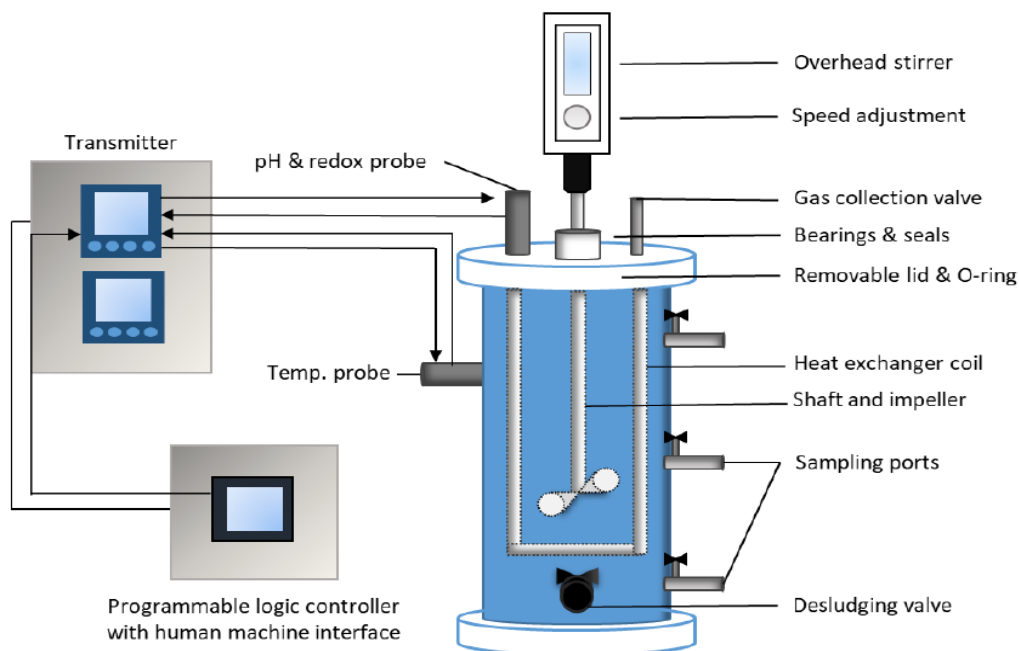


Figure 3.4: Schematic diagram of the 20 L bioreactors with the transmitter and the programmable logic controller

The required temperature was set on the HMI, regulated automatically in each bioreactor and measured using Mettler Toledo PT100 temperature sensors. The temperature of the water in the water bath was regulated using a proportional-integral-derivative (PID) controller that switched an element on and off when the temperature deviated within 0.1°C of the set point.

Booster pumps in the water bath were used to separately pump heated water via hosing from the water bath to each reactor when the temperature dropped within 0.1°C of the set point and, stop pumping when the water temperature increased by the same margin. Within each reactor, latent heat in the water from the water bath was transferred by thermal conduction and convection to the bulk liquid through heat exchange coils (Figure 3.5).

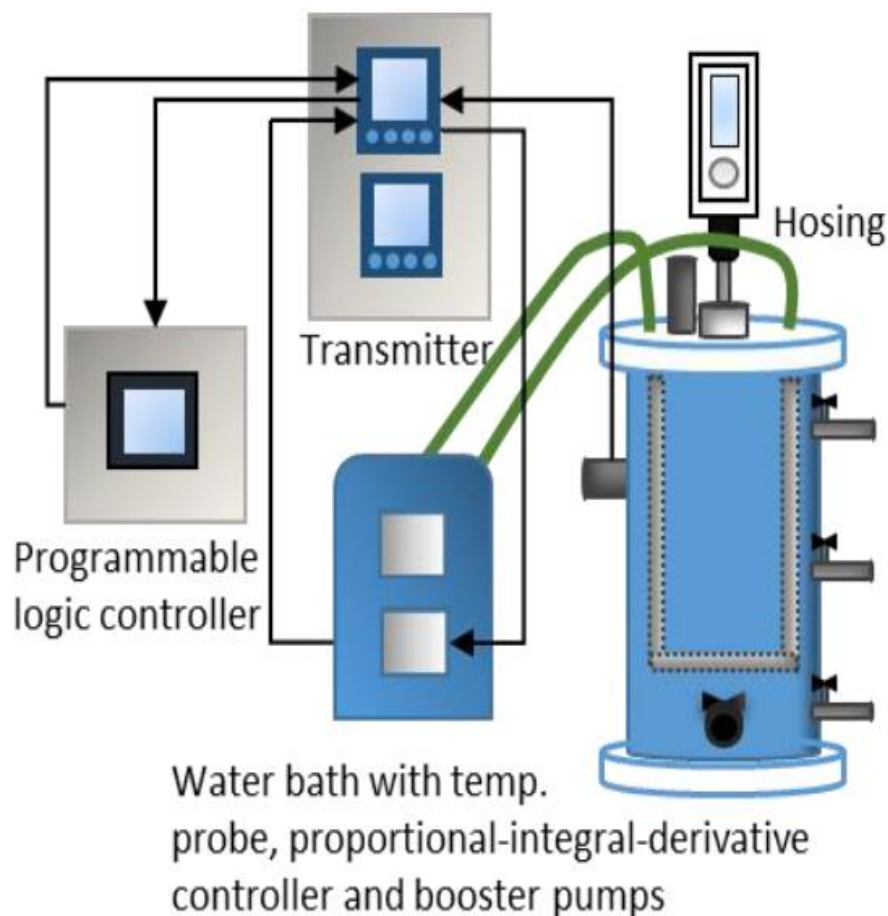


Figure 3.5: Schematic diagram of the 20 L reactors connected to control system

The ASBRs operated at different reaction time and settling time to optimise the five steps of the ASBR process (filling, reacting, settling, decanting and idling). Each of the reactors were initially operated at a reaction time of 20 days (4 weeks) and settling time of 5 days. This was then reduced to 21 days digestion time and 3 days settling time. They also operated at different mixing mode i.e. reactor 1 (ASBR1) operated at intermittent mixing (300 rpm for 5 to 10 min/day) while reactor 2 (ASBR2) operated at continuous mixing at 300 rpm.

3.3.2.1. Sampling

Samples of mixed liquor were taken from each of the BMP tests [at baseline (0 days), after 5 days, after 20 days and at the end of the tests] and the ASBRs (on weekly basis) via syringe tubes. The amounts taken are tabulated below (Table 3.4).

Table 3.4: Volume of samples extracted from the biochemical methane potential tests and the anaerobic sequencing batch reactor

Immediate analyses		Later analyses +/-or Storage
BMP	2× 15 mL + 2× 50 mL	3× 50 mL (baseline) + 5× 50 mL (final)
ASBR	1× 50 mL	5× 50 mL

BMP= biochemical methane potential ASBR= anaerobic sequencing batch reactor

3.4. Analytical methods

The six batches of tannery wastewater collected in Section 3.2 were first characterised individually before being blended. General physicochemical analyses were performed on the BMP tests and ASBRs collected samples. The various parameters measured are listed in Table 3.5. The pH of all the samples was measured using a pH 700 meter (Eutech, Singapore, Singapore).

The samples were analysed in duplicate for total COD (COD_t), soluble COD (COD_s), total organic carbon (TOC), BOD, total ammonium nitrogen (TAN) (NH_4-N), total volatile organic acids (VOA_t) as acetic acid equivalent (AAE), for total nitrogen (TN), chlorides (Cl^-), total phosphate (TP) as phosphorus ($PO_4^{2-}P$) and total alkalinity (alk) as calcium carbonate ($CaCO_3$). A Merck Spectroquant Pharo® 100 instrument (Darmstadt, Germany) together with Merck cell tests or kits were used for these analyses following the manufacturer's instructions. Refer to Table 3.6 for the methods and Appendix B for the test instructions. Oil and grease (OG) concentrations were determined for all the samples including the inoculum and the substrate by A.L. Abbot and Associates (PTY) Ltd (Cape Town, South Africa) using the SABS 1051 prescribed standard method.

The total solids (TS) and VS of the inoculum and substrate as well as of the collected samples were determined according to the APHA (2005) standard methods. The samples were first dried in the oven at 105°C overnight then calcined in the furnace at 550°C for 2 h.

Metal concentrations (Al, Cd, Cr, Co, Cu, Fe, Ni, Pb, and Zn) and other cations (Ca, Cl, K, Mg, and Na) were quantified by inductively coupled plasma (ICP) atomic emission spectroscopy

(AES) using a Thermo ICap 6200 ICP-AES instrument, while ultra-trace analyses were performed by ICP-mass spectrometry (MS) using an Agilent (Santa Clara, USA) 7900 ICP-MS instrument.

The characterisation of the six batches of tannery wastewater was performed on whole samples while all the BMP tests and ASBRs except pH, COD_s, BOD, TOC, OG, TS were performed on filtered samples (i.e. soluble fraction). The samples were filtered through 0.45 µm Millipore membrane filters membrane syringe filters (Darmstadt, Germany) and/ or diluted with dH₂O when necessary.

Table 3.5: Physicochemical parameters measured in this study

Parameters	6 TWW Batches	Blended	BMP tests				ASBR
			Days 0	5 days	20 days	Final	Weekly basis
pH	√	√	√	√	√	√	√
COD _t (mg/L)	√	√	√				√
Alk (mg/L)	√	√	√			√	√
COD _s (mg/L)			√	√	√	√	√
TOC (mg/L)	√	√	√	√	√	√	√
BOD (mg/L)	√	√					
VOA (mg/L)	√	√	√	√			√
P (mg/L)	√	√	√			√	√
TN (mg/L)						√	√
TAN (mg/L)							
Cl ⁻ (mg/L)	√		√			√	√
NO ₃ (mg/L)							
SO ₄ ²⁻ (mg/L)			√			√	√
S ²⁻ (mg/L)							√
FOG (mg/L)		√	√			√	√
Metals		√	√			√	√
Cations		√	√			√	√
TS (mg/L)		√	√			√	√
VS (mg/L)		√	√			√	√

TWW= tannery wastewater BMP= biochemical potential test ASBR= anaerobic digestion reactor

COD_s= soluble chemical oxygen demand Alk= alkalinity COD_t= total chemical oxygen demand TOC= total organic carbon BOD= biochemical oxygen demand VOA= volatile organic acid TN= total nitrogen TAN= total ammonium nitrogen FOG= fat oil and gas TS= total solid VS= volatile solid

Table 3.6: Analytical methods used in this study

Parameters	Methods	References
COD_s (mg/L)	Oxidation of water sample with hot sulfuric solution of potassium dichromate	Merck cell kit cat no: 14541
COD_t (mg/L)		Merck cell kits cat no: 14555
Alk (mgCaCO₃/L)	Reaction of the protonatable substances contained in water with resulting in a change of the pH and the colour of an indicator in direct proportion to the acid capacity	Merck cell kits cat no: 01758
TOC (mg/L)	Digestion of carbon-containing compounds with sulfuric acid and peroxodisulfate to form CO ₂	Merck cell kits cat no: 14879
VOA (mg/L)	Reaction of VOA with diole to form fatty acid esters, which are subsequently converted into hydroxamic acids and further into red complexes	Merck cell kits cat no: 01809
P (mg/L)	Reaction of orthophosphate ions with molybdate ions to form molybdophosphoric acid which is then reduced to phosphomolybdenum with Ascorbic acid	Merck cell kits cat no: 00673
TN (mg/L)	Transformation of organic and inorganic nitrogen compounds into nitrate with an oxidizing agent. This nitrate then reacts with 2,6 dimethylphenol to 4-nitro-2,6-dimethylphenol	Merck cell kits cat no: 14763
TAN (mg/L)	Reaction of NH ₃ with hypochlorite ions to form monochloramine, which in turn reacts with a substituted phenol to form a blue indophenol derivative	Merck cell kits cat no: 00683

COD_s= soluble chemical oxygen demand COD_t= total chemical oxygen demand Alk= alkalinity TOC= total organic carbon VOA= volatile organic acid TN= total nitrogen TAN= total ammonium nitrogen

3.5. Biogas analysis

The gas ports from the 2 L BMP bioreactors and 20 L bioreactors (Sections 3.3.1 & 3.3.2) were connected to individual gas sampling bags. Quantitative and qualitative analyses of the biogas were performed when sufficient biogas was produced (> ~200 ml). The volume of biogas was determined using a graduated gas-tight syringe. The CH₄, CO₂, and oxygen (O₂) content (%vol), as well as the H₂S content [parts per million (ppm)] of the gas were determined

using a Geotech biogas 5000 analyser (Warwickshire, England) (Figure 3.6) according to the manufacturers' instructions.



Figure 3.6: Biogas analyser

3.6. Analysis of methanogenic and sulfidogenic microbial communities

3.6.1. Sample collection

Samples were collected from each of the BMP reactors on day 0, within 1 week of starting to produce biogas (± 2 days), when gas production stopped (after 3 days) and at the end of the study (2 to 3 weeks). For the ASBRs, weekly samples were taken starting from day 0. This was done using the method described in Section 3.3.2.1.

3.6.2. DNA extraction

Genomic Deoxyribonucleic acid (DNA) was immediately extracted from all the samples using the DNeasy PowerSoil kit (Qiagen, Hilden, Germany) according to the manufacturer's protocol. A Genova Nano micro-volume spectrophotometer (Jenway, Staffordshire, UK) was used to quantify the concentration. The extracted DNA was frozen at $-20\text{ }^{\circ}\text{C}$ until analysed.

3.6.3. Next generation sequencing

To investigate the distribution of methanogens and SRB in the reactors, *mcrA* and *dsrB* were chosen as the genes of interest. As mentioned in Sections 2.3.1.4 and 2.3.1.5, both genes have previously been established as good phylogenetic markers for methanogenic archaea and SRB (Steinberg & Regan, 2008; Alvarado et al., 2014; Madden et al., 2014). Therefore, genomic DNA samples from selected BMP reactors (based on SO_4^{2-} concentration and ISR) were subjected to NGS, while for the ASBRs, NGS was performed on samples taken at the

beginning of the experiment and every 2 weeks thereafter. The samples were processed on Illumina MiSeq at Molecular Research DNA (MR DNA, Shallowater, TX, USA).

The *mcrA* and *dsrB* gene fragments in the genomic DNA were first amplified using the HotStarTaq Plus Master Mix Kit (Qiagen) according to the manufacturer's protocol. The primer pair designed by Luton et al. (2002) was used for the amplification of the *mcrA* gene while the *dsrB* gene was amplified using primers DSRp2060F (Wagner et al., 1998) and DSR4R (Geets et al., 2006) as described in Table 3.7. The PCR amplification conditions for both genes were as follows: initial denaturation at 95°C for 5 min, followed by 30 cycles of denaturation at 95°C for 30 sec, annealing at 53°C for 40 sec and extension at 72°C for 1 min.

After amplification, PCR products were analysed utilising a 2% agarose gel to determine the relative intensity of bands. Multiple samples were pooled together in equal proportions based on their molecular weight and DNA concentrations. These pooled samples were purified using calibrated Ampure XP beads (Beckman Coulter, Brea California, USA) then used to prepare Illumina DNA library on a MiSeq following the manufacturer's protocols. Sequence data were processed using MR DNA analysis pipeline. In summary, sequences were joined, sequences <150 bp removed and sequences with ambiguous base calls removed. Sequences were quality filtered using a maximum expected error threshold of 1.0 and dereplicated. The dereplicated or unique sequences were denoised; unique sequences identified with sequencing or PCR point errors were removed, followed by chimera removal, thereby providing a denoised sequence or OTU (operational taxonomic unit). Final OTUs were taxonomically classified using the basic logical alignment search tool (BLAST) against a curated database derived from the National Centre for Biotechnology Information (NCBI) database (www.ncbi.nlm.nih.gov).

Table 3.7: Primers sequences used for the amplification of the *mcrA* and *dsrB* genes

Primers	Sequence 5' → 3'	Product size (bp)	References
<i>mcrA</i> F	GGTGGTGTMGGATTCACACARTAYGCWACAGC	464-491	Luton et al., (2002)
<i>mcrA</i> R	TTCATTGCRTAGTTWGGRTAGT		
DSRp2060F	CAACATCGTYCAYACCCAGGG	350	Wagner et al., (1998)
DSR4R	GTGTAGCAGTTACCGCA		Geets et al., (2006)

F= forward R= reverse

degenerative bases (Y)= pYrimidine, (W)= Weak, (R)= purine, (M)= aMino

3.6.4. Quantitative real-time polymerase chain reaction

All the genomic DNA extracted in Section 3.6.2 were subjected to qRT-PCR for detection of the *mcrA* and *dsrB* genes. The order of the procedures used for the qRT-PCR and related procedures are shown schematically in Figure 3.7.

3.6.4.1. Optimisation of PCR Amplification of target genes

Optimisation of the conventional PCR for amplification of *mcrA* was performed to obtain a target gene to clone into a plasmid for use in the generation of the standard curve using different samples that had previously produced CH₄. Table 3.8 shows how the concentrations and volumes of PCR reagents were adjusted and the cycling programs changed from the method described by Yuan et al. (2018). No optimisation was needed for the method used to amplify the *dsrB* gene (Agrawal & Lal, 2009). PCR was performed using a Touchgene Gradient Thermal cycler (Techne Ltd., Cambridge, UK) or a T100 thermal cycler (Bio-Rad, Hercules, USA). The pairs of primers used were the same as the ones described in Table 3.7.

For the final procedure after optimisation, a fresh sample of the inoculum (Section 3.2) was collected, and genomic DNA extracted. The extracted genomic DNA was subjected to PCR to amplify the *mcrA* (464-491 bp) and *dsrB* (350 bp) genes using the same primers listed in Table 3.7. The optimised amplifications of both genes were carried out in a 50 µL reaction mixture which consisted of 5 µL of 10× DreamTaq buffer (Thermo Fisher Scientific, Waltham, USA), 5 µL (final concentration 0.2 mM) of dNTP mix (Thermo Fisher Scientific), 1 µL (2 µM final concentration) of each forward and reverse primer (IDT, Coralville, USA), 0.25 µL (5 U/µL) of DreamTaq polymerase (Thermo Fisher Scientific), 1 µL of the extracted DNA and water, nuclease free (Thermo Fisher Scientific) up to 50 µL. A negative control containing all the reagents but no DNA template, and a positive control containing DNA obtained from sugar molasses was included.

The final programme conditions were as follows: for the *mcrA* gene, the programme started with an initial denaturation at 95 °C for 3 min, followed by denaturation at 95 °C for 30 s, annealing at 55 °C for 30 s, extension at 72 °C for 1.5 min and final extension at 72 °C for 5 min. From denaturation to extension 40 cycles were repeated with the ramp in temperature for the first 5 cycles slowed to 0.1 °C/s to allow extension of mismatched primers as instructed by Luton et al. (2002). For the *dsrB* gene, the PCR programme was initial denaturation at 95 °C for 10 min, followed by 35 cycles of denaturation at 95 °C for 30 s, annealing at 55 °C for 40 s and extension at 72 °C for 1 min, followed by final extension at 72 °C for 10 min.

All the amplification products were separated by 1.5 % (w/v) agarose gel electrophoresis in 1× TAE buffer (Tris-acetate 40 mM and EDTA 1.0 mM) stained with Pronasafe (Conda,

Madrid, Spain) or ethidium bromide (Thermo Fischer Scientific). The GeneRuler 50 bp DNA ladder (Thermo Fisher Scientific) was used as a molecular size marker.

Table 3.8: Optimisation of conventional PCR for the *mcrA* gene

Samples	PCR optimisation	Program cycling
Sugar molasses & tannery sludge	The total volume of the reaction was 20 μ L. The concentrations of dNTP and primers were 0.2 mM and 3 μ M respectively and the volume of DNA was 5 μ L.	The cycling program used was as described by (Yuan et al., 2018)
Sugar molasses & Tannery sludge	The volume of DNA was decreased to 2 μ L.	Same as above
Sugar molasses & Tannery sludge	Same as above	The annealing temperature was increased from 50 to 55°C
Sugar molasses & Tannery sludge	Total volume of the reaction was increased to 25 μ L. The volume of DNA was increased to 2 and 4 μ L. The volumes of dNTP and DreamTaq buffer were increased to 2.5 μ L. The concentrations of primers 5 μ M.	The cycling program used was as described by (Rastogi et al., 2008)
Tannery sludge	DMSO was included in the reaction mixture	The cycling program used was as described by (Rastogi et al., 2008) annealing using a temperature gradient from 50 to 60°C
Tannery sludge	Fresh primers were used	As above
Tannery sludge	The total volume of the reaction was increased to 50 μ L.	The cycling program used was as described by (Luton et al., 2002) with a ramp rate of 0.1°C/s from the annealing to the extension temperature for the 5 first cycles

3.6.4.2. Standard plasmid construction

The amplicons were purified using the NucleoSpin kit (Machery-Nagel GmbH & Co., Düren, Germany) according to the manufacturer's instructions. The purified amplicons were ligated into the pGEM®-T and pGEM®-T Easy Vector (Promega, Madison, USA) according to the manufacturer's instructions and transformed into *Escherichia coli* JM109 high efficiency competent cells (Promega). After an overnight incubation at 37°C, white colonies were randomly selected from each Luria-Bertani (LB) agar plate and inoculated into 5 ml LB broth containing 5 µl of ampicillin (100 mg/ml). The cultures were incubated at 37°C in a shaking incubator operating at ≈ 160 rpm for 16 h. Plasmids were then isolated from the cultures using the High Pure plasmid isolation kit (Roche Diagnostics GmbH, Mannheim, Germany) following the manufacturer's protocol. Positive clones were verified by PCR amplification using the same primers and conditions as described in Section 3.6.4.1 and visualised on 1.5 % agarose gel stained with Pronasafe or ethidium bromide. The positive plasmids were sequenced at Inqaba Biotech (Pretoria, South Africa) using the primers described in Table 3.7. The sequences were aligned using DNA Baser Assembler software and compared to sequences available in GenBank.

A summary of section 3.6.2 to 3.6.4 is illustrated in Figure 3.7.

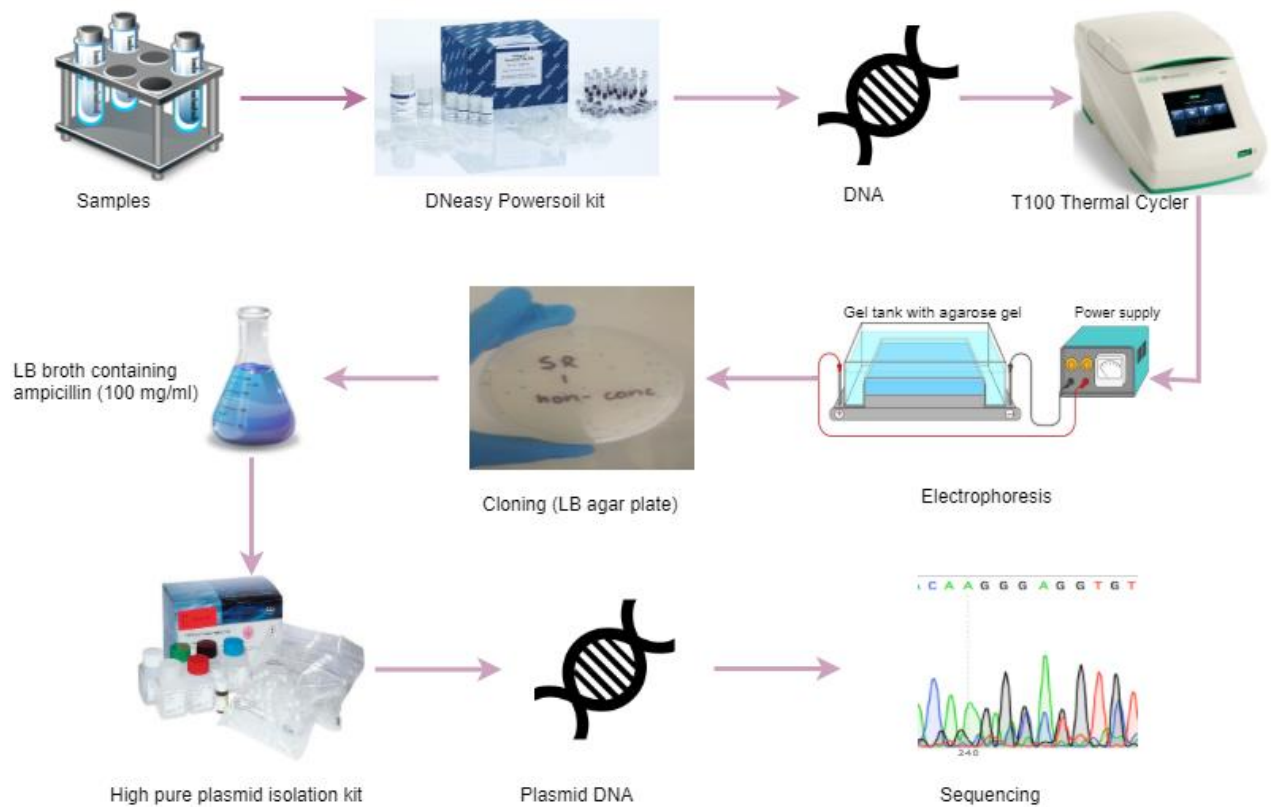


Figure 3.7: Schematic diagram of DNA extraction, quantitative PCR and cloning and isolating the amplicon standard

3.6.1. Standard curves

The concentration of purified plasmids was measured with a NanoDrop 2000 UV-VIS Spectrophotometer (Thermo Fisher Scientific). Standard curves were prepared by diluting each standard plasmid DNA (adjusted to 2.5 ng/ μ L) five times to obtain a 5-fold dilution series (from 2.5 to 8×10^{-4} ng/ μ L] for the *mcrA* and a 10-fold dilution series (from 2.5 to 25×10^{-6} ng/ μ L) for the *dsrB* as illustrated in Figure 3.8A and B respectively. The diluted plasmid DNA were then used to construct the standard curves used for the absolute quantification of the sample DNA and qPCR optimisation.

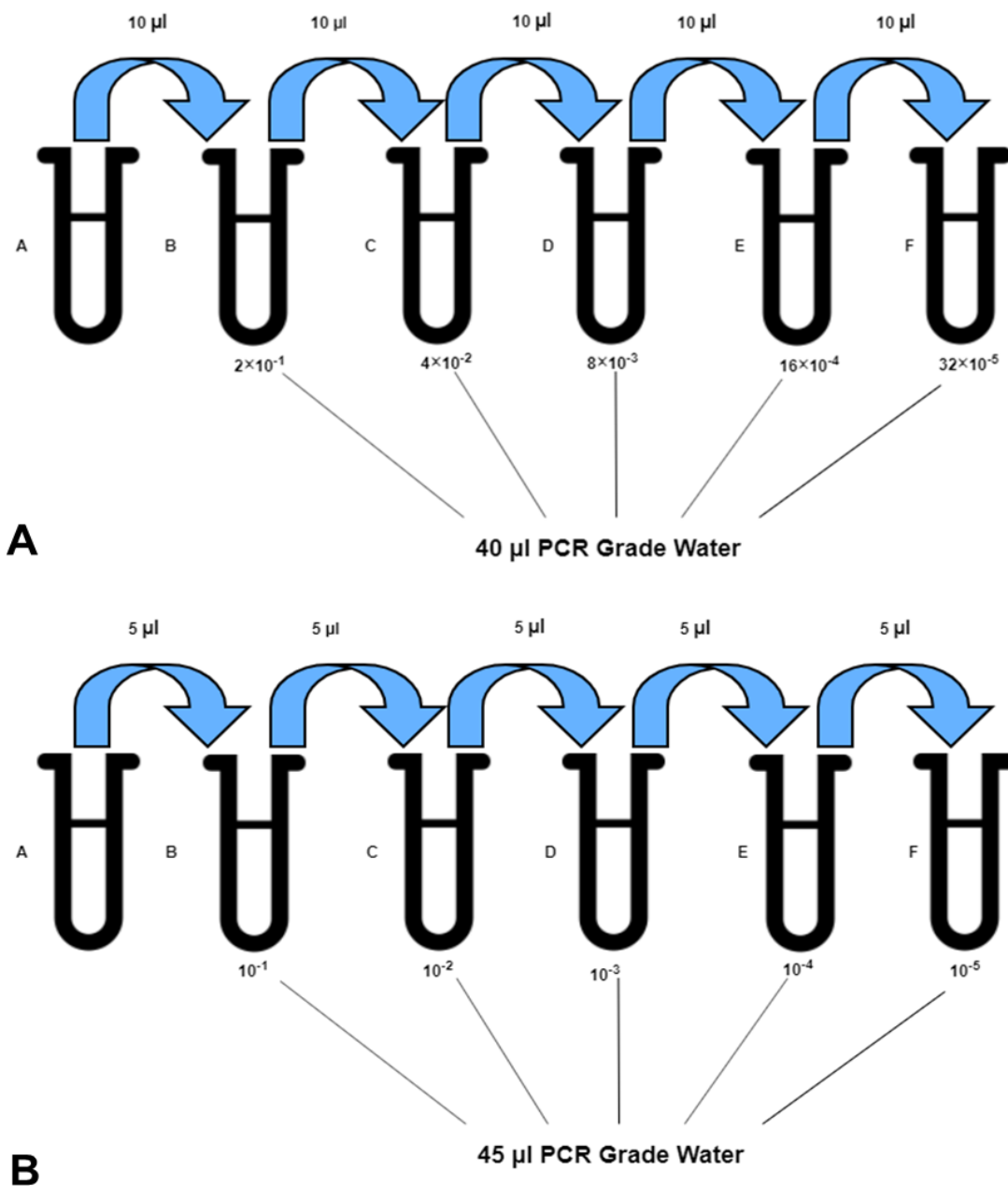


Figure 3.8: Serial dilution for standard curves from the original working solutions (A) *mcrA* gene (B) *dsrB* gene. PCR= polymerase chain reaction

3.6.2. Quantitative Real-Time PCR amplification of the target genes

Primer sequences used for the detection of the *mcrA* and *dsrB* genes were the same as listed in Table 3.7. Real-time PCR assays were carried out in a total volume of 20 μL consisting of 10 μL 2x SsoAdvanced universal SYBR Green Supermix (Bio-Rad), 3 μM of each primer and 5 μL template DNA (adjusted to 5 ng/ μL). All the PCR reactions of the samples were performed in triplicate on a CFX96 Real-Time PCR Detection System (Bio-Rad) with the following programme conditions: for the *mcrA* gene the programme started with an initial denaturation at 95 $^{\circ}\text{C}$ for 3 min, followed by denaturation at 95 $^{\circ}\text{C}$ for 30 s, annealing at 55 $^{\circ}\text{C}$ for 30 s, extension at 72 $^{\circ}\text{C}$ for 45 s. The thermocycling for the *dsrB* gene was as follows: initial denaturation 94 $^{\circ}\text{C}$ for 15 min followed by 40 cycles of denaturation at 94 $^{\circ}\text{C}$ for 30 s, annealing at 60 $^{\circ}\text{C}$ for 20 s and extension at 72 $^{\circ}\text{C}$ for 30 s (Agrawal & Lal, 2009).

To verify that the primer pairs generated the correct amplicon, the melt curve obtained from thermocycling was analysed (Morris et al., 2013). Melt curve analysis was performed from temperature 72-95 $^{\circ}\text{C}$ with a 1 $^{\circ}\text{C}$ hold for 5 s. All qRT-PCR analyses were performed in 6 runs. For every run, the standard curve (prepared in triplicate) and a no-template control were included.

Products from initial runs were also examined for specificity using 1.5% agarose gels, further cloned (Section 3.6.4.2) and sequenced at Inqaba Biotech using the relevant primer sets.

The total number of gene copies was calculated by converting the quantification cycle values to gene copy numbers using Equation 3.1 (Mahboudi et al., 2018).

$$\text{Copy numbers}/\mu\text{L} = \frac{\text{DNA concentration (ng}/\mu\text{L}) \times 6.022 \times 10^{23}}{\text{Size of DNA (bp)} \times 1 \times 10^9 \times 660} \quad \text{Equation 3.1}$$

Where 6.022×10^{23} represents Avogadro's number

660 is the average molecular weight of a dsDNA in g/mol

1×10^9 is used as conversion factor for converting ng

3.7. Statistical analysis

3.7.1. Biochemical methane potential test reactors and anaerobic sequencing batch reactors

The experimental data obtained were subjected to RSM using Design Expert® Software version 11. The aim was to determine the optimal conditions for CH_4 yield and biodegradability

of the substrate. In this study, CH₄, biogas, COD, TOC, SO₄²⁻ and VS were chosen as the response (output variables).

3.7.2. Next generation sequencing analysis

The data matrices were saved as Microsoft Excel files and analysed through the software Primer 7 (Primer-E Ltd, UK). The data was transformed (square-root) and a Bray-Curtis similarity matrix based on sample abundance of operational taxonomic units was used to (i) create non-metric multidimensional scaling (nMDS) plots, (ii) perform cluster analyses (group average linkages) and (iii) perform similarity percentage (SIMPER) analyses.

Statistical significance of biotic and abiotic data on sulfidogenic and methanogenic microbial community structure in BMP experiments was investigated through Primer 7. It should be reminded that to preserve reactor contents, samples were only taken for the full set of analyses (pH, COD, TOC, VOA, Alkalinity, VOA:Alk, NH₃, SO₄²⁻, N, COD:SO₄²⁻, C:N, FOG, TS, VS, and gene copy numbers) at the start of the experiments (initial) and at the end of the experiment (final). A truncated profile of parameters known to be most important for AD (pH, VOA, Alkalinity, VOA:Alk, NH₃, SO₄²⁻) as well as gene copy numbers, were also determined at the start of gas production.

In addition, analysis of similarity (ANOSIM, one-way, unordered, Spearman rank correlation) was performed on (i) the Bray-Curtis similarity matrices (NGS data), and (ii) Euclidean distance similarity matrices constructed from 4th root transformed and normalised data of the measured parameters. The factors that were investigated were: time (initial, start of gas production, final), initial SO₄²⁻ concentration, ISR, and a combined SO₄²⁻ concentration and ISR factor.

3.7.3. Quantitative real-time polymerase chain reaction analysis

Simple linear regression analysis was performed to describe the relationship of *mcrA* gene copy numbers with CH₄ yield as well as the relationship of *dsrB* gene copy numbers with SO₄²⁻ or S²⁻ concentrations. Values were plotted with a trend line for visual analysis. ANOVA was used to test the significance of regression coefficients at a 95% level of confidence.

3.8. Summary

Thirteen BMP tests were set-up based on CCD at different ISR (2 to 5) and SO₄²⁻ concentrations ranging from 665 to 2000 mg/L (mid to upper level expected for tannery effluents). Biogas production was measured throughout the study period, while physicochemical analyses were performed on samples taken at the start (baseline) and end

of the study. The BMP tests were followed by a series of scaled-up experiments, using two 20 L ASBRs at different mixing modes i.e. intermittent and continuous.

For microbial analyses, samples were collected from (i) the BMP reactors at baseline, when the reactors started to produce biogas, when biogas production stopped, and at the end of the study, and (ii) on a weekly basis from the ASBRs. Genomic DNA was extracted from those samples. The methanogenic and sulfate reducing microbial community structures were determined using NGS and, qRT-PCR was performed to determine copy numbers of the *mcrA* and *dsrB* genes. The results of the AD of the tannery effluent are discussed in Chapter 4 while the microbial results are discussed in Chapter 5.

CHAPTER 4. ANAEROBIC DIGESTION OF OSTRICH TANNERY WASTEWATER

4.1. Introduction

The findings presented in this Chapter provide fundamental information on the biodegradation of ostrich tannery wastewater using lab-scale digesters. The objectives were to determine the effects of ISR and SO_4^{2-} concentrations on the BMP of ostrich tannery wastewater, and to statistically analyse and validate the results (Section 4.3.6). Finally, the effect of mixing on AD was examined in scaled up experiments two 20 L ASBRs (Section 4.4).

4.2. Sample collection and characterisation

The physicochemical characteristics of the 6 batches of tannery wastewater collected in Section 3.2 are listed in Table 4.1 and these differed through all the batches. The pH value of all the batches fell within in the ideal range for AD of 6.3-7.8 (de Lemos Chernicharo, 2007). Most of the measured parameters were 2 to 4 times higher in batch 4 than the rest of the batches. This could be explained by seasonal sampling dates (June-winter). The COD varied from 4387 to 15690 mg/L, with the highest value being attributed to batch 4. Batch 1, 2, 3, 5 and 6 had $4.69 \leq TS \leq 8.38$ g/L and were considered as wet ($\leq 15\%$ TS) for AD whereas batch 4 had $TS = 19.4$ g/L and was considered as dry ($\geq 15\%$) for AD. According to Yan et al. (2015), dry substrates have higher BMP than wet substrates. Abbassi-Guendouz et al. (2012) showed that total CH_4 yield decreased with TS contents increasing from 10% to 25% in batch AD of cardboard under mesophilic conditions. Similarly, Forster-Carneiro et al. (2008) showed that biogas and CH_4 production decreased when the TS contents increased from 20 to 30% in dry batch AD of food waste.

Substrates with an optimal C/N ratio provide sufficient nutrients for microorganisms to maximise biogas production. In this study, the C/N ratio was 5.61; 14.38; 2.20 and 1.55 for batch 1, 2, 5 and 6 respectively, which were lower than the optimum range (20-35:1) (Jingura & Kamusoko, 2017). According to Siddique & Wahid (2018) lower C/N values lead to higher concentrations of NH_3 and methanogenic inhibition. When the C/N ratio is greater than the optimal value in the fermentation process, large amounts of VFAs are produced.

Table 4.1: Physicochemical characteristics of tannery wastewater batches collected in this study

Parameter	Batch 1	Batch 2	Batch 3	Batch 4	Batch 5	Batch 6	Mean	SD
TOC (mg/L)	2467	3380	4530	9080	485	820	3460	3148
COD (mg/L)	7945	8143	7903	15690	4387	7235	8551	3768
BOD (mg/L)	3532	1472	1542	1515	1531	1552	1857	821
VOA_t (mg/L AAE)	3070	2800	2440	2480	2120	1800	2452	456
TN (mg/L)	440	235	180	260	220	530	311	140
TAN (mg/L NH ₃ -N)	18.8	13.5	16.2	41.0	13.2	9.60	18.7	11.3
NO₃ (mg/L)	143.8	39.0	28.6	18.7	11.5	54.7	49.4	48.7
TP (mg/L PO ₄ ²⁻⁻ -P)	6.65	5.10	5.05	17.8	5.00	4.90	7.41	5.11
SO₄ (mg/L)	1114	626	352	424	173	1186	646	417
HS⁻ (mg/L)	ND	2.38	5.70	2.20	0.00	0.12	2.08	2.31
Cl (mg/L)	2038	1547	1294	1022	911	2369	1530	576
TS (g/L)	7.85	8.07	8.38	19.4	5.53	4.69	8.98	5.30
TVS (g/L)	3.61	4.06	4.97	14.6	2.82	2.32	5.40	4.61
K (mg/L)	11.7	19.9	13.2	12.3	10.7	6.6	12.4	4.3
Na (mg/L)	1477	1315	1953	2789	964	754	1542	740
Fe (µg/L)	3272	3081	606	497	193	282	1322	1446
Ca (mg/L)	11.7	24.0	24.2	6.9	17.6	16.8	16.9	6.8
Mg (mg/L)	19.4	15.5	39.5	55.3	14.9	13.2	26.3	17.2
Zn (µg/L)	1568	674	439	401	229	198	585	511
Cu (µg/L)	304	136	16.6	65.9	12.7	12.1	91.2	115
Co (µg/L)	7.7	4.7	1.6	1.9	44.2	1.9	10.3	16.8
Cd (µg/L)	2.27	1.08	0.18	0.27	0.18	0.18	0.69	0.85
Ni (µg/L)	73.1	18.4	18.7	21.3	5.6	8.4	24.2	24.7
Cr (µg/L)	766	57	1094	350	584	136	498	395
Pb (µg/L)	8.4	2.3	4.8	6.8	5.2	4.1	5.3	2.1
Al (µg/L)	1798	2366	583	624	85	101	926	941
Alk (g/L CaCO ₃)	245	236	330	264	297	308	280	37.0
EC (mS/cm)	8.22	8.27	8.81	11.87	4.04	3.61	7.47	3.13
pH	6.49	6.73	7.33	7.09	6.92	6.93	ND	ND
TVS:TS	0.46	0.50	0.59	0.76	0.51	0.49	ND	ND
BOD: COD	0.44	0.18	0.20	0.10	0.35	0.21	ND	ND
C: N	5.61	14.38	25.17	34.92	2.20	1.55	ND	ND
VFA:Alk	12.5	11.9	7.39	9.39	7.14	5.84	ND	ND
COD: SO₄	7.13	13.0	22.4	37.0	25.3	6.10	ND	ND
COD: TVS	2.20	2.00	1.59	1.07	1.56	3.12	ND	ND

TOC= total organic carbon COD= chemical oxygen demand VOA= volatile organic acid BOD= biochemical oxygen demand ND= not determined SD=standard deviation TN= total nitrogen TAN=total ammonium nitrogen TS: total solid TVS= total volatile solid TP= total phosphorous VFA= volatile fatty acid

The concentration of most metals (Na-Mg; Zn-Cu-Ni-Cd-Fe-Al; Ni-Pb; and Cr-Al) in the samples displayed a similar trend ($R^2= 0.73-0.99$), with the first 2 batches having the highest concentrations. The IC_{50} values for methanogens and acetogens have been reported as 11 g/L (Na), 28 g/L (K), 4.8 g/L (Ca), 4-8 mg/L (Cd), 100-400 mg/L (Ni), 17-58 mg/L (Zn), 67 mg/L (Pb), 8.3-3000 mg/L (Cr), and 0.7-5.65 g/L (Fe) (Abdel-shafy & Mansour, 2014; Lin, 1992; Zayed & Winter, 2000). The metal concentrations tabulated in Table 4.1 were below the IC_{50} . Some metals, such as Ni, Zn, Co, Cu and Ca are also necessary as metabolic co-factors, and in this study they were either within or below the optimal range for AD (Thanh et al., 2016).

A robust and well-acclimated inoculum was therefore needed. According to Holliger et al. (2016) the inoculum should (i) come from an active anaerobic digester that is digesting complex organic matter, (ii) have anaerobic sludge from a wastewater treatment plant and (iii) digested manure to provide a highly diverse microbial community able to digest a large variety of organic molecules. In this study, the inoculum was obtained by mixing mesophilic reactors, digested cow manure from a laboratory batch anaerobic reactor, granules from an up flow anaerobic sludge blanket reactor treating distillery and brewery wastewater, and tannery waste activated sludge (TWAS) (1:1:1:2). To shorten the experiment time, the inoculum was specifically adapted to the TWW to be tested by randomly feeding it with TWW.

4.3. Biochemical methane potential test

4.3.1. Specific methane production

The BMP experiments were terminated when volume of CH_4 (i.e. $BMP_{1\%}$) was $<1\%$ over 3 consecutive days as recommended by Hollinger et al. (2016). The specific CH_4 production (represented by the final value of the BMP curve) was evaluated, and results were grouped based on initial SO_4^{2-} concentrations in the BMP reactors.

A lag phase between 5 and 23 days in cumulative CH_4 production was observed in reactors operating at $ISR \geq 3$ and 1335 mg/L of SO_4^{2-} concentration (Figure 4.1). This lag phase can be called an acclimation period and is observed in reactors with inhibiting or toxic compounds (Rodriguez-chiang & Dahl, 2014). Cumulative CH_4 production ranged from 24 to 166 mL/gVS in these reactors, with the highest and lowest CH_4 being produced by R8 and R6 respectively. The low production in R6 can be attributed to its ISR of 5. High ISR causes an initial reactor overloading or substrate inhibition process (Eskicioglu & Ghorbani, 2011). In addition, in 4 of 5 replicates with $ISR= 3$, close to 50 days were required for CH_4 generation to complete. The cumulative CH_4 yield in these reactors ranged from 95 to 166 mL/gVS. The data obtained in this study were much lower than the 753 mL/gVS CH_4 yield reported by Achouri et al. (2017) in the AD of general TWW at a 37 days RT. Lower cumulative CH_4 (7.6 mL/gVS) was obtained by Saxena et al. (2019) who also worked on AD of TWW at 37 days retention time (RT).

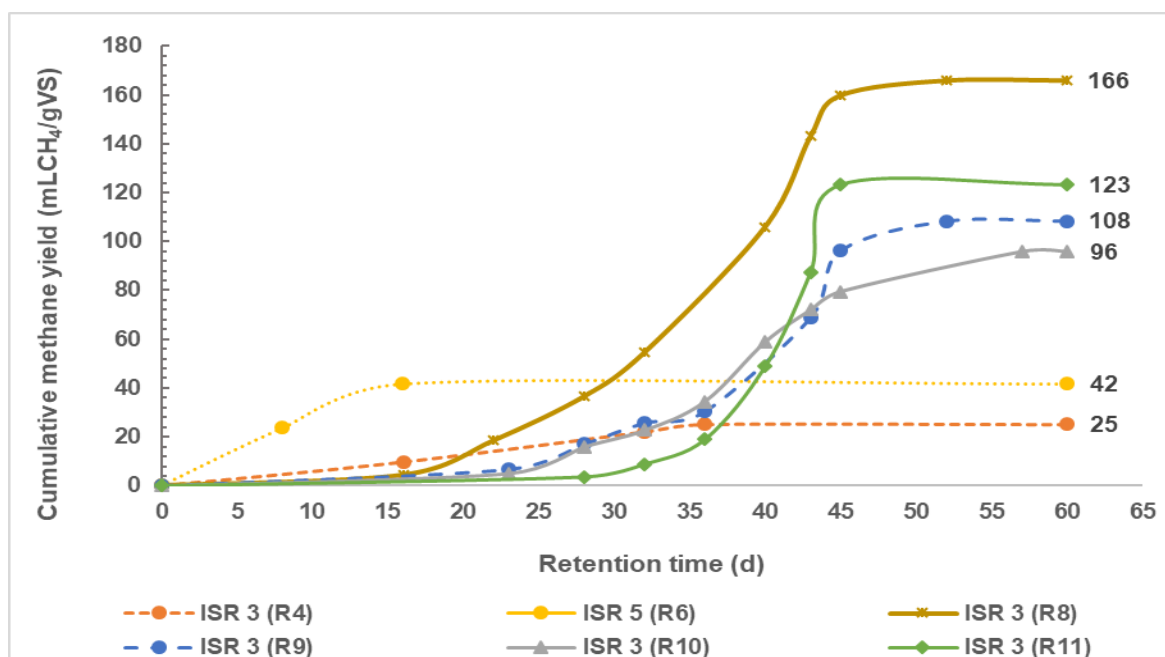


Figure 4.1: Cumulative methane yields from biochemical methane potential test reactors operating at inoculum to substrate ratio ≥ 3 and sulfate concentration of 1335 mg/L. ISR= inoculum to substrate ratio

In the second group, where reactors operated at $SO_4^{2-} \leq 710$ mg/L (mid concentration range from study site), no lag phase was experienced, and more than 92% of the cumulative CH_4 generation of 99-139 mL was obtained within 10 days of operation (Figure 4.2A). Finally, in the last category grouping reactors that operated at SO_4^{2-} concentration ≥ 1960 mg/L, inhibition of methanogens was observed in all reactors as illustrated in Figure 4.2B. R12 endured the longest lag phase (≈ 59 days) and only produced 1 mL CH_4 /gVS through the 60-day period, whereas R2 did not produce biogas at all. These results are very promising, and strongly suggest that by optimising the sludge recycle ratio and/or SRT, efficient AD can be achieved, provided the SO_4^{2-} concentration is kept below a particular (high) threshold.

In the majority of the reactors, CH_4 generation ceased between 16 and 52 days; additional weeks of digestion did not display any significant changes. However, the fact that CH_4 production ceased, does not mean that everything was degraded. Plus, the lag phases in some reactors does not necessarily mean that other metabolic processes did not occur. This is discussed in more detail in Sections 4.3.2 to 4.3.4.

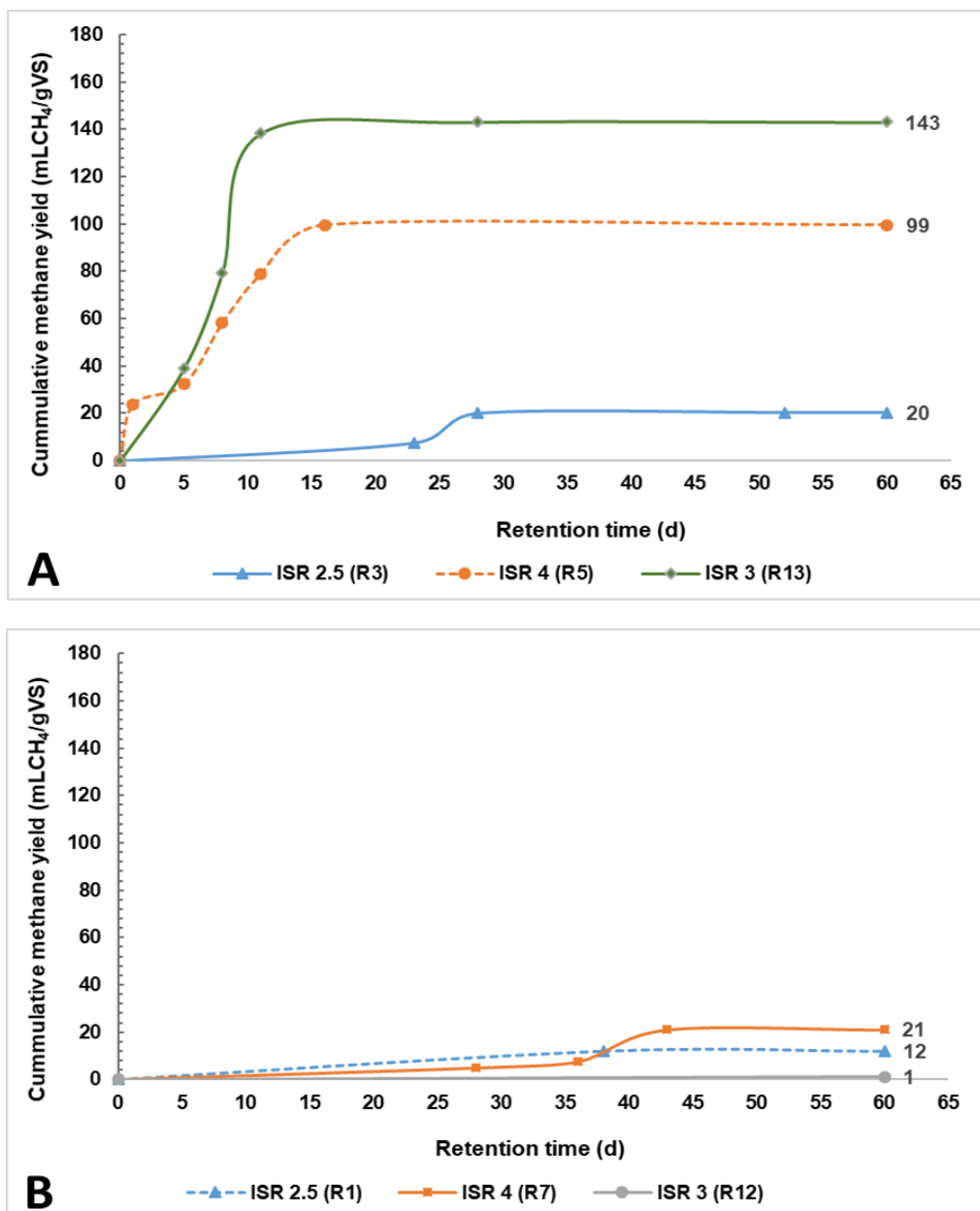


Figure 4.2: Cumulative methane yield from biochemical methane potential test reactors operating at sulfate concentration (A) ≤ 710 mg/L, (B) ≥ 1960 mg/L. ISR= inoculum to substrate ratio

4.3.2. Changes in pH, hydrolysis, acidogenesis and acetogenesis

Figure 4.3 shows the trend of pH through this study. In summary, the pH value remained in the optimum range (6.5-7.8) for methanogens (Regueiro et al., 2012; Carotenuto et al., 2016) in all the reactors for the first 20 days but was higher than the optimum range at the end of the study.

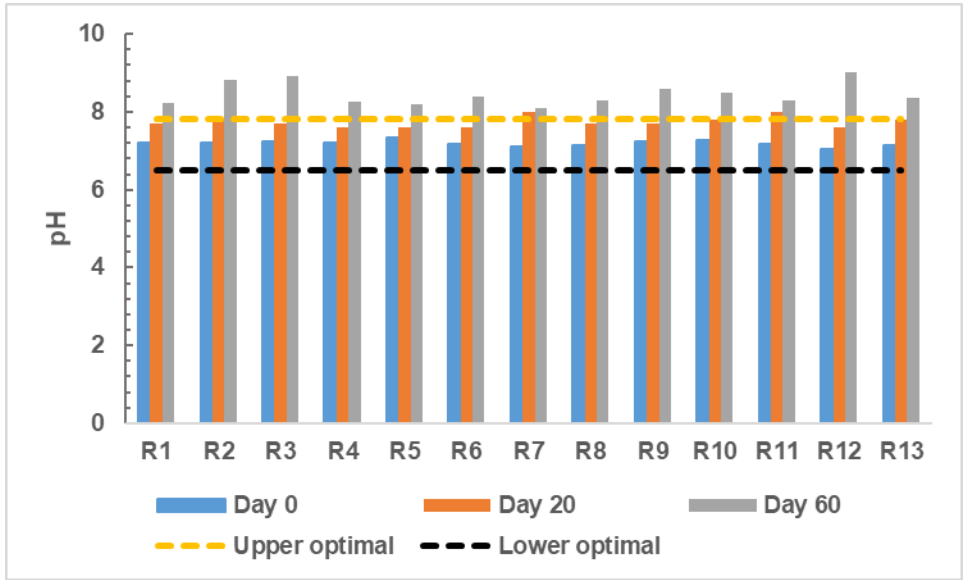


Figure 4.3: pH values measured in samples from biochemical methane potential test reactors

A 76-89% increase in NH_3 concentration (Figure 4.4) together with 38-80% reduction in fats oil and grease (FOG) concentration (Figure 4.5) and overall increase in VOA concentration (Figure 4.6A) were observed in most of the reactors after 20 days, clearly indicating that protein and lipid hydrolysis took place. With regards to NH_3 , the concentration fell above minimum inhibitory concentration (MIC) in all the reactors for the first 20 days of the experiment but fell well below this MIC by the end of the study as shown in Figure 4.4. Temporal NH_3 increases (25-147%) between day 0 and day 20 were observed in reactors operating at higher ISRs > 2.5 and/or lower $\text{SO}_4^{2-} \leq 1335 \text{ mg/L}$, while decreases between 5 to 51% were observed for reactors operating at lower ISRs ≤ 2.5 and/or higher $\text{SO}_4^{2-} \geq 1335 \text{ mg/L}$.

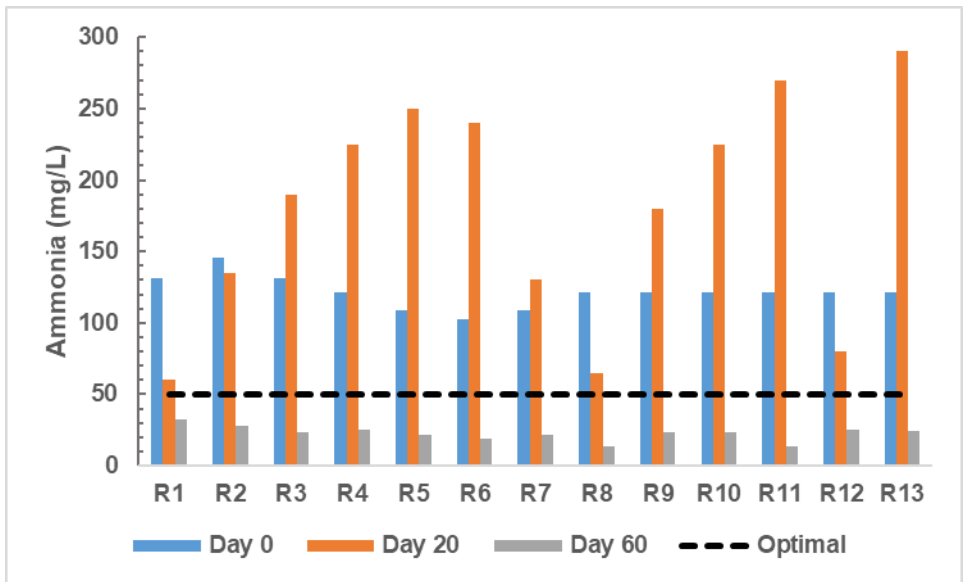


Figure 4.4: Ammonia concentrations measured in samples from biochemical methane potential test reactors

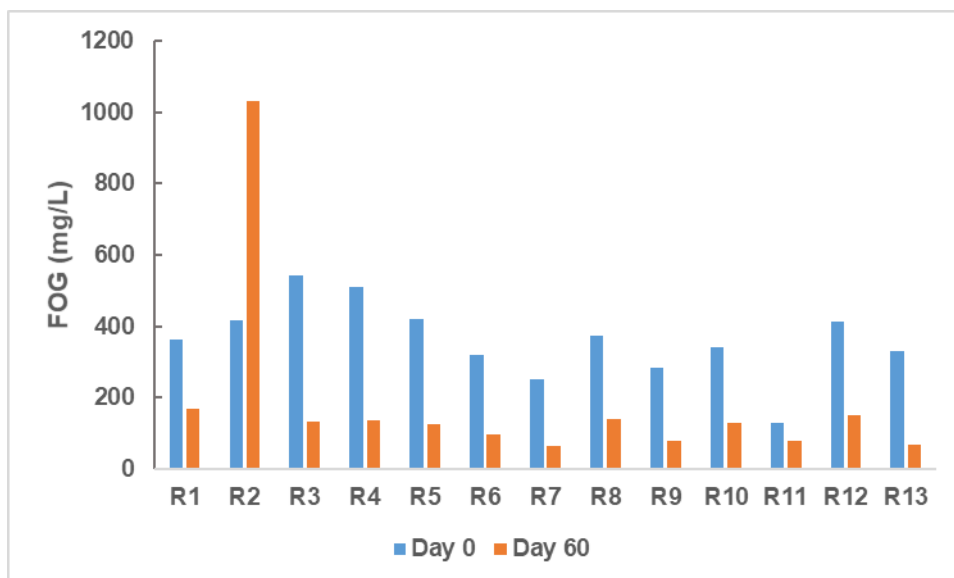


Figure 4.5: Fat oil and grease concentrations measured in samples from biochemical methane potential test reactors.

According to Li et al. (2014), alkalinity and VFA concentration are early warning parameters for anaerobic reactors stability, as they are both primarily derived from the decomposition of organic compounds during digestion (de Lemos Chernicharo, 2007). As described in Section 2.3.1, the VOA concentration depends on the balance between the breakdown of the product from the hydrolysis phase into VOA by acidogenic bacteria, and the consumption of the VOA by acetogens and/or acetoclastic methanogens. Increases of 13% and 14% in VOA concentrations were observed respectively in R1 and R12, while decreases ranging from 7 to 60% were observed in the rest of the reactors (Figure 4.6). Together with changes in the VOA concentrations, SO_4^{2-} was reduced (Figure 4.8) to H_2S (Figure 4.9), suggesting that both acidogenesis and acetogenesis occurred (Equations 4.1 to 4.5) during the lag phase. The accumulation of VOA in the two reactors (R1 and R12) operating at SO_4^{2-} concentration ≥ 1960 mg/L and $ISR \leq 3$ suggested the involvement of SRB in the breakdown of complex substrates (more details are given in Section 4.3.3).

The ratio VFA/Alkalinity was evaluated, and the results are shown in Figure 4.6. At the beginning of the experiment, VFA/Alkalinity ratios >0.4 were observed, indicating instability in methanogenesis and potential failure at start-up (Hampannavar & Shivayogimath, 2010). These ratios then stabilised in the range 0.3-0.4 after 20 days in all reactors with the exception of R3, R11 and R12. A comparison with Figure 4.2B and C shows that in 2 of these reactors (R3 and R12), minimal CH_4 was generated.

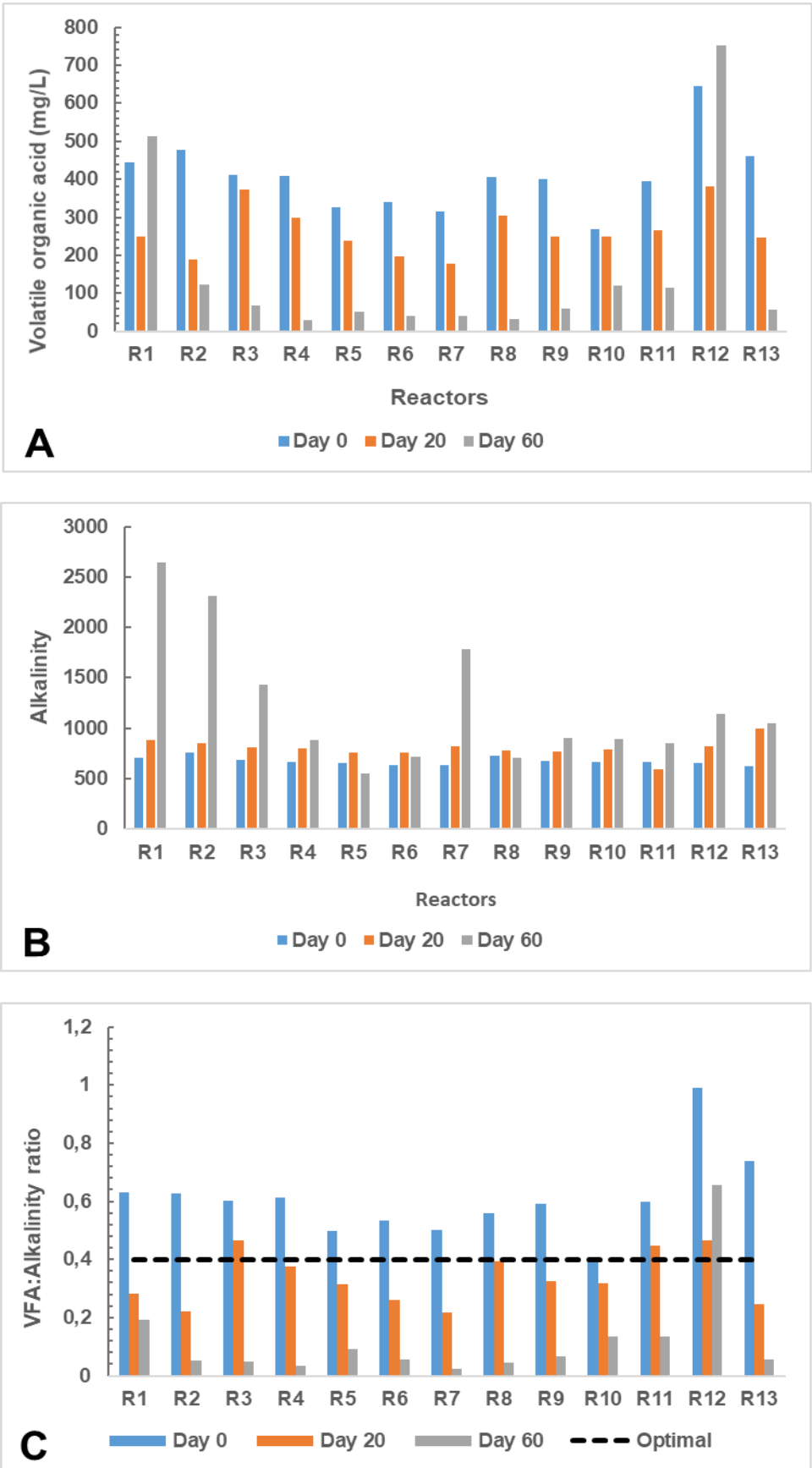
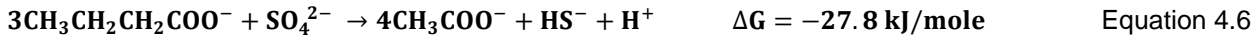
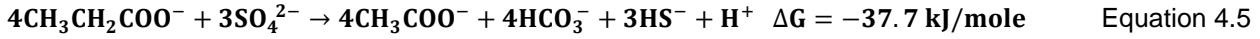
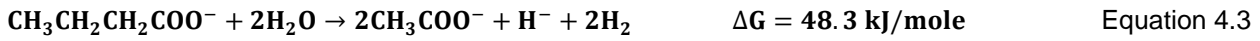
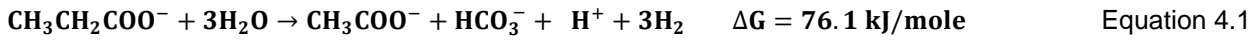


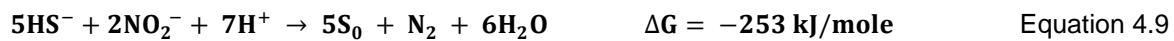
Figure 4.6: (A) Volatile organic acid concentrations, (B) Alkalinity concentrations, (C) Volatile fatty acid to alkalinity ratios measured in samples taken from biochemical methane potential test reactors



4.3.3. Sulfidogenesis and sulfide oxidation

The concentrations of soluble SO_4^{2-} and HS^- in the reactor contents, and H_2S (gas) were measured. However, due to the complexity of the physicochemical and biological processes, detailed mass balances for S were not determined. As displayed in Figure 4.8, SO_4^{2-} reductions occurred in all the reactors over the study period, with increases in H_2S concentration over the first 20 days of operation. However, after 60 days, no H_2S was measured.

It was assumed that sulfidogenesis was largely responsible for the simultaneous increase in H_2S concentration and reduction in SO_4^{2-} , and that SRB dominated not only HS^- generation, but also organic substrate utilisation in some reactors (Equations 4.5 to 4.6 and Equations 4.7 and 4.10). Furthermore, at $\text{pH} > 8$, H_2S is solubilised to HS^- , so that as the pH increased in the reactors (Figure 4.3), some of the HS^- may have precipitated the metals.



It was apparent that at least a fraction of the S^{2-} formed from sulfidogenesis was oxidised into elemental sulfur (S^0) because a white layer formed at the interface of the bulk liquid and head space in the reactors (Figure 4.7). Reyes-Avila et al. (2004), Cervantes et al. (2009) and Moraes et al. (2012) demonstrated this as the main intermediary product of HS^- and H_2S oxidation during treatment of various effluents. For Reyes-Avila et al. (2004) and Moraes et al. (2012), SO_4^{2-} was also re-formed in some instances by oxidation of $\text{S}_2\text{O}_4^{2-}$ and elemental S^0 .

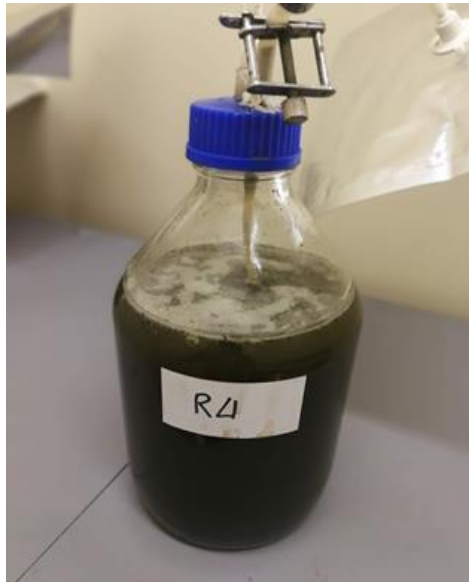


Figure 4.7: White layer forming at the bulk water – headspace interface of a biochemical methane potential test reactor (R4)

Chemolithotrophic sulfur oxidising bacteria (SOB) can simultaneously reduce oxidised N compounds (NO_2^- and NO_3^-) and oxidise S^{2-} under anoxic conditions (Equations 4.7-4.10). Other inorganic reduced S compounds such as thiosulfate ($S_2O_4^{2-}$) and S can also be used as electron donors by SOB. In this study, the notable decrease in NH_3 concentration between day 20 and day 62 in the reactors supports denitrification having taken place, which would have made NO_3^{2-} and NO_2^- available as electron donors for SOB. Furthermore, consumption of H^+ by SOB could explain the anomalous increase in alkalinity (Section 4.3.2) in some reactors.

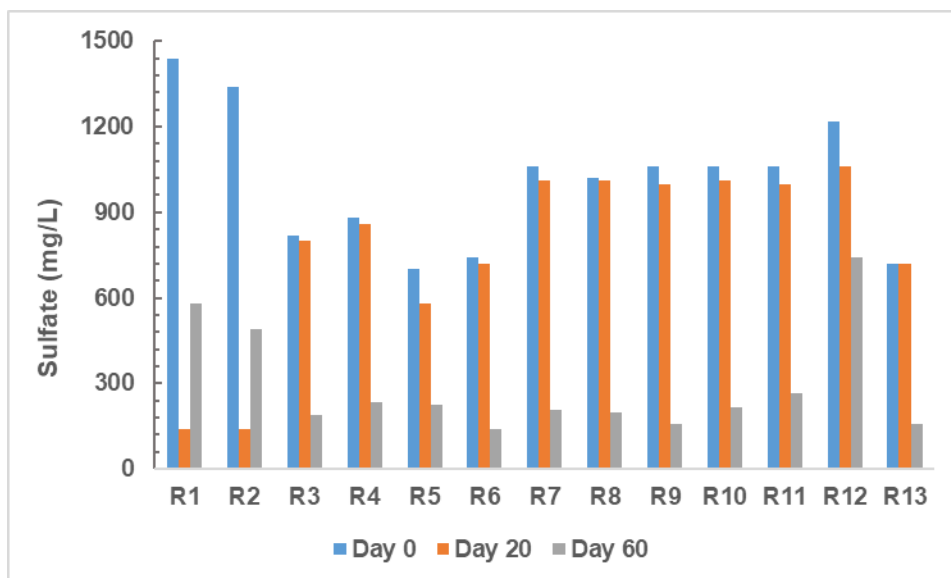


Figure 4.8: Sulfate concentrations in samples taken from biochemical methane potential test reactors

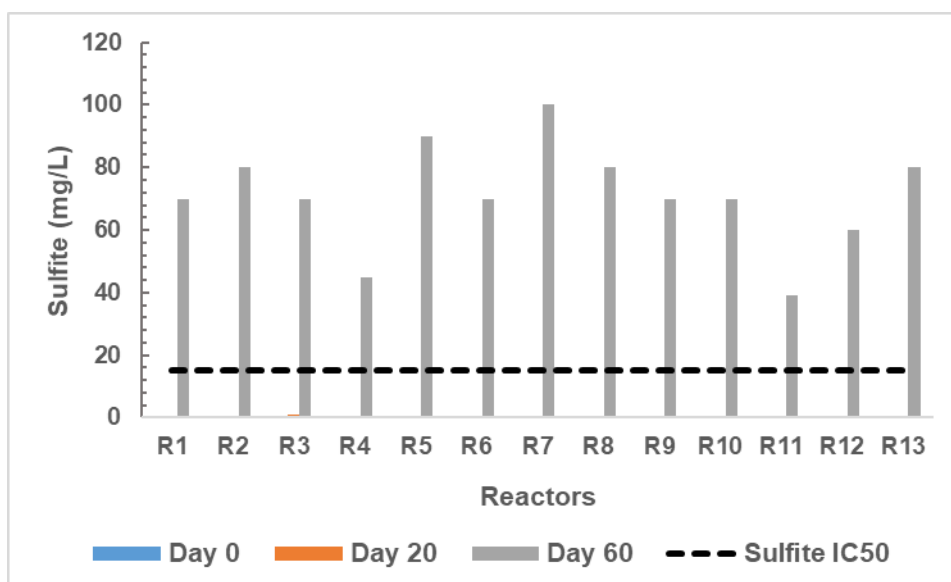


Figure 4.9: Sulfite concentrations in samples taken from biochemical methane potential test reactors

4.3.4. Methanogenesis

The interaction between methanogens and SRB is governed by several factors such as the COD: SO_4^{2-} ratio. According to Valdés et al. (2006), COD:ratio>10 should not represent a threat to process. Below this value, SO_4^{2-} reduction becomes predominant and a large fraction of the organic matter begins to be consumed through SO_4^{2-} reduction. In this study, as shown in Figure 4.10, COD: SO_4^{2-} ratios were constantly <10, suggesting that sulfidogenesis would be favoured over methanogenesis. However, Guerrero et al. (2013) and Omil et al. (1996) reported critical pro-methanogenic COD: SO_4^{2-} ratios <1 and 0.5 respectively, while Reilly & Colleran (2005) reported a COD: SO_4^{2-} ratio = 2 during mesophilic anaerobic treatment of SO_4^{2-} -containing wastewater. It was therefore hypothesised that (i) methanogenesis was favoured in reactors R5 and R13 where no lag phase for CH_4 generation was experienced ($ISR \geq 3$ and $SO_4^{2-} \leq 710$ mg/L), (ii) sulfidogenesis initially dominated, followed by methanogenesis in the reactors that generated CH_4 after lag phases, and (iii) sulfidogenesis was favoured, and methanogenesis was severely and continually inhibited in reactors with high SO_4^{2-} of ≥ 1960 mg/L (R1, R7, R12). This was supported by qualitative analysis of the biogas from R1 (129 mL biogas: 78 ppm H_2S , 0.1% O_2 , 0% CH_4). It was hypothesised that the physicochemical and biological milieu in R1 and R12 inhibited acetoclastic methanogens and/or acetogens, leading to an accumulation of VOA between day 20 and day 60 (Section 4.3.2), which intensified methanogenic inhibition.

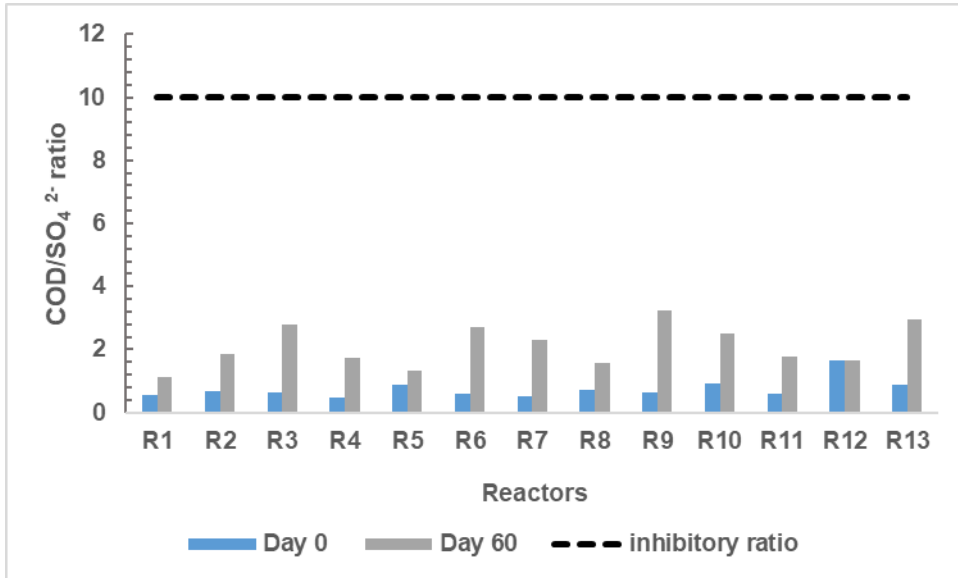


Figure 4.10: Chemical oxygen demand to sulfate ratios in samples taken from biochemical methane potential test reactors

4.3.5. Other factors contributing to methanogenic inhibition

Generally, an optimal C:N range of 20-30 and C:N:P:S of 500-600:15:5:1-3 provides a nutrient balance adequate for microbial growth and maintenance of a stable environment (Deublein & Steinhauser, 2008; Kameswari et al., 2014). In this study, the C:N range (Figure 3-10A) was below optimal in all reactors at the beginning and end of the study. The initial C:N:P ratios ranged from 280:37:1 to 111:26:1, indicating both N and P were limiting macronutrients. However, although there was a notable reduction in concentration, bioavailable (soluble) P was still present at day 62 (Figure 4.12).

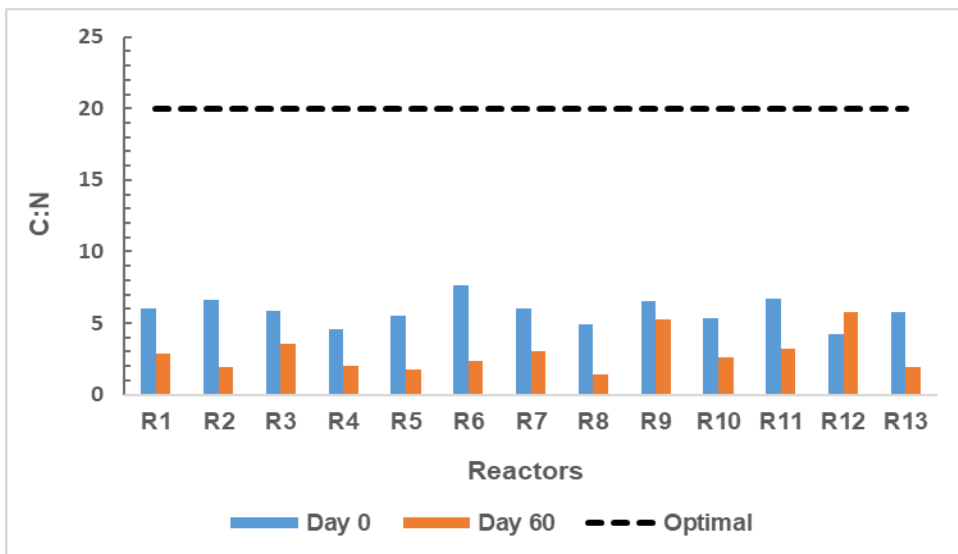


Figure 4.11: Carbon to nitrogen ratio in samples taken from the biochemical methane potential test reactors

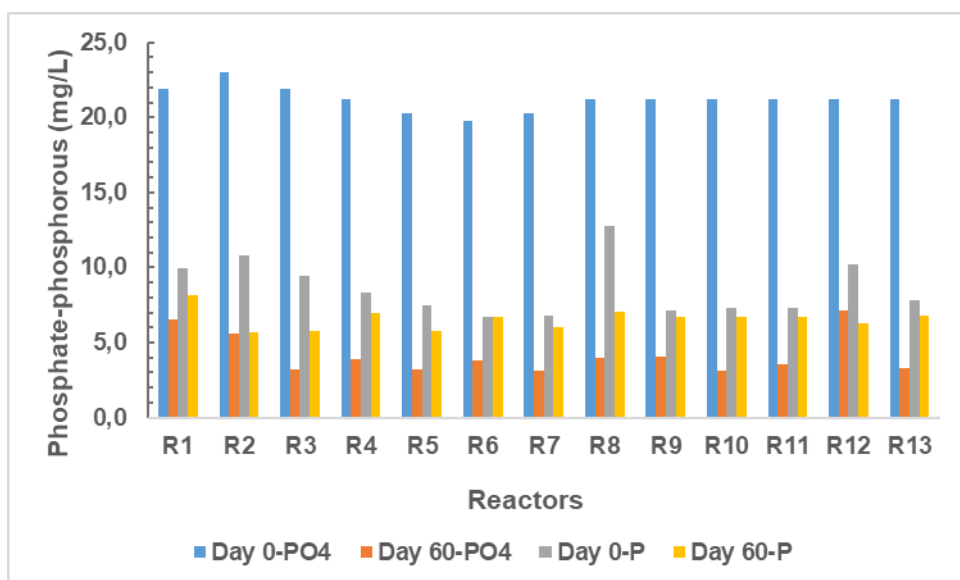


Figure 4.12: Phosphate and phosphorus concentrations in samples taken from biochemical methane potential test reactors

Macronutrients along with trace elements such as, iron (Fe), nickel (Ni), copper (Cu), zinc (Zn), cobalt (Co), molybdenum (Mo) and tungstate are essential for the activation or performance of enzymes and coenzymes involved in the methanogenic pathways (Ünal et al., 2012). However, these trace elements are required at low concentrations to avoid inhibition of AD (Jha & Schmidt, 2017). In this study, the concentrations of all the essential metals decreased, except for Ni in R1, R5, R7, R11, R12 and R13 as illustrated in Figure 4.13. The concentrations of most soluble metals decreased in the reactors, except for R7 and/or R12 Figure 4.13. In contrast, calcium (Ca) concentration increased simultaneously with a decrease in VOA, NH_3 and H_2S except in R2, R7 and R12 that operated at a high SO_4^{2-} concentration and/or lower ISR. Interestingly, the same reactors exhibited a low CH_4 yield and experienced longer lag phases. This could support the granule formation that was observed in the different reactors which may have formed in an effort to adapt and prevent metal toxicity or deficiency. Granule formation is achieved by excretion of soluble microbial products (SMPs) and extracellular polymeric substances (EPS) which play significant roles in chelating metals (Thanh et al., 2016).

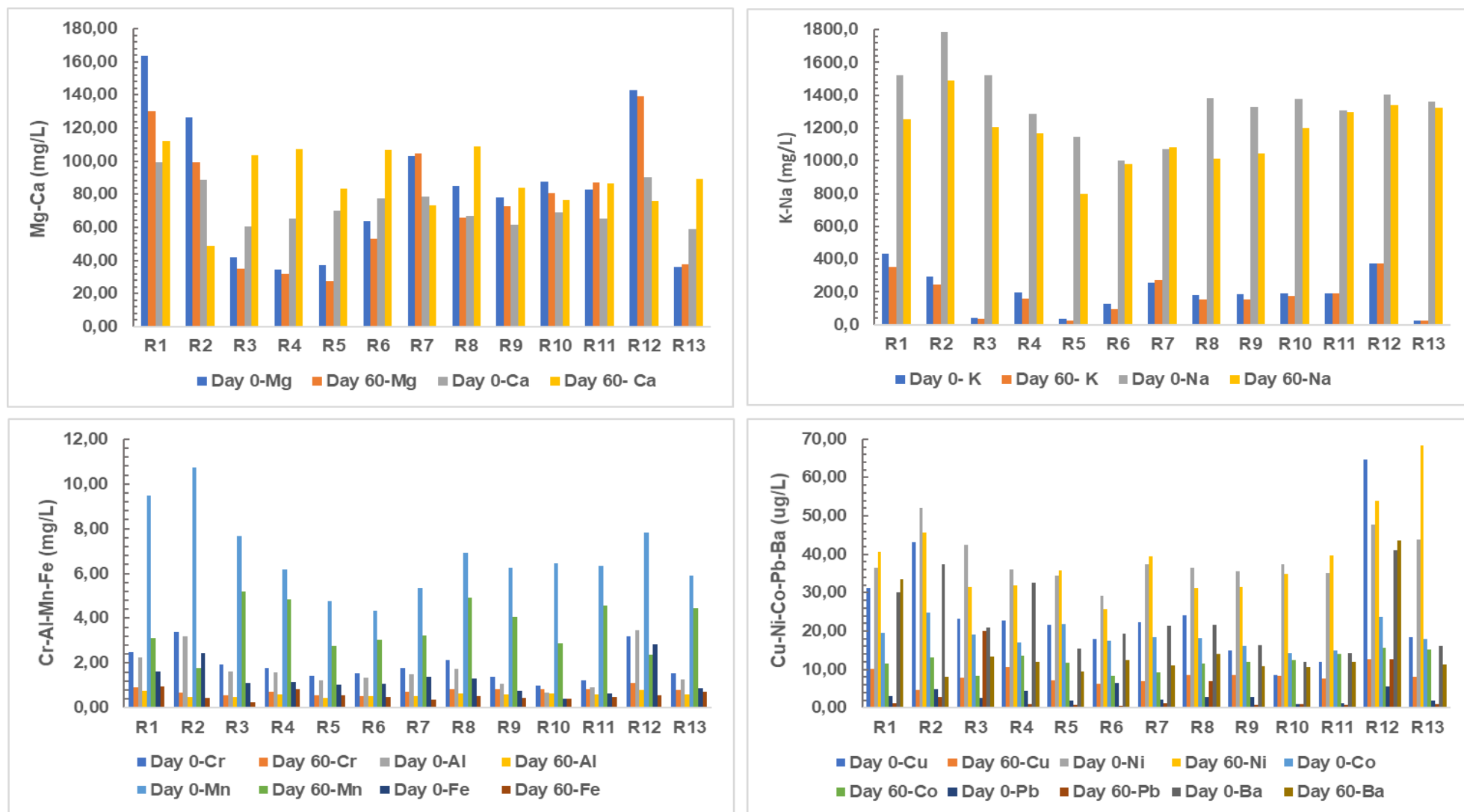


Figure 4.13: Change in soluble metal concentrations in samples taken from the biochemical methane potential test reactors

4.3.6. Statistical analysis

The use of Design-Expert software through CCD led to the utilisation of ANOVA, a regression analysis, determining the interaction effects of the process factors on CH₄, biogas, COD, TOC, SO₄²⁻ and VS and finding the optimum conditions for the process. Table 4.2 shows the experimental parameters applied and the measured responses. Only significant models (p <0.05) are further discussed in the next sections (4.3.6.1-4.3.6.4).

Table 4.2: Design matrix of central composite design and their corresponding responses

		Factor 1	Factor 2	Response 1	Response 2	Response 3	Response 4	Response 5	Response 6	Response 7
Std	Run	A: Sulfate concentration	B: ISR	TOC	Sulfate	TS	VS	COD	Cumulative methane	Biogas yield
		mg/L		%	%	%	%	%	mL/gVS	mL/gVS
3	1	1960	2.5	87.6	59.7	1.7	15.2	16,6	11	129.0
13	2	1335	2.0	93.1	63.4	19.2	11.5	13,8	0	0.0
8	3	710	2.5	76.2	77.1	20.1	28.5	19,2	20	83.6
5	4	1335	3.0	81.3	73.6	26.7	19.3	24.4	25	79.8
4	5	710	4.0	82.5	68.0	9.1	10.9	52.0	99	361.0
1	6	1335	5.0	88.3	81.1	26.0	55.0	10.8	42	180.2
7	7	1960	4.0	77.1	80.4	28.3	33.3	14.9	21	110.3
6	8	1335	3.0	82.7	80.4	30.5	26.1	43.6	166	337.1
2	9	1335	3.0	69.0	85.3	49.2	51.7	24.6	95	259.7
11	10	1335	3.0	61.3	79.6	37.0	40.8	43.0	108	265.1
9	11	1335	3.0	75.3	75.0	15.8	17.7	24.3	123	280.0
12	12	2000	3.0	23.2	49.3	27.5	19.0	39.3	1	9.1
10	13	665	3.0	78.5	77.8	35.4	29.0	25.5	143	290.1

ISR= inoculum to substrate ratio TOC= total organic ratio TS= total solid VS= volatile solid COD=chemical oxygen demand

4.3.6.1. Sulfate removal

Analysis of variance, regression and model validation

By analysing the measured SO_4^{2-} removal efficiency using Design-Expert software, the significance test for the regression model and the significance test of individual model coefficients were all determined. A backward stepwise regression model was selected for a quadratic model with no transformation. A simpler hierarchical model was obtained with a significant term, as shown in Table 4.3.

As tabulated below (Table 4.3), a coefficient of determination R^2 of 0.7023 was estimated for this model, suggesting that this quadratic model was only a reasonable fit for this data. Qiu et al. (2014) stipulated that a good model fit should yield an R^2 of at least 0.8. p-value of 0.0299 was obtained for this SO_4^{2-} removal model, indicating that the model was significant at a 5% significance level. In this case, AB (interaction between SO_4^{2-} concentration and ISR) was a significant model term at p-value= 0.0345. The significance of this model is supported by the F-value (4.72) that indicates that there was only a 2.99% chance that an F-value this large could occur due to noise.

Table 4.3: Results of analysis of variance for sulfate removal

Source	Sum of Squares	df	Mean Square	F-value	p-value	
Model	891.66	4	222.91	4.72	0.0299	significant
A-Sulfate concentration	13.83	1	13.83	0.2927	0.6033	
B-ISR	146.80	1	146.80	3.11	0.1160	
AB	305.95	1	305.95	6.47	0.0345	
A²	240.07	1	240.07	5.08	0.0542	
Residual	378.05	8	47.26			not significant
Lack of Fit	291.12	4	72.78	3.35	0.343	
Pure Error	86.93	4	21.73			
Cor Total	1269.71	12				
		$R^2 = 0.7023$		Adjusted $R^2 = 0.5534$		

Df= degree of freedom ISR= inoculum to substrate ratio AB= interaction between sulfate concentration and inoculum to substrate ratio A²= quadratic effect of sulfate concentration

The following quadratic model was found to represent the relationship between the response, also called the dependent variable (% SO_4^{2-} removal) and the independent variables

(SO_4^{2-} concentration and ISR). The final model terms of coded factors are presented in Equation 4.11 and Equation 4.12 for uncoded (actual) factors. Both equations can be used to make predictions about the response for given levels of each factor. By default, the high levels of the factors are coded as +1 and the low levels are coded as -1. However, Equation 4.11 is useful for identifying the relative impact of the factors by comparing the factor coefficients. In Equation 4.1,1 a positive sign before a term indicates an increasing effect, while a negative sign indicates a decreasing effect on SO_4^{2-} removal. The linear interaction term of SO_4^{2-} concentration and ISR (AB) shown in Equation 4.11 was significant with a p-value of 0.0345, indicating that they had a significant effect on SO_4^{2-} removal efficiency. This binary term shows that there is an increasing effect between SO_4^{2-} concentration and ISR on SO_4^{2-} removal.

$$\%SO_4^{2-}{}_{\text{removal}} = 78.68 + 6.78 B + 18.31 AB - 9.36 A^2 \quad \text{Equation 4.11}$$

$$\%SO_4^{2-}{}_{\text{removal}} = 114.51 - 0.01A - 19.86B + 0.02AB - 2.1 \times 10^{-5}A^2 \quad \text{Equation 4.12}$$

Where A is SO_4^{2-} concentration, B is the level of ISR, AB is the interaction between SO_4^{2-} concentration and ISR and A^2 is the quadratic effect of SO_4^{2-} concentration.

A diagnostic analysis was carried out to investigate the validity of the goodness of fit of the proposed model. This was done by plotting externally studentised residuals versus the predicted values for the SO_4^{2-} removal as illustrated in Figure 4.14. It was noticed that all colour points describing the values of SO_4^{2-} removal were within the limits (red lines) close to zero-axis, which led to the absence of constant error for SO_4^{2-} removal efficiency. Therefore, it can be concluded that all the values are constant and thus the F-tests were valid.

Interaction between sulfate concentration and inoculum to substrate ratio on sulfate removal

The effect of SO_4^{2-} concentration and ISR on SO_4^{2-} removal efficiency was studied. Their combined effect on this response is shown by a 2D contour and a 3D plot in Figure 4.15. A and B respectively. From the plots, it can be seen that both parameters had notable influences on the removal process because the contour plots become hot (red) and cold (blue) respectively at high and low SO_4^{2-} removal efficiencies. As the SO_4^{2-} concentration increased from 665 to 1333 mg/L and the ISR from 2.0 to 3.5, the SO_4^{2-} removal efficiency decreased from 80 to 76%. A positive trend (increase from 76 to 90%) was observed when SO_4^{2-} increased from 1333 to 2000 mg/L and ISR from 3.5 to 5. However, low removal efficiencies between 50 and 60% were observed when SO_4^{2-} concentration was increased from 1665 to

2000 mg/L and ISR below 2.5. According to (Montalvo et al., 2019) this low removal can be attributed to the inhibition of SRB.

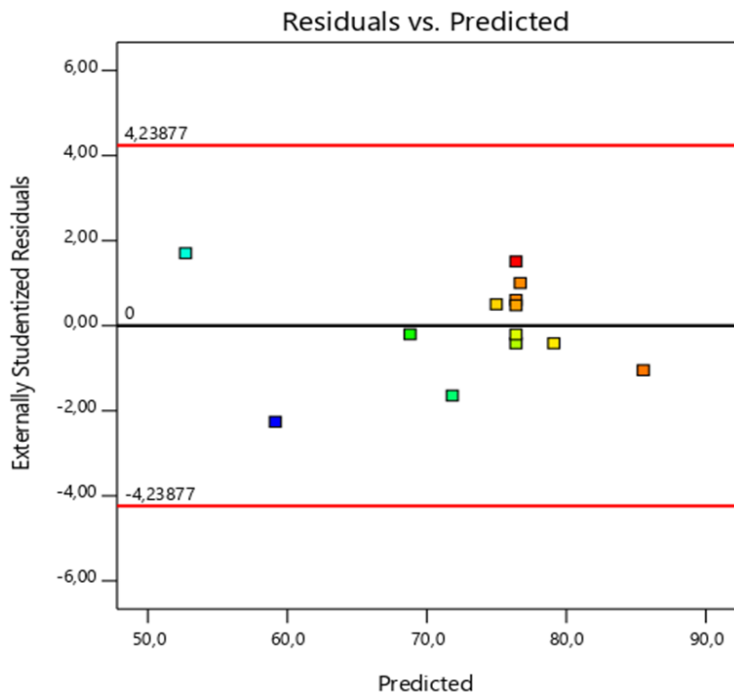


Figure 4.14: Sulfate removal diagnostic plot

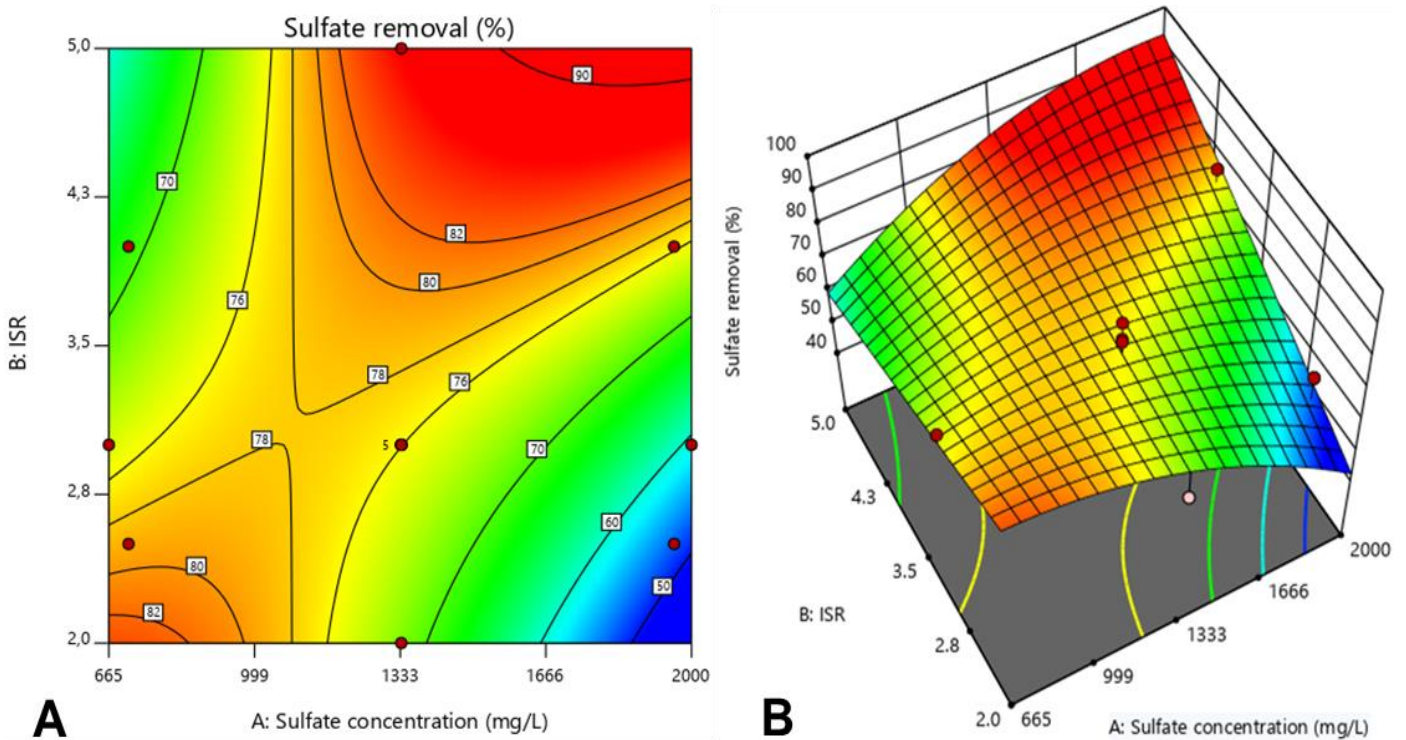


Figure 4.15: 2D contour plot (A) and 3D surface plot (B) of predicted model for sulfate removal. ISR= inoculum to substrate ratio

4.3.6.2. Removal of chemical oxygen demand

Analysis of variance, regression and model validation

For this response (COD removal), the predicted and actual values were reasonably good and were tested using ANOVA. A stepwise selection procedure (stepwise backwards) with an inverse transformation was used to deselect terms that did not contribute to the model. The resulting ANOVA Table 4.4 for the COD removal model outlines the analysis of variance for this response and shows the significant model terms affecting the removal of COD. This table also demonstrates additional analyses such as, $R^2= 0.8488$ and adjusted $R^2= 0.7409$ suggesting that this is a good model fit. The model was significant at a 5% significance level, as indicated by the very low p-value of 0.0086 that is less than 0.05. This significance is also confirmed by the large F-value of 7.86, for which there is only a 0.86% chance it could occur due to noise. In this case B^2 is a significant model term at p-value 0.0010.

Table 4.4: Results of analysis of variance for COD removal

Source	Sum of Squares	df	Mean Square	F-value	p-value	
Model	0.0050	5	0.0010	7.86	0.0086	significant
A-Sulfate concentration	0.0007	1	0.0007	5.43	0.0526	
B-ISR	0.0002	1	0.0002	1.81	0.2200	
AB	0.0006	1	0.0006	4.67	0.0676	
A²	0.0000	1	0.0000	0.2799	0.6131	
B²	0.0037	1	0.0037	29.05	0.0010	
Residual	0.0009	7	0.0001			not significant
Lack of Fit	0.0005	3	0.0002	1.76	0.2926	
Pure Error	0.0004	4	0.0001			
Cor Total	0.0059	12				
		$R^2= 0.8488$		Adjusted $R^2= 0.7409$		

ISR: Inoculum to substrate ratio df: domain of definition AB= interaction between sulfate concentration and inoculum to substrate ratio A^2 = quadratic effect of sulfate concentration B^2 = quadratic effect of inoculum to substrate ratio

The final models for describing the relationship between SO_4^{2-} and ISR are displayed in Equation 4.13 (coded) and Equation 4.14 (uncoded or actual factors).

$$\frac{1}{\text{COD}_{\text{removal}}} = 0.0302 + 0.0128A + 0.0085B + 0.0255AB + 0.0037A^2 + 0.0540 B^2 \quad \text{Equation 4.13}$$

$$\frac{1}{\text{COD}_{\text{removal}}} = 0.41 - 0.000092A - 0.20B + 0.000025AB + 8.31A^2 + 0.024B^2 \quad \text{Equation 4.14}$$

Where A is the SO_4^{2-} concentration and B the ISR, AB the interaction between SO_4^{2-} concentration and ISR, A^2 the quadratic effect of SO_4^{2-} and B^2 the quadratic effect of ISR.

The COD removal model validation was also investigated by plotting the externally studentised residuals against the predicted as illustrated in Figure 4.16. The figure indicates that the developed model is adequate owing to the residuals in prediction of the response being small, as the residuals tend to be close to the zero axis and within the limits.

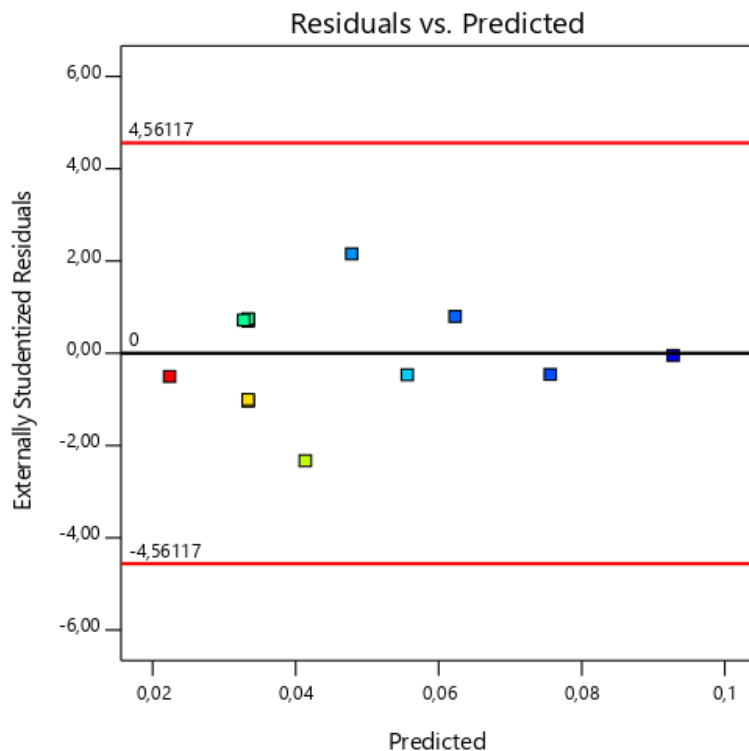


Figure 4.16: Diagnostic plot for chemical oxygen demand removal: Externally studentized residuals vs predicted

Interaction between sulfate concentration and inoculum substrate ratio on chemical oxygen demand removal

The efficiency of COD removal was highly influenced by SO_4^{2-} and ISR. The effect of these parameters is shown by a 2D contour plot and 3D plot in Figure 4.17A and B respectively. As illustrated in the contour (Figure 4.17A), maximum COD removal was found to be 65% at 665

mg/L SO_4^{2-} concentration and ISR of 3.7. A Decrease in COD removal (65-37%) was observed when increasing SO_4^{2-} concentration from 665 to 1333 mg/L. Further increase in SO_4^{2-} concentration led to significant decrease in COD removal. The same behaviour was observed by Valdés et al. (2006) in the anaerobic treatment of high SO_4^{2-} wastewaters. They observed a 12% decrease in COD removal when the inlet SO_4^{2-} concentration was increased from 150 to 900 mg/L. The decrease in COD removal with increasing SO_4^{2-} can be attributed to poor substrate degradation due to low microbial growth rate in the digester (Liu et al., 2018). For Valdés et al. (2006) this was attributed to the increasing S^{2-} concentration on reactor effluent: S^{2-} increases the O_2 demand of the treated water, notoriously reducing its quality. This simply implies that pre-treatment is required at high SO_4^{2-} concentration wastewater.

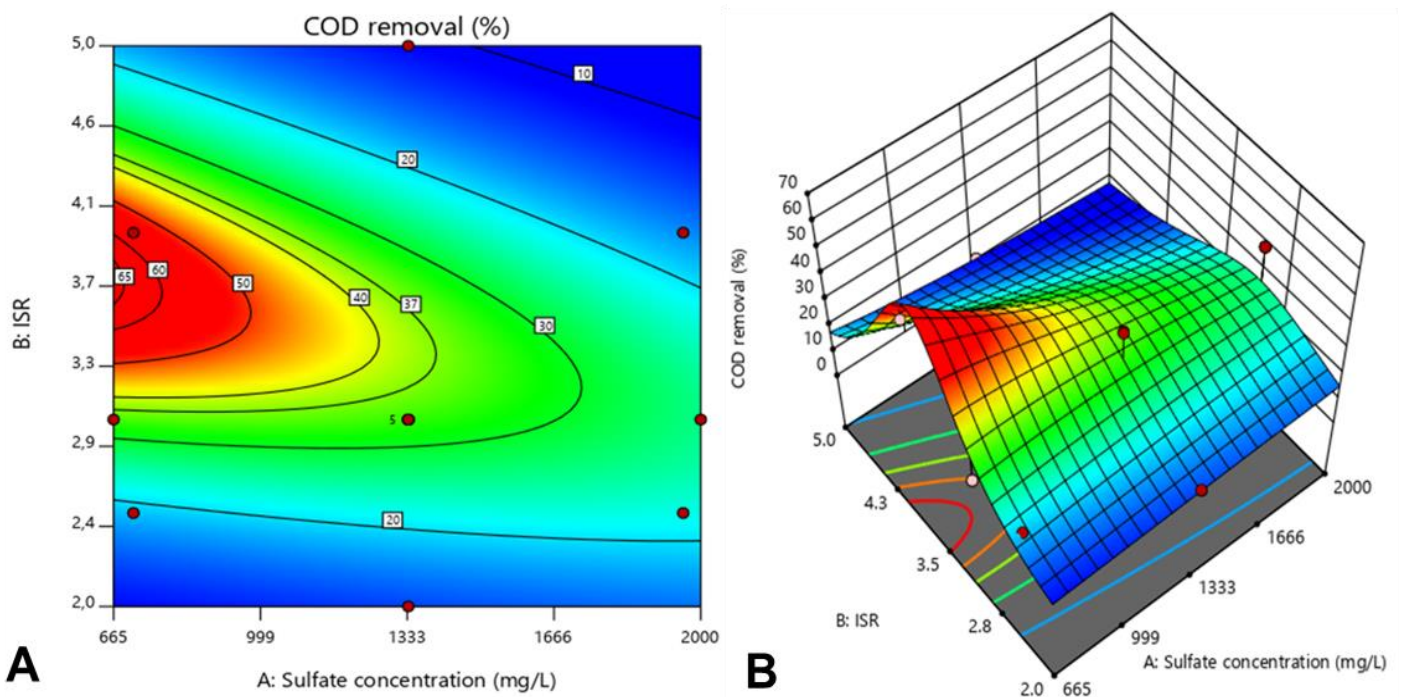


Figure 4.17: 2D contour plot (A) and 3D surface plot (B) of predicted model for chemical oxygen demand removal. ISR= inoculum to substrate ratio, COD= chemical oxygen demand

4.3.6.3. Cumulative methane yield

Analysis of variance, regression and model validation

For the CH_4 yield response, a backward stepwise regression model was selected for a quadratic model with no transformation. A simpler hierarchical model was achieved with significant terms, as shown in Table 4.5. P-value of 0.0059 was obtained for the model indicating that the model is significant at a 5% significance level. In this case A (SO_4^{2-}

concentration), A^2 (quadratic effect of SO_4^{2-}) and B^2 (quadratic effect of ISR) are significant model terms with respective p-value of 0.0048, 0.0147 and 0.0022. This is confirmed by the F-value of 9.01 that implies that there is only a 0.59% chance that an F-value this large could occur due to noise.

A coefficient of determination of 0.8656 was obtained for this model while the predicted R^2 of 0.5806 was in reasonable agreement with the Adjusted R^2 of 0.7695 (i.e. the difference was less than 0.2). Adequate precision measures the signal to noise ratio. For this response a signal to noise ratio of 8.014 was obtained, indicating an adequate signal. According to Nautiyal & Shukla (2018), a ratio greater than 4 is desirable, thus this model can be used to navigate the design space.

Table 4.5: Results of analysis of variance for methane yield

Source	Sum of Squares	df	Mean Square	F-value	p-value	
Model	39393.99	5	7878.80	9.01	0.0059	significant
A-Sulfate concentration	14422.17	1	14422.17	16.50	0.0048	
B-ISR	1723.63	1	1723.63	1.97	0.2030	
AB	1815.95	1	1815.95	2.08	0.1927	
A²	9061.51	1	9061.51	10.37	0.0147	
B²	19314.42	1	19314.42	22.09	0.0022	
Residual	6119.09	7	874.16			not significant
Lack of Fit	2948.29	3	982.76	1.24	0.4056	
Pure Error	3170.80	4	792.70			
Cor Total	45513.08	12				
	$R^2 = 0.8656$		Adjusted $R^2 = 0.7695$			

df= degree of freedom ISR= inoculum to substrate ratio AB= interaction between sulfate concentration and inoculum to substrate ratio A^2 = quadratic effect of sulfate concentration B^2 = quadratic effect of inoculum to substrate ratio

Interaction between the parameters were obtained and correlated with the response as represented in Equations 4.15 and 4.16. The final model terms of coded factors are presented in Equation 4.15 and Equation 4.16 for uncoded (actual) factors. In Equation 4.15, it can be seen that all the terms except B have a negative sign, indicating that they have a significant negative effect on CH_4 yield.

$$\text{Cumulative CH}_4 = 141.18 - 58.61A + 23.27B - 44.62AB - 59.16A^2 - 123.62B^2 \quad \text{Equation 4.15}$$

$$\text{Cumulative CH}_4 = -912.72 + 0.42A + 459.48B - 0.044AB - 0.00013A^2 - 54.94B^2 \quad \text{Equation 4.16}$$

Where A represents the SO_4^{2-} concentration, B the ISR, the AB the interaction between SO_4^{2-} concentration and ISR, A^2 the quadratic effect of SO_4^{2-} concentration and B^2 the quadratic effect of ISR.

A diagnostic analysis revealed that all colour points describing the values of CH_4 yield were within the limits (red lines) close to the zero-axis (Figure 4.18), which led to the absence of constant error for CH_4 yield. Therefore, it can be concluded that all the values are constant and thus the F-tests were valid.

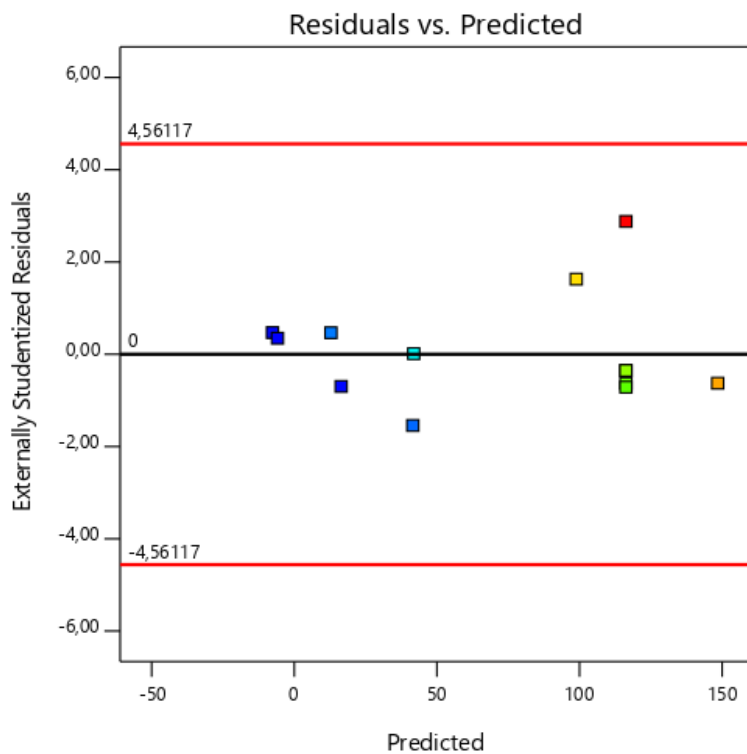


Figure 4.18: Diagnostic plot for cumulative methane: Externally studentized residuals vs predicted

Interaction between sulfate concentration and inoculum to sulfate ratio on cumulative methane yield

The combined effect of SO_4^{2-} concentration and ISR on cumulative CH_4 yield is shown in Figure 4.19A and B. Maximum CH_4 yield was found to be 160 mL/gVS at 999 mg/L SO_4^{2-} concentration and ISR of 3.8. With the increases of SO_4^{2-} concentration from 665 to

1335 mg/L and ISR from 2 to 3.5, 22.5% decrease of cumulative CH₄ (from 160 mg/L to 124 mg/L) production was observed. When the parameters were further increased, decrease of CH₄ still occurred. It was also observed on the 2D plot (Figure 4.19) that at ISR < 2.5 and at any SO₄²⁻ concentration point, the cumulative CH₄ was low (0-40 mLCH₄/gVS). Kawai et al. (2014) recorded high methane yield of 435 mL/g VS at an ISR of 3 in the AD of food waste, below this ratio they also observed a 38% decrease of CH₄ yield. According to Ohemengntiamoah & Datta (2019), low ISR causes an overloading of the system, leading to accumulation of VFAs, inhibition and decreased CH₄ yields. However, this is not in accordance with Feng et al. (2013), who recorded the highest CH₄ yield at ISR of 1 during the BMP test of vinegar residue. This demonstrates that ISR varies with the type of substrate under consideration.

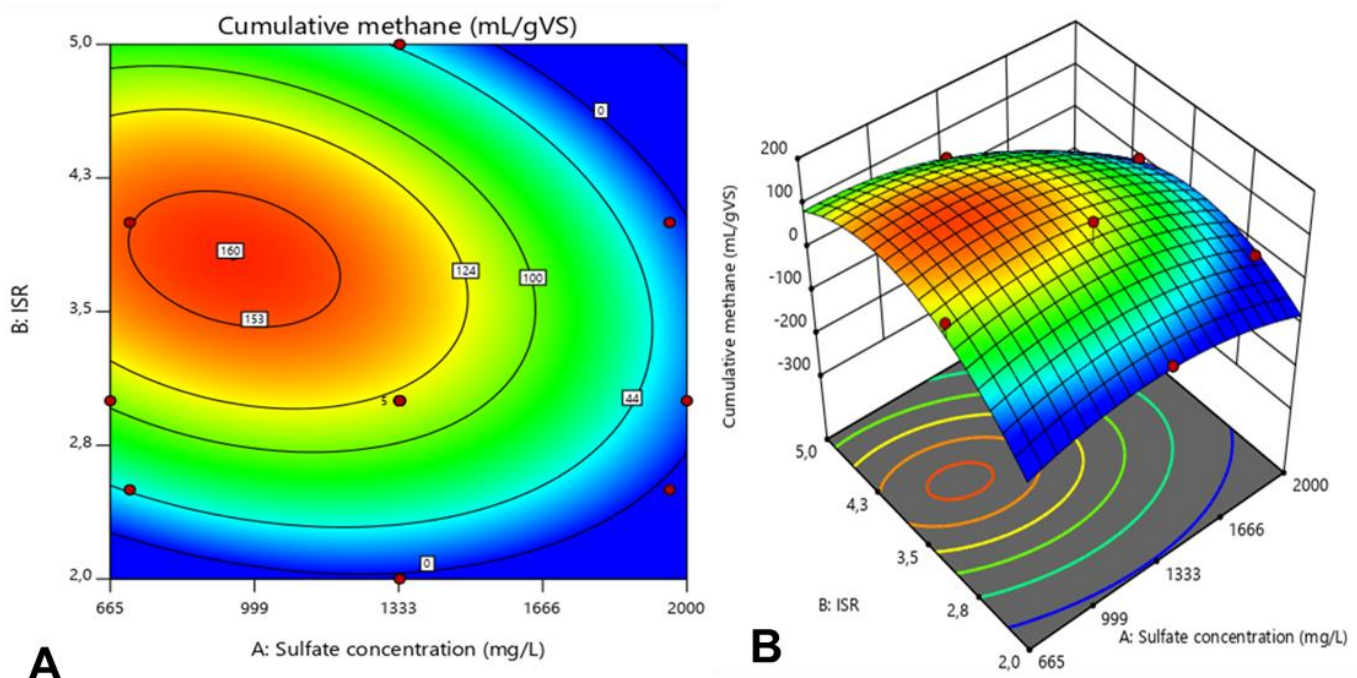


Figure 4.19: 2D contour plot (A) and 3D surface plot (B) of predicted model for cumulative methane. ISR= inoculum to substrate ratio

4.3.6.4. Biogas yield

Analysis of variance, regression and model validation

For the biogas response, a backward stepwise regression model was also selected for a quadratic model with no transformation. The ANOVA results for biogas yield obtained from CCD analysis are tabulated in Table 4.6. The model was significant at a 5% significance level with a p-value of 0.0258. In this case A, B² are significant model terms with respective p-value

of 0.0152 and 0.0181. The significance of this model is also confirmed by the model F-value of 5.22 implies the model is significant. There is only a 2.58% chance that an F-value this large could occur due to noise.

The Predicted R² of 0.5491 was in reasonable agreement with the Adjusted R² of 0.6376; i.e. the difference is less than 0.2. A ratio of 7.075 was determined for this model, indicating an adequate signal. This model can be also used to navigate the design space.

Table 4.6: Biogas yield analysis of variance

Source	Sum of Squares	df	Mean Square	F-value	p-value	
Model	1,644E+05	5	32872.99	5.22	0.0258	significant
A-Sulfate concentration	64209.37	1	64209.37	10.20	0.0152	
B-ISR	32115.75	1	32115.75	5.10	0.0584	
AB	5383.91	1	5383.91	0.8552	0.3858	
A²	24396.58	1	24396.58	3.88	0.0897	
B²	59269.39	1	59269.39	9.41	0.0181	
Residual	44067.00	7	6295.29			not significant
Lack of Fit	6448.65	3	2149.55	0.2286	0.8723	
Pure Error	37618.35	4	9404.59			
Cor Total	2.084E+05	12				
	R ² =0.7886		Adjusted R ² = 0.6376			

df= degree of freedom ISR= inoculum to substrate ratio AB= interaction between sulfate concentration and inoculum to substrate ratio A²= quadratic effect of sulfate concentration B²= quadratic effect of inoculum to substrate ratio

The interaction between SO_4^{2-} concentration and ISR was fitted to experimental data and regression equations in quadratic models were obtained. Equation 4.17 can be used to identify the relative impact of the factors by comparing the factor coefficients: B (ISR) is positive, indicating it has an increasing effect on biogas yield.

$$\text{Biogas yield} = 303.50 - 123.67A + 100.43B - 76.83AB - 97.07A^2 - 216.55B^2 \quad \text{Equation 4.17}$$

$$\text{Biogas yield} = -1670.62 + 0.664A + 842.90B - 0.077AB - 0.00022A^2 - 96.24B^2 \quad \text{Equation 4.18}$$

Where A is the SO_4^{2-} concentration, B the ISR, AB the interaction between SO_4^{2-} concentration and ISR, A² the quadratic effect of SO_4^{2-} concentration and B² the quadratic effect of ISR.

Figure 4.20 represents the diagnostic plot of biogas yield. It can be seen that the model is valid as all colour points describing the values of biogas yield were within the limits (red lines) close to zero-axis, which led to the absence of constant error for biogas yield.

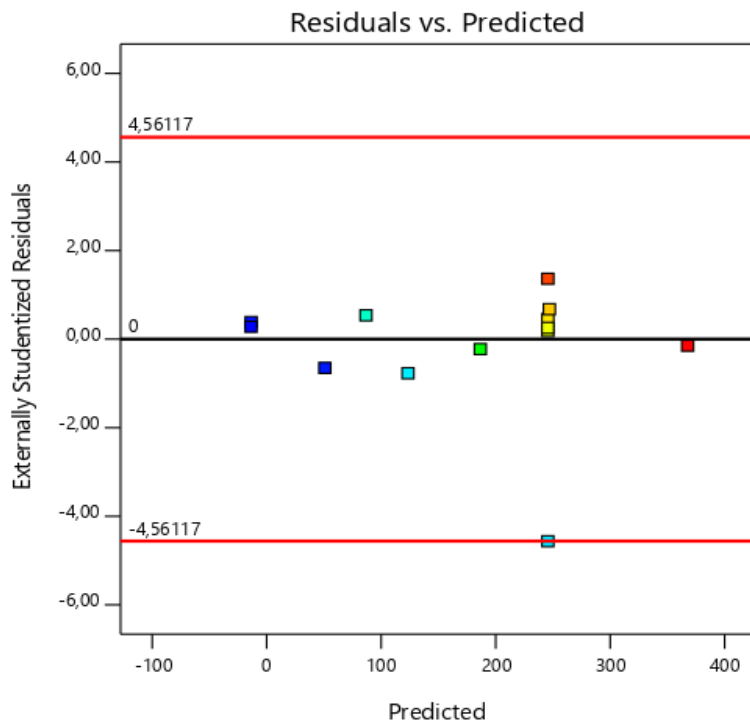


Figure 4.20: Biogas yield diagnostic plot

Interaction between sulfate concentration and inoculum to substrate ratio on biogas yield

The interaction between SO_4^{2-} concentration and ISR on biogas yield was similar to that obtained from the cumulative CH_4 yield. Maximum biogas yield was found to be 371 mL/gVS at 806 mg/L SO_4^{2-} concentration and ISR of 4.1. With the increases of SO_4^{2-} concentration from 665 to 1335 mg/L and ISR from 2 to 3.5, 22.5%, a decrease of biogas production (from 160 mg/L to 124 mg/L) was observed. When the parameters were further increased, decrease of biogas still occurred. At $ISR \leq 2.5$ and regardless of the SO_4^{2-} concentration, low biogas yield occurred (from 0-100 mL/gVS).

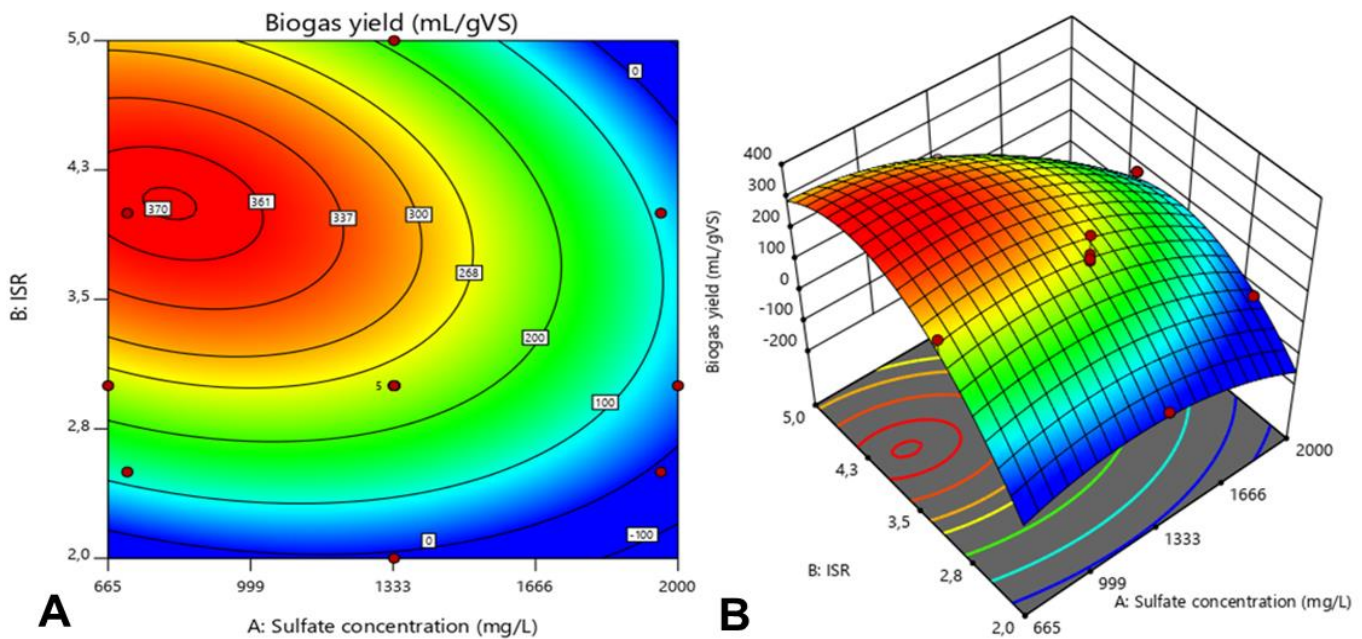


Figure 4.21: 2D contour plot (A) and 3D surface plot (B) of predicted model for biogas yield. ISR= inoculum to substrate ratio

4.3.6.5. Optimization

The process results were interrogated in order to ascertain the optimal parameters in terms of sulfate concentration and ISR for maximum CH₄ yield and COD, sulfate and solids reduction efficiencies (Table 4.7).

Table 4.7: Criteria for optimization of anaerobic digestion of tannery effluent

Name	Goal	Lower Limit	Upper Limit	Importance
A: Sulfate concentration	is in range	665	1000	3
B: ISR	is in range	2	4	3
TOC removal	maximize	23.2	93.1	3
Sulfate removal	maximize	49.3	85.3	3
TS removal	none	1.7	49.2	3
VS removal	none	10.9	55	3
COD removal	maximize	0.0167	0.0923	5
Cumulative methane	maximize	0	170	5
Biogas yield	is in range	0	370	5

ISR= inoculum to substrate ratio TOC total organic carbon TS= total solid VS= volatile solid COD= chemical oxygen demand. Importance level varies from the least important (value of 1), to the most important (value of 5)

The optimized numerical factors that were obtained are summarized in Table 4.8, which also shows the responses obtained by the software. The numerical optimization selected is the best combination of parameters that met all the goals with a desirability of 0.879.

Table 4.8: Optimized conditions in for methane generation and organic and solids removal in anaerobic digestion of ostrich tannery

Sulfate concentration	ISR	TOC removal	Sulfate removal	TS removal	VS removal	COD removal	Cumulative methane	Biogas yield	Desirability
983.687	3.687	76.302	75.850	28.606	30.232	44.597	160.154	362.446	0.879

ISR= inoculum to substrate ratio TOC total organic carbon TS= total solid VS= volatile solid COD= chemical oxygen demand

4.4. Anaerobic sequencing batch reactors

The biodegradability of ostrich tannery wastewater and its potential to produce CH₄ was then further investigated using results obtained from the BMP experiments in scaled-up reactors. Two 20 L ASBRs (namely ASBR1 and ASBR2) operating at ISR=3 and SO_4^{2-} concentration of 680 mg/L were used (i.e. no additional SO_4^{2-} was added to the ostrich tannery wastewater). These operating conditions were similar to those used for R8 and R13 during the BMP experiments (Section 4.3.6). However, ASBR1 operated at intermittent mixing (300 rpm for 5 to 10 min/day) while ASBR2 operated at continuous mixing at 300 rpm. The study was conducted for 50 days in two different operational runs. The first run at the start-up period of the ASBR operated for 30 days with a 5-day settling period before decanting. During the second run, the ASBRs operated for 20 days.

4.4.1. Process performance and stability

The CH₄ production, pH, COD concentration, COD removal efficiency, effluent VFA concentration, alkalinity, NH₃, SO_4^{2-}/S^{2-} concentration as well as the effect of mixing mode were used to assess the performance and stability of the ASBRs during the study. The results are shown on Figure 4.24 and Figure 4.25 and discussed in Sections 4.4.1.1 to 4.4.1.6.

4.4.1.1. Methane production

In Figure 4.22, it can be seen that CH₄ production increased gradually in both ASBRs with no significant lag phase during either run, indicating a good start-up and continuous growth of methanogenic microbial activity. In ASBR 2, the cumulative CH₄ yields from the two runs were 749 mL/gVS and 400 mL/gVS with biogas CH₄ content ranging between 2.8- 54.2% and 8.3-

54.6% respectively. Respective cumulative CH₄ yields of 95 mL/gVS and 11 mL/gVS were measured in runs 1 and 2 of ASBR1. These were significantly lower than those measured from ASBR2 and implied a serious process imbalance and a severe inhibition of methanogens. However, there was a decrease in yield between run 1 and run 2 in both ASBRs (Figure 4.22). This could be due to biomass washout that may have taken place during the decanting step as the sludge did not settle well. The yields from this study were comparable with previous studies treating ostrich tannery wastewater (Alemu & Lemma, 2016; Achouri et al., 2017; Mekonnen, Leta & Njau, 2017; Berhe & Leta, 2017; Saxena et al., 2019) as tabulated in Table 4.9.

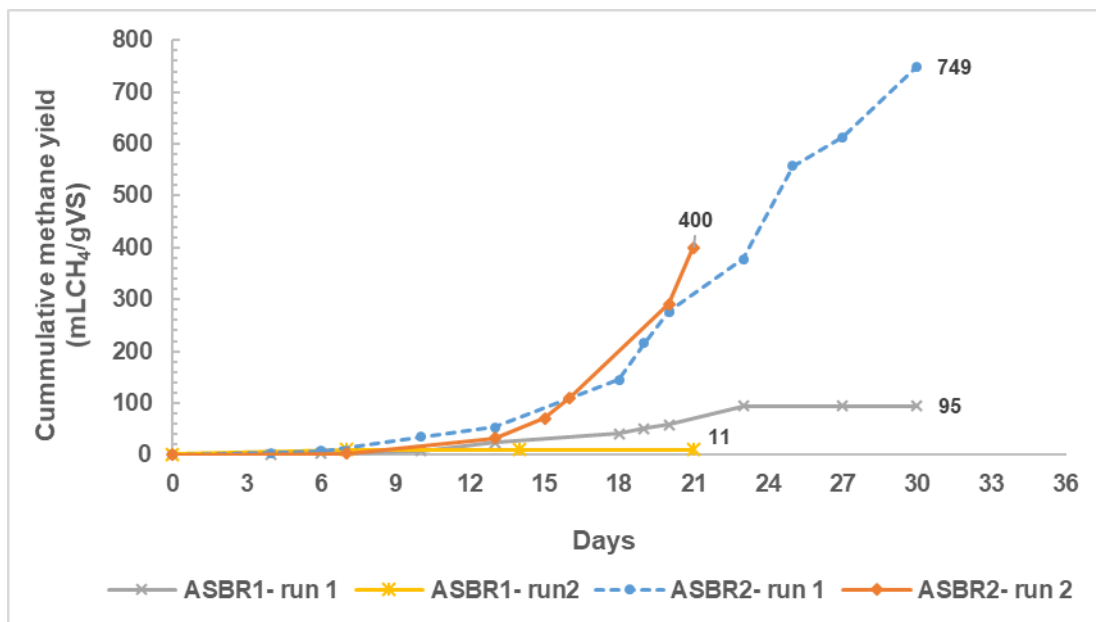


Figure 4.22: Anaerobic sequencing batch reactors 1 and 2 cumulative methane yield

4.4.1.2. pH

The pH of the ASBRs was maintained at 6.8 ± 0.2 and at a temperature of $37 \pm 2^\circ\text{C}$, as per Mpofo et al. (2019a). The reactors desirably operated under anaerobic conditions with an oxidation reduction potential that ranged between -395 and -539 mV in ASBR1 and between -385.2 and -517.5 mV, which was ideal for optimum methanogenic activity (Amani et al., 2010; G. Zupancic & Jemec, 2010).

4.4.1.3. Effect of mixing/ type of mixing

Experimental investigations have shown that the mixing mode and mixing intensity have direct effects on the biogas yield even though there are conflicting views on mixing design (Karim et al., 2005; Hoffmann et al., 2008; Kaparaju et al., 2008; Lindmark, Eriksson, et al., 2014;

Lindmark, Thorin, et al., 2014). In this study, in comparison to intermittent mixing, continuous mixing was shown to improve cumulative CH₄ from 99 mL/gVS in ASBR1 to 752 mL/gVS in ASBR2 in runs 1 and from 11 to 400 mL/gVS in ASBR1 and ASBR2 respectively in runs 2. This implies that better microbial adaptability occurred in the continuous mixing reactor (ASBR2) and it is in accordance with other studies (Zhang et al., 2020). However, conflicting results have also been reported. Kaparaju et al. (2008) observed an average of 7% CH₄ increase during intermittent mixing compared to continuous mixing in the thermophilic AD of manure. Dague et al. (1970) observed that shifting from continuous mixing to intermittent mixing (2 min of mixing/h) resulted in significantly higher gas production from municipal wastewater. On the other hand, Ong et al. (2002) did not find any significant difference between these 2 types of mixing in the AD of cattle manure slurry.

In general, the contents of small-scale reactors such as the BMP reactors used in this study are easily mixed when compared to pilot and full-scale reactors (Ndobeni, 2017). According to Lettinga et al. (2001) and Metcalf & Eddy (2003), ineffective mixing in a pilot scale reactor creates dead-zones, resulting in poor mass transfer and diffusion of the substrate from the bulk liquid to the biomass as compared to easily mixed contents of small-scale reactors. This could also help explain the low cumulative CH₄ yield in ASBR1.

It was also observed that a drop in CH₄ yield occurred between consecutive runs in both ASBRs (Figure 4.1.6), which was assumed to be due to washout of functional biomass due to inadequate settling. The biomass in the BMP reactors settled well, in contrast to the biomass in the ASBRs. During the settling phase, a significant volume of biogas was generated in the ASBR 2 (7% of the total in run 1). This suggested that sedimentation may have also provided closer microbial consortia proximity (juxtapositioning). Further studies on mixing and settling will be conducted in order to increase AD efficiency with successive runs.

4.4.1.4. Removal of chemical oxygen demand

The COD removal rate is commonly used to evaluate the performance of the AD process (Chowdhury et al., 2013; Achouri et al., 2017). As illustrated in Figure 4.23, the COD concentration in runs 1 and 2 of the ASBR1 varied between 1847 and 1375 mg/L and 1865 and 1560 mg/L respectively while in ASBR2, the COD concentration varied between 1690 and 398 mg/L and 1495 and 690 mg/L in run 1 and run 2 respectively. In terms of COD removal, 25.5% and 16.3% removal efficiencies were obtained respectively in run 1 and 2 of the ASBR1 and 76.5 and 55.2% were obtained in run 1 and run 2 of the ASBR2. This COD removal achieved in run 1 of the ASBR2 also agrees with the highest CH₄ production (Figure 4.22).

These removal efficiencies fall within the range of previous studies treating tannery wastewater. Mekonnen, Leta & Njau (2017) achieved 69-85% COD removal using a pilot scale ASBR. Results from Liu et al. (2017) showed COD removal efficiencies ranging from 36.2 to 68.3% in the AD of TWW using an UASB. Other comparable COD removal (75-82%) was reported by Mekonnen et al. (2016) in the co-digestion of TWW with cattle dung using an ASBR.

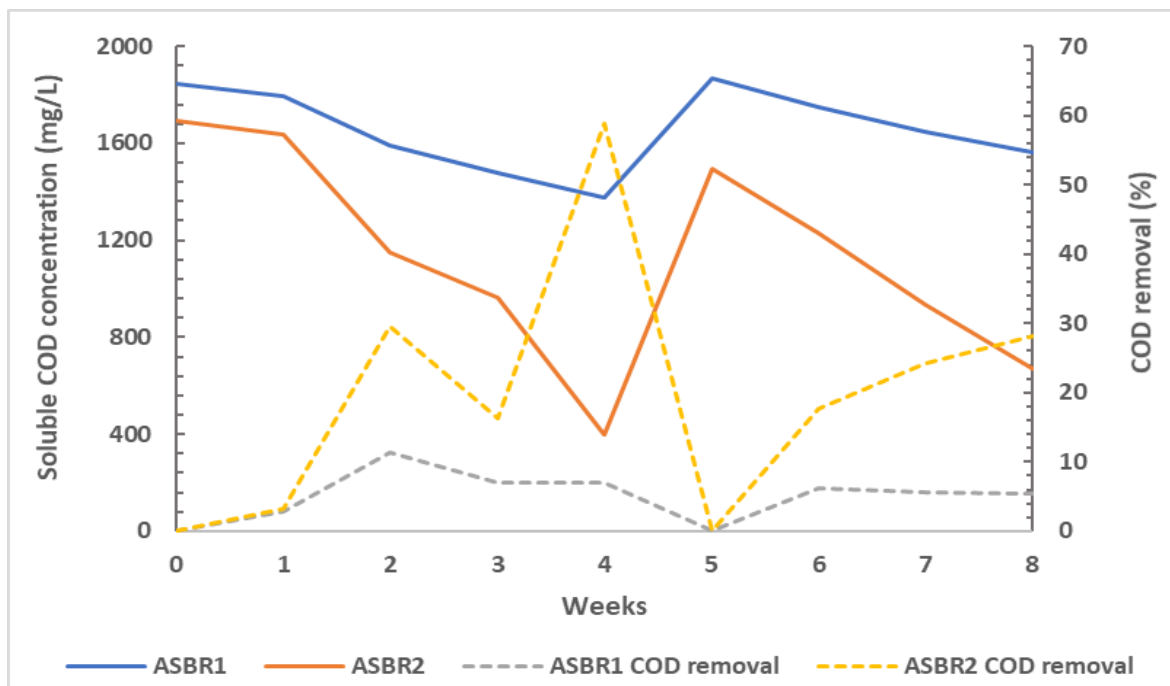


Figure 4.23: Weekly chemical oxygen demand concentration and removal efficiency. ASBR= anaerobic sequencing batch reactor, COD= chemical oxygen demand

4.4.1.5. Volatile organic acid and alkalinity

As with the BMP experiments, the implied imbalance between acidogenesis and methanogenesis led to the accumulation of VOA. The results illustrated in Figure 4.24A indicates that VOA concentration increased notably over the first week in both ASBRs due to mixing intensity that enhanced hydrolysis. This was reflected by a slight decrease in COD (Figure 4.23) and TOC (Figure 4.24E) and insignificant CH₄ generation (on an average 1.75 and 3.1% in ASBR1 and ASBR2 respectively). According to Lindmark et al. (2014) mixing also has an effect on the microbial consortia. McMahon et al. (2001) and Hoffmann et al. (2008) reported an increase in *Methanosarcina* spp. and *Methanobacteriaceae* during a destabilization of the AD process caused by a higher mixing intensity. *Methanosarcina* spp. increased in digesters with periodically high acetate levels and were abundant in all digesters with a history

of high VFA values. The microbial community structure is discussed more fully in Section 5.3.2.2.

The buffering capacity in both ASBRs was found to be unstable. As shown in Figure 4.24B, the reactors were only stabilised during weeks 3 and 4, which was reflected by an exponential rise of CH₄ content (on an average 17.34 and 50.9 % in ASBR1 and ASBR2 respectively) and decrease in COD (Figure 4.23) and TOC (refer to Figure 4.24E). From week 5 till the end of the study, the alkalinity concentration was below the effective digestion range of 1500-3000 mgCaCO₃/L (Gerardi, 2003; Marti, 2008; Kavitha, 2009). This coincided with the increased TOC concentrations. According to Gil et al. (2018), accumulation of TOC indicates a failure in the degradation pathway of the biodegradable matter of one or more of the groups of microorganisms involved in AD. This simultaneously decreased the production of CH₄ and may have led to the termination of the process.

As one of the critical parameters that indicates the stability of a system, the ratio VFA: Alkalinity was evaluated. Figure 4.24C shows that this ratio ranged between 0.09 and 0.92 in ASBR1 and between 0.22-0.86 in ASBR2.

4.4.1.6. Ammonia

As illustrated in Figure 4.24D, the measured weekly NH₃ concentrations were above the MIC (53 mg/L) reported in literature for AD (Rajagopal et al., 2013) in both ASBRs. The concentration peaked in weeks 3 and 4 and may have led to the ultimate termination of methanogenesis together with decrease in SO₄²⁻ concentration (Figure 4.25A). The S²⁻ concentrations fell below the range (IC₅₀ =14-125 mg/L at pH 7-8) found to inhibit methanogenesis during AD of suspended sludge in all the weeks except week 6 (Koster et al., 1986; McCartney, D. M. Oleszkiewicz, 1991; O'Flaherty & Colleran, 1999). The SO₄²⁻ concentration (Figure 4.25A) may have promoted SRB activity in acidogenesis and/or sulfidogenesis as observed from the high COD:SO₄²⁻ (Figure 4.25C). Furthermore, during gas sampling, the Geotech biogas 5000 analyser indicated that the biogas contained >>>>9999 ppm H₂S. It can therefore be assumed that SO₄²⁻ was transformed into H₂S gas.

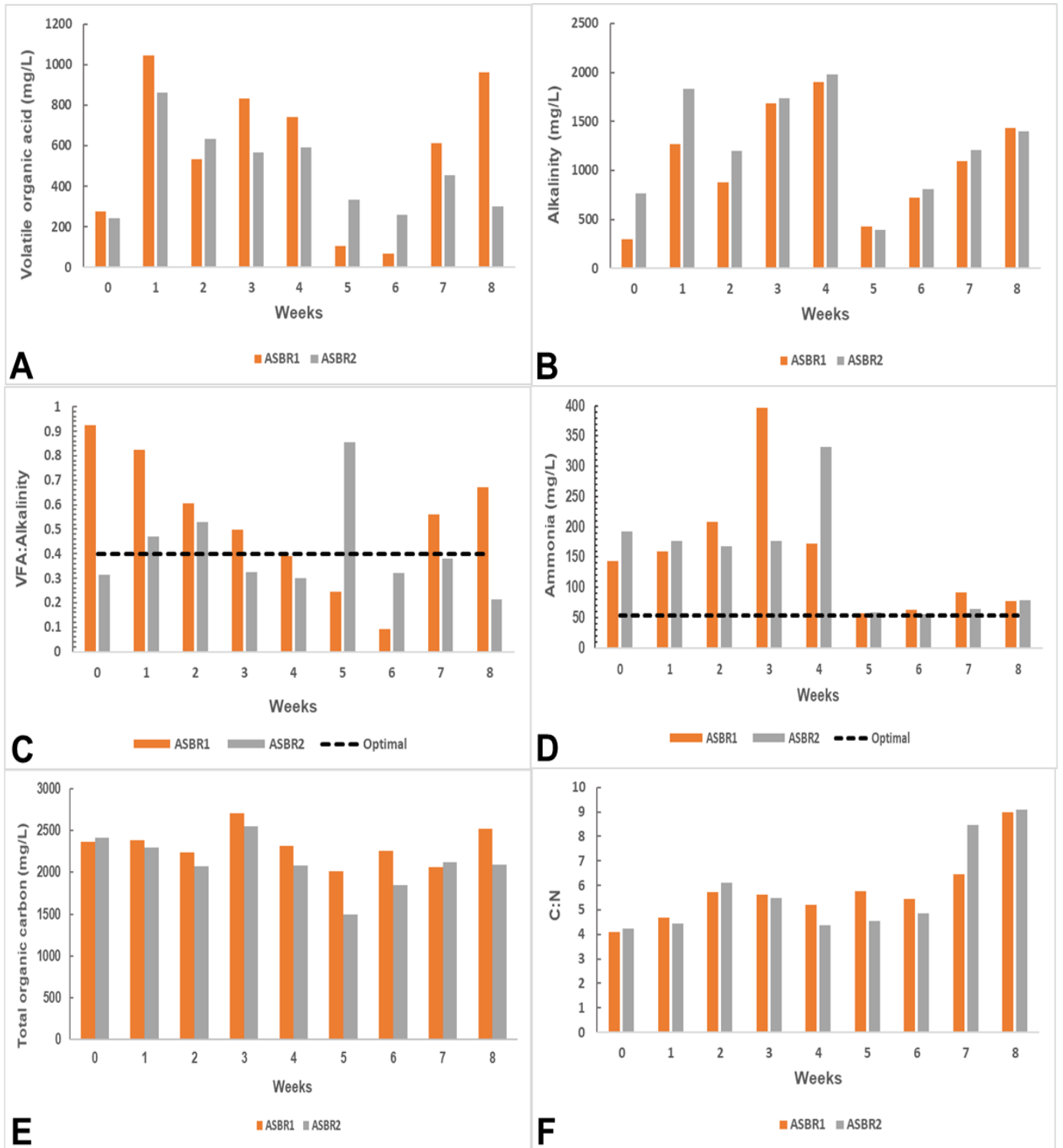


Figure 4.24: A=Volatile organic acid concentration, B= Alkalinity, C= Volatile fatty acid to Alkalinity ratio, D= Ammonia concentration, E= total organic carbon concentration F= carbon to nitrogen ratio in the anaerobic sequencing batch reactors

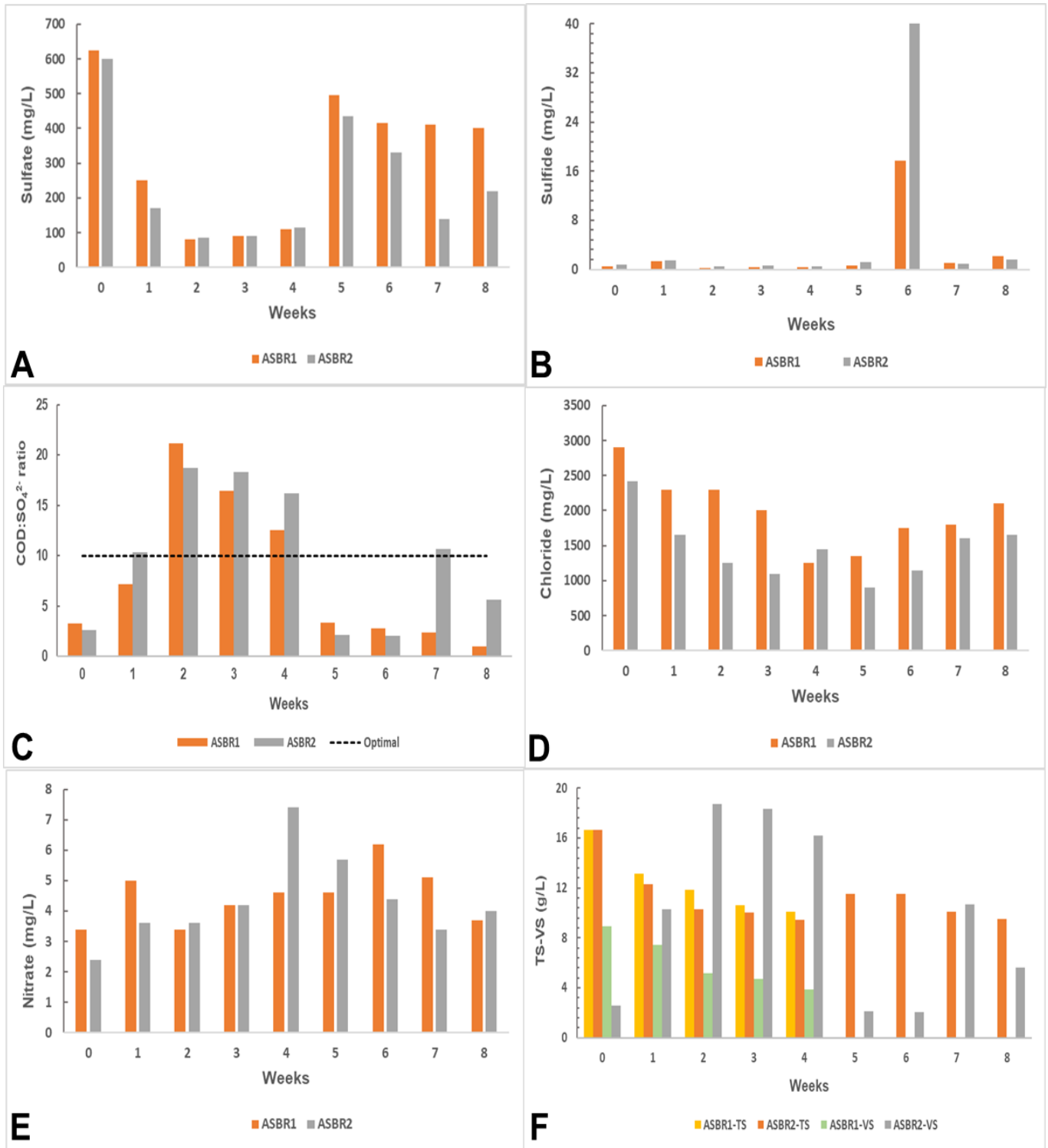


Figure 4.25: A= Sulfate concentration, B= sulfide concentration, C= chemical oxygen demand to sulfate ratio, D= chloride concentration, E= nitrate concentration, F= total solids and volatile solids in the anaerobic sequencing batch reactors. ASBR= anaerobic sequencing batch reactor

Table 4.9: Comparison of the results of this study with literature results on anaerobic digestion of tannery wastewater

Reactors	Batch digester	Batch digester	ASBR digester	2- stage ASBR	2- stage ASBR	Batch BMP	Batch BMP	2- stage ASBR	Batch BMP	ASBR digester	ASBR digester
Scale	lab-scale	Lab-scale	Pilot scale	Lab-scale	Lab- scale	Lab-scale	Lab-scale	Full-scale	Lab-scale	Pilot-scale	Pilot-scale
Reactor volume (L)	2	2		0.6	0.6	1	1	113 000*	2	20	20
Pre-treatment	-	Cavitation	-	Hydrolysis	Hydrolysis	-	Coagul.	Hydrolysis	-	-	-
Substrate	GTE	GTE	GTE	GTE	GTE	GTE	GTE	GTE	GTE	GTE	GTE
Co-substrate (type)	-	-	-	-	TWS	-	-	-	OSE	OSE	OSE
Co-substrate (%vol)	-	-	-	-	50	-	-	-	-	-	-
Operation mode	Batch	Batch	S-cont	S-cont.	S-cont.	Batch	Batch	S-cont.	Batch	Batch	Batch
Mixing mode	-	-	intermittent	-	-	-	-	-	intermittent	intermittent	continuous
Inoculum	Sewage	Sewage	Cow-dung	Manure	Manure	DAS	DAS	-	AS	AS	AS
Acclimation (days)	36	36	-	30	30	0	0	-	Long term	Long term	Long term
ISR (TVS/TVS)	-	-	-	-	-	1.5	1.5	-	2-5	3	3
RT (days)	35	35		20	20	37	37	-	16-60	20-30	20-30
Temp (°C)	37±0.2	37±0.2	31	38±2	38±2	35	35	-	37±2	37±2	37±2
OLR (gCOD/L.day ⁻¹)	-	-		2.1	2.8	-	-	1.0-2.2	-	-	-
Influent COD _t (g/L)	9.6	8.2		4.2	5.5	23.7	17.3	-	-	-	-
COD _t removal (%)	21	43		56	74	45	88	-	-	-	-
Influent CODs (g/L)	-	-	5.2-4.6	2.2	3.3	-	20.6	-	0.41-2.00	2.04	1.8
COD _s removal (%)	-	-	69-85	68	74	-	-	-	10.8-52.0	2.8-11.4	3.2-58.8
Biogas (mL/LRV.day ⁻¹)	-	-	-	-	-	-	-	230-319*	-	-	-
Biogas (mL/gVS)	66.7	136.7	-	-	-	≈653	≈737	-	4.97-361		
Biogas (mL/gCOD)	-	-		81	98	-	-	-	-	-	-
CH ₄ yield (mL/gVS)	7.6	26.5	-	-	-	437	703	-	1.02-166	11-99	400-749
CH ₄ yield (mL/gCOD)	-	-		56	61	-	-	-	-	-	-
Average CH ₄ (%)	11	19	55-70	45	61	58	84	61	9.30-44.8	-	-
References	Saxena et al., 2019	Saxena et al., 2019	Mekonnen, Leta & Njau, 2017	Berhe & Leta, 2018	Berhe & Leta, 2018	Achouri et al., 2017	Achouri et al., 2017	Alemu & Lemma, 2016	This study	This study	This study

*calculated from figures given in manuscript. Performance values expressed as averages where possible.

ISR = inoculum to substrate ratio RT = retention time OLR = organic loading rate COD_t = total chemical oxygen demand COD_s = soluble chemical oxygen demand RV = reactor volume ASBR = anaerobic sequencing batch reactor BMP = biochemical methane potential Cont. = continuous DAS = domestic anaerobic sludge GTE = general tannery effluent (combined beamhouse and tanyard) OSE = combined ostrich slaughterhouse effluent GTEV = general tannery effluent for vegetable tanning process

4.5. Summary

Biochemical methane potential tests were conducted in 2 L reactors to investigate the effect of ISR and SO_4^{2-} concentration on AD of TWW. From the results, it was evident that methanogenic inhibition was minimal when the reactors were operated $ISR \geq 3$ and/or lower SO_4^{2-} concentration ≤ 710 mg/L while high SO_4^{2-} concentration ≥ 1960 mg/L and $ISR < 3.0$ caused almost complete methanogenic inhibition regardless of corresponding ISR and SO_4^{2-} concentration, respectively. Based on RSM, the optimum operating conditions for maximal gas (CH_4 , biogas) and biodegradability were found to be 983.687 and 3.687 for SO_4^{2-} concentration and ISR respectively.

When the volume of the reactors was upscaled to 20 L, results showed that continuous mixing was more efficient than intermittent mixing. However, in full scale systems, the cost and complexity of continuous mixing is higher. It was assumed that biomass washout occurred during the decanting step due to the large drop of CH_4 production between successive runs in both ASBRs.

To further validate the observations and hypotheses developed in this Chapter, the methanogenic community and SRB involved in this study were investigated. These are reported in Chapter 5.

CHAPTER 5. INVESTIGATING THE DISTRIBUTION OF METHANOGENIC AND SULFIDOGENIC COMMUNITIES

5.1. Introduction

This chapter focuses on the methanogenic and sulfidogenic communities existing in the BMP test reactors and ASBRs. Section 5.3 discusses the microbial community analysis by NGS while Section 5.4 focuses on quantitative analysis of the target genes using qRT-PCR. It also investigates the correlations of these 2 communities with CH₄ production and SO₄²⁻ or S²⁻ concentration as well as the statistical significance of biotic and abiotic data on these communities' structure in the BMP experiments.

5.2. DNA extraction

As indicated in Section 3.6.1, a total of 52 and 20 samples (including the inoculum and substrate) were respectively collected from the BMP tests and the ASBRs. Genomic DNA was extracted from those samples and quantified using the Genova Nano micro-volume spectrophotometer (Jenway). The results are tabulated in Appendix C.

5.3. Next generation sequencing

5.3.1. Overall taxonomic comparison between methanogenic and sulfidogenic communities

The methanogenic and sulfidogenic communities contained in the selected 40 samples taken from the BMPs and the ASBRs were characterised by means of NGS at MR DNA using the *mcrA* and *dsrB* genes, respectively as phylogenetic markers. The phylogenetic study was performed at different taxonomic levels. These were kingdom, phylum, family, class, genus and species. However, this section briefly enumerates the different distributions based on sample abundance of operational taxonomic units up to the genus level. The analyses of species are described in detail in Section 5.3.2.

5.3.1.1. Methanogenic community

As expected, the phylogenetic analysis results showed that the methanogens in this study were exclusively archaea. They were divided into 6 classes and 15 families within the phylum *Euryarchaeota* and were comprised of 19 genera. Figure 5.1A illustrates the class distribution

of methanogens in the reactors. It shows that *Methanomicrobia* was the most dominant class with 41-78% of abundance followed by *Methanobacteria* (15.32-69.43%) and *Thermoplasmata* (2.17-11.65%). At abundance level, dominant methanogens belonged to family *Methanobacteriaceae* (15.28-68.80%), *Methanosaetaceae* (13.53-46.74%), *Methanosarcinaceae* (2.25-32.47%), *Methanomicrobiaceae* (0.48-40.75%) and *Methanomassiliicoccaceae* (1.98-11.10%) (Figure 5.1B). However, in contrast to other methanogenic environments, which typically host many genera (Angel et al., 2011), the diversity of this study was low. Furthermore, out of the 23 genera represented, only 5 were dominant. These were *Methanosarcina*, *Methanosaeta*, *Methanoculleus*, *Methanobacterium* and *Methanomassiliicoccus* (Figure 5.1C). This indicates that the 3 forms of methanogenesis can occur in this study: (i) acetoclastic methanogenesis by members of the genus *Methanosaeta* and *Methanosarcina* which use acetate to produce CH₄. However, some species of *Methanosarcina* are facultative acetoclastic methanogens which use H₂/CO₂ and C-1 compounds in addition to acetate for methanogenesis (Venkiteshwaran et al., 2015); (ii) hydrogenotrophic methanogenesis by members of the genus *Methanoculleus* and *Methanobacterium* which grow and produce CH₄ from H₂/CO₂ and formate and (iii) methylotrophic methanogenesis by members of the genus *Methanomassiliicoccus* which produce CH₄ from methylated compounds (Kröniger et al., 2017). Salvador et al. (2013) also reported the endurance of methanogenic archaea in continuous anaerobic bioreactors treating oleate-based wastewater, with *Methanobacterium* and *Methanosaeta* being the predominant genera of hydrogenotrophic and acetoclastic methanogens, respectively.

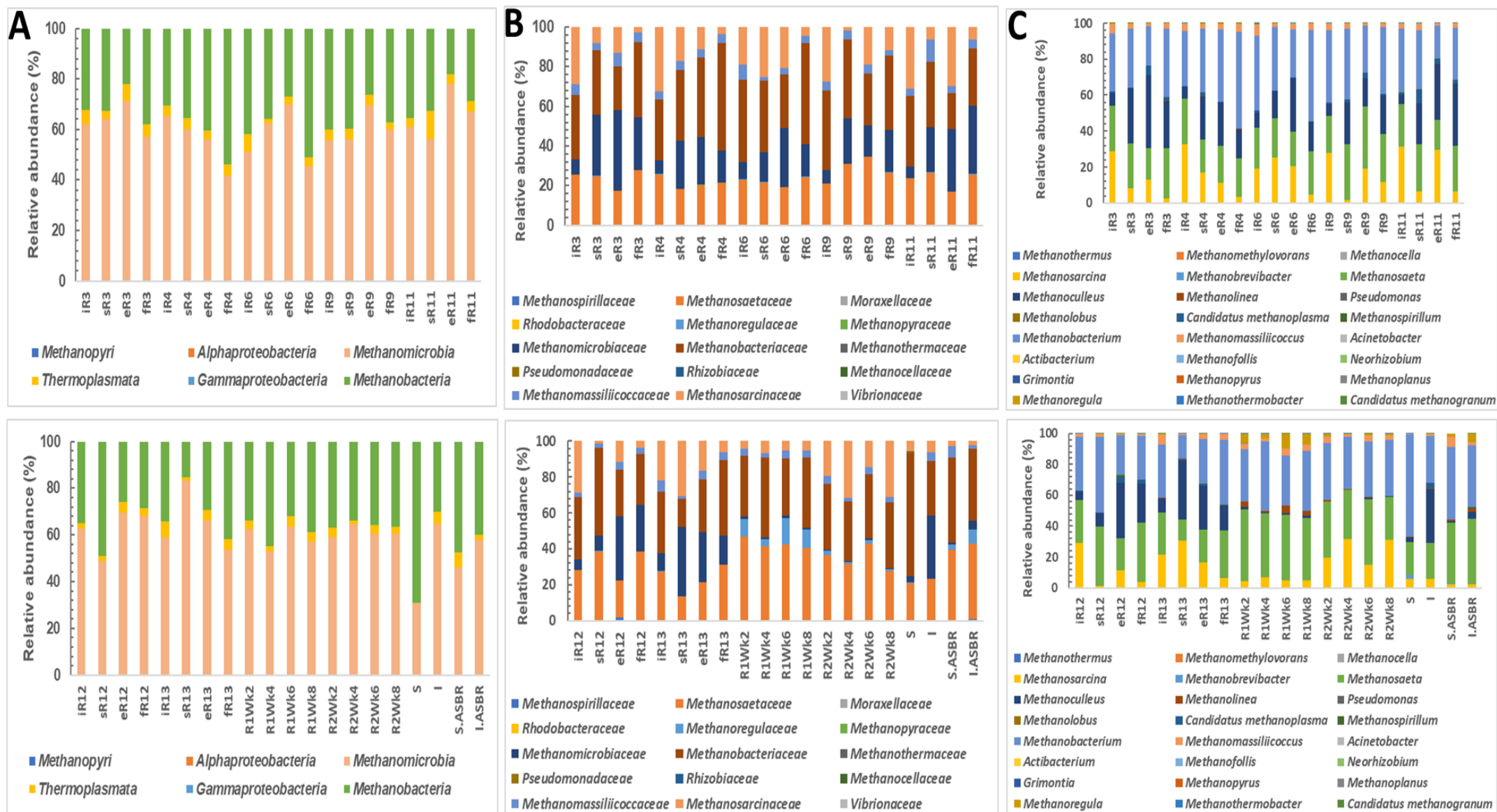


Figure 5.1: Methanogenic distribution in the study (A) class (B) family (C) genera. I= initial, S= start of gas production, E= end of gas production, F= final (end of study), WK = week, S= substrate, I= inoculum, ASBR= anaerobic sequencing batch reactor

5.3.1.2. Sulfidogenic community

As revealed by the NGS results, the sulfidogenic community in the digesters was more diverse than the methanogenic community. The univariate indices indicate that richness, Shannon diversity and Pielou evenness were higher in the sulfidogenic community than in the methanogenic community (Appendix E). The results show that this community was composed of numerous phyla such as *Chlorobi*, *Nitrospirae*, *Firmicutes* and *Proteobacteria*. However, only 2 were dominant i.e. *Proteobacteria* and *Firmicutes* as illustrated in Figure 5.2.

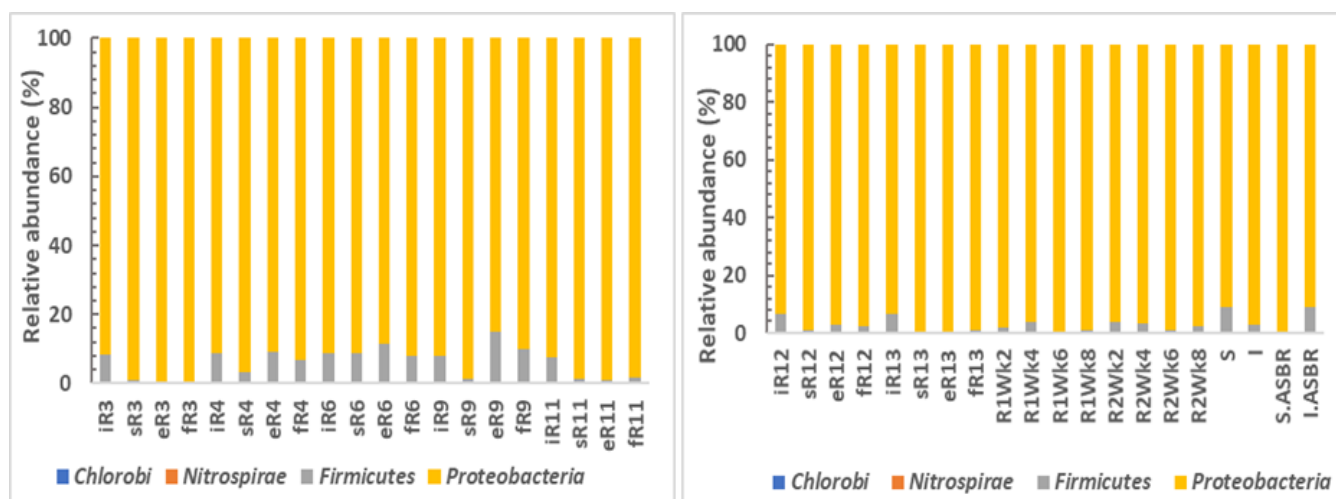


Figure 5.2: Sulfidogenic community phylum distribution. I= initial, S= start of gas production, E= end of gas production, F= final (end of study), WK = week, S= substrate, I= inoculum, ASBR= anaerobic sequencing batch reactor

The values of relative abundance of SRBs show that *Deltaproteobacteria* represented the most abundant class in this study (88.54-99.88%) followed by *Clostridia* (0.22-11.44%) (Figure 5.3A). Li et al. (2015) reported that members of the class *Deltaproteobacteria* can be observed in most sulfate-rich environments. These were then distributed into 16 families. Figure 5.3B represents the family distribution of the SRB in the reactor samples. From that figure, it can be seen that at relative abundance level, *Desulfovibrionaceae* (4.03-95.46%), *Desulfobulbaceae* (0.87-60.06%), *Desulfobacteraceae* (0.66-50.72%), *Desulfomicrobiaceae* (0.50-43.58%), *Syntrophobacteraceae* (0.82-32.17%) and *Peptococcaceae* (0.46-14.88%) were the most dominant families. A total of 27 genera were identified in this study, with the most predominant being *Desulfovibrio* (4.00-95.43%) followed by *Desulfobulbus* (1.50-60.04%), *Desulfomicrobium* (0.50-43.58%), *Syntrophobacter* (0.47-32.00) and *Desulfobacterium* (0.28-30.81%). According to Houari et al. (2017), the most remarkable characteristic of members of the genus *Desulfobulbus* is their ability to oxidize propionate in the presence of SO_4^{2-} to acetate, and to ferment pyruvate and lactate to a mixture of acetate and propionate.

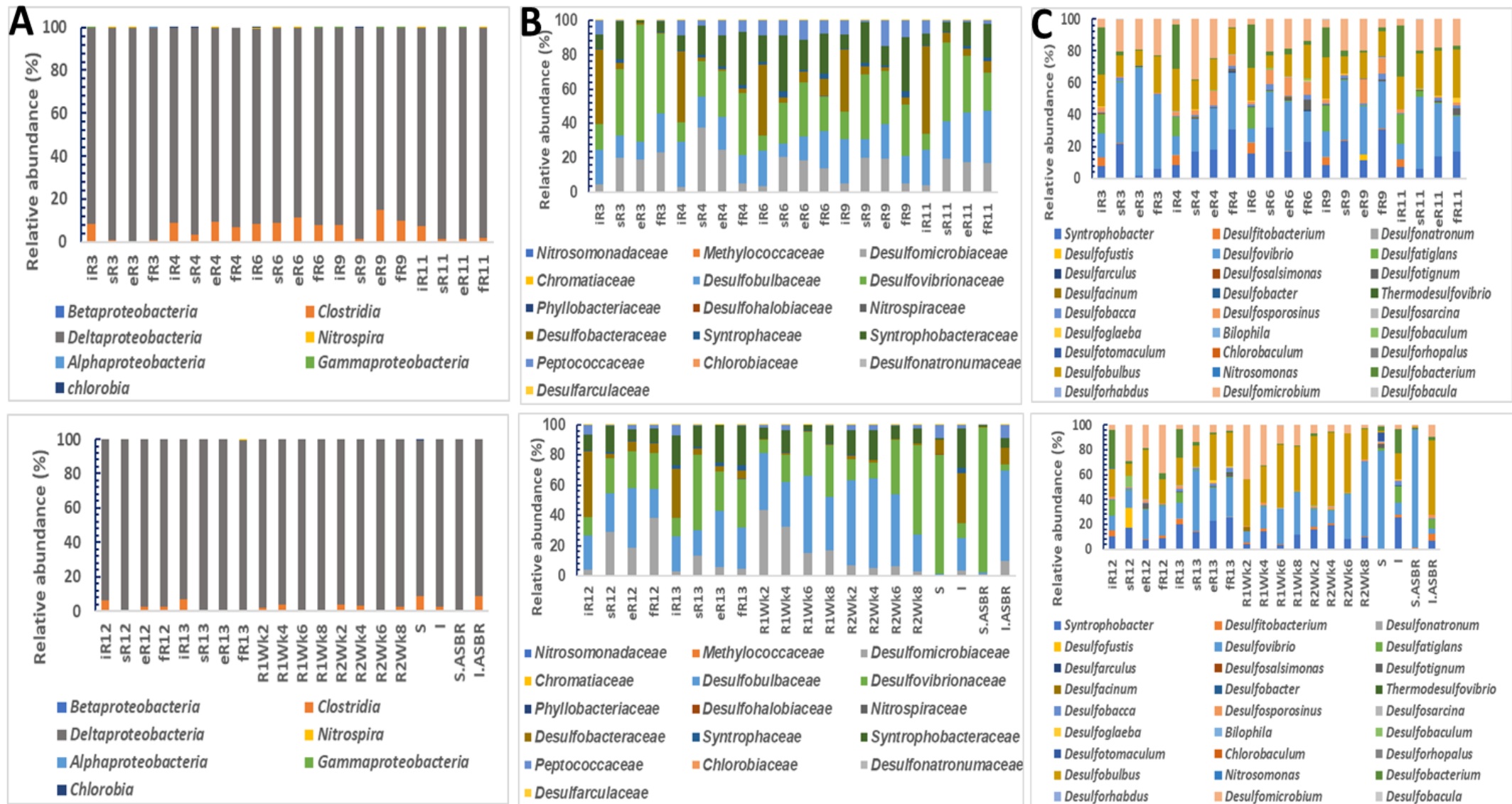


Figure 5.3: Sulfidogenic community distribution (A) class (B) family (C) genera. I= initial, S= start of gas production, E= end of gas production, F= final (end of study), WK = week, S= substrate, I= inoculum, ASBR= anaerobic sequencing batch reactor

5.3.2. Selection of sulfidogenic and methanogenic microbial communities during anaerobic digestion of ostrich tannery wastewater

5.3.2.1. Sulfidogenic microbial community

The microbial community species from the different BMP tests and ASBRs were compared by statistical analysis of the NGS results. The results were visualized by the spatial distribution of points representing samples and reactors in nMDS plots (Figure 5.4) with cluster analyses (Figure 5.5).

The nMDS plots depicting similarities in the sulfidogenic microbial community samples have stress values of 0.1 (Figure 5.5A) and 0.02 (Figure 5.5B) for the BMPs and ASBRs respectively, which represent ideal ordinations with little chance of misinterpretation. According to Wilson et al. (2013), stress values less than 0.1 represent 2D ordinations with little risk of misinterpretation, values less than 0.2 correspond to useful ordinations, and values over 0.2 represent nearly random plots.

The nMDS plot in Figure 5.5A revealed that the initial samples from the BMPs were strongly influenced by the inoculum as they are closely clustered together at 85% similarity level, while the rest of the samples are clustered together at 60% similarity level. The shade plot (Figure 5.6) based on Bray-Curtis similarity also clearly showed the same clustering pattern observed in the nMDS analysis. Uncultured *Syntrophobacter* sp., *Desulfobacterium autotrophicum*, *Desulfatiglans anilini* and uncultured *Desulfobulbus* sp. were found to be the most abundant species in the inoculum and the initial samples. From the substrate, the initial samples also selected *Desulfovibrio fructosivorans* (2.82-11.25%) which is known to differ from all other described *Desulfovibrio* species by the ability to use fructose or lactase (Martins et al., 2009). However, the relative abundance of this species decreased with time. Interestingly, there was a shift in the community structure in the samples taken between t=0 (baseline) and start of gas production, end of gas production and end of study (shown by arrows on Figure 5.5). The increase of some species was observed when the reactors started to produce biogas. At high level of abundance these species were *Desulfomicrobium* sp. enrichment culture (13.35-37.52%), *Desulfovibrio aminophilus* (13.93-43.4%) and *Desulfobulbus rhabdoformis* in some samples. According to Kushkevych et al. (2017), these detected species are acetogenic microorganisms which oxidize organic compounds incompletely to acetate and CO₂, which could be useful to other SRBs and methanogens. *Desulfovibrio aminophilus* has previously been reported to play an important metabolic role in anaerobic digesters by using single amino acids if SO₄²⁻ is present (Baena et al., 1998).

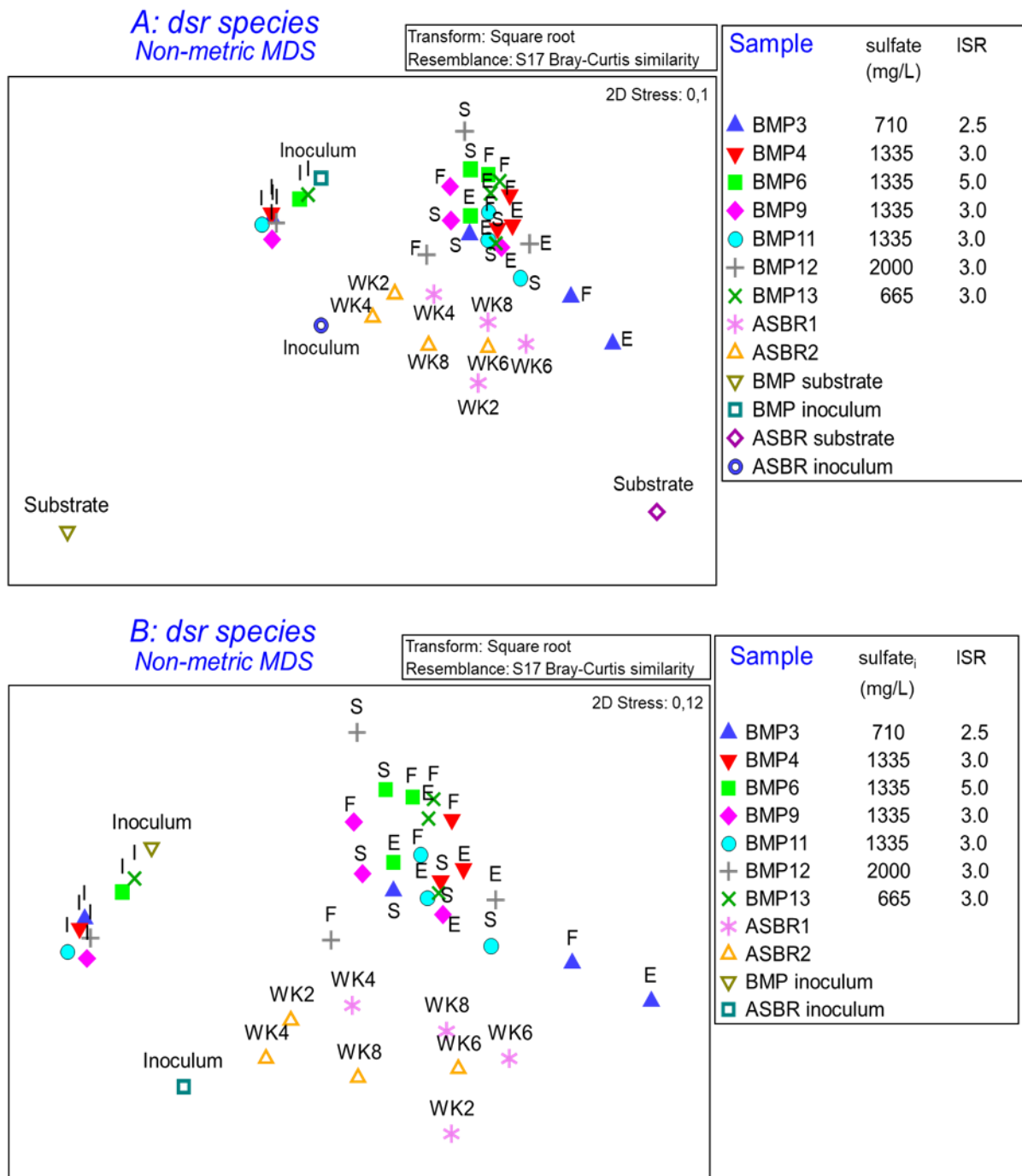


Figure 5.4: Non-metric multidimensional scaling plots of *dsr* amplicon sequencing results: (A) all samples, and (B) all samples excluding substrates. I= initial, S= start of gas production, E= end of gas production, F= final (end of study), WK = week

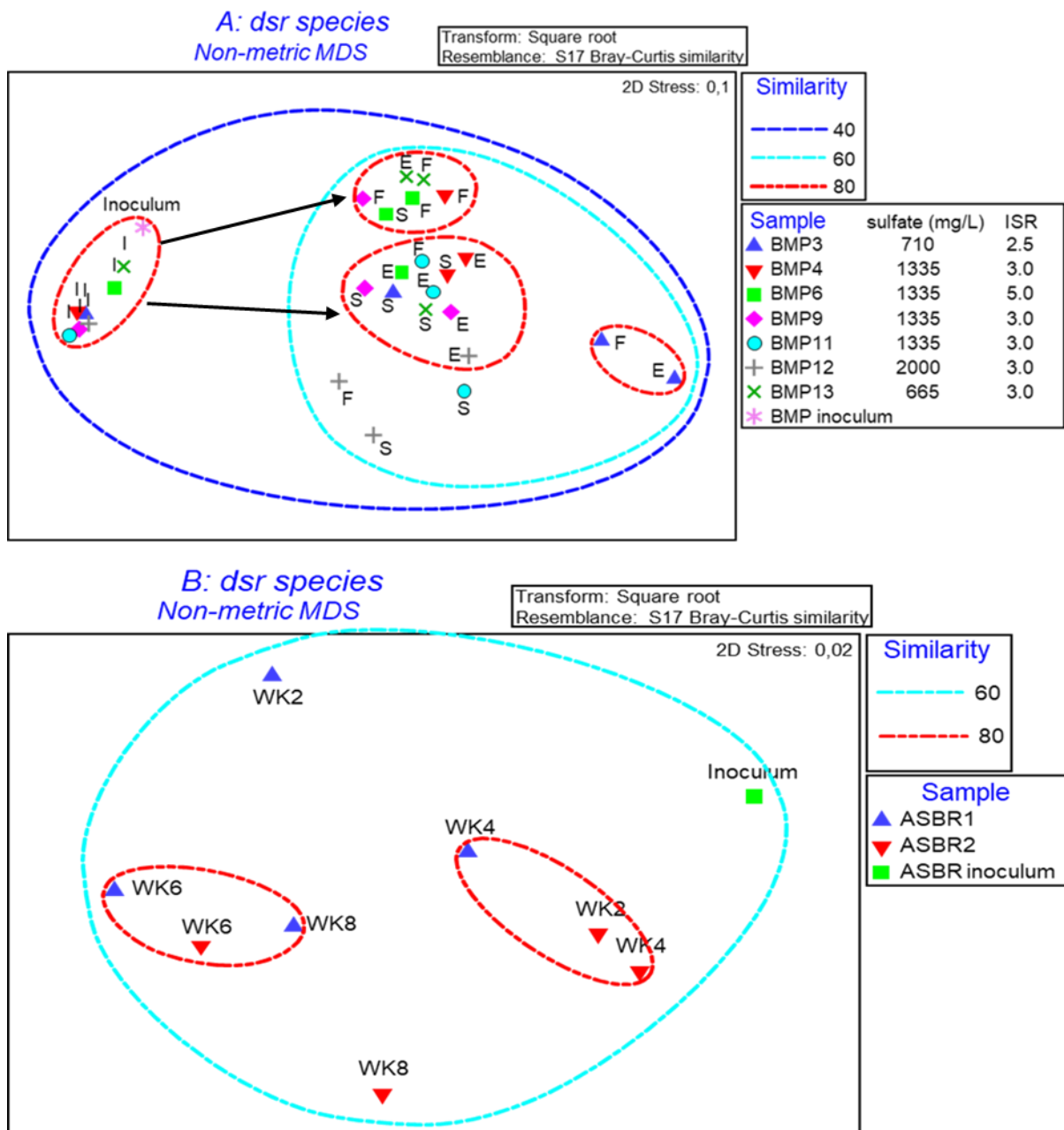


Figure 5.5: Non-metric multidimensional scaling plots of *dsr* amplicon sequencing results: (A) all samples, and (B) all samples excluding substrates. I= initial, S= start of gas production, E= end of gas production, F= final (end of study), WK = week

In an attempt to determine whether the sulfidogenic microbial community may be impacted by SO_4^{2-} concentration, the BMPs were grouped based on initial SO_4^{2-} concentrations i.e. ≤ 710 , $=1335$ and $=2000$ mg/L. It is worth noting that contrary to what was expected, the relative abundance of the main species in the phyla *Proteobacteria* did not change with the increase in influent SO_4^{2-} concentration (Figure 5.6). According to Plugge et al. (2011) and Cetecioglu et al. (2019), this could be explained by the metabolic flexibility of SRB, which allows some of

them to act as fermenters when SO_4^{2-} is not available. This was in line with Jiang et al. (2019) but not consistent with the observations of Lu et al. (2017). The former studied the spatial separation and bio-chain cooperation between sulfidogenesis and methanogenesis in an ABR remediating sugar wastewater, while the latter studied the sulfidogenesis process to strengthen re-granulation for biodegradation of methanolic wastewater and microorganisms' evolution in an UASB reactor. They noted considerable shifts in the microbial community with a decrease in the $COD:SO_4^{2-}$ ratio (via increased SO_4^{2-} concentration) from 20 to 2.0. However, in this study, high relative abundance (15,91%) of *Desulfofustis glycolicus* was detected in the BMP test (BMP12) operating at $SO_4^{2-} = 2000$ mg/L at the start of gas production, while the other reactors contained <0.03% of this species. *Desulfofustis glycolicus* has been reported by Friedrich & Schink (2008) to reduce SO_4^{2-} , SO_3^{2-} and elemental S^0 to H_2S . This agrees with the results of the BMPs outlined in CHAPTER 4. The produced H_2S might have an inhibitory effect on some methanogenic species, which might have lowered the CH_4 generation (Isa et al., 1986b; Cetecioglu et al., 2019).

For the ASBRs, the nMDS plot shows that both reactors were influenced by the inoculum as all the weekly samples were clustered close to the inoculum at 60% similarity level (Figure 5.5B). Figure 5.7 summarizes all species containing the *dsrB* gene with >1% of population in any one sample. An uncultured *Desulfobulbus sp.* was found to be the most dominant species in the inoculum and also detected at high abundance in the ASBRs. The first runs also selected *Desulfovibrio aminophilus* from the substrate, however at low abundance (6.08-14.27%).

As shown in Figure 5.5A, a shift in the *dsrB*-containing community structure was observed between week 2 and week 4 in the first run of ASBR1. In contrast, week 4 showed 80% community structure similarity to weeks 2 and 4 in ASBR2 (Figure 5.5), indicating that the 3 weeks are colonized by the same phylotypes and also the acclimation of the bacterial communities in ASBR1. When comparing both ASBRs, high relative abundance (32.27-43.46%) of *Desulfomicrobium sp.* enrichment culture was observed in run 1 of ASBR1, while in ASBR2, a low relative abundance (4.58-6.32%) of this species was found. It can be hypothesized that this difference in species selection was due to the different mixing protocols, and may have contributed to the difference in the ultimate performance of the two ASBRs. In run 2, both ASBRs were dominated by *Desulfovibrio aminophilus* (25.77-27.62% in ASBR1 and 26.18-48.65% in ASBR2) obtained from the new substrate and by *Desulfobulbus rhabdoformis* while the abundance of uncultured *Desulfobulbus sp.* obtained from the inoculum decreased (Figure 5.7).

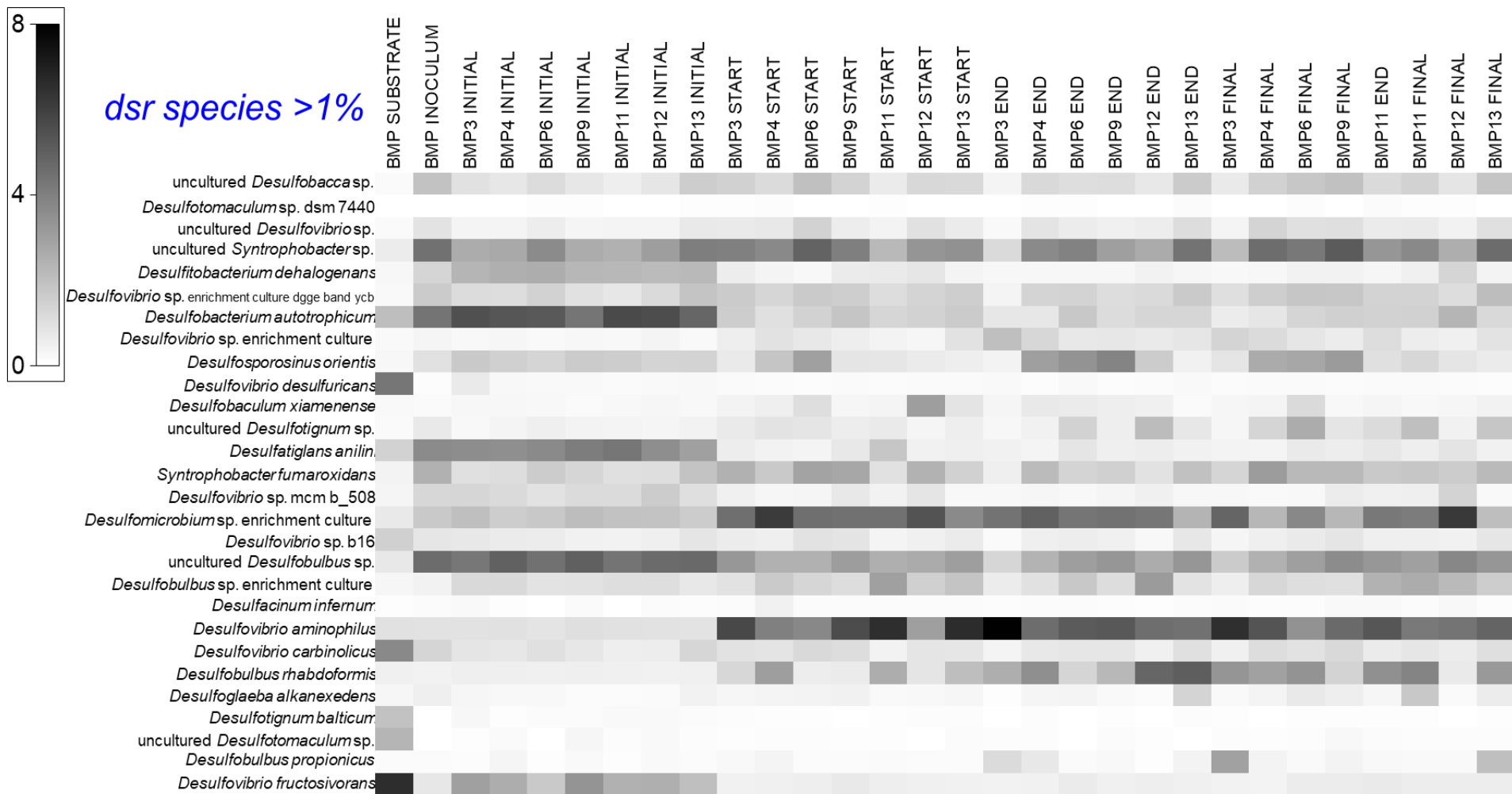


Figure 5.6: Shade plot of square root transformed Bray-Curtis similarity data from dsr amplicon sequencing, with group average linkages between samples, and index of association of species standardised by total resemblance. Inclusive of all species >1% of population in any one sample (28 of 78 species).

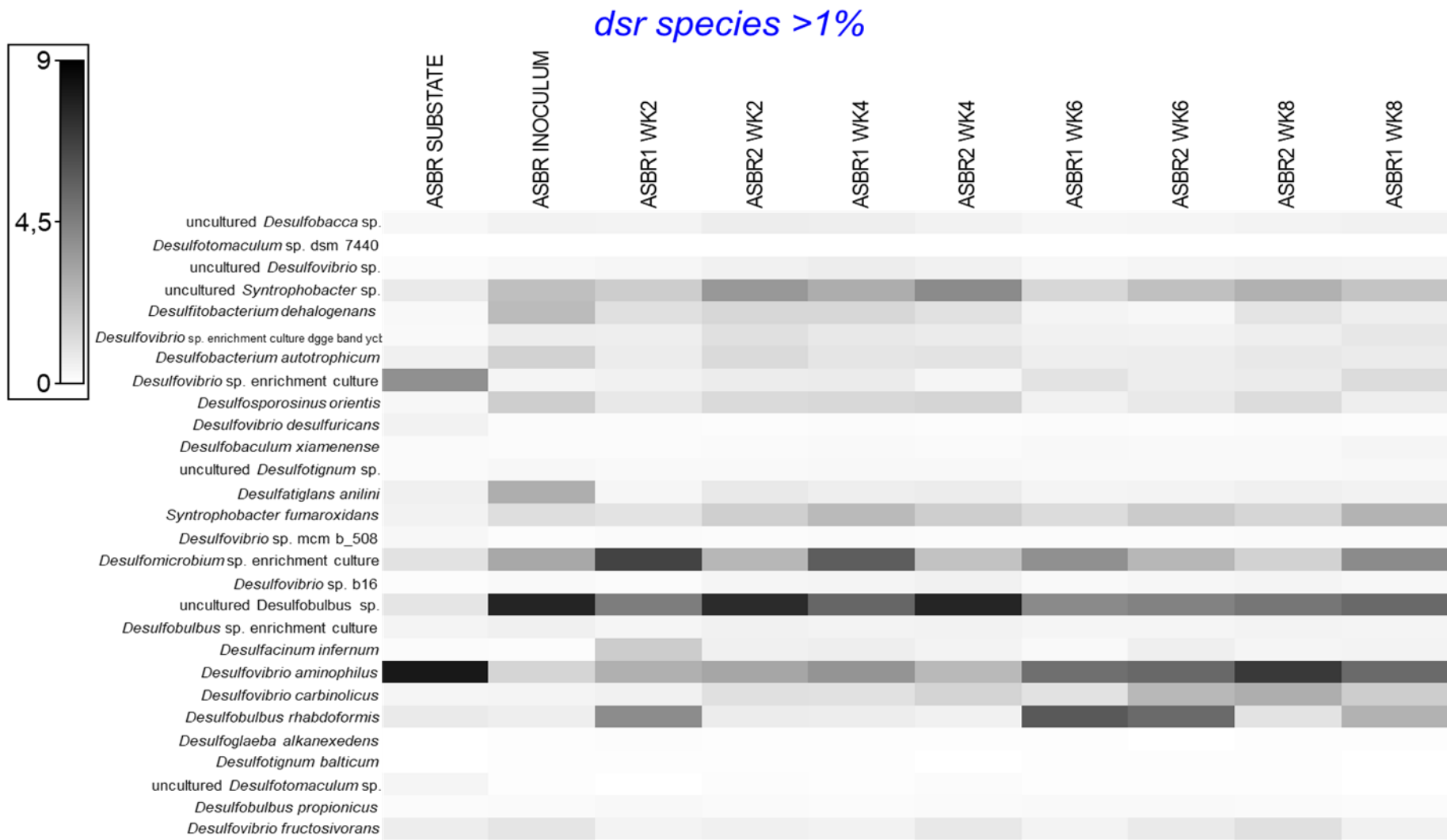


Figure 5.7: Shade plot of square-root transformed data from dsr amplicon sequencing of samples from anaerobic sequencing batch reactors. Inclusive of all species >1% of population in any one sample (28 of 78 species). WK = week

5.3.2.2. Methanogenic community

Like the sulfidogenic community, the methanogenic community species from the different BMP tests and ASBRs were compared by statistical analysis of the NGS results. The results were visualized by the spatial distribution of points representing samples and reactors (Figure 5.8) in nMDS plots overlaid with results of cluster analyses (Figure 5.9).

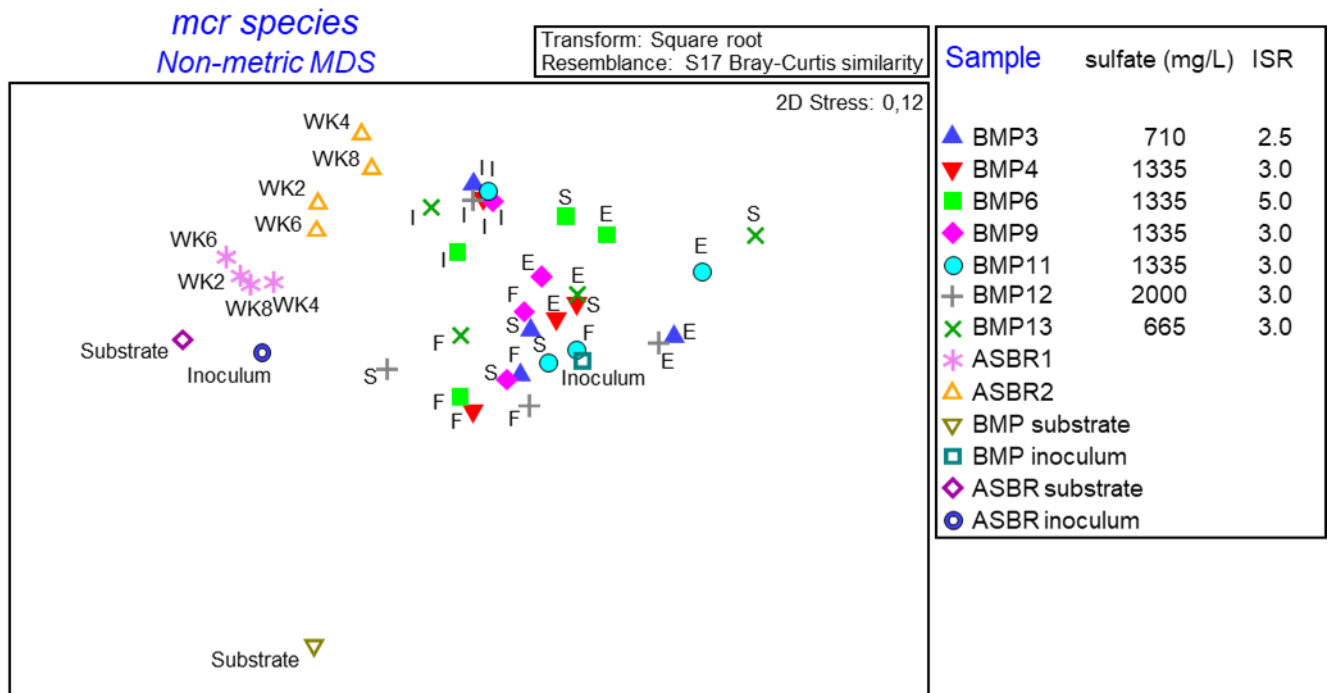


Figure 5.8: Non-metric multidimensional scaling plots of *mcr* amplicon sequencing results. I= initial, S= start of gas production, E= end of gas production, F= final (end of study), WK= week

The stress values of the nMDS plot of the BMPs species (Figure 5.9A) and the ASBRs (Figure 5.9B) were 0.11 and 0.01 respectively. Although the stress value of the BMPs is slightly higher than the ideal value of 0.1, this plot still represents a useful ordination for visualizing similarities in archaeal communities (Wilson et al., 2013).

Unlike the sulfidogenic community where the initial reactor samples were well clustered together with the inoculum, the methanogenic community was not strongly influenced by the inoculum (Figure 5.9). It was hypothesized that there was a rapid change in these very sensitive communities due to exposure to O₂ and/or the new substrate during the reactor set-up. Figure 5.10 summarizes archaeal species containing the *mcrA* gene for each of the BMP tests. A total of 42 species were identified. However, only those >1% of population in any one sample were included in the shade plot. *Methanoculleus bourgensis* and *candidatus*

Methanoplasma termitum were found abundantly in the inoculum, but they were not detected in the initial samples. Methanogens have long been considered strictly anaerobic and O₂-sensitive microorganisms, but their ability to survive O₂ stress has also been reported (Ueki et al., 1997; Ma et al., 2012; Lyu & Lu, 2017). *Methanobacterium* sp., *Methanosaeta* sp., *Methanobacterium petrolearium* and *Methanosarcina mazei* were found resilient to change due to exposure to O₂ and their tenacious resistance to O₂ exposure was also reported by Liu et al. (2008).

The nMDS in Figure 5.9A also shows that all the samples with the exception of the substrate were clustered together at 80% level of similarity. In other words, relatively small changes in the *mcrA*-containing archaeal community structures were observed during the biodegradation of ostrich tannery wastewater and its potential to produce CH₄. SIMPER analyses across all the sampling periods in each test were performed, and they revealed similarities of 83.38, 85.98, 84.81, 86.07, 83.25, 80.66, 80.41% in BMPs 3, 4, 5, 9, 11, 12 and 13 respectively (Appendix F).

From Figure 5.10, it can also be seen that the methanogenic community was negatively influenced in the reactor operating at $SO_4^{2-} \geq 1960$ mg/L. In comparison to the other reactors at the start of gas production, an absence of *Methanosarcina mazei* and a lower abundance of *Methanoculleus chikugoensis* (0.17%) was found. It was hypothesized that these species are less tolerant to higher SO_4^{2-} concentration. Instead, this reactor (BMP12) contained higher relative abundances of *Methanosaeta* sp. and *Methanosaeta concilli*, suggesting low concentration of acetate, because according to Venkiteshwaran et al. (2015), *Methanosaeta* species have a relatively slow growth rate but possess a high affinity for acetate and hence dominate at low acetate concentration. However, the VOA concentration in this reactor at the start of biogas generation (382 mg/L) was slightly higher than in the other reactors (198-374 mg/L), which contradicted this hypothesis. The absence of *Methanosarcina mazei* was therefore hypothesised to be responsible for the low CH₄ production at $SO_4^{2-} \geq 1960$ mg/L.

In the ASBRs, the methanogenic community was influenced by both the substrate and the inoculum. The nMDS plot in Figure 5.9B indicates 90% species similarities. High relative abundance of *Methanobacterium* sp. was found in the inoculum, but temporal fluctuations in the relative abundance of this species was seen in both ASBRs (Figure 5.10), which coincided with fluctuating VOA concentrations (Figure 4.6A). Two well-known acetoclastic methanogenic species i.e. *Methanosaeta* sp. and *Methanosaeta concilli* and one hydrogenotrophic methanogen species, *Methanobacterium petrolearium* obtained from the substrate were also detected in both ASBRs at high abundance (10.8-27.7%, 5-

19.2% and 16.3-34.8% respectively) indicating that acetoclastic and hydrogenic methanogenesis took place. Little changes occurred in the community during the study. SIMPER indicated average similarities of 91.93 and 90.62% in ASBR1 ASBR2 respectively (Appendix F).

When comparing both ASBRs, 14.79 of average dissimilarity percentage between the various sample groups was obtained based on their Bray-Curtis similarity resemblance (Appendix F). The SIMPER analyses also showed that *Methanosaeta* sp. was the most dominant species in ASBR1 while in ASBR2, *Methanosarcina mazei* dominated. It can therefore be hypothesized that *Methanosarcina mazei* may have contributed to the higher CH₄ production in ASBR2. For Vrieze et al. (2012) *Methanosarcina mazei* is a very robust methanogen and is crucial for anaerobic digestion at high OLR. As illustrated in Figure 5.11, *Methanosarcina mazei* was detected in both ASBRs with better survival and higher relative abundance in ASBR2 (14.7-31.6%) than in ASBR1 (4.3-6.8%). According to Zhang et al. (2020), this selection is due to continuous mixing, and is in accordance with the results obtained by McMahon et al. (2001) and Hoffmann et al. (2008), who observed an increase in *Methanosarcina* spp. in continuously stirred anaerobic digesters treating animal manure. In this study it also resulted in high cumulative CH₄ yield (749 and 400 mL/gVS respectively in runs 1 and 2 of ASBR2, versus 96 and 11 mL/gVS run1 and 2 of ASBR1).

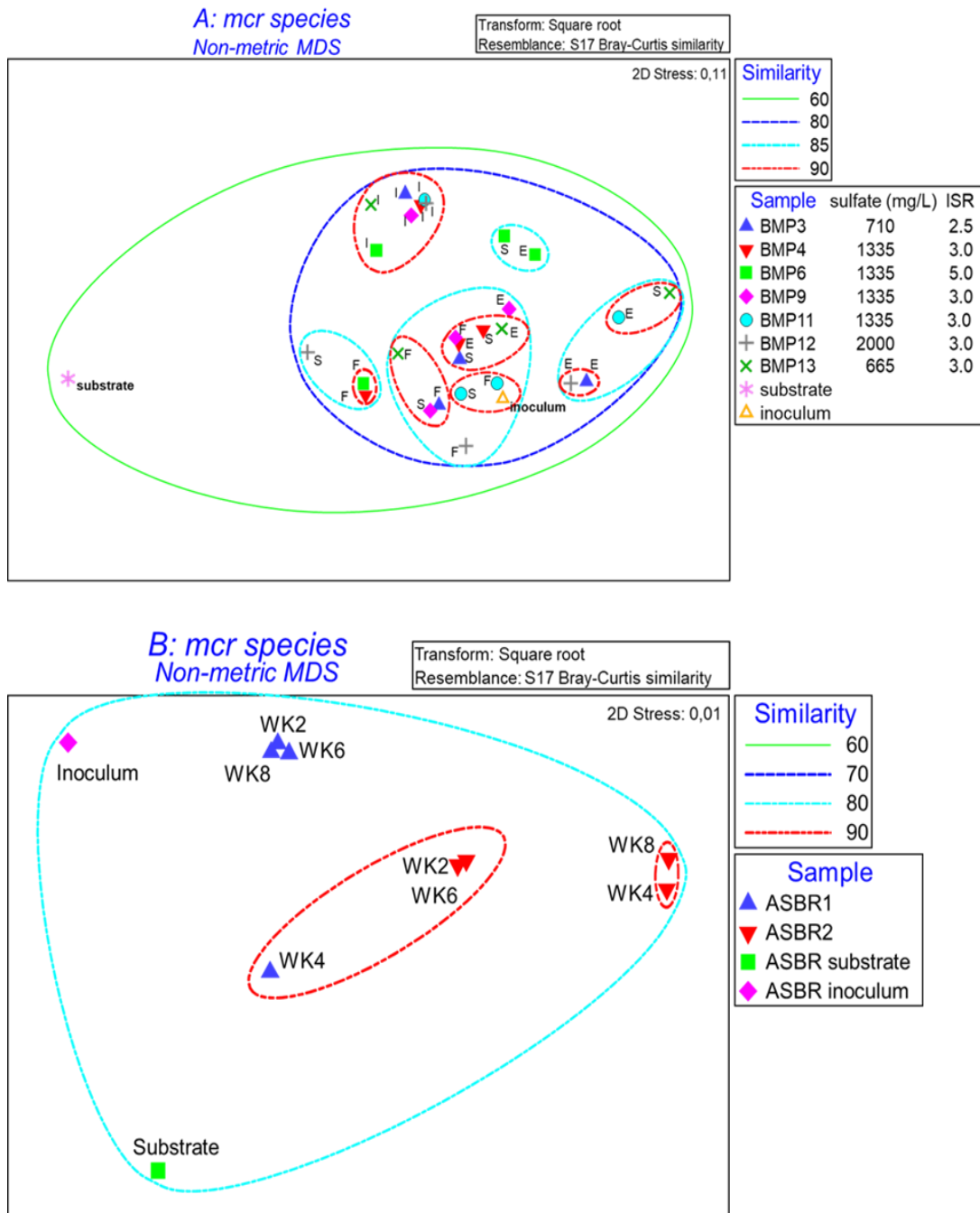


Figure 5.9: Non-metric multi-dimensional scaling plots overlaid with cluster plots (group average linkage) of *mcr* amplicon sequencing results of samples from (A) biochemical methane potential test reactors and inoculum, and (B) anaerobic sequencing batch reactors and inoculum. I = initial, S = start of gas production, E = end of gas production, F = final (end of study), WK = week

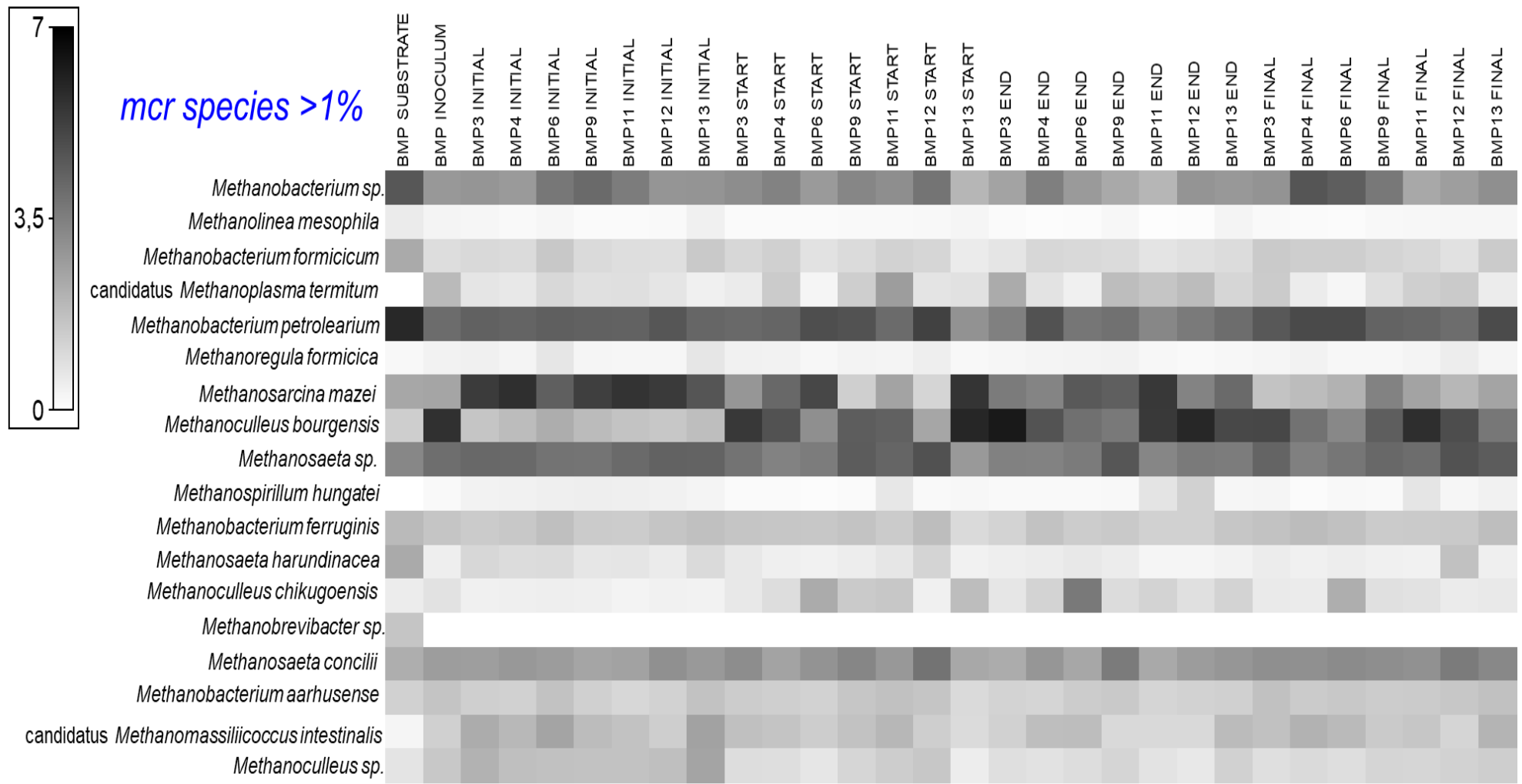


Figure 5.10: Shade plot of square root transformed data from *mcr* amplicon sequencing of samples from biochemical methane potential test reactors. Inclusive of all species >1% of population in any one sample (18 of 42 species)

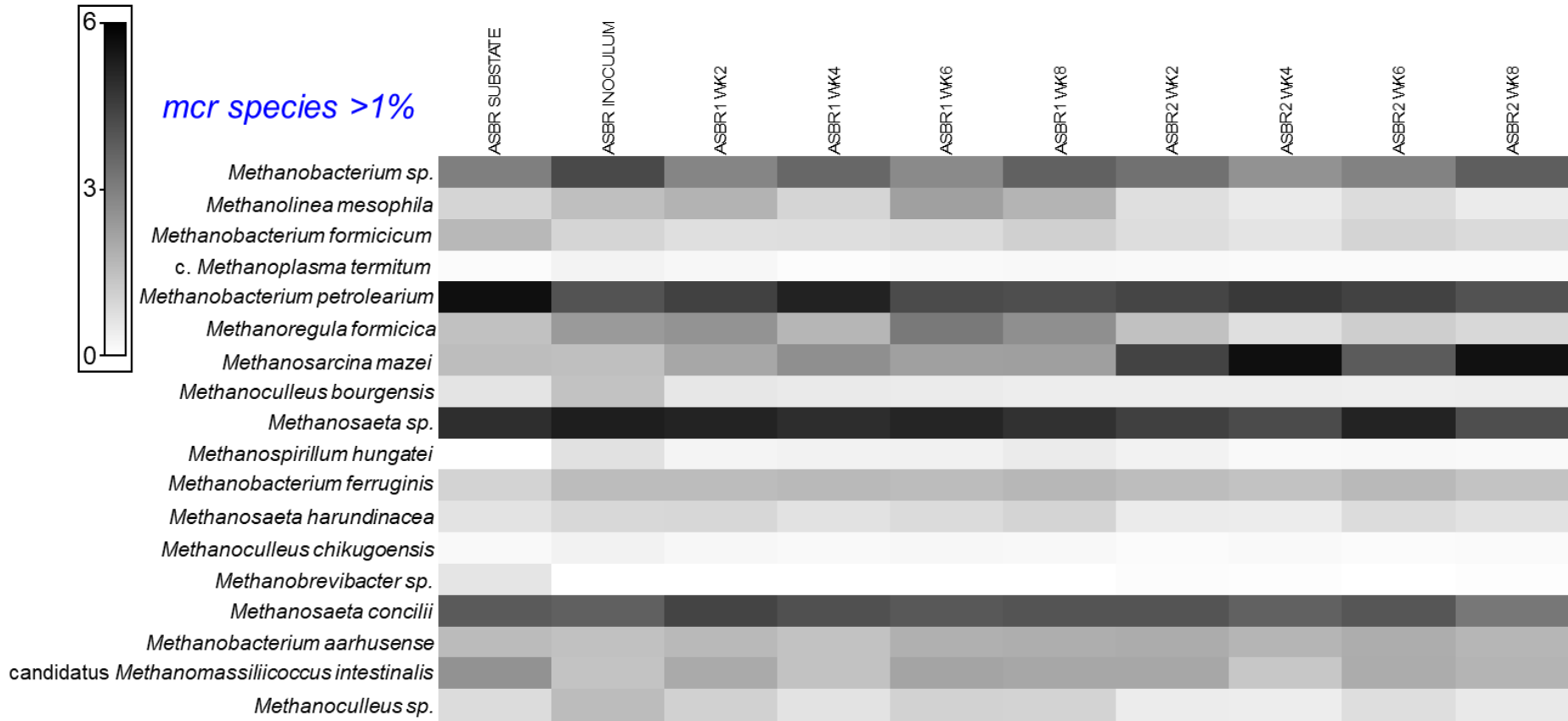


Figure 5.11: Shade plot of square root transformed data from mcr amplicon sequencing of samples from anaerobic sequencing batch reactors. Inclusive of all species >1% of population in any one sample (18 of 42 species)

5.4. Quantitative real-time polymerase chain reaction

5.4.1. Optimisation of the PCR amplification of target genes

As previously mentioned, methanogens and SRB play an important role in AD for the degradation of organic material and production of CH₄. Therefore, monitoring these communities is crucial for understanding and improving the performance of anaerobic reactors. In this study, to measure methanogenic and sulfidogenic activities from the reactors, qRT-PCR was conducted.

The target genes (*mcrA* and *dsrB*) were successfully amplified by conventional PCR using genomic DNA extracted from a fresh inoculum collected as described in Section 3.2 using the methods and PCR conditions described by Luton et al. (2002) and Agrawal & Lal (2009) and specific primer sets. They were then separated on a 1.5% agarose gel electrophoresis (Figure 5.12 and Figure 5.13). The expected single product size between 464-491 bp was obtained for the *mcrA* gene while the *dsrB* gene yielded an expected product size of 350 bp. The amplicons were then purified, cloned and plasmids isolated. The isolated plasmids were subjected to PCR to verify that the correct genes were cloned. Furthermore, they were sequenced and were found to have >90% identity to the *mcrA* and *dsrB* genes (Table 5.1).

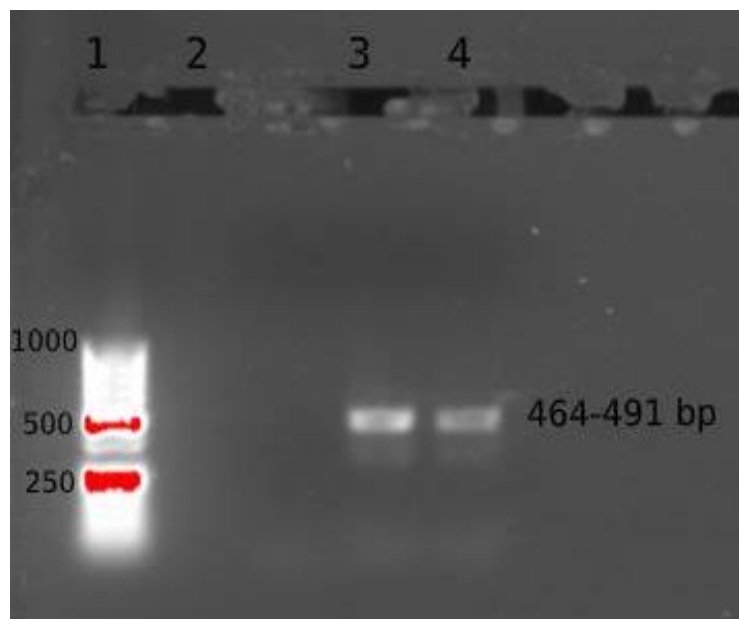


Figure 5.12: 1.5% agarose gel electrophoresis showing the amplification of the *mcrA* gene after conventional PCR, lane 1: gene ruler, lane 2 negative control, lanes 3-4: inoculum sample

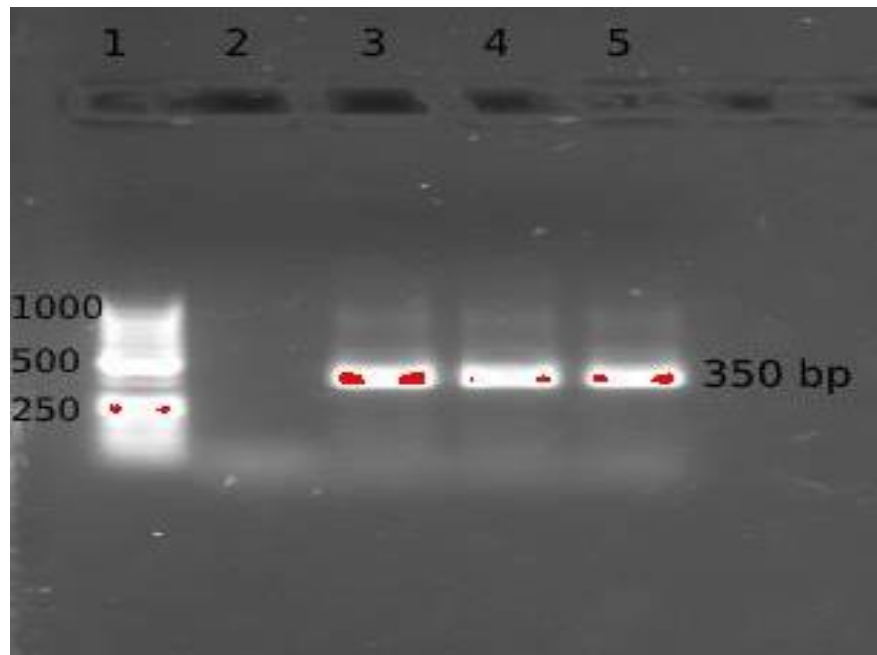


Figure 5.13: 1.5% agarose gel electrophoresis showing the amplification of the *dsrB* gene after conventional PCR, lane 1: gene ruler, lane 2 negative control, lanes 3-5: inoculum sample

Table 5.1: *mcrA* and *dsrB* genes sequences identification

Plasmid name	Total score	Query cover (%)	Description	ID sequence (%)	Accession Number
S1	636	87	<i>mcrA</i> gene	98.87	EU636869.1
S1B	636	87	<i>mcrA</i> gene	98.87	EU636869.1
S2	642	82	<i>mcrA</i> gene	100	KC292223.1
S3	433	80	<i>mcrA</i> gene	91.19	LC002167.1
S4	435	82	<i>mcrA</i> gene	90.77	LC002167.1
A	467	100	<i>dsrB</i> gene	96.44	AY626029.2
B	291	72	<i>dsrB</i> gene	95.58	KF269054.1
C	462	100	<i>dsrB</i> gene	98.58	AY626029.2
D	281	76	<i>dsrB</i> gene	98.10	AY626029.2
E	550	99	<i>dsrB</i> gene	99.22	AY626029.2
F	541	99	<i>dsrB</i> gene	98.41	AY626029.2
G	377	99	<i>dsrB</i> gene	98.18	AY626029.2
H	432	97	<i>dsrB</i> gene	96.37	AY626029.2
I	426	99	<i>dsrB</i> gene	99.23	AY626029.2

ID= identity

5.4.2. Standard curves

Triplicate serial dilutions of isolated plasmids were used for the preparation of standard curves. The linearity and reproducibility of the standard curves were tested. The *mcrA* gene standard curve was linear from 4.77×10^9 to 1.53×10^6 copies per μl while the *dsrB* gene was linear from 6.52×10^9 to 6.52×10^6 copies per μl . This was applied in all runs of this study.

As shown in Figure 5.14 and Figure 5.15, the derivative melting curve obtained from both genes exhibited a single peak, indicating that single amplicons were generated by qRT-PCR and no primer-dimers occurred. However, because 2 types of single peaks (shown by arrows in Figure 5.14) were obtained when performing qRT-PCR on genomic DNA extracted from the BMPs and the ASBRs with the *mcrA*, one random product was evaluated using 1.5% agarose gel electrophoresis together with 2 standard dilutions (Figure 5.16) to investigate if non-specific amplification of DNA other than *mcrA* occurred. Single bands of about 464-491 bp were visualised in the agarose gel, indicating that different species of methanogens were amplified. This is confirmed by Luton et al. (2002), who designed the degenerate primer pairs used for the amplification of the *mcrA* gene. They successfully evaluated the primers against 23 species of methanogens representing all five recognized orders of this group of archaea, generating PCR products ranging between 464 and 491 bp.

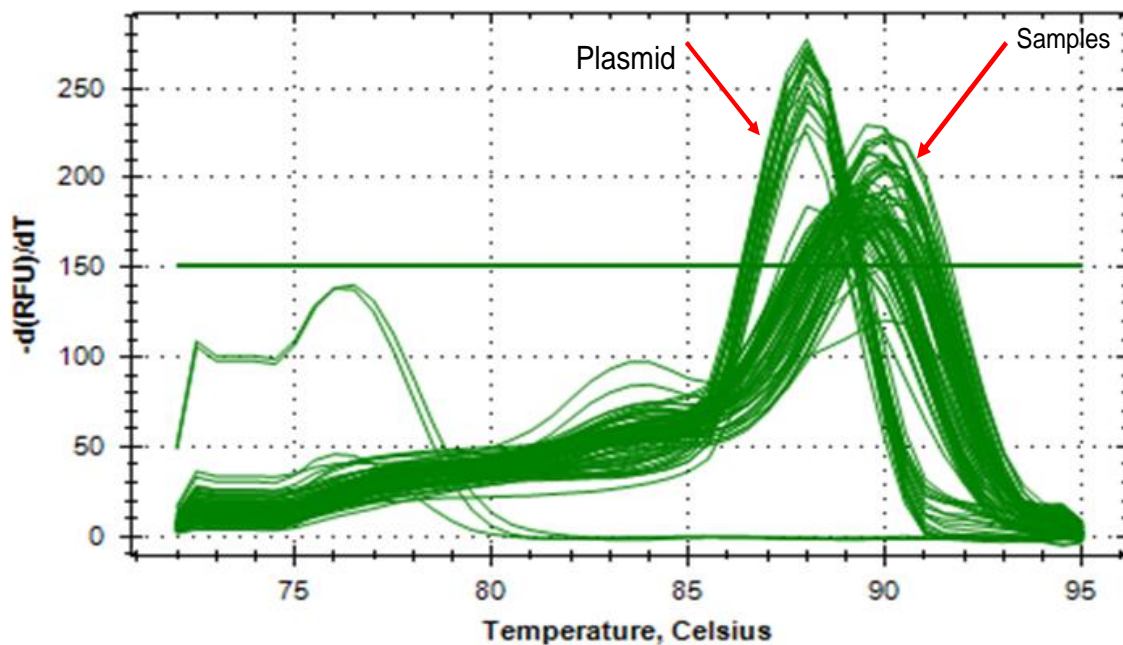


Figure 5.14: *mcrA* gene melt curve analysis

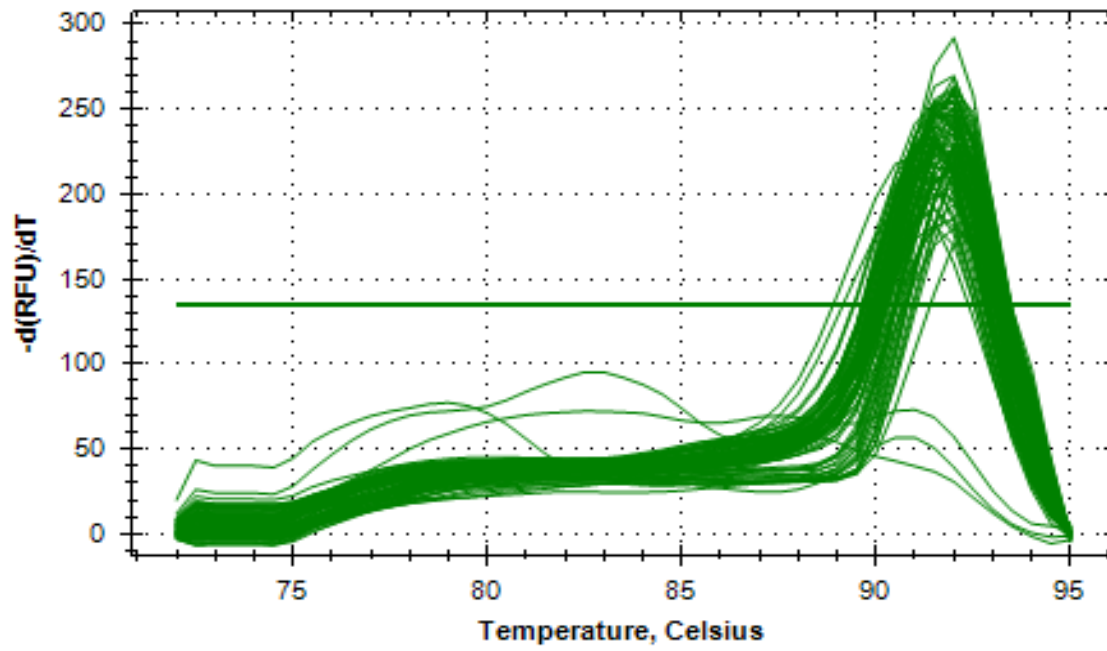


Figure 5.15: *dsrB* gene melt curve analysis

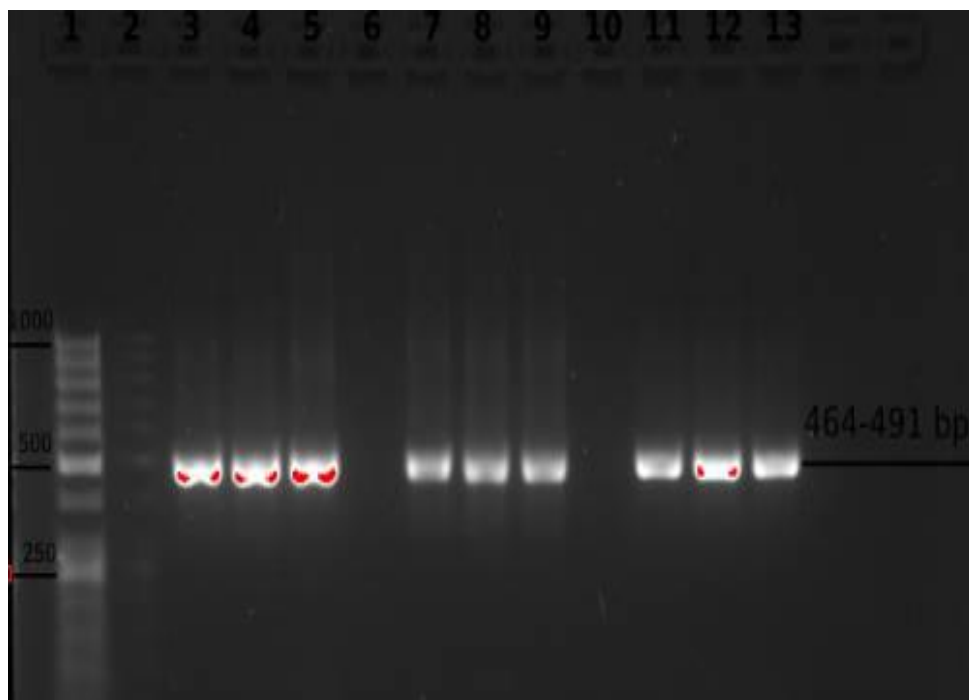


Figure 5.16: *mcrA* gene agarose gel electrophoresis after qPCR, lane 1: gene ruler, lane 2 negative control, lanes 3-5: standard 2, lanes 7-9: reactor sample, lanes 11-13: standard

5.4.3. Biochemical Potential test

5.4.3.1. Quantitative real-time polymerase chain reaction of the *mcrA* gene

All the BMP qRT-PCR analyses were performed in 2 x 96 well plates, with slopes of -6.071 and -4.883 which corresponded to amplification efficiencies of 46.12 and 60.26, respectively and high correlation coefficients ($R^2= 0.995$) and ($R^2= 0.993$) as shown in Appendix E. The efficiencies were comparable with previous efficiencies i.e. higher than Yuan et al. (2018) (42–59%) but lower than Morris et al. (2013) (110.5%). This difference could be explained by PCR inhibitors such as metals (which are abundant in tannery effluents as shown in Table 4.1). The average Ct of the 'no template' control was 37.80, confirming that no primer dimers were present. The *mcrA* gene copy numbers per ng DNA were calculated from the qRT-PCR results using Equation 3.1. These ranged from 4.18×10^5 to 2.51×10^6 at baseline, 3.06×10^6 to 6.46×10^6 at the start of gas production, 6.11×10^5 to 4.77×10^6 when the reactor stopped producing CH₄ and 3.63×10^5 to 1.57×10^6 at the end of the digestion (Figure 5.17). The figure illustrates that the graphs show a common trend, where the *mcrA* gene copy numbers were significantly higher ($P < 0.001$) when the reactors started producing gas, and subsequently decreased. A similar trend was obtained by Morris et al. (2013) with 3 samples of biomass taken from 4 different H₂/CO₂ enriched bioreactors. The relatively high copy numbers at the start of gas production confirmed that methanogens play an important role in AD. The data obtained by Morris et al. (2013) were 2 to 3 orders of magnitude lower than those obtained in this study (10^3 to 10^4 copies per ng DNA versus 10^6 to 10^7 copies per ng DNA in this study). This difference may be due to the type of sample and the diversity of methanogens in the samples, or the nature of the biomass. It may also be that the reactors in this study had more growth compared to Morris et al. (2013) and also to some organisms having multiple gene copies.

The presence of a gene (in this case *mcrA*) indicates that an organism may have the capability of synthesizing an enzyme, but cannot confirm that it is actually being expressed. However, detection of a particular gene is still a good indicator of functional selection (Cooper, 2000). Performing qRT-PCR using RNA may be preferable to the use of DNA because it indicates that the genes have been transcribed into RNA (which is then used as a template for production of the target enzyme). However, RNA is generally present in small amounts and degrades very easily in harsh environments like tannery effluent once the cells are lysed. So ultimately, the results may be less accurate (Zaiko et al., 2018).

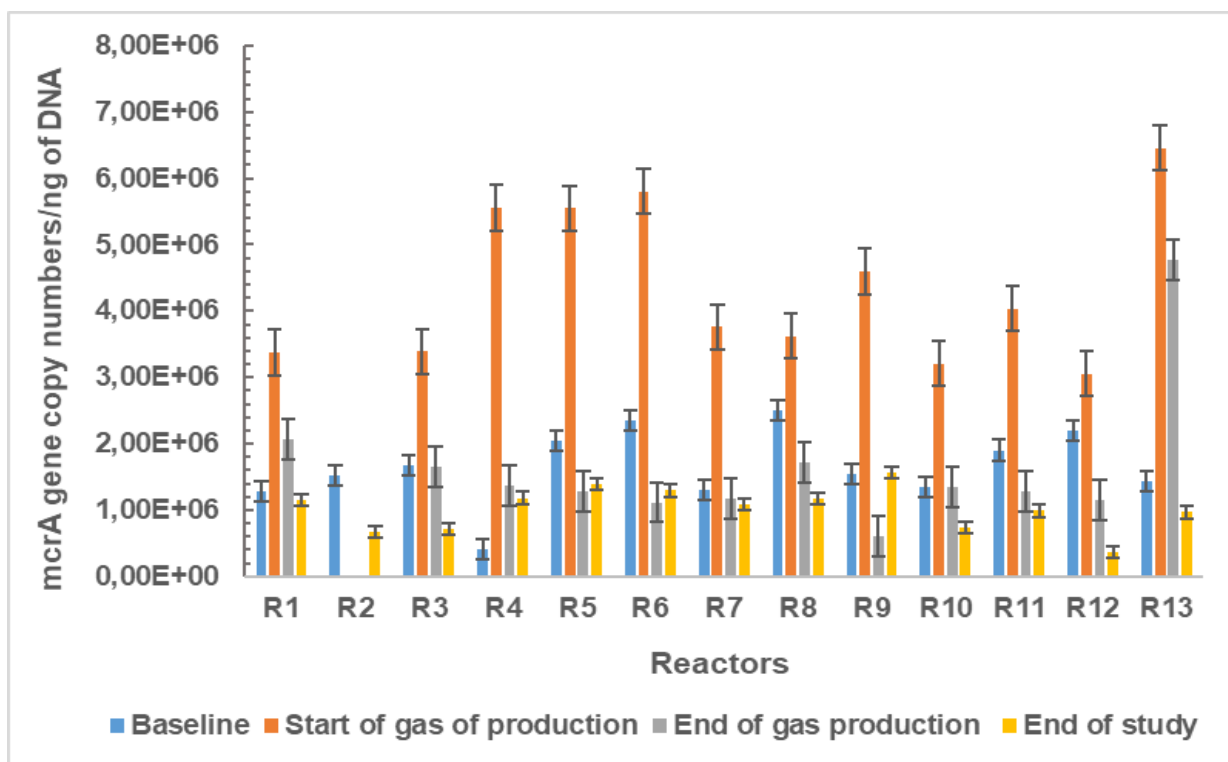


Figure 5.17: *mcrA* gene copy numbers in the biochemical methane potential tests. All measurements were performed independently in triplicate and error bars represent standard deviations

5.4.3.2. Correlation between methanogens and methane production

The relationship between *mcrA* copy numbers and CH₄ generation was further investigated by correlation analysis. As expected, the applied analysis described in Section 3.7.1 revealed in the BMP tests a positive significant correlation between *mcrA* gene copy numbers and specific CH₄ yield when the reactors started producing gas, $R^2= 0.7009$ with $P<0.01$ (Figure 5.18), indicating that the production of CH₄ is significantly and positively related to *mcrA* gene copy numbers. This significant correlation obtained confirmed findings from previous studies that demonstrated the relationship between *mcrA* gene copy numbers and CH₄ production. The R values obtained were not as high as those obtained by Waghmode et al. (2015) from rice cultivation ($R^2= 0.964$, $P<0.001$) and Morris et al. (2013) from 4 continuously 2 L bioreactors ($R^2= 0.9779$, $P<0.01$, with copies also expressed in DNA). According to Morris et al. (2013), this difference may be due to the type of substrate used, the measurement methods of CH₄ production, or the diversity of methanogens in the samples. However, some authors like Kanaparthi et al. (2017) did not find a linear correlation between rates and copy numbers even though the low rates of CH₄ emission were in accordance with the low copy numbers of *mcrA*

genes per gram dry weight moss detected in the moss stands collected from several temperate forests.

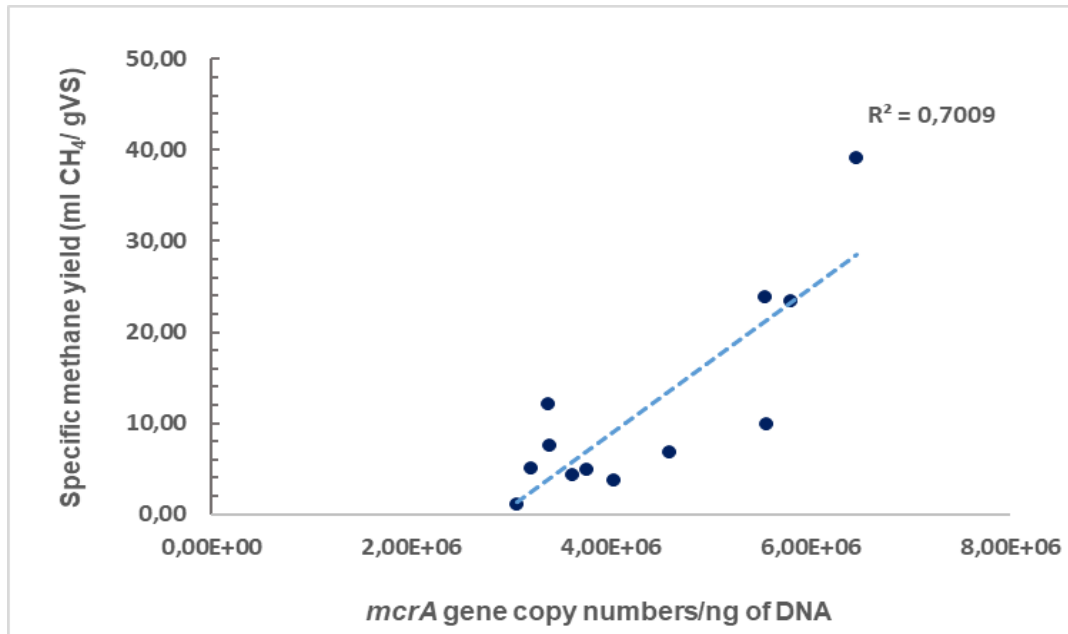


Figure 5.18: Correlation between *mcrA* gene copy numbers and specific methane yield in the biochemical methane potential tests

5.4.3.3. Quantitative real-time polymerase chain reaction of the *dsrB* gene

Like the *mcrA* gene, *dsrB* gene copy numbers were calculated from the qRT-PCR results. All the analyses were performed in 2 x 96 well microliter plates and critical parameters were as follows: slopes -4.496 and -5.304, y-intercepts 8.404 and 6.929, correlation coefficients 0.988 and 0.976 and efficiencies 54.35 and 68.9% and average Ct of the 'no-template' control of 34.72. However, the efficiencies were lower than the efficiency obtained by Cetecioglu et al. (2019) (103-109%). The copy numbers ranged from 5.13×10^4 to 1.73×10^5 per ng DNA at baseline, from 1.53×10^5 to 8.44×10^5 per ng DNA when the reactors started producing gas, from 1.20×10^5 to 6.55×10^5 per ng DNA when they stopped producing gas and from 1.97×10^5 to 7.04×10^5 per ng DNA at the end of the study as shown in Figure 5.19. However, no common trend was observed. As demonstrated previously by Islamud-Din et al. (2014), variation in the copy numbers of the *dsrB* gene are in line with variations in the availability of organic matter and the SO_4^{2-} concentrations.

In this study, however, inconsistency was observed. As observed in Figure 5.19, the *dsrB* gene copy numbers kept on increasing until the end of the experimental period in (i) R2 and R4 operating both at $SO_4^{2-} = 1335$ mg/L and ISR of 2 and 3, respectively, and (ii) R5 operating at $SO_4^{2-} = 710$ mg/L and ISR of 4. In R10 and R13, operating at ISR= 3 both and $SO_4^{2-} = 1335$ and 665 mg/L respectively, they increased when those reactors started producing biogas to decrease again from then until the end of the study. An increase of copy numbers was observed from baseline to the end of biogas production in (i) R1 operating at $SO_4^{2-} = 710$ mg/L and (ii) R8 and R11 operating both at $SO_4^{2-} = 1960$ mg/L and ISR= 3. In those reactors, copy numbers decreased at the end of the study. In the rest of the reactors, *dsrB* gene copy numbers increased when the reactors started to produce biogas, they then decreased when the reactors stopped producing biogas to increase again at the end of the study. These results indicate that *dsrB* gene copies are not affected by SO_4^{2-} concentration. Correlation analysis indicated $R^2 = 0.039$ and $P > 0.05$ (Section 5.4.3.4). Furthermore, as discussed in Section 5.3.2.1, it was observed that only the relative abundance of *Desulfofustis glycolicus* differed significantly in the BMPs (from 15,91% in BMP12 to < 0.035 in the rest of the reactors).

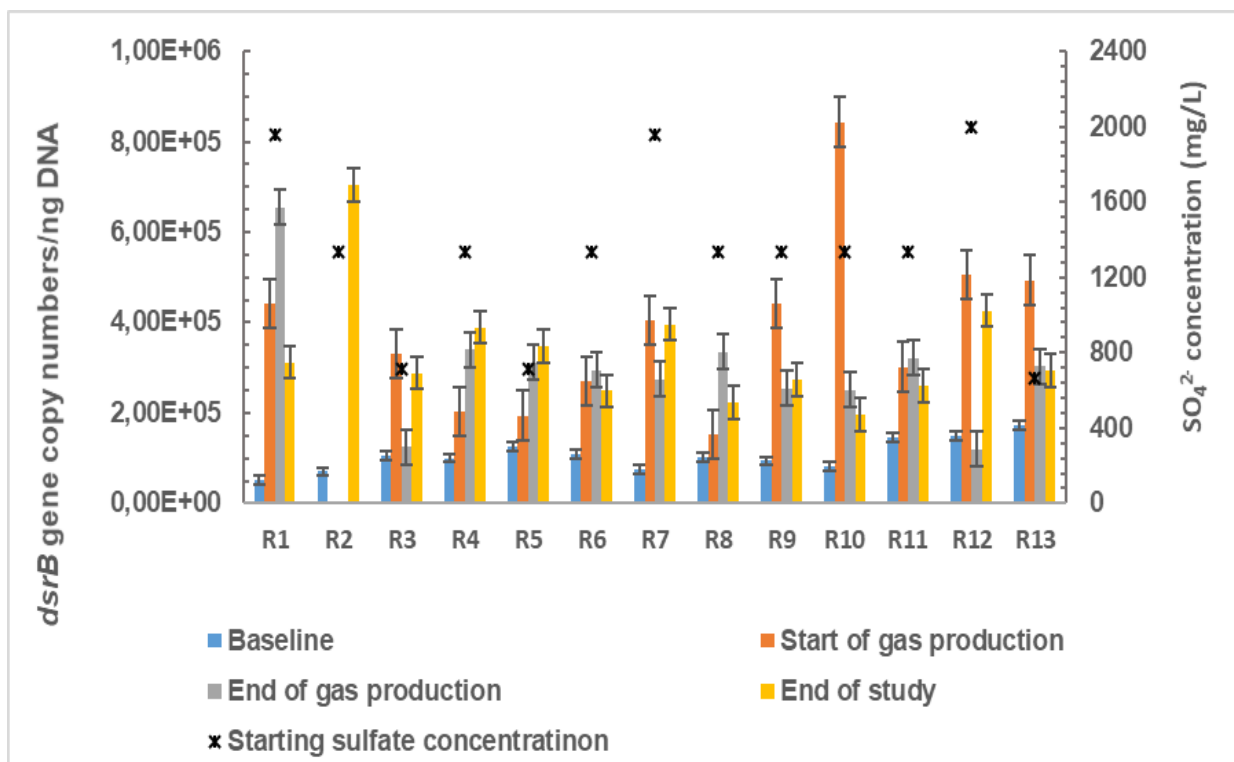


Figure 5.19: *dsrB* gene copy numbers per ng DNA contained in the biochemical methane potential tests. All measurements were performed independently in triplicate and error bars represent standard deviations

5.4.3.4. Correlation between sulfate reducing bacteria and sulfate or sulfide

The relationship between SRB and SO_4^{2-} or S^{2-} concentrations was also investigated by correlation analysis. Contrary to what was expected, no significant correlations ($P>0.05$) were detected between SO_4^{2-} concentrations contained in the BMP tests and *dsrB* gene copies (Figures not shown, Table 5.6). This is in accordance with studies conducted by Cetecioglu et al. (2019), whom also found no significant correlation between SO_4^{2-} concentrations and *dsrB* gene copies in anaerobic digesters treating coffee production wastewater. According to the authors, this is because some SRB act as fermenters and do not use SO_4^{2-} until insufficient carbon source is present. Shi et al. (2019) found that the *dsrB* gene abundance negatively correlated with the concentrations of SO_4^{2-} ($R^2 = -0.363$, $P < 0.05$) from six sites at the Xiaowan reservoir on the Lancang River. They attributed this negative correlation to microbial SO_4^{2-} reduction by enzymes produced from the *dsrB* gene. Contradictory results were reported by Niu et al. (2018), who obtained a significant positive correlation between SO_4^{2-} concentrations and *dsrB* gene abundance ($R^2 = 0.477$, $P < 0.05$). Likewise, He et al. (2010) also found a significant positive correlation between SO_4^{2-} concentrations and *dsrB* gene abundance in anaerobic paddy soil amended with rice straw ($R^2 = 0.759$, $P < 0.05$). In this study, the correlation analysis revealed that the *dsrB* gene copy numbers in the BMP tests had a significant correlation with H_2S ppm ($R^2 = 0.8293$, $P < 0.001$) as shown in Figure 5.20 and Table 5.6, indicating that the production of H_2S was significantly and positively related to *dsrB* gene copy numbers.

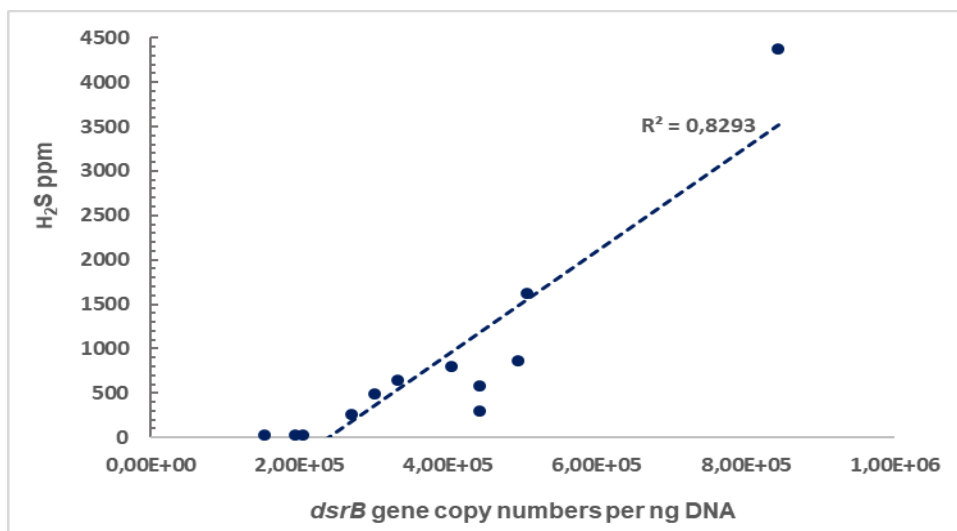


Figure 5.20: correlation between *dsrB* gene copy numbers and hydrogen sulfide gas produced in the biochemical methane potential tests

5.4.3.5. Other correlations

To detect correlations between the various physicochemical parameters that were measured (CHAPTER 4) and *mcrA* copy numbers in the BMP tests, data were subjected to analysis using the method described in Section 3.7.3. No correlations were obtained between *mcrA* copy numbers and VOA, NH_3 , SO_4^{2-} concentrations as well as C:N in the reactors (Figures not shown), even though in some instances the concentrations were found below or above the MIC reported in the literature (CHAPTER 4). However, there was a weak linear relationship between *mcrA* copy numbers and the initial and final alkalinity concentrations ($R^2 = 0.1507$ and $R^2 = 0.2749$ respectively, Figure 5.21). This is because buffering capacity controls AD stability and mitigates process imbalances (Molinuevo-salces et al., 2010; Procházka et al., 2012).

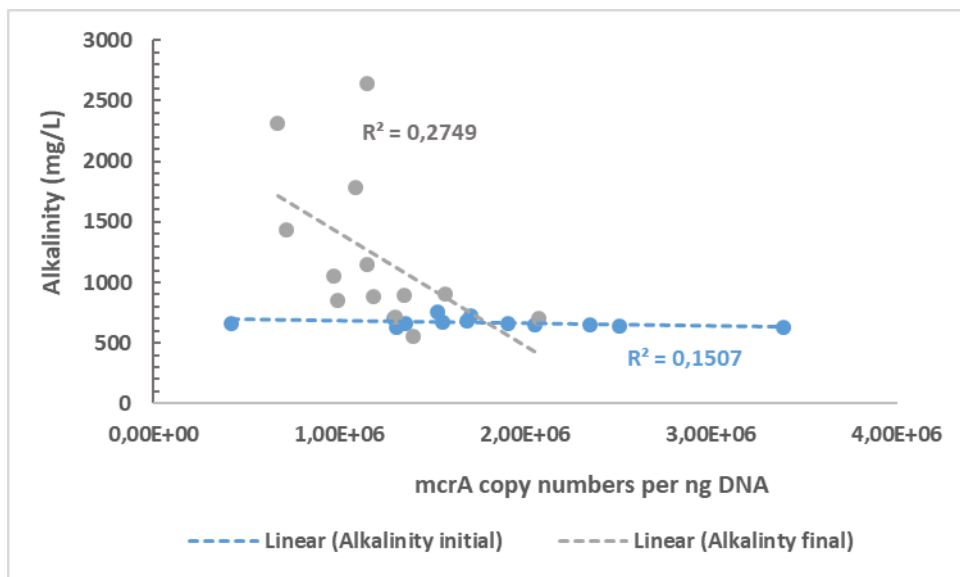


Figure 5.21: Correlation between *mcrA* copy numbers and alkalinity concentration contained in the biochemical potential tests

Statistical significance of abiotic data on sulfidogenic and methanogenic microbial community structure in BMP experiments were also investigated. Non-metric MDS plots were constructed using Bray-Curtis similarity matrices derived from square root transformed species abundance data for both the *mcrA* and *dsrB* NGS species datasets and, compared with principal component analyses (PCA) plots constructed from 4th root transformed and normalised data (Figure 5.22 and Figure 5.23). In the case of PCA, 80% and 83% of the results were explained by PC1 and PC2 for all parameters and truncated parameters (pH, VOA, Alkalinity, VOA:Alk, NH_3 , SO_4^{2-}) respectively, which both included the *mcrA* copy numbers in the datasets. Similarly, 80 and 85% of the results were explained by PC1 and PC2 for all parameters and

truncated parameters, respectively, which both included the *dsrB* copy numbers in the datasets.

Analysis of similarity (ANOSIM, one-way, unordered, Spearman rank correlation) was performed on (i) the Bray-Curtis similarity matrices (NGS data), and (ii) Euclidean distance similarity matrices constructed from 4th root transformed and normalised data of the measured parameters.

The factors that were investigated were: time (initial, start of gas production, final), initial SO_4^{2-} concentration, ISR, and a combined SO_4^{2-} concentration and ISR factor. In the case of all permutations for both the biotic and abiotic data, the only significant difference ($P < 0.05$) was determined for the factor “time” (Table 5.2). There was a significant change ($P < 0.01$) in the similarity of the truncated physicochemical data profiles between samples taken at the start of biogas production and the final samples (Table 5.2, Figure 5.22 and Figure 5.23). However, there was no significant ($P > 0.05$) change in the methanogenic or SRB community profiles during this time (Table 5.2, Figure 5.22 and Figure 5.23). It can therefore be deduced that both communities were established once biogas generation commenced, and were responsible for ongoing physicochemical changes thereafter. To determine which measured parameters that most significantly affected the selection of methanogenic and SR microbial communities, BEST analyses of Spearman rank correlations were performed on the Bray-Curtis similarity data of the functional microbial community structures and the Euclidian distance of the transformed and normalised data for the full and truncated datasets of the measured parameters (Table 5.3).

From the BEST analyses (Table 5.3), it can be seen that the changes in the similarity profiles of the functional microbial communities in initial and final samples that were investigated were driven by NH_3 , TOC and Alkalinity, while SO_4^{2-} , and N & pH, were also important drivers for changes in the SRB and methanogenic community structures, respectively. The results of the combinations of parameters giving the highest rho values in the initial and final samples are shown visually as bubble overlays on the same nMDS plots constructed from the NGS data (Figure 5.22E and Figure 5.23E). With the exception of N, all of these parameters were included in the truncated datasets. The truncated datasets also included changes that took place in the investigated microbial community structure at the start of gas generation and, should theoretically provide a better breakdown of the parameters driving the temporal community shifts.

Table 5.2: Results of ANISOM with time factor (R values)

	Global	Pairwise comparisons		
		Initial & start of gas generation	Initial & final	Start of gas generation & final
Methanogenic spp.				
NGS data <i>mcrA</i>	0.551**	0.601**	0.938**	0.015
All parameters	0.959**	-	0.959**	-
Truncated parameters	0.795**	0.848**	0.908**	0.867**
Sulfate reducing spp.				
NGS data <i>dsrB</i>	0.784**	0.997**	0.966**	0.104
All parameters	0.963**	-	0.961**	-
Truncated parameters	0.835**	0.905**	0.942**	0.853**

Significance levels: *0.05 > p ≥ 0.01 **p < 0.01

NGS=next generation sequencing

Table 5.3: Results of BEST analysis: rho values and 'best' correlated parameters

Microbial community structure (NGS)	Measured parameters	
	All	Truncated
Methanogenic: Initial & final	0.851** (NH ₃ , pH, TOC, Alk, N)	-
Methanogenic: Initial, start of gas generation, final	-	0.415** (NH ₃ , pH, VOA)
Sulfate reducing: Initial & final	0.947** (NH ₃ , TOC, Alk, SO ₄ ²⁻)	-
Sulfate reducing: Initial, start of gas generation, final	-	0.693** (pH, VOA:Alk, <i>dsrB</i> copies)

Significance levels: *0.05 > p ≥ 0.01 **p < 0.01

NGS=next generation sequencing, TOC= total organic carbon, VOA= volatile organic acid, Alk= alkalinity

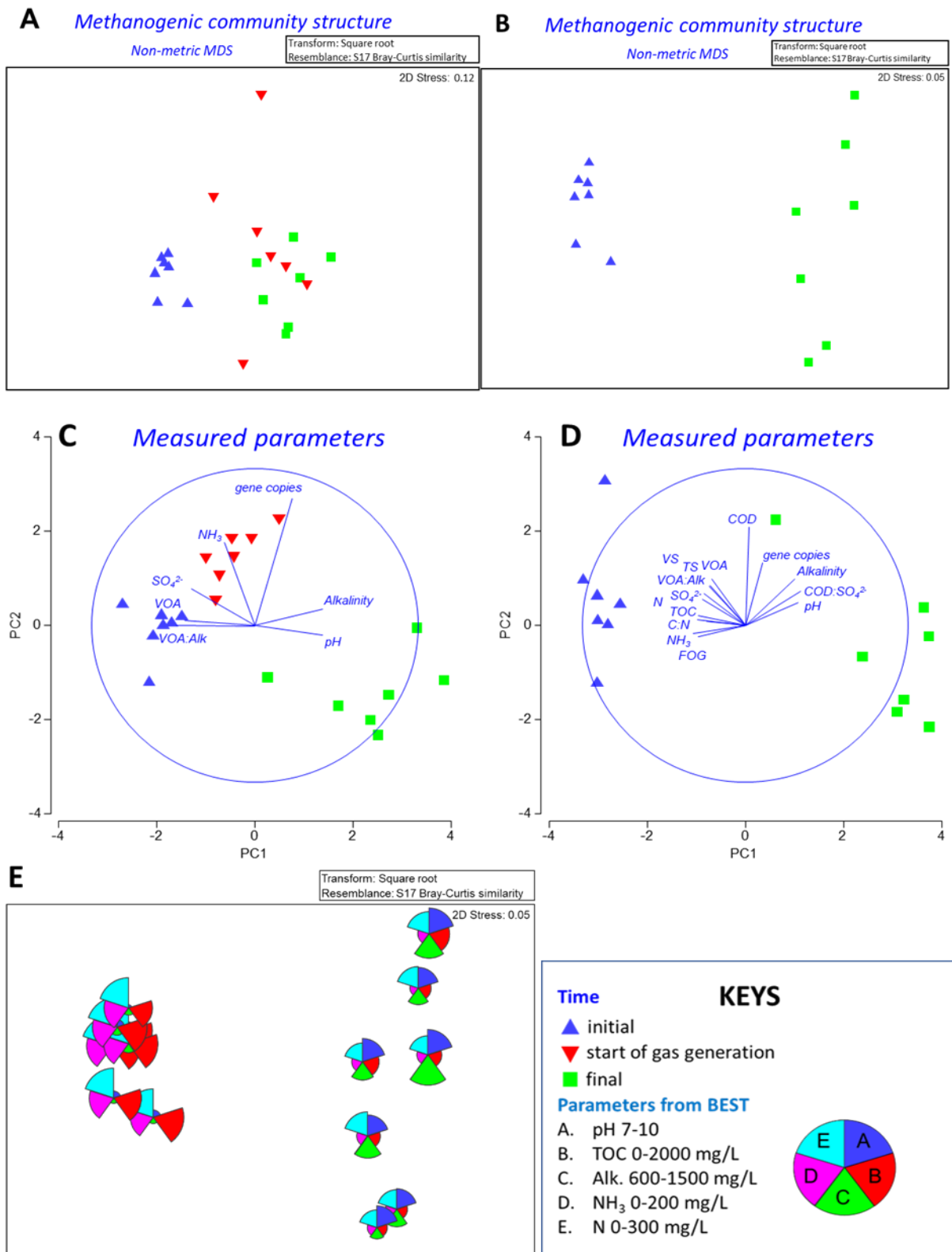


Figure 5.22: Similarity plots at different time instances (see key) of: methanogenic archaeal community structures (A,B), measured parameters (C,D) and bubble overlay on plot A of measured parameters determined to be most significant for community selection by BEST analysis (E).

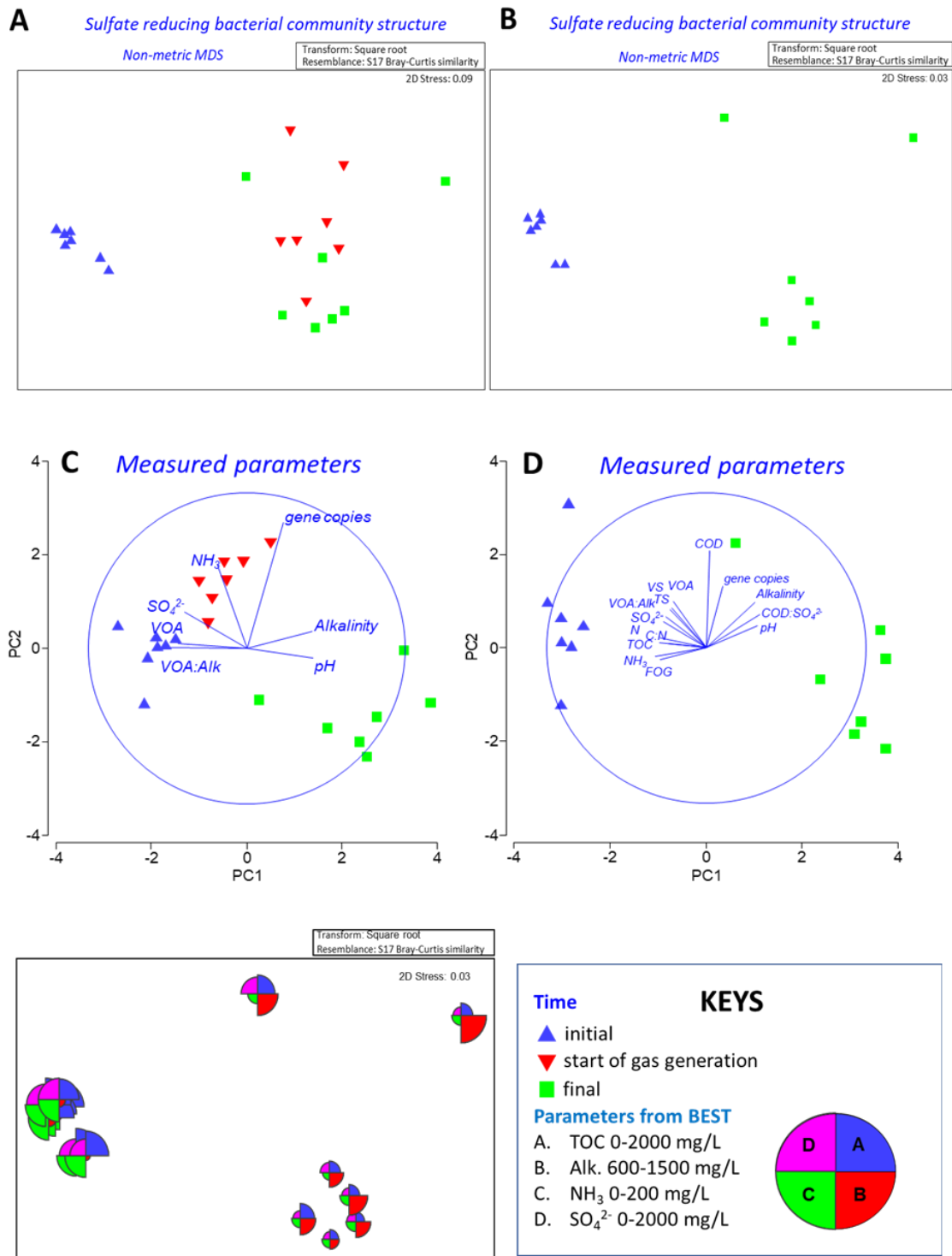


Figure 5.23: Similarity plots at different time instances (see key) of: sulfate reducing bacterial community structures (A,B), measured parameters (C,D) and bubble overlay on plot A of measured parameters determined to be most significant for community selection by BEST analysis (E)

5.4.3.6. Competition between methanogens and sulfate reducing bacteria shown by *mcrA* and *dsrB* gene copy numbers

The competition between methanogens and SRB shown by the *mcrA* and *dsrB* gene copy numbers was further investigated. This was once again grouped based on initial SO_4^{2-} concentration. As shown in Figure 5.24, a clear competition for substrate existed between these 2 communities as they both increased in all the categories at the start of gas production. As the *dsrB* gene copy numbers were notably lower than the *mcrA* copy, the results are displayed on a different figure (Figure 5.25). The results strongly suggest that the SRB did not outcompete the methanogens, even in the presence of high SO_4^{2-} concentration. This was in line with findings by Cetecioglu et al. (2019) whom also found that H_2 -consuming methanogens were not outcompeted by H_2 -consuming SRB in high SO_4^{2-} coffee production wastewater. Sulfate reducing bacteria utilise a number of different metabolic pathways (Section 2.3.1.5). Based on the data obtained in this study, it is not possible to speculate on which pathways the different DSR community members utilised.

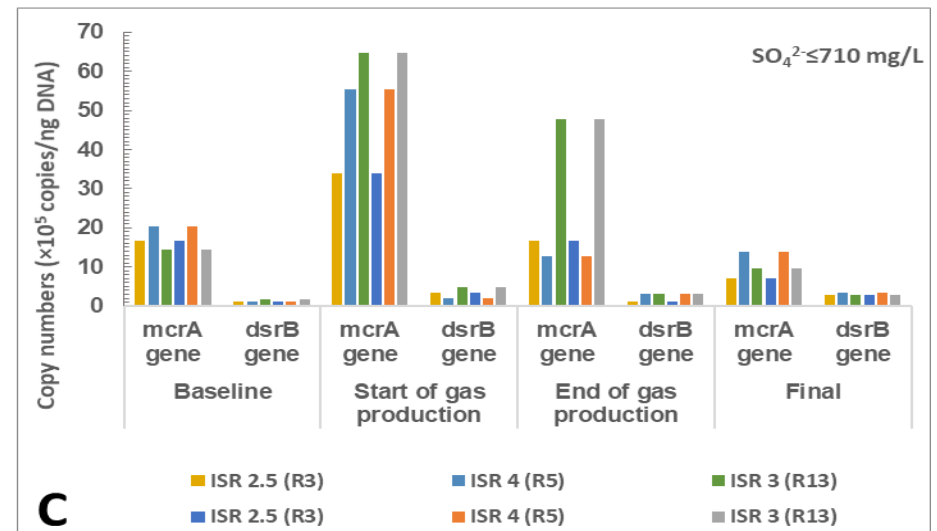
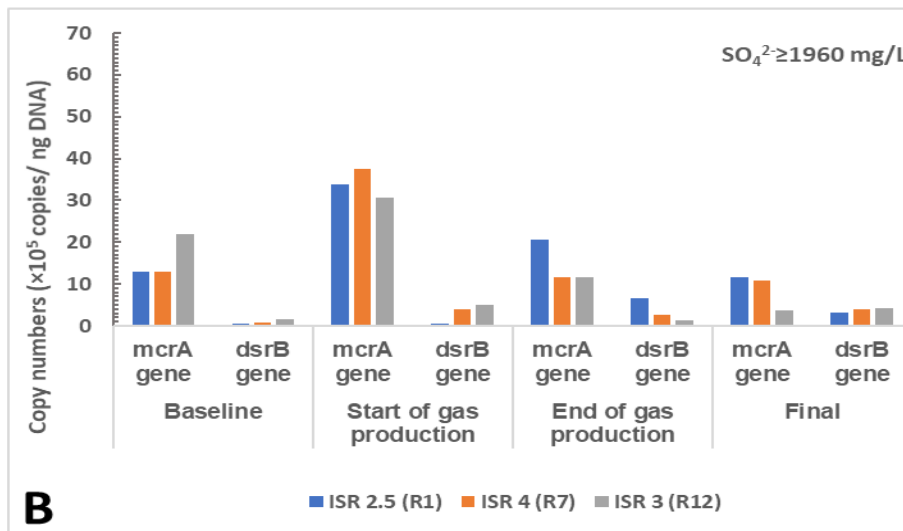
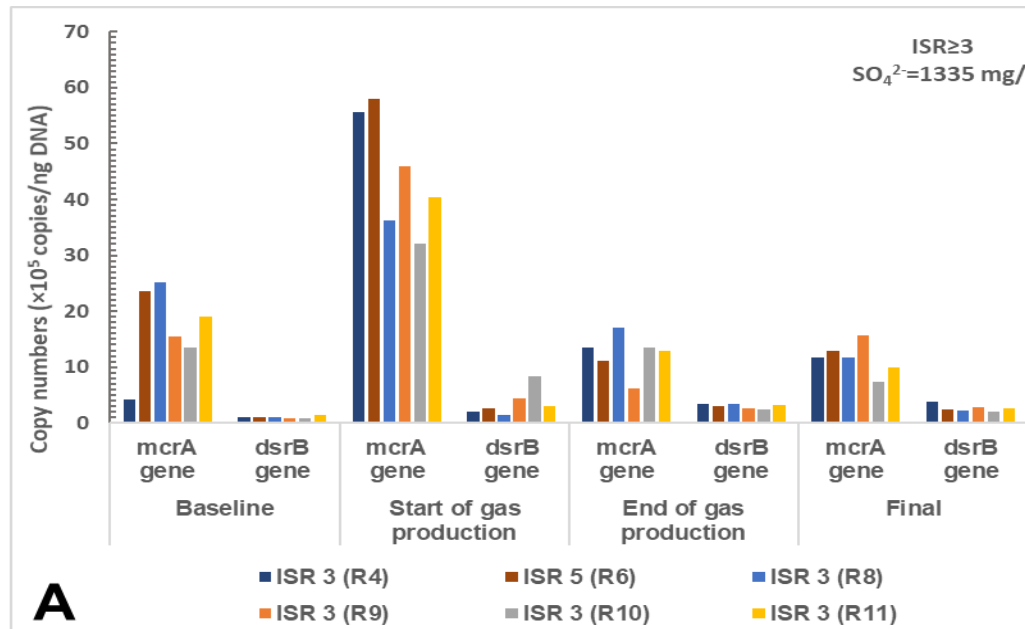


Figure 5.24: Competition between *mcrA* and *dsrB* genes in the biochemical methane potential tests operating at (A) inoculum to substrate ratio ≥ 3 and sulfate concentration of 1335 mg/L, (B) sulfate concentration ≤ 710 mg/L and (C) sulfate concentration ≥ 1960 mg/L. ISR= inoculum to substrate ratio

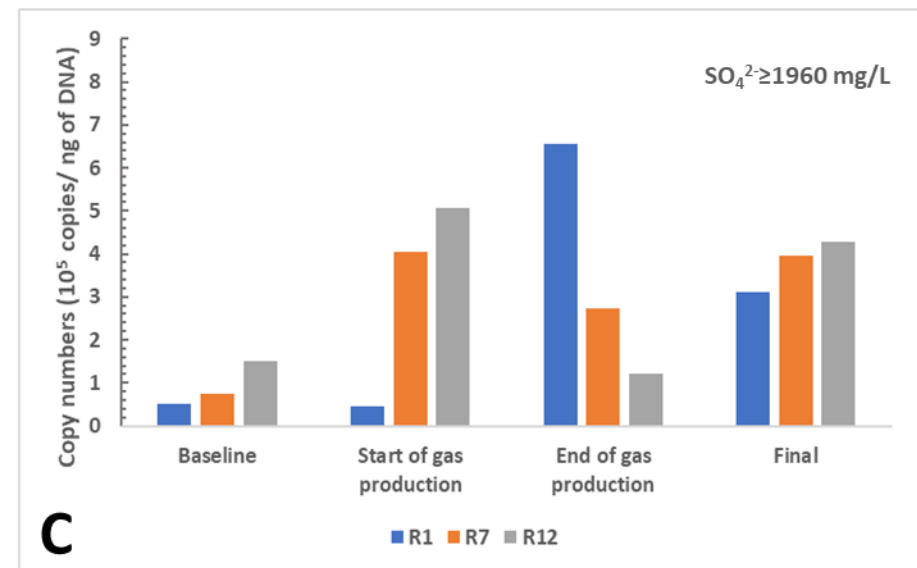
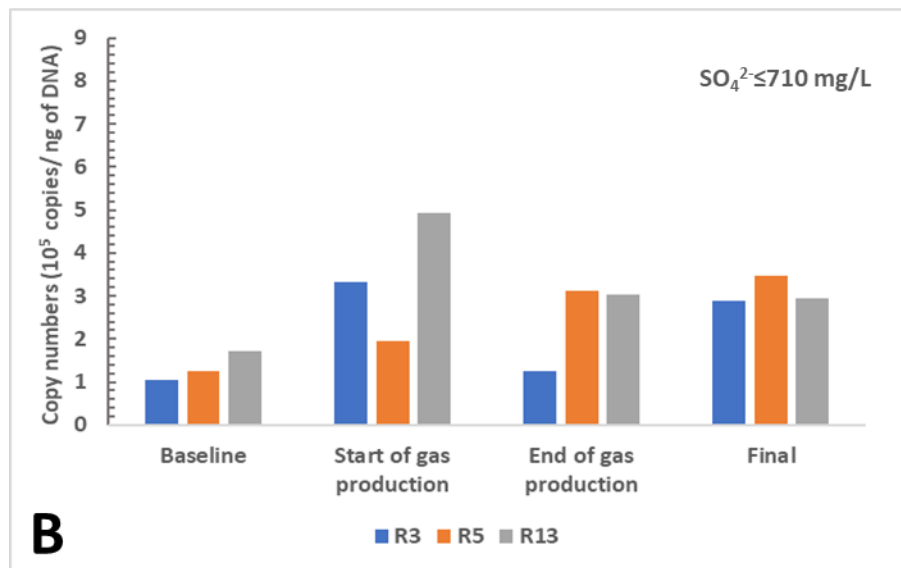
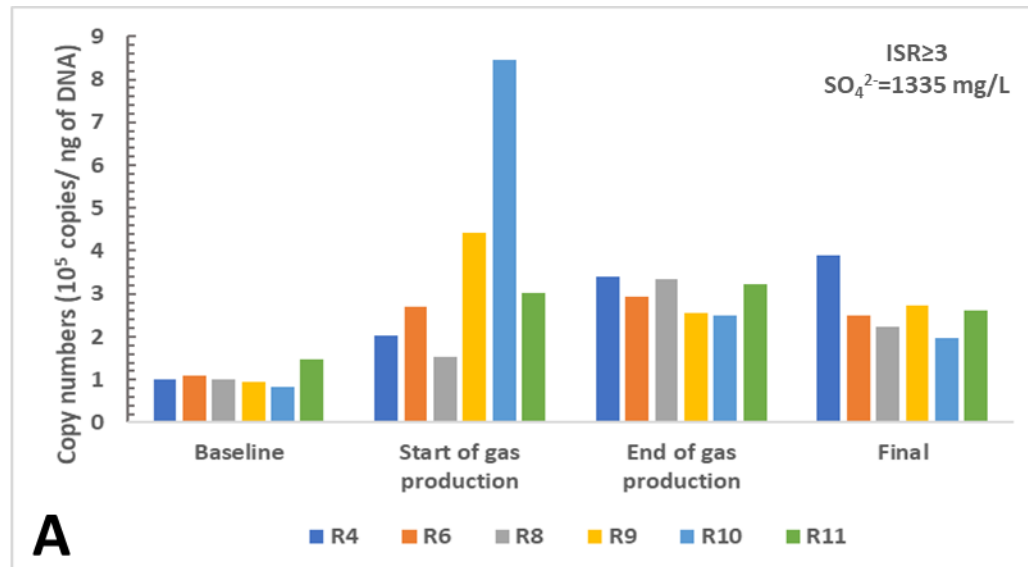


Figure 5.25: *dsrB* gene copy competition (A) inoculum to substrate ratio ≥ 3 and sulfate concentration of 1335 mg/L, (B) sulfate concentration ≤ 710 mg/L and (C) sulfate concentration ≥ 1960 mg/L. ISR= inoculum to substrate ratio

5.4.4. Anaerobic sequencing batch reactors

The genomic DNA extracted from the ASBRs were also subjected to qRT-PCR to amplify the *mcrA* and *dsrB* genes. All the qRT-PCR analyses for both reactors were performed in 1 x 96 well microtiter plate for each gene. The critical parameters for the genes are displayed in Table 5.4 and total *mcrA* and *dsrB* copy numbers were calculated from qRT-PCR results. These are discussed in the following sections.

Table 5.4: *mcrA* and *dsrB* genes quantitative polymerase chain reaction critical parameters for the anaerobic sequencing batch reactors

	<i>mcrA</i> gene	<i>dsrB</i> gene
slopes	4.877	5.290
y-intercept	8.894	6.125
correlation coefficient	0.990	0.9975
Efficiency (%)	33.75	54.5
average Ct	35.15	31.72

C_t= cycle threshold

5.4.4.1. Quantitative real-time polymerase chain reaction of the *mcrA* gene

The substrate and the inoculum had respectively 9.72×10^6 and 1.13×10^6 *mcrA* gene copy numbers per ng DNA. As showed in Figure 5.26, the *mcrA* gene copy numbers in ASBR1 ranged from 8.23×10^6 to 1.26×10^7 copy per ng DNA whereas in ASBR2, they ranged from 9.32×10^6 to 1.32×10^7 per ng DNA. Copy numbers increased rapidly in ASBR1 at the start of the experiment and reached a maximum at week 4 (1.26×10^7 copy per ng DNA) which was also reflected by an exponential rise of CH₄ content and decrease in COD. They decreased thereafter at week 5. A stable number of approximately 1×10^7 copy numbers per ng DNA was reached from week 5 to week 7 which then slightly decreased by $\approx 6\%$ in week 8 from 1.01×10^7 copy to 9.55×10^6 copy per ng DNA indicating inhibition of methanogens. A similar trend to ASBR1 was obtained in ASBR2 (Figure 5.26) i.e. the *mcrA* copy numbers gradually increased from baseline to reach their maximum at week 4 to decrease thereafter until week 7. However,

unlike in ASBR1 where inhibition of methanogenesis was observed in week 8, copy numbers in this reactor increased by 22%, which corresponded to an increase of *Methanobacterium* sp. and *Methanosarcina mazei* (Figure 5.11).

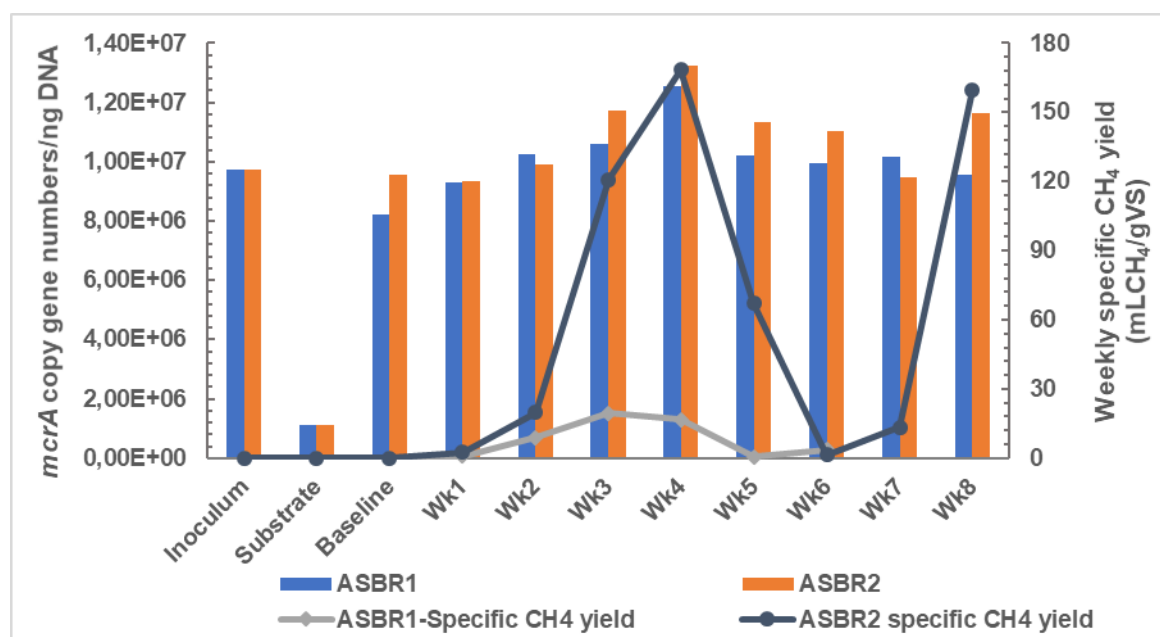


Figure 5.26: *mcrA* copy numbers per ng DNA contained in the anaerobic sequencing batch reactors. Wk= week, ASBR= anaerobic sequencing batch reactor

Several other orders of magnitude of *mcrA* gene copy numbers were reported from anaerobic digesters, rice field soils, wastewater plant sludges, lake sediments, etc. (Steinberg & Regan, 2009; Morris et al., 2015; Vaksmaa, 2017; Cetecioglu, Dol, Taylor, Purdy, et al., 2019) (Table 5.7).

When comparing both ASBRs, ASBR2 had higher copy numbers of *mcrA*, but the difference was not significant ($P > 0.05$). It was therefore postulated that *M. mazei* was selected by the physicochemical conditions associated with continuous mixing, and that from a functional perspective, this archaeal species was associated with significantly higher CH₄ generation than the other methanogenic species present. Thus, the predominance of *Methanosarcina mazei* may be a better indicator for understanding the efficiency of AD in this study.

It was also observed that the *mcrA* copy numbers peaked in weeks 3 and 4 in both ASBRs, which was in accordance with the alkalinity concentrations. Both reactors were seen to have stabilized with alkalinity concentrations found within the effective digestion range of 1500-3000 mgCaCO₃/L (Gerardi, 2003; Marti, 2008; Kavitha, 2009), discussed more fully in Section 4.4.1.5. Subsequently, a decrease in *mcrA* gene copy numbers was observed from week 5 in

both ASBRs. This was not only due to the alkalinity concentration found below the effective digestion range of 1500-3000 mgCaCO₃/L, but also to the increased TOC concentrations that indicates a failure in the degradation pathway of the biodegradable matter of one or more of the groups of microorganisms involved in AD (discussed more fully in Chapter 4 Section 4.4.1.5 and Figure 4.24E). Significant positive correlations ($P < 0.05$, $R^2 = 0.448$ in ASBR1 and $P < 0.05$ and $R^2 = 0.5711$ in ASBR2) (Figure 5.27) were obtained between *mcrA* gene copies and alkalinity concentration. As previously mentioned, this is because buffering capacity controls AD stability and mitigates against process imbalances (Molinuevo-salces et al., 2010; Procházka et al., 2012). According to Procházka et al. (2012), higher buffer capacity allows higher OLR without accumulation of VFA. These results were in line with a previous study, where the microbial archaeal communities significantly increased together with the alkalinity concentration (Silva et al., 2015). This was also reflected in CH₄ generation rates, i.e. increased *mcrA* copy numbers corresponded to increased CH₄ production as shown in Figure 5.26.

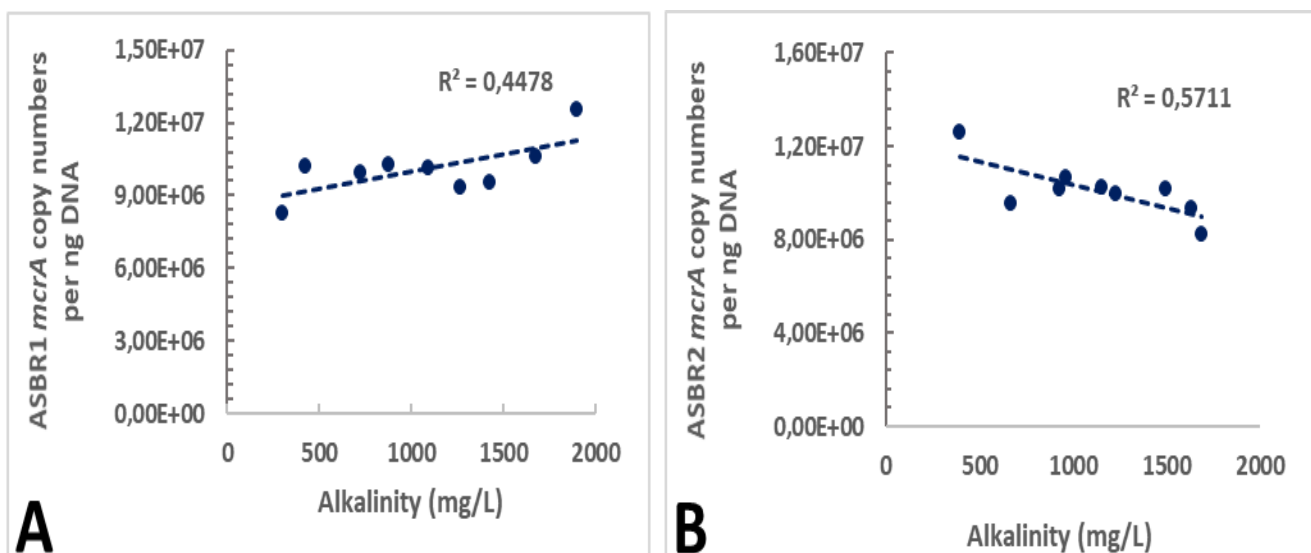


Figure 5.27: Correlation between *mcrA* copy numbers and alkalinity concentration contained in the anaerobic sequencing batch reactors. ASBR= anaerobic sequencing batch reactor

Later, copy numbers were normalized to TS and VS. According to Blagodatskaya et al. (2003), Joergensen & Emmerling (2006), Muñoz et al. (2017) and Welz et al. (2018), this parameter can be used as a proxy for biomass. When normalised to gTS, the copy numbers were 1 to 2 orders of magnitude higher than those obtained per ng of DNA in both reactors. Figure 5.28 showed the behaviour of the *mcrA* gene copy numbers per gTS inside both ASBRs. Increases were observed from week 0 to week 4 in both ASBRs where they reached their highest values

(6.41×10^8 and 8.48×10^8 copy numbers per gTS respectively in ASBR1 and ASBR2). 34.46 and 40.42% decrease were observed respectively in ASBR1 and ASBR2 after the decanting between weeks 4 and 5.

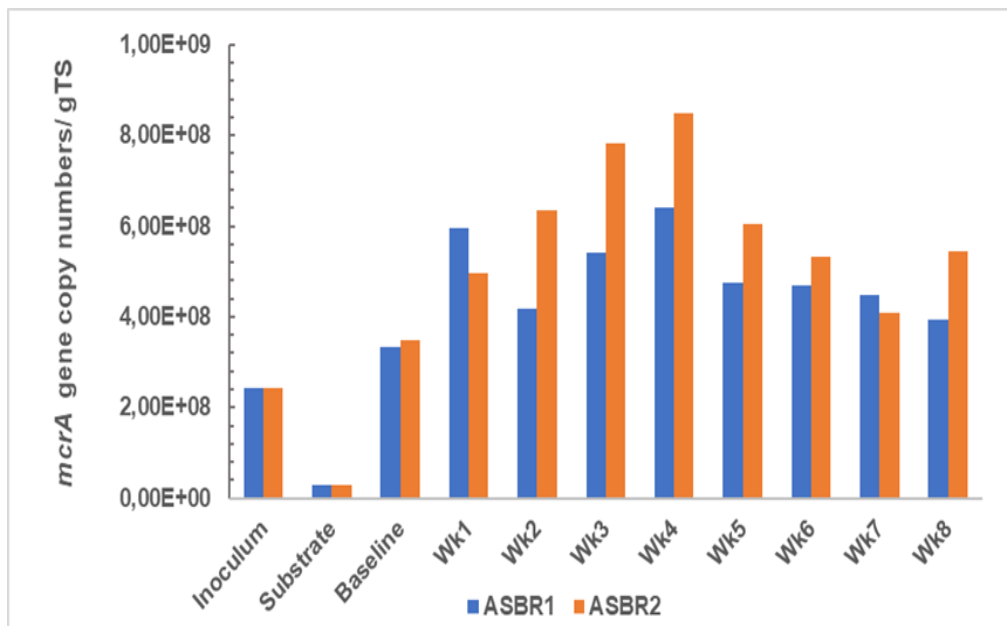


Figure 5.28: *mcrA* gene copy numbers per gTS contained in the anaerobic sequencing batch reactors. Wk= week, ASBR= anaerobic sequencing batch reactor

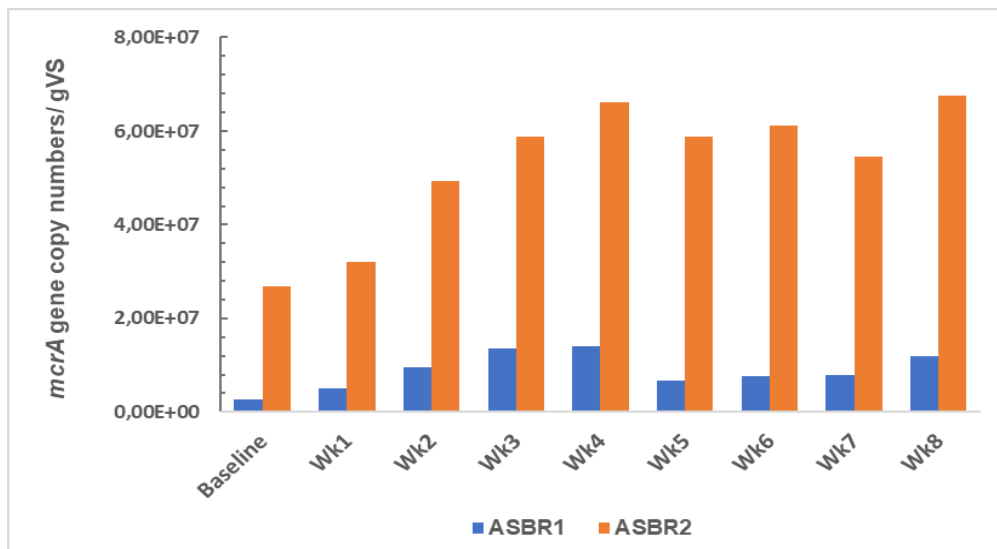


Figure 5.29: *mcrA* gene copy numbers per gVS contained in the anaerobic sequencing batch reactors. Wk= week, ASBR= anaerobic sequencing batch reactor

Like in the BMP tests, significant correlations ($P < 0.05$) were obtained between *mcrA* gene copy numbers expressed in ng DNA, gTS and VS and specific CH_4 yield in both ASBRs. With

copies in ng DNA, a coefficient correlation of $R^2 = 0.5275$ with $P < 0.05$ was obtained in ASBR1 while ASBR2 had a better correlation ($R^2 = 0.7552$, $P < 0.01$) (Figure 5.30A and C respectively, Table 5.5). As shown in Figure 5.30B and E and Table 5.5, $R^2 = 0.489$ with $P = 0.036$ and $R^2 = 0.7436$ with $P < 0.01$ were respectively obtained in ASBR1 and ASBR2 when CH_4 was correlated with copy numbers per gTS. Expressed in gVS, copy numbers also significantly ($P < 0.05$) correlated with specific CH_4 yield ($R^2 = 0.5823$ and $R^2 = 0.4809$ in ASBR1 and ASBR2 respectively as shown in Figure 5.30C and F and Table 5.5. All these correlations were similar or lower than the BMPs and comparable to correlations determined by Morris et al. (2015), Waghmode et al., 2015 and Cetecioglu et al. (2019) (Table 5.7).

Table 5.5: *mcrA* gene copy numbers correlation coefficient and level of significance with methane production. Statistically significant coefficients are printed in bold

ASBR1	mL CH_4 per gVS		mL CH_4 per gTS	
	R^2	P-value	R^2	P-value
Copy per ng DNA	0.5275	0.0267	ND	ND
Copy per gTS	ND	ND	0.489	0.036
Copy per gVS	0.5823	0.0211	ND	ND
ASBR2				
Copy per ng DNA	0.7552	< 0.01	ND	ND
Copy per gTS	ND	ND	0.7436	< 0.01
Copy per gVS	0.4809	0.038	ND	ND

ASBR= Anaerobic sequencing batch reactor ND = not determined TS= total solid VS= volatile solid

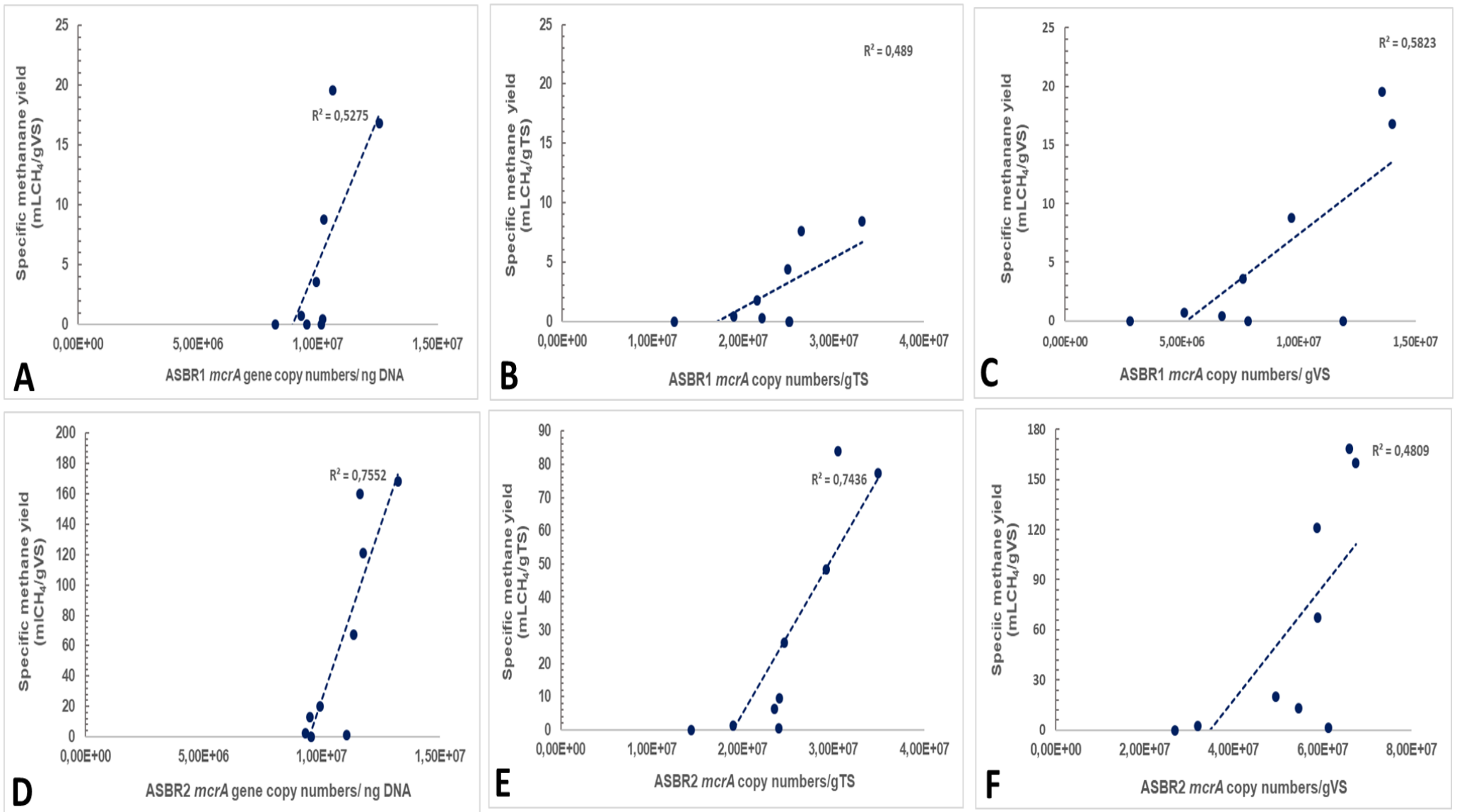


Figure 5.30: Correlations between *mcrA* gene copy numbers and methane yield in the anaerobic sequencing batch reactors. ASBR= anaerobic sequencing batch reactor

5.4.4.2. Quantitative real-time polymerase chain reaction of the *dsrB* gene

The total *dsrB* copy numbers per ng DNA and per gTS was calculated from qRT-PCR results. The substrate and the inoculum had 4.95×10^5 and 4.25×10^5 copy numbers per ng DNA respectively. In ASBR1, the *dsrB* gene varied between 2.70×10^5 to 1.12×10^6 copy numbers per ng DNA while in ASBR2, the abundance was in the magnitude of 10^5 . They varied between 2.27×10^5 to 6.72×10^5 copy numbers per ng DNA, indicating that sulfidogenesis was more favoured in ASBR1, which may have contributed to the lower production CH_4 in this digester. In addition, the *dsrB* gene copy numbers exhibited more temporal fluctuation in ASBR1 than ASBR2. As shown in Figure 5.31, an increase of copies was observed in ASBR1 from baseline to week 1 (2.70×10^5 to 7.53×10^5 copy numbers per ng DNA). This was followed by a slight decrease in week 2, and again in week 3. No change was observed between week 3 and week 4. On a process level this was characterised by an increase of S^{2-} concentration from 0.6 to 17.75 mg/L, which was assumed to be due to the introduction of the new substrate during the second run. As described more fully in Section 5.3.2.1, the second run in both reactors was dominated by *Desulfovibrio aminophilus* obtained from the new substrate, and by *Desulfobulbus rhabdoformis* developed during the process. The *dsrB* gene copy numbers per ng DNA then drastically decreased by 40% (from 5.52×10^5 to 4.58×10^5) from week 6 to week 7 until the last week. In ASBR2, a more stable performance was achieved as copy numbers did not vary from week 0 until week 5, minimizing the production of H_2S .

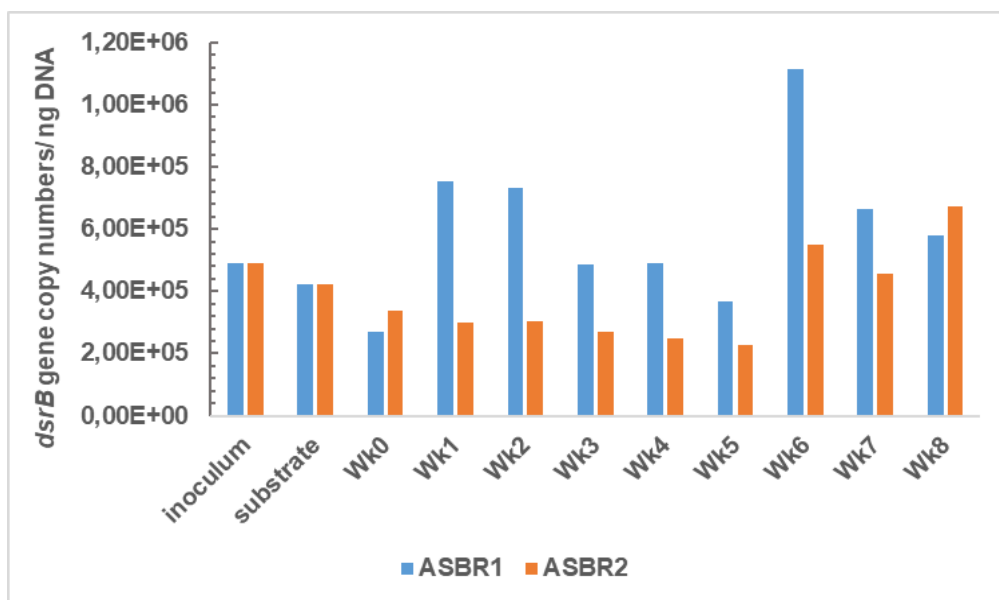


Figure 5.31: *dsrB* gene copy numbers per ng DNA contained in the anaerobic sequencing batch reactors. Wk= week, ASBR= anaerobic sequencing batch reactor

Furthermore, comparisons of the abundance of SRB in the ASBRs with the abundance in other environments, all determined with the same detection method (qPCR targeting the *dsrB* gene), revealed that the levels were lower than those described previously in paddy soils (10^6 – 10^8), but similar or higher than those described in estuary sediments (10^5 – 10^9) and in marine environments (10^6 – 10^8) (Niu et al., 2018; He et al., 2010; Shi et al., 2019).

Like in the BMPs, no correlations were found with SO_4^{2-} in both ASBRs. Correlations were instead obtained with S^{2-} . In ASBR1, the S^{2-} concentration positively correlated with both *dsrB* gene copy numbers expressed in ng per DNA and gTS at coefficients 0.6189 (Figure 5.32A) and 0.4595 (Figure 5.32B) at level of significance $P < 0.05$. However, the *dsrB* gene copy numbers obtained in ASBR2 (in ng DNA and gTS) did not significantly correlate with S^{2-} ($P > 0.05$) (Table 5.6, Figures not shown), even though the highest S^{2-} concentration corresponded to the highest *dsrB* gene copy numbers. As mentioned earlier in Section 5.4.3.1, copy numbers in DNA can give a good indication of underlying function but their presence does not always correlate 100% with activity. This could explain the results obtained in ASBR2. It should be noted that S^{2-} concentrations were not measured in the BMP tests and ASBRs produced over range H_2S gas that could not be recorded as shown in Appendix G.

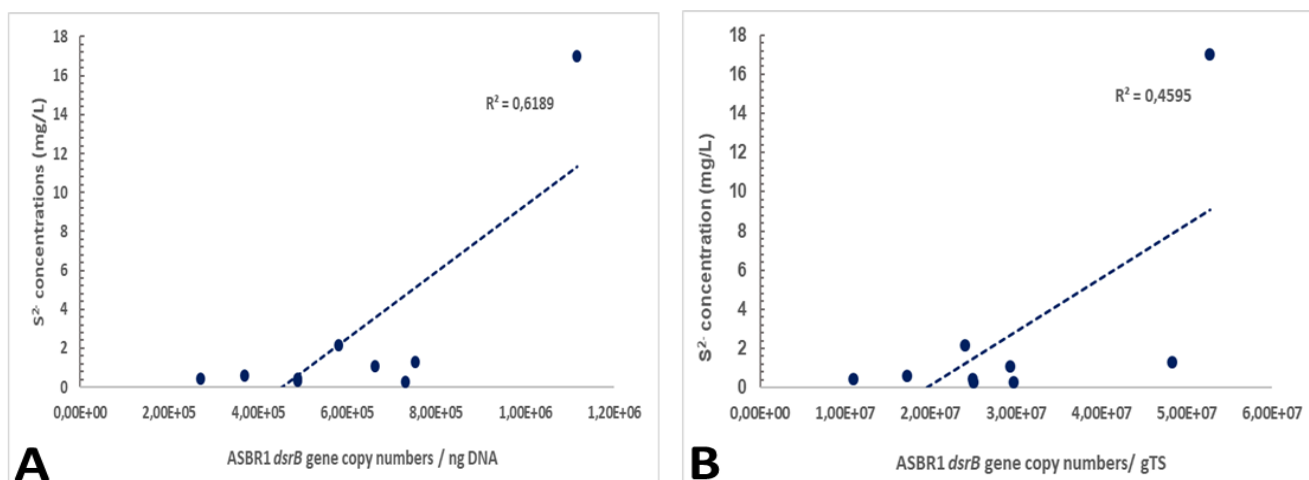


Figure 5.32: Correlation analysis between sulfide concentrations contained in anaerobic sequencing batch reactor with *dsrB* gene copy numbers expressed in (A) ng DNA (B) gTS. ASBR= anaerobic sequencing batch reactor

Table 5.6: Correlations analysis between *dsrB* copy numbers and sulfate and sulfide concentrations in the reactors

ASBR1	SO_4^{2-} conc. (mg/L)		S^{2-} conc. (mg/L)		H_2S (ppm)	
	R ²	P-value	R ²	P-value	R ²	P-value
Copy per ng DNA	0.0430	0.5926	0.6189	0.0119**	ND	ND
Copy per gTS	0.0656	0.5059	0.459	0.0448		
ASBR2						
Copy per ng DNA	0.0001	0.9331	0,2027	0,2239	ND	ND
Copy per gTS	0.0001	0.9331	0,2045	0.2239		
BMP						
Copy per ng DNA	0.039	0.5358	ND	ND	0.8293	<0.0001

ASBR= anaerobic sequencing batch reactor

ppm= part per million

ND= not determined

Table 5.7: Comparison of the results of this study with literature results

Substrate	Target gene	Abundance	Variable	Correlation coefficient (R ²)	P-value	References
Paddy soil amended with rice straw	<i>dsrB</i>	1.99×10 ⁶ -1.96×10 ⁸ /gds	SO ₄ ²⁻	0.759	0.029	He et al., 2010
Anaerobic biomass	<i>mcrA</i>	1.20×10 ³ -7.90×10 ⁴ / ng DNA	CH ₄	0.9779*	<0.01	Morris et al., 2013
Anaerobic biomass	<i>mcrA</i>	10 ⁴ -10 ⁵ / ng DNA	CH ₄	0.70	0.038	Morris et al., 2015
Moss stands	<i>mcrA</i>	10 ⁴ -10 ⁵ copies per gdw*	CH ₄	NG	> 0.05	Kanaparthi et al., 2017
Estuary sediments	<i>dsrB</i>	1.50×10 ⁵ -4.66×10 ⁸ /gs	SO ₄ ²⁻	0.477	< 0.05	Niu et al., 2018
Paddy rhizosphere soil	<i>mcrA</i>	3.40×10 ² -5.00×10 ² /gds	CH ₄	-0.390	< 0.01	Yuan et al., 2018
Coffee production wastewater	<i>mcrA</i>	1.1×10 ⁵ - 1.6×10 ⁶	CH ₄	0.720	< 0.01	Cetecioglu et al., 2019
	<i>dsrB</i>	NG	SO ₄ ²⁻	0.302	> 0.05	
River	<i>dsrB</i>	3.80 × 10 ⁶ -3.50 × 10 ⁸ /gwwt.	SO ₄ ²⁻	-0.363	< 0.05	Shi et al., 2019
Ostrich tannery wastewater	<i>mcrA</i>	3.63×10 ⁵ to 6.46×10 ⁶ /ng DNA	CH ₄	0.7009	<0.01	This study (BMP)
	<i>dsrB</i>	7.05×10 ⁴ -8.44×10 ⁵ /ng DNA	H ₂ S	0.8293	<0.001	
Ostrich tannery wastewater	<i>mcrA</i>	8.23×10 ⁶ -1.26×10 ⁷ /ng DNA	CH ₄	0.528	0.0267	This study (ASBR1)
	<i>dsrB</i>	2.70×10 ⁵ -1.12×10 ⁶ /ng DNA	S ²⁻	0.619	0.0119	

continued

Ostrich tannery wastewater	<i>mcrA</i>	9.32×10 ⁶ -1.32×10 ⁷ /ng DNA	CH ₄	0.755	< 0.01	This study (ASBR2)
	<i>dsrB</i>	2.27×10 ⁵ -6.72×10 ⁵ /ng DNA	S ²⁻	0,2027	NS	
Ostrich tannery wastewater	<i>mcrA</i>	2.77×10 ⁶ -1.40×10 ⁶ /g VS	CH ₄	0.582	0.0211	This study (ASBR1)
Ostrich tannery wastewater	<i>mcrA</i>	2.68×10 ⁷ -6.75×10 ⁷ /g VS	CH ₄	0.481	0.038	This study (ASBR2)
Ostrich tannery wastewater	<i>mcrA</i>	3.95×10 ⁸ -6.41×10 ⁸ /gTS	CH ₄	0.489	0.036	This study (ASBR1)
	<i>dsrB</i>	1.10×10 ⁷ -5.27×10 ⁷ /g TS	S ²⁻	0.459	0.0448	
Ostrich tannery wastewater	<i>mcrA</i>	3.49×10 ⁸ -8.48×10 ⁸ /gTS	CH ₄	0.743	< 0.01	This study (ASBR2)
	<i>dsrB</i>	1.21×10 ⁷ -3.14×10 ⁷ /g TS	S ²⁻	0,2045	NS	

gds= gdw= gram dry weight NG= not given, NS= not significant

5.5. Summary

Next generation sequencing was conducted on selected BMP samples (based on SO_4^{2-} concentration) and on ASBR biweekly samples. Results from the BMPs indicated that initial SO_4^{2-} concentration did not have an effect on the main or most dominant sulfidogenic species. Only *Desulfofustis glycolicus*, known to reduce SO_4^{2-} to H_2S was found at high RA (15,91%) in the test operating at $SO_4^{2-} \geq 1960$ mg/L compared to the other tests (<0.003% RA). These results strongly suggested that the produced H_2S inhibited some methanogenic species, with resultant decreased CH_4 production. With regards to the methanogenic community, a rapid change, probably caused by O_2 exposure was observed in the initial samples as they were not strongly influenced by the inoculum. The results also showed that the methanogenic community was negatively influenced in the reactor operating at $SO_4^{2-} \geq 1960$ mg/L at the start of biogas production by the absence of *Methanosarcina mazei* which seemed to also have an important role in this study. Statistically, the ANOSIM results revealed that only the factor time (initial, start of gas production, final) had a significant effect on both communities' structure. The community were established when gas production started. Additionally, BEST analyses of Spearman rank correlations revealed that the changes in the sulfidogenic community structure were driven by combinations of pH, concentrations of NH_3 , VOA, TOC and alkalinity, and VOA:alkalinity and *dsrB* copy numbers, while the methanogenic structure changes were driven by pH, and NH_3 , VOA, TOC, alkalinity and N concentrations.

When the volume of the reactors was upscaled to 20 L, results demonstrated that mixing mode impacted the functional microbial communities that were investigated. Continuous mixing promoted better survival and high abundance of *Methanosarcina mazei* in ASBR2 (14.7-31.6%) than in ASBR1 (4.3-6.8%). *Methanosaeta* sp. dominated in ASBR1 while in ASBR2, *Methanosarcina mazei* was the most dominant species. These results suggest that promotion of *Methanosarcina mazei* may be key in obtaining high process efficiencies in terms of methane yield.

In addition to the sequence analysis, the *mcrA* and *dsrB* genes were also quantified to determine the copy numbers in the methanogens and SRB. Results revealed that the *mcrA* gene copy numbers were significantly higher ($P < 0.001$) in the BMPs when the reactors started producing gas and decreased when gas production ceased. In contrast, no common trend was observed with the *dsrB* gene, confirming that initial SO_4^{2-} concentration had no significant effect on the MCS and overall microbial function. In the ASBRs, higher copy numbers of *mcrA* were found in ASBR2 when compare with ASBR1. However, the difference was not significant.

Finally, correlation analysis revealed a direct link i.e. positive correlation between (i) *mcrA* gene copies and alkalinity concentration in the BMPs and the ASBRs, (ii) *mcrA* gene copies and specific CH₄ yield in the BMPs and the ASBRs, (iii) *dsrB* genes copies and H₂S gas in the BMPs and (iv) *dsrB* genes copies and S²⁻ concentration in ASBR1. Contrary to what was expected, no correlation was observed between *dsrB* genes copies and SO₄²⁻ concentrations. This is almost certainly because some SRB act as fermenters with or without SO₄²⁻.

CHAPTER 6. CONCLUSION AND RECOMMENDATIONS

6.1. Conclusions

The aim of this study was to quantify copy numbers of *mcrA* and *dsrB* genes and correlate these respectively with the efficiency of methane generation and sulfate/sulfide concentrations in anaerobic digesters treating ostrich tannery wastewater. BMP tests were conducted to determine the effects of SO_4^{2-} and ISR on AD of ostrich tannery wastewater. It was deduced that at an average expected in ostrich tannery from the tannery, and high ISR, this ostrich tannery wastewater is an excellent candidate for AD. However, pre-treatment to reduce the SO_4^{2-} is required at high concentrations. Based on the model derived from the results, a combination of $SO_4^{2-} = 983.687$ and $ISR = 3.687$ was required for optimal gas (CH_4 , biogas) and biodegradability. To try and maximize AD efficiency, two 20 L operated at different mixing mode. High cumulative CH_4 generation was achieved (789 mL/gVS in 25 days) in ASBR2 operating at continuous mixing while in ASBR1 operating at intermittent mixing only 95 mL CH_4 /gVS was produced in 25 days, suggesting that continuous is more efficient than intermittent mixing. During the second run however, a decline in cumulative CH_4 generation was observed. It was therefore assumed that biomass washout occurred during decanting.

From a microbiology point of view however, NGS results showed that initial SO_4^{2-} concentration and ISR did not have a significant effect on the methanogenic and sulfidogenic structure. This was statistically confirmed by ANOSIM, which revealed that only the factor time (initial, start of gas production, final) had a significant effect on the both communities' structure. The communities were established once biogas generation commenced, and were responsible for ongoing physicochemical changes thereafter. However, it should also be noted that *Desulfofustis glycolicus* and *Methanosarcina mazei* played important roles by producing notable H_2S and CH_4 respectively. In the ASBRs, results strongly demonstrated that mixing mode influenced the communities by producing *Desulfomicrobium* sp. enrichment culture and *Methanosarcina mazei*.

Furthermore, the quantification of *mcrA* by qRT-PCR demonstrated to be a valuable gene for use in the investigation of methanogens as significant positive correlations ($P < 0.05$) between the copy numbers and CH_4 yield were obtained in the BMPs and ASBRs. The *dsrB* gene on the other hand positively correlated with H_2S in the BMPs and with S^{2-} concentration in ASBR1 but not with SO_4^{2-} .

6.2. Recommendations

Based on the general findings reported in this study, it can be concluded that monitoring the various consortia involved in AD could provide valuable information. Investigations that would aid in the further improvement of the application of AD in the treatment of ostrich tannery wastewater are highlighted in the following:

- Pre-treatment of high SO_4^{2-} to avoid development of unwanted SRB species known to reduce SO_4^{2-} to H_2S
- Since it was demonstrated that initial sulfate and/or ISR did not significantly affect the methanogenic and sulfidogenic communities the effects of carbon sources should be tested
- Continuous mixing shown to be more efficient, however, in full scale systems, the cost and complexity of continuous mixing is higher. Therefore, manipulation of operational conditions to promote the growth methanogens specially *Methanosarcina mazei* is required
- Different decanting methods are required to avoid biomass washout

REFERENCES

- Abbassi-guendouz, A., Brockmann, D., Trabaly, E., Dumas, C., Delgenès, J., Steyer, J. & Escudié, R. 2012. Total solids content drives high solid anaerobic digestion via mass transfer limitation. *Bioresource Technology*, 111: 55–61. <http://dx.doi.org/10.1016/j.biortech.2012.01.174>.
- Abdallh, M.N., Abdelhalim, W.S. & Abdelhalim, H.S. 2016. Biological Treatment of Leather Tanneries Wastewater Effluent- Bench Scale Modeling. *International Journal of Engineering Science and Computing*, 6(9): 2271–2286.
- Abdallh, M.N., SayedAbdelhalim, W. & SayedAbdelhalim, H. 2016. Biological Treatment of Leather Tanneries Wastewater Effluent- Bench Scale Modeling. *International Journal of Engineering Science and Computing*, 6(9): 2271–2286.
- Abdel-shafy, H.I. & Mansour, M.S.M. 2014. Biogas production as affected by heavy metals in the anaerobic digestion of sludge. *Egyptian Journal of Petroleum*, 23(4): 409–417. <http://dx.doi.org/10.1016/j.ejpe.2014.09.009>.
- Acharya, B.K., Mohana, S. & Madamwar, D. 2008. Anaerobic treatment of distillery spent wash – A study on upflow anaerobic fixed film bioreactor. *Bioresource Technology*, 99: 4621–4626.
- Achouri, O., Panico, A., Ph, D., Derbal, K., Ph, D. & Pirozzi, F. 2017. Effect of Chemical Coagulation Pretreatment on Anaerobic Digestion of Tannery Wastewater. *Journal of Environmental Engineering*: 1–5.
- Adzitey, F., Huda, N. & Ali, G.R.R. 2013. Molecular techniques for detecting and typing of bacteria, advantages and application to foodborne pathogens isolated from ducks. *3 Biotech*, 3(2): 97–107.
- Agrawal, A. & Lal, B. 2009. Rapid detection and quantification of bisulfite reductase genes in oil field samples using real-time PCR. *FEMS Microbiology Ecology*, 69(2): 301–312.
- Akpomie, O.O. & Ejechi, O. 2016. Bioremediation & Biodegradation Bioremediation of Soil Contaminated with Tannery Effluent by Combined Treatment with Cow Dung and Microorganisms Isolated from Tannery Effluent. *Journal of bioremediation & biodegradation*, 7(4): 354–359.
- Alemu, T. & Lemma, E. 2016. Performance of Pilot Scale Anaerobic-SBR System Integrated with Constructed Wetlands for the Treatment of Tannery Wastewater. *Environmental Processes*: 815–827. <http://dx.doi.org/10.1007/s40710-016-0171-1>.
- Alvarado, A., Montañez-hernández, L.E., Palacio-molina, S.L., Oropeza-navarro, R. & Miriam, P. 2014. Microbial trophic interactions and mcr A gene expression in monitoring of anaerobic digesters. *Frontiers in Microbiology*, 5: 1–14.

- Álvarez, A. & Soto, M. 2012. Anaerobic Treatment of Domestic Wastewater. In D. J. Caruana & A. E. Olsen, eds. *Anaerobic Digestion: Processes, Products and Applications*. New York.
- Amani, T., Nosrati, M. & Sreekrishnan, T.R. 2010. Anaerobic digestion from the viewpoint of microbiological, chemical, and operational aspects-a review. *Environmental Reviews*, 278: 255–278.
- Anderson, K., Sallis, P. & Uyanik, S. 2003. Anaerobic treatment processes. In M. Duncan & N. Horan, eds. *Handbook of Water and Wastewater Microbiology*. Amsterdam: Academic Press.
- Angel, R., Matthies, D. & Conrad, R. 2011. Activation of Methanogenesis in Arid Biological Soil Crusts Despite the Presence of Oxygen. *PLoS one*, 6(5): 1–8.
- Angelidaki, I., Alves, M., Bolzonella, D., Borzacconi, L., Campos, J.L., Guwy, A.J., Kalyuzhnyi, S., Jenicek, P. & Lier, J.B. Van. 2009. Defining the biomethane potential (BMP) of solid organic wastes and energy crops: a proposed protocol for batch assays. *Water Science and Technology*, 59(5): 927–934.
- Apaydin, O. & Kurt, U. 2009. An Investigation on the treatment of tannery wastewater by Electrocoagulation. *Global NEST Journal*, 11(4): 546–555.
- APHA. 2005. *Standard Methods for the Examination of Water and Wastewater*. 21st ed. Washington DC: American Public Health Association/American Water Works Association/Water Environment Federation, Washington DC.
- Ayoub, G.M., Hamzeh, A. & Semerjian, L. 2011. Post treatment of tannery wastewater using lime/bittern coagulation and activated carbon adsorption. *Desalination*, 273(2–3): 359–365. <http://dx.doi.org/10.1016/j.desal.2011.01.045>.
- Aziz, A., Basheer, F., Sengar, A., Ullah, S. & Haq, I. 2019. Biological wastewater treatment (anaerobic-aerobic) technologies for safe discharge of treated slaughterhouse and meat processing wastewater. *Science of the Total Environment*, 686: 681–708. <https://doi.org/10.1016/j.scitotenv.2019.05.295>.
- Baena, S., Fardeau, M., Labat, M., Garcia, B.O. & Patel, B.K.C. 1998. *Desulfovibrio aminophilus* sp. nov., a Novel Amino Acid Degrading and Sulfate Reducing Bacterium from an Anaerobic Dairy Wastewater Lagoon. *Systematic and applied microbiology*, 21(4): 498–504. [http://dx.doi.org/10.1016/S0723-2020\(98\)80061-1](http://dx.doi.org/10.1016/S0723-2020(98)80061-1).
- Bailón-Salas, A.M., Medrano-Roldán, H., Valle-Cervantes, S., Ordaz-Díaz, L.A., Urtiz-Estrada, N. & Rojas-Contreras, J.A. 2017. Review of molecular techniques for the identification of bacterial communities in biological effluent treatment facilities at pulp and paper mills. *BioResources*, 12(2): 4384–4409.
- Banu, J.R. & Kaliappan, S. 2007. Treatment of tannery wastewater using hybrid upflow

- anaerobic sludge blanket reactor. *J. Environ. Eng. Sci*, 6: 415–421.
- Berhe, S. & Leta, S. 2018. Anaerobic co-digestion of tannery waste water and tannery solid waste using two-stage anaerobic sequencing batch reactor : focus on performances of methanogenic step. *Journal of Material Cycles and Waste Management*, 0(0): 0. <http://dx.doi.org/10.1007/s10163-018-0706-9>.
- Berhe, S. & Leta, S. 2017. Two Phase Anaerobic Co Digestion of Tannery Wastewater and Dairy Wastewater : Effect of Operational Parameters on Performance of Hydrolytic – Acidogenic Step. *International Journal of Sustainable and Green Energy*, 6(1): 1–9.
- Bhardwaj, S. & Payal, D. 2017. A Review : Advantages and Disadvantages of Biogas. *International Research Journal of Engineering and Technology*, 4(10): 890–893.
- Bhattacharyya, D. & Singh, K.S. 2010. Understanding the Mixing Pattern in an Anaerobic Expanded Granular Sludge Bed Reactor: Effect of Liquid Recirculation. *Journal of Environmental Engineering*, 136(6): 576–584.
- Bijmans, M.F.M., Buisman, C.J.N., Meulepas, R.J.W. & Lens, P.N.L. 2011. Sulfate Reduction for Inorganic Waste and Process Water Treatment. In *Comprehensive Biotechnology*. Wageningen: Elsevier B.V.: 435–446. <http://dx.doi.org/10.1016/B978-0-08-088504-9.00471-2>.
- Bio-Rad. 2006. *Real-Time PCR Applications Guide*.
- Black, M., Canova, M., Rydin, S., Scalet, B.M., Roudier, S. & Sancho, L.D. 2013. *BAT refernce document for the Tanning of Hides and Skins*. Luxembourg: European Commission.
- Blagodatskaya, E. V., Blagodatskii, S.A. & Anderson, T.H. 2003. Quantitative isolation of microbial DNA from different types of soils of natural and agricultural ecosystems. *Microbiology*, 72(6): 744–749.
- Blaut, M. 1994. Metabolism of methanogens. *Antonie van Leeuwenhoek*, 66: 187–208.
- Bodík, I., Herdová, B. & Kratochvíl, K. 2000. The Application of Anaerobic Filter for Municipal Wastewater Treatment. *Chemical papers*, 54(3): 159–164.
- Borja, R. & Banks, C.J. 1994. Anaerobic digestion of palm oil mill effluent using an up-flow anaerobic sludge blanket reactor. *Biomass and Bioenergy*, 6(5): 381–389.
- Boulanger, A., Pinet, E., Bouix, M., Bouchez, T. & Mansour, A.A. 2012. Effect of inoculum to substrate ratio (I/S) on municipal solid waste anaerobic degradation kinetics and potential. *Waste Management*, 32(12): 2258–2265. <http://dx.doi.org/10.1016/j.wasman.2012.07.024>.
- Brankatschk, R., Bodenhausen, N., Zeyer, J. & Bürgmann, H. 2012. Simple Absolute Quantification Method Correcting for Quantitative PCR Efficiency Variations for Microbial Community Samples. *Applied and Environmental Microbiology*, 78(12): 4481–4489.

- Caporaso, J.G., Lauber, C.L., Walters, W.A., Berg-lyons, D., Huntley, J., Fierer, N., Owens, S.M., Betley, J., Fraser, L., Bauer, M., Gormley, N., Gilbert, J.A., Smith, G. & Knight, R. 2012. Ultra-high-throughput microbial community analysis on the Illumina HiSeq and MiSeq platforms. *The International Society for Microbial Ecology Journal*, 6: 1621–1624.
- Carotenuto, C., Guarino, G., Morrone, B. & Minale, M. 2016. Temperature and pH Effect on Methane Production from Buffalo Manure Anaerobic Digestion. *International Journal of Heat and Technology*, 34(2): S425–S429.
- Cervantes, F.J., Meza-Escalante, E.R., Texier, A.C. & Gómez, J. 2009. Kinetic limitations during the simultaneous removal of p-cresol and sulfide in a denitrifying process. *Journal of Industrial Microbiology and Biotechnology*, 36(11): 1417–1424.
- Cetecioglu, Z., Dol, J., Taylor, J. & Purdy, K.J. 2019. COD / sulfate ratio does not affect the methane yield and microbial diversity in anaerobic digesters. , 155: 444–454.
- Cetecioglu, Z., Dol, J., Taylor, J., Purdy, K.J. & Eyiced, Ö. 2019. COD/sulfate ratio does not affect the methane yield and microbial diversity in anaerobic digesters. *Water Research*, 155: 444–454.
- Chang, Y., Peacock, A.D., Long, P.E., Stephen, J.R., Kinley, J.P.M.C., Macnaughton, S.J., Hussain, A.K.M.A., Saxton, A.M. & White, D.C. 2001. Diversity and Characterization of Sulfate-Reducing Bacteria in Groundwater at a Uranium Mill Tailings Site. , 67(7): 3149–3160.
- Chaudhary, P.P., Sirohi, K.S., Singh, D. & Saxena, J. 2011. Methyl Coenzyme M Reductase (mcrA) Gene Based Phylogenetic Analysis of Methanogens Population in Murrah Buffaloes (*Bubalus bubalis*). *The Journal of Microbiology*, 49(4): 558–561.
- Chistoserdova, L., Vorholt, J.A., Thauer, R.K. & Lidstrom, M.E. 1998. C-1 Transfer Enzymes and Coenzymes Linking Methylotrophic Bacteria and Methanogenic Archaea. *Science*, 281: 99–102.
- Chowdhury, M., Mostafa, M.G., Biswas, T.K. & Saha, A.K. 2013. Treatment of leather industrial effluents by filtration and coagulation processes. *Water Resources and Industry*, 3: 11–22.
- Cioabla, A.E., Ionel, I., Dumitrel, G. & Popescu, F. 2012. Comparative study on factors affecting anaerobic digestion of agricultural vegetal residues. *Biotechnology for biofuels*, 5(1): 39.
- Cooper, G.M. 2000. *The Cell: A Molecular Approach*. 2nd ed. Sunderland: Sinauer Associates.
- Costa, C.R., Botta, C.M.R., Espindola, E.L.G. & Olivi, P. 2008. Electrochemical treatment of tannery wastewater using DSA® electrodes. *Journal of Hazardous Materials*, 153(1–2): 616–627.

- Cruz-Salomón, A., Ríos-Valdovinos, E., Pola-Albores, F., Lagunas-Rivera, S., Meza-Gordillo, R., Ruíz-Valdiviezo, V.M. & Cruz-Salomón, K.C. 2019. Expanded granular sludge bed bioreactor in wastewater treatment. *Global Journal of Environmental Science and Management*, 5(1): 119–138.
- D'haene, B., Vandesompele, J. & Hellemans, J. 2010. Accurate and objective copy number profiling using real-time quantitative PCR. *Methods*, 50(4): 262–270. <http://dx.doi.org/10.1016/j.ymeth.2009.12.007>.
- Dague, R.R., McKinney, R.E. & Pfeffer, J.T. 1970. Solids retention in anaerobic waste treatment systems. *Journal of the Water Pollution Control Federation*, 42(2 Part 2): R29–R46.
- Dargo, H. & Ayalew, A. 2014. Tannery Wastewater Treatment: A review. *International Journal of Emerging Trends in Science and Technology*, 1(9): 1488–1494.
- Daud, M.K., Rizvi, H., Akram, M.F., Ali, S., Rizwan, M., Nafees, M. & Jin, Z.S. 2018. Review of Upflow Anaerobic Sludge Blanket Reactor Technology: Effect of Different Parameters and Developments for Domestic Wastewater Treatment. , 2018.
- Deng, L., Liu, Y., Zheng, D., Wang, L., Pu, X. & Song, L. 2017. Application and development of biogas technology for the treatment of waste in China. *Renewable and Sustainable Energy Reviews*, 70(December 2016): 845–851. <http://dx.doi.org/10.1016/j.rser.2016.11.265>.
- Deublein, D. & Steinhauser, A. 2008. *Biogas from Waste and Renewable Resources*. Weinheim: Wiley-VCH.
- Dhawane, S.H., Kumar, T. & Halder, G. 2015. Central composite design approach towards optimization of flamboyant pods derived steam activated carbon for its use as heterogeneous catalyst in transesterification of Hevea brasiliensis oil. *Energy Conversion and Management*, 100: 277–287. <http://dx.doi.org/10.1016/j.enconman.2015.04.083>.
- Dixit, S., Yadav, A., Dwivedi, P.D. & Das, M. 2015. Toxic hazards of leather industry and technologies to combat threat: a review. *Journal of Cleaner Production*, 87: 39–49.
- Duarte, A.G., Santos, A.A. & Pereira, I.A.C. 2016. Electron transfer between the QmoABC membrane complex and adenosine 5' -phosphosulfate reductase. *Biochimica et Biophysica Acta*, 1857: 380–386. <http://dx.doi.org/10.1016/j.bbabi.2016.01.001>.
- Durai, G. & Rajasimman, M. 2011. Biological Treatment of Tannery Wastewater- A review. *Journal of Environmental Science and Technology*, 4(1): 1–17.
- Ebrahimi-nik, M., Heidari, A., Ramezani, S., Asadi, F., Younesi, H., Duc, D., Jeon, B., Hoon, J., Rene, E.R., Banu, J.R., Ravindran, B., Manh, C., Hao, H., Guo, W., Wang, S., Jena, U., Das, K.C., Taylor, P., Mussoline, W., Esposito, G., Giordano, A., Jordaan, G.P., Epa, U.S., The, F.O.R., Of, T., Slaughterhouse, P., In, W., Town, C., Dolejs, P., El, G.,

- Vejmelkova, D., Pecenka, M., Polaskova, M., Bartacek, J., Town, C., Madrid, V.M., Aller, R.C., Aller, J.Y., Chistoserdov, A.Y., Holliger, C., Alves, M., Andrade, D., Angelidaki, I., Astals, S., Baier, U., Bougrier, C., Buf, P., Carballa, M., Wilde, V. De, Ebertseder, F., Fernández, B., Ficara, E., Fotidis, I., Frigon, J., Laclos, H.F. De, Ghasimi, S.M., Hack, G., Hartel, M., Heerenklage, J., Horvath, I.S., Jenicek, P., Koch, K., Krautwald, J., Lizasoain, J., Liu, J., Mosberger, L., Nistor, M., Oechsner, H., Oliveira, J.V., Paterson, M., Pauss, A., Pommier, S., Porqueddu, I., Raposo, F., Ribeiro, T., Pfund, F.R., Strömberg, S., Torrijos, M., Hack, G., Andrade, D., Bougrier, C. & Koch, K. 2016. Towards a standardization of biomethane potential tests Czech Republic. *Water Science & Technology*, 74(11): 2515–2522. <https://doi.org/10.1016/j.jclepro.2018.07.134>.
- El-sheikh, M.A., Saleh, H.I., Flora, J.R. & Abdel-ghany, M.R. 2011. Biological tannery wastewater treatment using two stage UASB reactors. *Desalination*, 276: 253–259.
- Elbeshbishy, E., Nakhla, G. & Hafez, H. 2012. Biochemical methane potential (BMP) of food waste and primary sludge: Influence of inoculum pre-incubation and inoculum source. *Bioresource Technology*, 110: 18–25. <http://dx.doi.org/10.1016/j.biortech.2012.01.025>.
- Elsheikh, M.A.S. 2009. Tannery wastewater pre-treatment. *Water Science and Technology*, 60(2): 433–440.
- Emana, M. & Dawit, M. 2017. Two-stage anaerobic sequence batch digestion of composite tannery wastewater. *African Journal of Environmental Science and Technology*, 11(11): 578–586.
- Eskicioglu, C. & Ghorbani, M. 2011. Effect of inoculum/substrate ratio on mesophilic anaerobic digestion of bioethanol plant whole stillage in batch mode. *Process Biochemistry*, 46(8): 1682–1687. <http://dx.doi.org/10.1016/j.procbio.2011.04.013>.
- Esposito, G., Frunzo, L., Liotta, F., Panico, A. & Pirozzi, F. 2012. Bio-Methane Potential Tests To Measure The Biogas Production From The Digestion and Co-Digestion of Complex Organic Substrates. *The Open Environmental Engineering Journal*, 5: 1–8.
- European Commission. 2003. Integrated Pollution Prevention and Control (IPPC). , (February).
- Fazli, P., Man, H.C., Shah, U.K. & Idris, A. 2013. Characteristics of Methanogens and Methanotrophs in Rice Fields: A Review. *Asia-Pacific Journal of Molecular Biology and Biotechnology*, 21(1): 3–17.
- Feng, L., Li, Y., Chen, C., Liu, X., Xiao, X., Zhang, R., He, Y. & Liu, G. 2013. Biochemical Methane Potential (BMP) of Vinegar Residue and the Influence of Feed to Inoculum Ratios on Biogas Production. *BioResources*, 8(2): 2487–2498.
- Ferry, J.G. 2010. The chemical biology of methanogenesis. *Planetary and Space Science*, 58(14–15): 1775–1783.

- Forster-Carneiro, T., Pérez, P. & Romero, L.I. 2008. Influence of total solid and inoculum contents on performance of anaerobic reactors treating food waste. *Bioresource Technology*, 99: 6994–7002.
- Forster, S., Lappin-scott, H.M., Snape, J.R. & Porter, J. 2003. Rains, drains and active strains: towards online assessment of wastewater bacterial communities. *Journal of Microbiological Methods*, 55: 859–864.
- Franke-whittle, I.H., Walter, A., Ebner, C. & Insam, H. 2014. Investigation into the effect of high concentrations of volatile fatty acids in anaerobic digestion on methanogenic communities. *Waste Management*, 34(11): 2080–2089.
- Freitag, T.E. & Prosser, J.I. 2009. Correlation of Methane Production and Functional Gene Transcriptional Activity in a Peat Soil. *Applied and Environmental Microbiology*, 75(21): 6679–6687.
- Friedrich, M. & Schink, B. 2008. *The Proteobacteria, Bergey's Manual of Systematic Bacteriology*. D. J. Brenner, N. R. Krieg, & J. T. Staley, eds. New York: Springer.
- Friedrich, M.W. 2005. Methyl-Coenzyme M Reductase Genes : Unique Functional Markers for Methanogenic and Anaerobic Methane-Oxidizing Archaea. In *Methods in Enzymology*. Elsevier Inc.: 428–442.
- Ganesh, R. & Ramanujam, R.A. 2009. Biological waste management of leather tannery effluents in India: current options and future research needs. *International Journal of Environmental Engineering*, 1(2): 165–186.
- Gargaud, M. 2015. Synonyms Synonyms. *Encyclopedia of Astrobiology*.
- Geets, J., Borremans, B., Diels, L., Springael, D., Vangronsveld, J., van der Lelie, D. & Vanbroekhoven, K. 2006. DsrB gene-based DGGE for community and diversity surveys of sulfate-reducing bacteria. *Journal of Microbiological Methods*, 66: 194–205.
- Gerardi, M.H. 2003. *The microbiology of anaerobic digesters*. Hoboken: John Wiley & Sons, Inc.
- Ghanimeh, S.A., Al-sanioura, D.N., Saikaly, P.E. & El-fadel, M. 2018. Correlation between system performance and bacterial composition under varied mixing intensity in thermophilic anaerobic digestion of food waste. *Journal of Environmental Management*, 206: 472–481.
- Gil, A., Siles, J.A., Serrano, A., Chica, A.F. & Mart, M.A. 2018. Effect of Variation in the C/[N+P] Ratio on Anaerobic Digestion. *Environmental Progress & Sustainable Energy*, 00(00): 1–9.
- Goswami, S. & Mazumder, D. 2014. Scope of biological treatment for composite tannery wastewater. *International Journal of Environmental Sciences*, 5(3): 607–622.

- Goswami, S. & Mazumder, D. 2013. Treatment of Chrome Tannery Wastewater by Biological Process - A Mini Review. *International Journal of Environment and Ecological Engineering*, 7(11): 798–804.
- Guan, J., Xia, L., Wang, L., Liu, J., Gu, J. & Mu, B. 2013. International Biodeterioration & Biodegradation Diversity and distribution of sulfate-reducing bacteria in four petroleum reservoirs detected by using 16S rRNA and dsrAB genes. *International Biodeterioration & Biodegradation*, 76: 58–66. <http://dx.doi.org/10.1016/j.ibiod.2012.06.021>.
- Guerrero, L., Chamy, R., Jeison, D., Montalvo, S., Huiliñir, C., Guerrero, L., Chamy, R., Jeison, D. & Montalvo, S. 2013. Behavior of the anaerobic treatment of tannery wastewater at different initial pH values and sulfate concentrations. *Journal of Environmental Science and Health , Part A*, 48: 1073–1078.
- Guo, J., Peng, Y., Ni, B.-J., Han, X., Fan, L. & Yuan, Z. 2015. Dissecting microbial community structure and methane-producing pathways of a full-scale anaerobic reactor digesting activated sludge from wastewater treatment by metagenomic sequencing. *Microbial Cell Factories*, 14: 33.
- Hagman, L., Blumenthal, A., Eklund, M. & Svensson, N. 2018. The role of biogas solutions in sustainable biorefineries. *Journal of Cleaner Production*, 172: 3982–3989.
- Hampannavar, S. & Shivayogimath, C. 2010. Anaerobic treatment of sugar industry wastewater by Upflow anaerobic sludge blanket reactor at ambient temperature. *International Journal of Environmental Sciences*, 1(4): 631–639.
- Haydar, S. & Aziz, J.A. 2009. Coagulation-flocculation studies of tannery wastewater using cationic polymers as a replacement of metal salts. *Water Science and Technology*, 59(2): 381–390.
- Haydar, S., Aziz, J.A. & Ahmad, M.S. 2007. Biological Treatment of Tannery Wastewater Using Activated Sludge Process. *Pakistan journal of engineering and applied sciences*, 1: 61–67.
- He, J.Z., Liu, X.Z., Zheng, Y., Shen, J.P. & Zhang, L.M. 2010. Dynamics of sulfate reduction and sulfate-reducing prokaryotes in anaerobic paddy soil amended with rice straw. *Biology and Fertility of Soils*, 46(3): 283–291.
- Hickey, R.F., Wu, W.M., Veiga, M.C. & Jones, R. 1991. Start-up, operation, monitoring and control of high-rate anaerobic treatment systems. *Water Science and Technology*, 24(8): 207–255.
- Hobbs, S., Landis, A.E., Rittmann, B.E., Young, M.N. & Parameswaran, P. 2018. Enhancing anaerobic digestion of food waste through biochemical methane potential assays at different substrate: inoculum ratios. *Waste Management*, 71: 612–617. <https://doi.org/10.1016/j.wasman.2017.06.029>.

- Hobbs, S.R., Landis, A.E., Rittmann, B.E., Young, M.N. & Parameswaran, P. 2018. Enhancing anaerobic digestion of food waste through biochemical methane potential assays at different substrate: inoculum ratios. *Waste Management*, 71: 612–617. <https://doi.org/10.1016/j.wasman.2017.06.029>.
- Hoffmann, R.A., Garcia, M.L., Veskivar, M., Karim, K., Al-dahhan, M.H. & Angenent, L.T. 2008. Effect of Shear on Performance and Microbial Ecology of Continuously Stirred Anaerobic Digesters Treating Animal Manure. *Biotechnology and Bioengineering*, 100(1): 38–48.
- Holliger, C., Alves, M., Andrade, D., Angelidaki, I., Astals, S., Baier, U., Bougrier, C., Buf, P., Carballa, M., Wilde, V. De, Ebertseder, F., Fernández, B., Ficara, E., Fotidis, I., Frigon, J., Laclos, H.F. De, Ghasimi, S.M., Hack, G., Hartel, M., Heerenklage, J., Horvath, I.S., Jenicek, P., Koch, K., Krautwald, J., Lizasoain, J., Liu, J., Mosberger, L., Nistor, M., Oechsner, H., Oliveira, J.V., Paterson, M., Pauss, A., Pommier, S., Porqueddu, I., Raposo, F., Ribeiro, T., Pfund, F.R., Strömberg, S., Torrijos, M., Hack, G., Andrade, D., Bougrier, C. & Koch, K. 2016. Towards a standardization of biomethane potential tests. *Water Science & Technology*, 74(11): 2515–2522.
- Hook, S.E., Wright, G. & McBride, B.W. 2010. Methanogens: Methane Producers of the Rumen and Mitigation Strategies. *Hindawi Publishing Corporation*, 2010: 50–60.
- Houari, A. El, Ranchou-peyruse, M., Ranchou-peyruse, A., Dakdaki, A., Guignard, M., Idouhammou, L., Bennisse, R. & Bouterfass, R. 2017. *Desulfobulbus oligotrophicus* sp. nov., a sulfate-reducing and propionate-oxidizing bacterium isolated from a municipal anaerobic sewage sludge digester. *International Journal of Systematic and Evolutionary Microbiology*, 67: 275–281.
- Igoni, A.H., Abowei, M.F.N., Ayotamuno, M.J. & Eze, C.L. 2008. Effect of Total Solids Concentration of Municipal Solid Waste on the Biogas Produced in an Anaerobic Continuous Digester. *Agricultural Engineering International: the CIGR Ejournal*, X: 1–11.
- Insam, H. & Wett, B. 2008. Control of GHG emission at the microbial community level. *Waste Management*, 28: 699–706.
- Isa, Z., Grusenmeyer, S. & Verstraete, W. 1986a. Sulfate Reduction Relative. *Applied and Environmental Microbiology*, 51(3): 572–579.
- Isa, Z., Grusenmeyer, S. & Verstraete, W. 1986b. Sulfate Reduction Relative to Methane Production in High-Rate Anaerobic Digestion: Microbiological Aspects. *Applied and Environmental Microbiology*, 51(3): 580–587.
- Islamud-Din, N., Hesham, A.E.L., Ahmad, A., Daqiang, C. & Khan, S. 2014. PCR-DGGE and real-time PCR *dsrB*-based study of the impact of heavy metals on the diversity and abundance of sulfate-reducing bacteria. *Biotechnology and Bioprocess Engineering*, 19(4): 703–710.

- Jha, P. & Schmidt, S. 2017. Reappraisal of chemical interference in anaerobic digestion processes. *Renewable and Sustainable Energy Reviews*, 75: 954–971.
- Jiang, Y., Li, H., Qin, Y., Liang, Y., Wu, C., Liu, K. & Yu, F. 2019. Spatial separation and bio-chain cooperation between sulfidogenesis and methanogenesis in an anaerobic baffled reactor with sucrose as the carbon source. *International Biodeterioration and Biodegradation*, 138: 99–105. <https://doi.org/10.1016/j.ibiod.2019.01.004>.
- Jing, Z., Hu, Y., Niu, Q., Liu, Y., Li, Y. & Wang, X.C. 2013. Bioresource Technology UASB performance and electron competition between methane-producing archaea and sulfate-reducing bacteria in treating sulfate-rich wastewater containing ethanol and acetate. *Bioresource Technology*, 137: 349–357.
- Jingura, R.M. & Kamusoko, R. 2017. Methods for determination of biomethane potential of feedstocks: a review. *Biofuel Research Journal*, 14: 573–586.
- Joergensen, R.G. & Emmerling, C. 2006. Methods for evaluating human impact on soil microorganisms based on their activity, biomass, and diversity in agricultural soils. *Journal of Plant Nutrition and Soil Science*, 169(3): 295–309.
- Juottonen, H., Galand, P.E. & Yrjälä, K. 2006. Detection of methanogenic Archaea in peat: comparison of PCR primers targeting the mcrA gene. *Research in Microbiology*, 157: 914–921.
- Kabdasli, I., Tunay, O. & Orhon, D. 1999. Wastewater control and management in a leather tanning district. *Water Science and Technology*, 40: 261–267.
- Kameswari, K., Kalyanaraman, C., Umamaheswari, B. & Thanasekaran, K. 2014. Enhancement of biogas generation during co-digestion of tannery solid wastes through optimization of mix proportions of substrates. *Clean Technologies and Environmental Policy*, 16: 1067–1080.
- Kanaparthi, D., Reim, A., Martinson, G.O., Pommerenke, B. & Conrad, R. 2017. Methane emission from feather moss stands. *Global Change Biology*, 10: 1–12.
- Kaparaju, P., Buendia, I., Ellegaard, L. & Angelidakia, I. 2008. Effects of mixing on methane production during thermophilic anaerobic digestion of manure: Lab-scale and pilot-scale studies. *Bioresource Technology*, 99: 4919–4928.
- Karakashev, D., Batstone, D.J. & Angelidaki, I. 2005. Influence of Environmental Conditions on Methanogenic Compositions in Anaerobic Biogas Reactors. *Applied and Environmental Microbiology*, 71(1): 331–338.
- Karamperis, K., Wadge, S., Koromina, M. & Patrinos, G.P. 2020. Genetic Testing. In *Applied Genomics and Public Health*. New York: Elsevier Inc.: 189–208. <http://dx.doi.org/10.1016/B978-0-12-813695-9.00010-8>.

- Karim, K., Hoffmann, R., Klasson, K.T. & Al-dahhan, M.H. 2005. Anaerobic digestion of animal waste: Effect of mode of mixing. *Water Research*, 39: 3597–3606.
- Kariyama, I.D., Zhai, X. & Wu, B. 2018. Influence of mixing on anaerobic digestion efficiency in stirred tank digesters: A review. *Water Research*, 143: 503–517.
- Kavitha. 2009. *Feasibility study of upflow anaerobic filter for pre-treatment of municipal wastewater*. National University of Singapore, Kent Ridge.
- Kaviyaran, K. 2014. Application of UASB Reactor in Industrial Wastewater Treatment – A Review. *International Journal of Science & Engineering Research*, 5(1): 584–589.
- Kawai, M., Nagao, N., Tajima, N., Niwa, C., Matsuyama, T. & Toda, T. 2014. The effect of the labile organic fraction in food waste and the substrate / inoculum ratio on anaerobic digestion for a reliable methane yield. *Bioresource Technology*, 157: 174–180. <http://dx.doi.org/10.1016/j.biortech.2014.01.018>.
- Khan, M.A., Mohsin, J. & Faheem, S.M. 2013. Monitoring Microbial Diversity of a Full-Scale Municipal Wastewater Treatment Plant in Dubai. *APCBEE Procedia*, 5: 102–106. <http://dx.doi.org/10.1016/j.apcbee.2013.05.018>.
- Kim, M., Ahn, Y. & Speece, R.E. 2002. Comparative process stability and efficiency of anaerobic digestion ; mesophilic vs . thermophilic. *Water Research*, 36: 4369–4385.
- Koschorreck, M. 2008. Microbial sulphate reduction at a low pH. *FEMS Microbiology Ecology*, 64(3): 329–342.
- Koster, I.W., Rinzema, A. & De Vegt, A.L. 1986. Sulfide inhibition of the methanogenic activity of granular sludge at various pH-levels. *Water Research*, 20(12): 1561–1567.
- Krishnamoorthi, S., Sivakumar, V. & Saravanan, K. 2009. Treatment and Reuse of Tannery Waste Water by Embedded System. *Modern Applied Science*, 3(1): 129–134.
- Kristjanson, J.K., Schönheit, P. & Thauer, R.K. 1982. Different K_S values for hydrogen of methanogenic bacteria and sulfate reducing bacteria: an explanation for the apparent inhibition of methanogenesis by sulfate. *Archives of Microbiology*, 131: 278–282.
- Kröniger, L., Gottschling, J. & Deppenmeier, U. 2017. Growth Characteristics of *Methanomassiliococcus luminyensis* and Expression of Methyltransferase Encoding Genes. *Archaea*, 2017: 1–12.
- Kurt, U., Apaydin, O. & Gonullu, M.T. 2007. Reduction of COD in wastewater from an organized tannery industrial region by Electro-Fenton process. *Journal of Hazardous Materials*, 143: 33–40.
- Kushkevych, I., Vítězová, M., Vítěz, T. & Bartoš, M. 2017. Production of biogas: relationship between methanogenic and sulfate-reducing microorganisms. *Open Life Sciences*: 82–91.

- Langeveld, J.W.A., Dixon, J. & Jaworski, J.F. 2010. Development Perspectives Of The Biobased Economy : A Review. *Crop Science*, 50: 142–151.
- Lastella, G., Testa, C., Cornacchia, G., Notornicola, M. & Voltasio, F. 2002. Anaerobic digestion of semi-solid organic waste : biogas production and its purification. *Energy Conversion Management*, 43: 63–75.
- Latha, A., Raj, G.S., Kaushik, G. & Sabari, S.K. 2016. Treatment of Tannery Effluent by U.A.S.B Reactor Method. *International Journal for Research in Applied Science & Engineering Technology*, 4(4): 170–176.
- Latif, M.A., Ghufuran, R., Wahid, Z.A. & Ahmad, A. 2011. Integrated application of upflow anaerobic sludge blanket reactor for the treatment of wastewaters. *Water Research*, 45(16): 4683–4699. <http://dx.doi.org/10.1016/j.watres.2011.05.049>.
- Lay, J.-J., Li, Y.-Y. & Noike, T. 1997. Influences of pH and Moisture Content on the Methane production in High-Solids Sludge Digestion. *Water Research*, 31(6): 1518–1524.
- Lee, C., Kim, J., Hwang, K., Flaherty, V.O. & Hwang, S. 2009. Quantitative analysis of methanogenic community dynamics in three anaerobic batch digesters treating different wastewaters. *Water Research*, 43: 157–165.
- Lefebvre, O., Vasudevan, N., Torrijos, M., Thanasekaran, K. & Moletta, R. 2006. Anaerobic digestion of tannery soak liquor with an aerobic post-treatment. *Water Research*, 40: 1492–1500.
- de Lemos Chernicharo, C.A. 2007. *Biological Wastewater Treatment Series: Anaerobic Reactors*. London: IWA Publishing.
- Lens, P.N.L., Visser, A., Janssen, A.J.H., Hulshoff Pol, L.W. & Lettinga, G. 1998. Biotechnological Treatment of Sulfate-Rich Wastewaters. *Critical Reviews in Environmental Science and Technology*, 28(1): 41–88. <http://www.tandfonline.com/action/journalInformation?journalCode=best20%5Cnhttp://dx.doi.org/10.1080/10643389891254160>.
- Lettinga, G., Rebac, S. & Zeeman, G. 2001. Challenge of psychrophilic anaerobic wastewater treatment. *Trends in Biotechnology*, 19(9): 363–370.
- Li, L., He, Qingming, Wei, Y., He, Qin & Peng, X. 2014. Early warning indicators for monitoring the process failure of anaerobic digestion system of food waste. *Bioresource Technology*, 171: 491–494. <http://dx.doi.org/10.1016/j.biortech.2014.08.089>.
- Li, W. cheng, Wang, C., Tian, Z., Zhang, H., Gao, Y., Zhang, Y., Yang, M., Li, Y.-Y. & Nishimura, O. 2015. Anaerobic treatment of p-acetamidobenzene sulfonyl chloride (p-ASC) -containing wastewater in the presence or absence of ethanol in a UASB reactor. *International Biodeterioration & Biodegradation*, 98: 81–88. <http://dx.doi.org/10.1016/j.ibiod.2014.09.002>.

- Lier, J.B., Zee, F.P., Frijters, C.T.M.J. & Ersahin, M.E. 2015. Celebrating 40 years anaerobic sludge bed reactors for industrial wastewater treatment. *Reviews in Environmental Science and Bio/Technology*, 14(4): 681–702.
- Life Technologies. 2012. *Real-time PCR handbook*. Carlsbad: Life Technologies Corporation.
- Lin, C.-Y. 1992. Effect of heavy metals on volatile fatty acid degradation in anaerobic digestion. *Water Research*, 26(2): 177–183.
- Lindmark, J., Eriksson, P. & Thorin, E. 2014. The effects of different mixing intensities during anaerobic digestion of the organic fraction of municipal solid waste. *Waste Management*, 34(8): 1391–1397. <http://dx.doi.org/10.1016/j.wasman.2014.04.006>.
- Lindmark, J., Thorin, E., Bel, R. & Dahlquist, E. 2014. Effects of mixing on the result of anaerobic digestion: Review. *Renewable and Sustainable Energy Reviews*, 40: 1030–1047. <http://dx.doi.org/10.1016/j.rser.2014.07.182>.
- Liu, C., Miyaki, T., Toshihiro, A. & Oyaizu, H. 2008. Evaluation of Methanogenic Strains and Their Ability to Endure Aeration and Water Stress. *Current Microbiology*, 56: 214–218.
- Liu, T., Sun, L. & Nordberg, Å. 2018. Substrate-Induced Response in Biogas Process Performance and Microbial Community Relates Back to Inoculum Source. *Microorganisms*, 6(80).
- Liu, W.-H., Zhang, C.-G., Gao, P.-F., Liu, H., Song, Y.-Q. & Yang, J.-F. 2017. Advanced treatment of tannery wastewater using the combination of UASB , SBR , electrochemical oxidation and BAF. *Journal of Chemical Technology & Biotechnology*, 92: 588–597.
- Lofrano, G., Belgiorno, V., Gallo, M. & Raimo, A. 2006. Toxicity reduction in leather tanning wastewater by improved coagulation flocculation process. *Global NEST Journal/Global NEST: the international Journal*, 8(2): 151–158.
- Lofrano, G., Meriç, S., Emel, G. & Orhon, D. 2013. Chemical and biological treatment technologies for leather tannery chemicals and wastewaters: A review. *Science of the Total Environment*, 461–462: 265–281.
- Lu, X., Zhen, G., Ni, J., Kubota, K. & Li, Y. 2017. Sulfidogenesis process to strengthen re-granulation for biodegradation of methanolic wastewater and microorganisms evolution in an UASB reactor. *Water Research*, 108: 137–150. <http://dx.doi.org/10.1016/j.watres.2016.10.073>.
- Luptakova, A. & Kusnierova, M. 2005. Bioremediation of acid mine drainage contaminated by SRB. *Hydrometallurgy*, 77(1–2): 97–102.
- Luton, P.E., Wayne, J.M., Sharp, R.J. & Riley, P.W. 2002. The mcrA gene as an alternative to 16S rRNA in the phylogenetic analysis of methanogen populations in landfill. *Microbiology*, 148(2002): 3521–3530.

- Lyu, Z. & Lu, Y. 2017. Metabolic shift at the class level sheds light on adaptation of methanogens to oxidative environments. *Nature Publishing Group*, 12(2): 411–423. <http://dx.doi.org/10.1038/ismej.2017.173>.
- Ma, K., Conrad, R. & Lu, Y. 2012. Responses of Methanogen *mcrA* Genes and Their Transcripts to an Alternate Dry / Wet Cycle of Paddy Field Soil. *Applied and Environmental Microbiology*, 78(2): 445–454.
- Madden, P., Al-raei, A.M., Enright, A.M., Chinalia, F.A. & Beer, D. De. 2014. Effect of sulfate on low-temperature anaerobic digestion. *frontiers in Microbiology*, 5: 1–15.
- Maddocks, S. & Jenkins, R. 2016. *Quantitative PCR: Things to Consider*. London: Elsevier Inc.
- Madrid, V.M., Aller, R.C., Aller, J.Y. & Chistoserdov, A.Y. 2006. Evidence of the activity of dissimilatory sulfate-reducing prokaryotes in nonsulfidogenic tropical mobile muds. *FEMS microbiology ecology*, 57: 169–181.
- Mahboudi, H., Heidari, N.M., Rashidabadi, Z.I., Anbarestani, A.H., Karimi, S. & Darestani, K.D. 2018. Prospect and Competence of Quantitative Methods via Real-time PCR in a Comparative Manner: An Experimental Review of Current Methods. *The Open Bioinformatics Journal*, 11(1): 1–11.
- Manariotis, I.D. & Grigoropoulos, S.G. 2006. Municipal-Wastewater Treatment Using Upflow-Anaerobic Filters. *Water Environmental Research*, 78(3): 233–242.
- Mandal, T., Dasgupta, D., Mandal, S. & Datta, S. 2010. Treatment of leather industry wastewater by aerobic biological and Fenton oxidation process. *Journal of Hazardous Materials*, 180(1–3): 204–211.
- Mannucci, A., Munz, G., Mori, G. & Lubello, C. 2010. Anaerobic treatment of vegetable tannery wastewaters: A review. *Desalination*, 264(1–2): 1–8. <http://dx.doi.org/10.1016/j.desal.2010.07.021>.
- Manyi-loh, C.E., Mamphweli, S.N., Meyer, E.L. & Okoh, A.I. 2013. Microbial Anaerobic Digestion (Bio-Digesters) as an Approach to the Decontamination of Animal Wastes in Pollution Control and the Generation of Renewable Energy. *International Journal of Environmental Research and Public Health*, 10: 4390–4417.
- Marilynn, R., Fairfax, M. & Salimnia, H. 2010. Quantitative PCR : An Introduction. In *Molecular Diagnostics: Techniques and Applications for the Clinical Laboratory*. Academic Press Inc.
- Marti-herrero, J. 2011. Reduced hydraulic retention times in low-cost tubular digesters: Two issues. *Biomass and bioenergy*, 35: 4481–4484.
- Marti, I.. 2008. *Study of the effect of process parameters on the thermophilic anaerobic*

digestion of sewage sludge, evaluation of a thermal sludge pre-treatment and overall energetic assessment. Autonomous University of Barcelona, Cerdanyola del Valles.

- Martins, M., Faleiro, M.L., Barros, R.J., Veríssimo, A.R., Barreiros, M.A. & Costa, M.C. 2009. Characterization and activity studies of highly heavy metal resistant sulphate-reducing bacteria to be used in acid mine drainage decontamination. *Journal of Hazardous Materials*, 166: 706–713.
- Massé, D.I. & Masse, L. 2000. Treatment of slaughterhouse wastewater in anaerobic sequencing batch reactors. *Canadian Agricultural Engineering*, 41(3): 131–137.
- Matangue, M.T.A. & Campos, C.M.M. 2011. Determination of Kinetic Parameters of an Upflow Anaerobic Sludge Blanket Reactor (UASB), Treating Swine Wastewater. *Science and Agrotechnology Journal*, 35(6): 1204–1210.
- Mathuriya, A.S. 2014. Enhanced tannery wastewater treatment and electricity generation in microbial fuel cell. *Environmental Engineering and Management Journal*, 13(12): 2945–2954.
- Mazumder, D., Mukherjee, S. & Ray, P.K. 2008. Treatment of tannery wastewater in a hybrid biological reactor. *International Journal of Environment and Pollution*, 34(1–4): 43–56.
- McCartney, D. M. Oleszkiewicz, J.A. 1991. Sulfide inhibition of anaerobic degradation of lactate and acetate. *Water Research*, 25(2): 203–209.
- McCartney, C.A., Bull, I.D. & Dewhurst, R.J. 2013. Chemical markers for rumen methanogens and methanogenesis. *Animal*, 7(s2): 409–417.
- Mcmahon, K.D., Stroot, P.G., Mackie, R.I. & Raskin, L. 2001. Anaerobic codigestion of municipal solid waste and biosolids under various mixing conditions- II: microbial population dynamics. *Water Research*, 35(7): 1817–1827.
- Meegoda, J.N., Li, B., Patel, K. & Wang, L.B. 2018. A review of the processes, parameters, and optimization of anaerobic digestion. *International Journal of Environmental Research and Public Health*, 15(10).
- Mekonnen, A., Leta, S. & Nicholas, K. 2017. Anaerobic treatment of tannery wastewater using ASBR for methane recovery and greenhouse gas emission mitigation. *Journal of Water Process Engineering*, 19: 231–238.
- Mekonnen, A., Leta, S. & Njau, K.N. 2016. Anaerobic co-treatment of tannery wastewater and cattle dung for biogas production using a pilot scale anaerobic sequencing batch reactor (ASBR). *International Journal of Scientific & Engineering Research*, 7(6): 633–649.
- Mekonnen, A., Leta, S. & Njau, K.N. 2017. Kinetic analysis of anaerobic sequencing batch reactor for the treatment of tannery wastewater. *African Journal of Environmental Science and Technology*, 11(6): 339–348.

- Méndez-Acosta, H.O., Snell-Castro, R., Alcaraz-González, V., González-Alvarez, V. & Pelayo-ortiz, C. 2010. Anaerobic treatment of Tequila vinasses in a CSTR-type digester. *Biodegradation*, 21: 357–363.
- de Mes, T.Z.D., Stams, A.J.M., Reith, J.H. & Zeeman, G. 2003. Methane production by anaerobic digestion of wastewater and solid wastes.
- Metcalf & Eddy. 2003. *Wastewater Engineering, Treatment and reuse*. 4th ed. New Y.
- Midha, V. & Dey, A. 2008. Biological treatment of tannery wastewater for sulphide removal. *International Journal of Chemical Sciences*, 6(2): 472–486.
- Moestedt, J., Nilsson, S. & Schnürer, A. 2013. The effect of substrate and operational parameters on the abundance of sulphate-reducing bacteria in industrial anaerobic biogas digesters. *Bioresource Technology*, 132: 327–332. <http://dx.doi.org/10.1016/j.biortech.2013.01.043>.
- Molinuevo-salces, B., García-gonzález, M.C., González-fernández, C., José, M., Morán, A. & Gómez, X. 2010. Anaerobic co-digestion of livestock wastes with vegetable processing wastes: A statistical analysis. *Bioresource Technology*, 101(24): 9479–9485. <http://dx.doi.org/10.1016/j.biortech.2010.07.093>.
- Montalvo, S., Huiliñir, C., Borja, R. & Castillo, A. 2019. Anaerobic digestion of wastewater rich in sulfate and sulfide: effects of metallic waste addition and micro-aeration on process performance and methane production. *Journal of Environmental Science and Health, Part A*: 1–9. <https://doi.org/10.1080/10934529.2019.1623597>.
- Montero, B., Sales, D. & Solera, R. 2009. Analysis of methanogenic activity in a thermophilic-dry anaerobic reactor: Use of fluorescent in situ hybridization. *Waste Management*, 29(3): 1144–1151.
- Moraes, B.S., Souza, T.S.O. & Foresti, E. 2012. Effect of sulfide concentration on autotrophic denitrification from nitrate and nitrite in vertical fixed-bed reactors. *Process Biochemistry*, 47(9): 1395–1401. <http://dx.doi.org/10.1016/j.procbio.2012.05.008>.
- Morero, B., GropPELLI, E.S. & Campanella, E.A. 2016. Evaluation of biogas upgrading technologies using a response surface methodology for process simulation Evaluation of biogas upgrading technologies using a response surface methodology for process simulation. *Journal of Cleaner Production*, 141(September 2017): 978–988. <http://dx.doi.org/10.1016/j.jclepro.2016.09.167>.
- Morris, R., Schauer-gimenez, A., Bhattad, U., Kearney, C., Struble, C.A., Zitomer, D. & Maki, J.S. 2013. Methyl coenzyme M reductase (mcrA) gene abundance correlates with activity measurements of methanogenic H₂/CO₂-enriched anaerobic biomass. *Microbial biotechnology*, 7(1): 77–84.
- Morris, R.L., Tale, V.P., Mathai, P.P., Zitomer, D.H. & Maki, J.S. 2015. mcrA Gene abundance

- correlates with hydrogenotrophic methane production rates in full-scale anaerobic waste treatment systems. *Letters in Applied Microbiology*, 62: 111–118.
- Muller, A.L., Kjeldsen, K.U., Rattei, T., Pester, M. & Loy, A. 2015. Phylogenetic and environmental diversity of DsrAB-type dissimilatory (bi) sulfite reductases. *International Society for Microbial Ecology*, 9: 1152–1165.
- Muñoz, K., Buchmann, C., Meyer, M., Schmidt-Heydt, M., Steinmetz, Z., Diehl, D., Thiele-Bruhn, S. & Schaumann, G.E. 2017. Physicochemical and microbial soil quality indicators as affected by the agricultural management system in strawberry cultivation using straw or black polyethylene mulching. *Applied Soil Ecology*, 113: 36–44. <http://dx.doi.org/10.1016/j.apsoil.2017.01.014>.
- Mustapha, U., Loveth, E.C., Bashir, M.M., Balarabe, M.I., Bashir, S., Tijjani, T.U., Anthony, O.A. & Muhammad, A.I. 2017. Bioremediation of Total Soluble Salt of Tannery Effluent Using Halophilic Microbial Consortium Email address: *International Journal of Ecotoxicology and Ecobiology*, 2(3): 109–118.
- Mutungwazi, A., Mukumba, P. & Makaka, G. 2018. Biogas digester types installed in South Africa : A review. *Renewable and Sustainable Energy Reviews*, 81: 172–180.
- Muyzer, G. & Stams, A.J.M. 2008. The ecology and biotechnology of sulphate-reducing bacteria. *Nature Reviews Microbiology*, 6(6): 441–454.
- Nacheva, P.M., Chávez, G.M. & Herrera, M.J. 2004. Alternative treatment strategy for tannery water reuse and material recovery. *Water Science and Technology*, 5(2): 121–130.
- Nasir, I.M., Ghazi, T.I.M. & Omar, R. 2012. Anaerobic digestion technology in livestock manure treatment for biogas production : A review. *Eng. Life Sci*, 12(3): 258–269.
- Nautiyal, A. & Shukla, S.R. 2018. Silver nanoparticles catalyzed reductive decolorization of spent dye bath containing acid dye and its reuse in dyeing. *Journal of Water Process Engineering*, 22: 276–285. <https://doi.org/10.1016/j.jwpe.2018.02.014>.
- Ndegwa, P.M., Hamilton, D.W., Lalman, J.A. & Cumba, H.J. 2005. Optimization of anaerobic sequencing batch reactors treating dilute swine slurries. *American Society of Agricultural Engineers*, 48(4): 1575–1584.
- Ndobeni, A. 2017. *Effect of temperature and carbon to nitrogen ratio on the performance of an upflow anaerobic sludge blanket reactor treating sugarcane molasses*. Cape Peninsula University of Technology.
- Ndon, U. & Dague, R. 1997. Effects of Temperature and Hydraulic Retention Time on Anaerobic Sequencing Batch Reactor Treatment of Low-Strength Wastewater. *Water Research*, 31(10): 2455–2466.
- Nelson, M.C., Morrison, M. & Yu, Z. 2011. Bioresource Technology A meta-analysis of the

- microbial diversity observed in anaerobic digesters. *Bioresource Technology*, 102(4): 3730–3739.
- Niu, Z. shun, Pan, H., Guo, X. pan, Lu, D. pei, Feng, J. nan, Chen, Y. ru, Tou, F. yun, Liu, M. & Yang, Y. 2018. Sulphate-reducing bacteria (SRB) in the Yangtze Estuary sediments: Abundance, distribution and implications for the bioavailability of metals. *Science of the Total Environment*, 634: 296–304. <https://doi.org/10.1016/j.scitotenv.2018.03.345>.
- O’Flaherty, V. & Colleran, E. 1999. Effect of sulphate addition on volatile fatty acid and ethanol degradation in an anaerobic hybrid reactor. *Bioresource Technology*, 68(2): 101–107.
- O’Reilly, C. & Colleran, E. 2005. Microbial sulphate reduction during anaerobic digestion: EGSB process performance and potential for nitrite suppression of SRB activity. *Water Sci Technol*, 52(1–2): 371–376.
- Ohemeng-ntiamoah, J. & Datta, T. 2019. Perspectives on variabilities in biomethane potential test parameters and outcomes : A review of studies published between 2007 and 2018. *Science of the Total Environment*, 664: 1052–1062.
- Ohimain, E.I. & Izah, S.C. 2017. A review of biogas production from palm oil mill effluents using different configurations of bioreactors. *Renewable and Sustainable Energy Reviews*, 70: 242–253.
- Omil, F., Lens, P., Hulshoff, L. & Lettinga, G. 1996. Effect of Upward Velocity and Sulphide Concentration on Volatile Fatty Acid Degradation in a Sulphidogenic Granular Sludge Reactor. *Process Biochemistry*, 31(7): 699–710.
- Ong, H.K., Greenfield, P.F. & Pullammanappallil, P.C. 2002. Effect of Mixing on Biomethanation of Cattle-Manure Slurry. *Environmental Technology*, 23: 1081–1090.
- Paramaguru, G., Kannan, M. & Lawrence, P. 2017. Effect of pH on Biogas Production through Anaerobic Digestion of Food Waste. *Journal of Advanced Engineering Research*, 4(1): 59–62.
- Patil, P.D., Gude, V.G., Reddy, H.K., Muppaneni, T. & Deng, S. 2012. Biodiesel Production from Waste Cooking Oil Using Sulfuric Acid and Microwave Irradiation Processes. *Journal of Environmental Protection*, 3: 107–113.
- Pavani, S., Rao, Y.M. & Kumar, Y.S. 2016. Use of Box-Behnken Experimental design for Optimization of process Variables in Iontophoretic delivery of Repaglinide. *Journal of Young pharmacist*, 8(4): 350–355.
- Pfaffl, M.W. 2004. Quantification strategies in real-time PCR. In *A-Z of quantitative PCR*. 87–112. <http://www.gene-quantification.de/chapter-3-pfaffl.pdf>.
- Plugge, C.M., Zhang, W., Scholten, J.C.M. & Stams, A.J.M. 2011. Metabolic flexibility of sulfate-reducing bacteria. *frontiers in Microbiology*, 2(81): 1–8.

- Pokorna, D. & Zabranska, J. 2015. Sulfur-oxidizing bacteria in environmental technology. *Biotechnology Advances*, 33(6): 1246–1259. <http://dx.doi.org/10.1016/j.biotechadv.2015.02.007>.
- Polizzi, C., Alatríste-mondragón, F. & Munz, G. 2018. The role of organic load and ammonia inhibition in anaerobic digestion of tannery fleshing. *Water Resources and Industry*, 19: 25–34.
- Porwal, H.J., Mane, A. V & Velhal, S.G. 2015. Biodegradation of dairy effluent by using microbial isolates obtained from activated sludge. *Water Resources and Industry*, 9: 1–15.
- Procházka, J., Dolejš, P., Máca, J. & Dohányos, M. 2012. Stability and inhibition of anaerobic processes caused by insufficiency or excess of ammonia nitrogen. *Applied Microbiology and Biotechnology*, 93: 439–447.
- Pycke, B.F.G., Etchebehere, C., Caveye, P. Van De, Negroni, A., Verstraete, W. & Boon, N. 2011. A time-course analysis of four full-scale anaerobic digesters in relation to the dynamics of change of their microbial communities. *Water Science and Technology*: 769–776.
- Qiu, P., Cui, M., Kang, K., Park, B., Son, Y., Khim, E., Jang, M. & Khim, J. 2014. Application of Box–Behnken design with response surface methodology for modeling and optimizing ultrasonic oxidation of arsenite with H₂O₂. *Central European Journal of Chemistry*, 12(2): 164–172.
- Quail, M.A., Smith, M., Coupland, P., Otto, T.D., Harris, S.R., Connor, T.R., Bertoni, A., Swerdlow, H.P. & Gu, Y. 2012. A tale of three next generation sequencing platforms: comparison of Ion Torrent, Pacific Biosciences and Illumina MiSeq sequencers. *BMC Genomics*, 13(341).
- Rajagopal, R., Masse, D.I. & Singh, G. 2013. A critical review on inhibition of anaerobic digestion process by excess ammonia. *Bioresource Technology*, 143: 632–641.
- Raposo, F., Fern, V., Rubia, M.A. De, Borja, R., B, F., Fern, M., Frigon, J.C., Cavinato, C., Demirer, G., Fern, B., Menin, G., Peene, A., Scherer, P., Torrijos, M., Uellendahl, H., Wierinck, I. & Wilde, V. De. 2011. Biochemical methane potential (BMP) of solid organic substrates: evaluation of anaerobic biodegradability using data from an international interlaboratory study. *Journal of Chemical Technology & Biotechnology*, 86: 1088–1098.
- Rastogi, G., Ranade, D.R., Yeole, T.Y., Patole, M.S. & Shouche, Y.S. 2008. Investigation of methanogen population structure in biogas reactor by molecular characterization of methyl-coenzyme M reductase A (mcrA) genes. *Bioresource Technology*, 99: 5317–5326.
- Regueiro, L., Veiga, P., Figueroa, M., Alonso-gutierrez, J., Stams, A.J.M., Lema, J.M. &

- Carballa, M. 2012. Relationship between microbial activity and microbial community structure in six full-scale anaerobic digesters. *Microbiological Research*, 167(10): 581–589. <http://dx.doi.org/10.1016/j.micres.2012.06.002>.
- Reyes-Avila, J., Razo-Flores, E. & Gomez, J. 2004. Simultaneous biological removal of nitrogen, carbon and sulfur by denitrification. *Water Research*, 38(14–15): 3313–3321.
- Rodriguez-chiang, L.M. & Dahl, O. 2014. Effect of Inoculum to Substrate Ratio on the Methane Potential of Microcrystalline Cellulose Production. *BioResources*, 10(1): 898–911.
- Ros, M. & Gantar, A. 1998. Possibilities of reduction of reciepoint loading of tannery wastewater in Slovenia. *Water Science and Technology*, 37(8): 145–152.
- Routh, T. 2000. Anaerobic treatment of vegetable tannery wastewater by UASB process. *Indian Journal of Environmental Health*, 20(2): 115–123.
- Sabumon, P. 2016. Perspectives on Biological Treatment of Tannery Effluent. *Advances Recycling Waste Management*, 1(1): 1–10.
- Sabumon, P.C. 2016. Advances in Recycling & Waste Management : Open Access. *Advances in Recycling & Waste Management*, 1(1): 1–10.
- Sahota, S., Shah, G., Ghosh, P., Kapoor, R., Sengupta, S., Singh, P., Vijay, V., Sahay, A., Kumar, V. & Shekhar, I. 2018. Review of trends in biogas upgradation technologies and future perspectives. *Bioresource Technology Reports*, 1: 79–88.
- Sahu, O.P. & Chaudhari, P.K. 2013. Review on Chemical treatment of Industrial Waste Water. *Journal of Applied Sciences and Environmental Management*, 17(2): 241–257.
- Salvador, A.F., Cavaleiro, A.J., Sousa, D.Z., Alves, M.M. & Pereira, M.A. 2013. Endurance of methanogenic archaea in anaerobic bioreactors treating oleate-based wastewater. *Applied Microbiology and Biotechnology*, 97: 2211–2218.
- Sarker, S., Lamb, J.J., Hjelme, D.R. & Lien, K.M. 2018. Overview of recent progress towards in-situ biogas upgradation techniques. *Fuel*, 226: 686–697. <https://doi.org/10.1016/j.fuel.2018.04.021>.
- Sawyerr, N., Trois, C., Workneh, T. & Okudoh, V. 2019. An Overview of Biogas Production: Fundamentals , Applications and Future Research. *International Journal of Energy Economics and Policy*, 9(2): 105–116.
- Saxena, S., Saharan, V.K. & George, S. 2019. Modeling & simulation studies on batch anaerobic digestion of hydrodynamically cavitated tannery waste effluent for higher biogas yield. *Ultrasonics - Sonochemistry*, 58: 104692. <https://doi.org/10.1016/j.ultsonch.2019.104692>.
- Schonheit, P., Kristjansson, J.K. & Thauer, R.K. 1982. Kinetic mechanism for the ability of sulfate reducers to out-compete methanogens for acetate. *Archives of Microbiology*, 132:

285–288.

- Setya, A., Murillo, M. & Leustek, T. 1996. Sulfate reduction in higher plants: Molecular evidence for a novel 5' -adenylylsulfate reductase. *Proceedings of the National Academy of Sciences of the United States of America*, 93: 13383–13388.
- Shalu & Bishnoi, N.R. 2016. A Review on Up flow Anaerobic Sludge Blanket Reactor used in Wastewater Treatment. *International Journal of Research in Management, Science & Technology*, 4(3): 6–10.
- Shammas, N.K. & Wang, L.K. 2007. Anaerobic Digestion. In L. K. Wang, N. K. Shammas, & Y.-T. Hung, eds. *Handbook of Environmental Engineering: Biosolids Treatment Processes*. New Jersey: Humana Press Inc.
- Shi, H. 2009. Industrial wastewater-types, amounts and effects. In *Point sources of Pollution: Local effects and their Control*. Beijing: Eolss.
- Shi, J., Zhang, B., Wang, Y. & Fu, J. 2019. Effects of hydropower dam construction on sulfur distribution and sulfate-reducing prokaryotes assemblage. *Science of the Total Environment*. 1–11. <https://doi.org/10.1016/j.scitotenv.2019.135819>.
- Shi, X., Leong, K.Y. & Ng, H.Y. 2017. Bioresource Technology Anaerobic treatment of pharmaceutical wastewater : A critical review. *Bioresource Technology*, 245: 1238–1244.
- Shin, G.S., Han, G., Lim, J., Lee, C. & Hwang, S. 2010. A comprehensive microbial insight into two-stage anaerobic digestion of food waste-recycling wastewater. *Water Research*, 44(17): 4838–4849.
- Shizas, I. & Bagley, D.M. 2002. Improving anaerobic sequencing batch reactor performance by modifying operational parameters. *Water Research*, 36: 363–367.
- Siddique, N.I. & Wahid, Z.A. 2018. Achievements and perspectives of anaerobic co-digestion: A review. *Journal of Cleaner Production*, 194: 359–371. <https://doi.org/10.1016/j.jclepro.2018.05.155>.
- Silva, A.J., Pozzi, E., Foresti, E. & Zaiat, M. 2015. The influence of the buffering capacity on the production of organic acids and alcohols from wastewater in anaerobic reactor. *Applied Biochemistry and Biotechnology*, 175: 2258–2265.
- Da Silva, C., Astals, S., Peces, M., Campos, J.L. & Guerrero, L. 2018. Biochemical methane potential (BMP) tests: Reducing test time by early parameter estimation. *Waste Management*, 71: 19–24. <https://doi.org/10.1016/j.wasman.2017.10.009>.
- Sivakumar, P., Bhagiyalakshmi, M. & Anbarasu, K. 2012. Anaerobic treatment of spoiled milk from milk processing industry for energy recovery – A laboratory to pilot scale study. *Fuel*, 96: 482–486.
- Smith, C.J. & Osborn, A.M. 2009. Advantages and limitations of quantitative PCR (Q-PCR)-

- based approaches in microbial ecology. *FEMS microbiology ecology*, 67: 6–20.
- Song, Z. & Williams, C.J. 2003. Tannery Wastewater Treatment Using an Upflow Anaerobic Fixed Biofilm Reactor (UAFBR). *Environmental Engineering Science*, 20(6): 587–599.
- Song, Z., Williams, C.J. & Edyvean, R.G.J. 2004. Treatment of tannery wastewater by chemical coagulation. *Desalination*, 164(3): 249–259.
- Song, Z., Williams, C.J.M. & Edyvean, R.G.J. 2000. Sedimentation of Tannery wastewater. *Water Research*, 34(7): 2171–2176.
- Staley, B.F., Iii, F.L.D.L.R., Barlaz, M.A. & Icrobiol, A.P.P.L.E.N.M. 2011. Effect of Spatial Differences in Microbial Activity, pH, and Substrate Levels on Methanogenesis Initiation in Refuse. *Applied and Environmental Microbiology*, 77(7): 2381–2391.
- Steinberg, L.M. & Regan, J.M. 2009. mcrA -Targeted Real-Time Quantitative PCR Method To Examine Methanogen Communities □. , 75(13): 4435–4442.
- Steinberg, L.M. & Regan, J.M. 2008. Phylogenetic Comparison of the Methanogenic Communities from an Acidic, Oligotrophic Fen and an Anaerobic Digester Treating Municipal Wastewater Sludge. *Applied and Environmental Microbiology*, 74(21): 6663–6671.
- Streit, K.F., Rodrigues, M.A.S. & Ferreira, J.L. 2014. Electrodialysis Treatment of Tannery wastewater. In *Topics in Mining, Metallurgy and Materials Engineering*. Springer-Verlag Berlin Heidelberg.
- Sundar, V.J., Ramesh, R., Rao, P.S., Saravanan, P., Sridharnath, B. & Muralidharan, C. 2001. Water Management in Leather Industry. *Journal of Scientific and Industrial Research*, 60: 443–450.
- Sung, S. & Dague, R.R. 1995. Laboratory studies on the anaerobic sequencing batch reactor. *Water Environment Research*, 67(3): 294–301.
- Supaphol, S., Jenkins, S.N., Intomo, P., Waite, I.S. & Donnell, A.G.O. 2011. Bioresource Technology Microbial community dynamics in mesophilic anaerobic co-digestion of mixed waste. *Bioresource Technology*, 102(5): 4021–4027.
- Swartz, C.D., Jackson-Moss, C., Rowswell, R.A., Mpofo, A.B. & Welz, P.J. 2017. *Water and Wastewater Management in the Tanning and Leather Finishing Industry: Natsurv 10*. Pretoria: Water Research Commission Report TT 713/17.
- Świątczak, P., Cydzik-kwiatkowska, A. & Rusanowska, P. 2017. Microbiota of anaerobic digesters in a full-scale wastewater treatment plant. *Archives of Environmental Protection*, 43(3): 53–60.
- Tansengco, M., Herrera, D., Tejano, J., Yao, M., Beraye, R.J. & Esguerra, R. 2015. Biological Treatment of Meat Processing Wastewater using Anaerobic Sequencing Batch Reactor

- (ASBR). *International Research Journal of biological Sciences*, 4(3): 66–75.
- Tchobanoglous, G., Burton, F.L. & Stensel, H.D. 2003. *Wastewater Engineering: Treatment and Reuse*. 4th ed. New York: McGraw-Hill Education.
- Thanh, P.M., Ketheesan, B., Yan, Z. & Stuckey, D. 2016. Trace metal speciation and bioavailability in anaerobic digestion: A review. *Biotechnology Advances*, 34(2): 122–136.
- Tunay, O., Kabdasli, I., Orhon, D. & Genceli, E.A. 1995. Characterization and pollution profile of leather tanning industry in Turkey. *Water Science & Technology*, 32(12): 1–9.
- Ueki, A., Ono, K., Tsuchiya, A. & Ueki, K. 1997. Survival of methanogens in air-dried paddy field soil and their heat tolerance. *Water Science and Technology*, 36(6–7): 517–522. [http://dx.doi.org/10.1016/S0273-1223\(97\)00563-5](http://dx.doi.org/10.1016/S0273-1223(97)00563-5).
- Ünal, B., Perry, V.R., Sheth, M., Gomez-Alvarez, V., Chin, K.J. & Nüsslein, K. 2012. Trace elements affect methanogenic activity and diversity in enrichments from subsurface coal bed produced water. *Frontiers in Microbiology*, 3: 1–14.
- UNIDO. 2011. *Introduction to treatment of tannery effluents*. Vienna.
- Vaksmas, A. 2017. McrA primers for the detection and quantification of the anaerobic archaeal methanotroph 'Candidatus Methanoperedens nitroreducens'. *Applied Microbiology and Biotechnology*: 1631–1641. <http://dx.doi.org/10.1007/s00253-016-8065-8>.
- Valdés, F., Chamy, R. & Vergara, C. 2006. Effect of sulphate concentration and sulphide desorption on the combined removal of organic matter and sulphate from wastewaters using expanded granular sludge bed (EGSB) reactors. *Electronic Journal of Biotechnology*, 9(4): 370–378.
- Venkateshwaran, K., Bocher, B., Maki, J. & Zitomer, D. 2015. Relating Anaerobic Digestion Microbial Community and Process Function. *Microbiology insights*, 8: 37–44.
- Vijayaraghavan, K. & Murthy, D.V.S. 1997. Effect of toxic substances in anaerobic treatment of tannery wastewaters. *Bioprocess Engineering*, 16: 151–155.
- Vivekanandhan, V. & Mohan, S. 2018. Treatment of Tannery Wastewater in an EGSB (Expanded Granular Sludge Blanket) Reactor. *International Journal of Scientific Research and Reviews*, 7(3): 957–967.
- Vrieze, J. De, Hennebel, T., Boon, N. & Verstraete, W. 2012. Bioresource Technology Methanosarcina: The rediscovered methanogen for heavy duty biomethanation. *Bioresource Technology*, 112: 1–9. <http://dx.doi.org/10.1016/j.biortech.2012.02.079>.
- Waghmode, T.R., Haque, M., Kim, S.Y. & Kim, P.J. 2015. Effective Suppression of Methane Emission by 2-Bromoethanesulfonate during Rice Cultivation. *PLoS*, 10(11): 1–13.
- Wagner, M., Roger, A.J., Flax, J.L., Brusseau, G.A. & Stahl, D.A. 1998. Phylogeny of

- Dissimilatory Sulfite Reductases Supports an Early Origin of Sulfate Respiration. *Journal of Bacteriology*, 180(11): 2975–2982.
- Wang, B., Strömberg, S., Nges, I.A., Nistor, M. & Liu, J. 2016. Impacts of inoculum pre-treatments on enzyme activity and biochemical methane potential. *Journal of Bioscience and Bioengineering*, 121(5): 557–560. <http://dx.doi.org/10.1016/j.jbiosc.2015.10.004>.
- Wang, H., Fotidis, I.A. & Angelidaki, I. 2015. Ammonia effect on hydrogenotrophic methanogens and syntrophic acetate-oxidizing bacteria. *FEMS Microbiology Ecology*, 91(11): 1–8.
- WBA. 2013. Biogas-An important renewable energy source. *World bioenergy association*.
- Welz, P.J., Khan, N. & Prins, A. 2018. The effect of biogenic and chemically manufactured silver nanoparticles on the benthic bacterial communities in river sediments. *Science of the Total Environment*, 644: 1380–1390.
- Wilson, L.P., Loetscher, L.H., Sharvelle, S.E. & Long, S.K. De. 2013. Microbial community acclimation enhances waste hydrolysis rates under elevated ammonia and salinity conditions. *Bioresource Technology*, 146: 15–22. <http://dx.doi.org/10.1016/j.biortech.2013.06.081>.
- World Bank Group. 2007. Environmental , Health , and Safety Guidelines for Tanning and Leather Finishing. : 1–21.
- Xiangwen S, Dangcong P, Zhaohua T, X.J. 2008. Treatment of brewery wastewater using anaerobic sequencing batch reactor (ASBR). *Bioresource Technology*, 99: 3182–3186.
- Yan, Z., Song, Z., Li, D., Yuan, Y., Liu, X. & Zheng, T. 2015. The effects of initial substrate concentration, C/N ratio, and temperature on solid-state anaerobic digestion from composting rice straw. *Bioresource Technology*, 177: 266–273. <http://dx.doi.org/10.1016/j.biortech.2014.11.089>.
- Young, J.C. & McCarty, P.L. 1969. The anaerobic filter for waste treatment. *Journal of the Water Pollution Control Federation*, 41(5).
- Yuan, J., Yuan, Y., Zhu, Y. & Cao, L. 2018. Effects of different fertilizers on methane emissions and methanogenic community structures in paddy rhizosphere soil. *Science of the Total Environment*, 627: 770–781. <https://doi.org/10.1016/j.scitotenv.2018.01.233>.
- Zaiko, A., Pochon, X., Garcia-vazquez, E., Olenin, S. & Wood, S.A. 2018. Advantages and Limitations of Environmental DNA/RNA Tools for Marine Biosecurity: Management and Surveillance of Non-indigenous Species. *Frontiers in Marine Science*, 5(322).
- Zayed, G. & Winter, J. 2000. Inhibition of methane production from whey by heavy metals-- protective effect of sulfide. *Applied microbiology and biotechnology*, 53(6): 726–731.
- Zelege, J., Lu, S., Wang, J., Huang, J., Li, B. & Ogram, A. V. 2013. Methyl Coenzyme M

- Reductase A (*mcrA*) Gene-Based Investigation of Methanogens in the Mudflat Sediments of Yangtze River Estuary, China. *Microbial Ecology*, 66: 257–267.
- Zhang, C., Su, H., Baeyens, J. & Tan, T. 2014. Reviewing the anaerobic digestion of food waste for biogas production. *Renewable and Sustainable Energy Reviews*, 38: 383–392.
- Zhang, J., Qi, Q., Mao, L., He, Y., Loh, K. & Tong, Y.W. 2020. Mixing strategies - activated carbon nexus: Rapid start-up of thermophilic anaerobic digestion with the mesophilic anaerobic sludge as inoculum. *Bioresource Technology*: 123401. <https://doi.org/10.1016/j.biortech.2020.123401>.
- Zhang, L., Shen, Z., Fang, W. & Gao, G. 2019. Composition of bacterial communities in municipal wastewater treatment plant. *Science of the Total Environment*, 689: 1181–1191. <https://doi.org/10.1016/j.scitotenv.2019.06.432>.
- Zhang, Y., Yu, G., Yu, L., Abdul, M., Siddhu, H., Gao, M., Abdeltawab, A.A., Al-deyab, S.S. & Chen, X. 2016. Computational fluid dynamics study on mixing mode and power consumption in anaerobic mono- and co-digestion. *Biore*, 203: 166–172.
- Zheng, M., Yan, Z., Zuo, J. & Wang, K. 2014. Concept and application of anaerobic suspended granular sludge bed (SGSB) reactor for wastewater treatment. *Front. Environ. Sci. Eng*, 8(5): 797–798.
- Ziganshin, A.M., Liebetrau, J., Pröter, J. & Kleinstüber, S. 2013. Microbial community structure and dynamics during anaerobic digestion of various agricultural waste materials. *Applied Microbiology and Biotechnology*, 97: 5161–5174.
- Zongo, I., Merzouk, B., Palm, K., Wethe, J., Maiga, H., Leclerc, J. & Lapique, F. 2012. Study of an electrocoagulation (EC) unit for the treatment of industrial effluent of Ouagadougou, Burkina Faso. *Advances in Applied Science Research*, 3(1): 572–582.
- Zouboulis, A., Peleka, E. & Ntolia, A. 2019. Treatment of Tannery Wastewater with Vibratory Shear-Enhanced Processing Membrane Filtration. *Separations*, 6(2): 20.
- Zupancic, G. & Jemec, A. 2010. Anaerobic digestion of tannery waste: Semi-continuous and anaerobic sequencing batch reactor processes. *Bioresource Technology*, 101: 26–33.
- Zupancic, G.D. & Jemec, A. 2010. Anaerobic digestion of tannery waste : Semi-continuous and anaerobic sequencing batch reactor processes. *Bioresource Technology*, 101: 26–33.

APPENDICES

Appendix A: Biochemical methane potential tests setup

Table A1: Biochemical chemical potential tests setup

Run								Factor 1	Factor 2
Unit	mg	mg	mg	mg	mg	L		A: SO_4^{2-} conc	B: ISR
	MgSO4	K2SO4	Half of J	+	SO ₄ Conc	OS vol	Target		
1	2824,4	1996,8	1100,75	2201,5	1130,5	1,7	3332	1960	2,5
2	1822,3	1288,3	710,2	1420,4	1409,8	2,12	2830,2	1335	2
3	98,1	69,4	38,25	76,5	1130,5	1,7	1207	710	2,5
4	1220,6	862,9	475,7	951,4	944,3	1,42	1895,7	1335	3
5	60,0	42,4	23,4	46,8	691,6	1,04	738,4	710	4
6	730,6	516,5	284,75	569,5	565,25	0,85	1134,75	1335	5
7	1727,9	1221,6	673,4	1346,8	691,6	1,04	2038,4	1960	4
8	1220,6	862,95	475,7	951,4	944,3	1,42	1895,7	1335	3
9	1220,6	862,95	475,7	951,4	944,3	1,42	1895,7	1335	3
10	1220,6	862,95	475,7	951,4	944,3	1,42	1895,7	1335	3
11	1220,6	862,95	475,7	951,4	944,3	1,42	1895,7	1335	3
12	2432,1	1719,5	947,85	1895,7	944,3	1,42	2840	2000	3
13	0	0	0	0	944,3	1,42	944,3	665	3

Appendix B: Analytical treatment methods

Chemical Oxygen demand (COD)

- Switch on the thermoreactor (TR) and set the temperature at 148°C
- Suspend the bottom sediment in the reaction cell by swirling
- Carefully transfer 1 ml of the pre-treated sample with the pipette down inside the
- Vigorously mix the contents of the cell
- Heat the cell in the preheated TR for 2h
- Remove the hot cell from the TR and allow it to cool in a test-tube rack
- Swirl the cell after 10 min and return to the rack for complete cooling to room temperature

- Measure in the photometer (PM)

Total Organic Carbon (TOC)

- Switch on the TR and set the temperature at 120°C
- Place 1 ml of the pre-treated sample into a suitable cell tube
- Add and mix 9 ml of distilled water
- Add and mix 2 drops of reagent TOC-1K
- Adjust the pH below 2.5 with H₂SO₄ if necessary
- Stir for 10 min at minimum speed
- Pipette 3 ml of the solution into a reaction cell
- Add 1 level grey micro-spoon of reagent TOC-2K
- Immediately close the cell tightly with an aluminium cap
- Heat the tube standing on its head in the preheated TR for 2h
- Remove the tube from the TR and allow it to cool in a test-tube rack standing on its head for 60 min
- Turn the tube upright and measure in the PM within 10 min

Acid Capacity

- Filter the samples
- Pipette 4 ml of reagent AC-1 into a clean test tube
- Add 1 ml of the pre-treated sample and mix
- Add 0.5 ml reagent AC-2 with pipette and mx
- Measure the sample in the PM

Volatile Organic Acids (VOA)

- Pipette 0.75 ml of reagent OA-1 into clean round cell
- Add 0.5 ml reagent OA-2 with pipette
- Add 0.5 ml of pre-treated sample with pipette
- Close the cell tightly and mix
- Heat the cell at 100°C in the pre-treated TR for 15 min, then cool to room temperature under running water
- Add 1 ml reagent OA-3 with pipette
- Add 1 ml reagent OA-3 with pipette
- Add 1 ml reagent OA-4 with pipette, close the cell tightly and mix

- Add 1 ml reagent OA-5 with pipette, close the cell tightly and mix.
- Leave to stand for 1 min, then measure the sample in the PM

Sulfate

- Filter the samples through a 0.45 µm membrane filter
- Pipette 1.0 ml of pre-treatment sample into a reaction cell and mix
- Add 1 level green micro spoon of reagent SO₄-1K (in the cap of the SO₄-1K bottle)
- Close the cell tightly, and shake vigorously until reagent is completely dissolved
- Leave to stand for exactly 2 min, then measure the sample in the PM

Ammonium (NH₄⁺)

- Filter the sample
- Pipette 5 ml of reagent NH₄-1
- Add 0.1 ml of the pre-treated sample with pipette and mix
- Add 1 level blue micro spoon of reagent NH₄-2 and shake vigorously until the reagent is completely dissolved
- Leave to react for 15 min, then fill the sample into a 10 mm cell, and measure in the PM

Total Phosphorus

- Switch on the TR and set the temperature at 120°C
- Pipette 0.2 ml of the pre-treated sample into a reaction cell
- Add 1 dose of reagent P-1K, close the cell tightly and mix
- Heat the cell in in the pre-treated TR for 30 min
- Allow to cool to room temperature in a rack
- Shake vigorously after cooling and add 5 drops reagent P-2K, close the cell tightly and mix
- Add 1 dose of reagent P-3K, close tightly and shake vigorously until the reagent is completely dissolved
- Leave to stand for 5 min then measure the sample in the PM

Total Nitrogen (N)

- Switch on the TR and set the temperature at 120°C
- Pipette 1 ml of the pre-treated sample into an empty cell tube
- Add and mix 9 ml of distilled water
- Add and mix 1 level blue micro spoon of reagent N-1K

- Add 6 drops of reagent N-2K, close and mix
- Heat the cell in the preheated TR for 1h
- Allow to cool to room temperature in a test rack
- Shake briefly after 10 min
- Pipette 1 ml of the digested sample into a reaction tube cell
- Add 1 ml reagent N-3K with pipette, close the tube tightly and mix
- Leave to stand for 10 min
- Measure in the PM

Biological oxygen demand (BOD)

- Check the pH of the sample, specified range pH 6 – 8. If required, add dilute sodium hydroxide solution or sulfuric acid drop by drop to adjust the pH
- Fill 2 oxygen reaction bottles each with pre-treated sample and 2 glass beads to overflowing. Close bubble-free with the slanted ground-glass stoppers
- Fill 2 oxygen reaction bottles each with inoculated nutrient-salt solution and 2 glass beads to overflowing. Close bubble-free with the slanted ground-glass stoppers
- Use one bottle of pre-treated sample and one of inoculated nutrient-salt solution for the measurement of the initial oxygen concentration
- Incubate one bottle of pre-treated sample and one of inoculated nutrient-salt solution closed in a thermostatic incubation cabinet at $20 \pm 1^\circ\text{C}$ for 5 days
- After incubation, use one bottle of pre-treated sample and one of inoculated nutrient salt solution for the measurement of the final oxygen concentration
- Add 5 drops of BOD-1K and then 10 drops of BOD-2K, close bubblefree, and mix for approx. 10 seconds. Reaction time: 1 minute
- Add 10 drops of BOD-3K, reclose, and mix
- Fill the solution into a round cell and measure in the PM

Appendix C: Genomic DNA samples concentration

Table C1: DNA reaction

Samples	Initial conc. (ng/ul)	Initial Vol (ul)	dH2O to add
iR1	7,6	30,92	16,08
iR2	8,7	27,01	19,99
iR3	10,2	23,04	23,96
iR4	7,1	33,10	13,90
iR5	9,9	23,74	23,26
iR6	17,1	13,74	33,26
iR7	16,4	14,33	32,67
iR8	14,1	16,67	30,33
iR9	15,3	15,36	31,64
iR10	11,5	20,43	26,57
iR11	15,5	15,16	31,84
iR12	23,1	10,17	36,83
iR13	21,8	10,78	36,22
Inoculum	98,6	2,38	44,62
substrate	5,9	39,83	7,17
sR1	7,2	32,64	14,36
sR2			
sR3	18	13,06	33,94
sR3	6,4	36,72	10,28
sR4	16,3	14,42	32,58
sR5	22,1	10,63	36,37
sR6	28,6	8,22	38,78
sR7	33,2	7,08	39,92
sR8	32,6	7,21	39,79
sR9	12,7	18,50	28,50
sR10	23,4	10,04	36,96
sR11	6,9	34,06	12,94
sR12	25,8	9,11	37,89
sR13	23	10,22	36,78
eR1	13,3	17,67	29,33
eR1	13,1	17,94	29,06

eR2			
eR3	9,2	25,54	21,46
eR3	25	9,40	37,60
eR4	24,2	9,71	37,29
eR5			
eR6	12,6	18,65	28,35
eR7			
eR8	19,6	11,99	35,01
eR9	26,5	8,87	38,13
eR10	5,4	43,52	3,48
eR11	13,5	17,41	29,59
eR12	26,6	8,83	38,17
eR13	13,1	17,94	29,06
fR1	11,5	20,43	26,57
fR2	16,7	14,07	32,93
fR3	21,5	10,93	36,07
fR4	21,6	10,88	36,12
fR5	17,8	13,20	33,80
fR6	18,8	12,50	34,50
fR7	15,3	15,36	31,64
fR8	20,3	11,58	35,42
fR9	15,8	14,87	32,13
fR10	14,5	16,21	30,79
fR11	10,5	22,38	24,62
fR12	16,7	14,07	32,93
fR13	13,5	17,41	29,59
BR1			
Wk0	30,5	8,2	41,8
Wk1	35,2	7,1	42,9
Wk2	34	7,4	42,6
Wk3	36	6,9	43,1
Wk4	43,6	5,7	44,3
Wk5	23,2	10,8	39,2
Wk6	34,7	7,2	42,8
Wk7	28,2	8,9	41,1
Wk8	28,3	8,8	41,2
Subs	5,3	47,2	2,8

Inoculum	64,4	3,9	46,1
BR2			
Wk0	20,1	12,4	37,6
Wk1	40,9	6,1	43,9
Wk2	27	9,3	40,7
Wk3	47,7	5,2	44,8
Wk4	36,1	6,9	43,1
Wk5	20,4	12,3	37,7
Wk6	32,5	7,7	42,3
Wk7	27,6	9,1	40,9
Wk8	29,2	8,6	41,4

Appendix D: Preparation of buffers and reagents

Preparation of 50 × TAE buffer

- Dissolve 242 g Tris in 500 ml H₂O
- Add 100 ml 0.5 M Na₂EDTA (pH 8.0) and 57.1 ml glacial acetic acid
- Adjust volume to 1 L with H₂O
- Store at room temperature

Preparation of 1% agarose gel

- Dissolve 1 g in 100 ml 1 × TAE buffer
- Heat the mixture in a microwave until all the agarose powder is dissolved and the mixture is clear (Check every 30 sec to avoid the mixture to solidify)
- Cool at room temperature
- Add 5 µl of Pronasafe

Appendix E: Univariate analysis indices

DIVERSE

Univariate Diversity indices

Name: 060220PWdsr2061F-zotus.fa.species.txt

Data type: Abundance

Sample	S	N	d	J'	H'(loge)	1-Lambda'
iR3	54	33456	5.087	0.5755	2.296	0.8426
sR3	56	31497	5.31	0.5157	2.076	0.8112
eR3	47	32990	4.421	0.3344	1.287	0.5593
fR3	50	32701	4.714	0.4597	1.799	0.7461
iR4	54	33737	5.083	0.5593	2.231	0.8317
sR4	53	32501	5.005	0.5265	2.091	0.7997
eR4	53	32554	5.004	0.5575	2.213	0.85
fR4	48	32505	4.524	0.5877	2.275	0.8454
iR6	55	33274	5.186	0.5686	2.279	0.8456
sR6	52	31821	4.919	0.5914	2.337	0.8612
eR6	55	32368	5.2	0.5674	2.274	0.8493
fR6	56	32642	5.292	0.6462	2.601	0.8995
iR9	52	33180	4.899	0.5804	2.293	0.8541
sR9	57	32117	5.396	0.5299	2.142	0.8214
eR9	51	32533	4.812	0.556	2.186	0.8417
fR9	53	32488	5.005	0.5865	2.329	0.8499
iR11	52	33696	4.892	0.5319	2.102	0.8163
sR11	53	32828	5	0.4859	1.929	0.7592
eR11	54	32507	5.101	0.5667	2.261	0.848
fR11	55	32453	5.199	0.612	2.453	0.8835
iR12	56	33101	5.285	0.5402	2.175	0.8271
sR12	49	31188	4.639	0.5918	2.303	0.8521
eR12	51	32819	4.808	0.5634	2.215	0.85
fR12	57	32306	5.393	0.4992	2.018	0.7867
iR13	58	32720	5.483	0.5811	2.36	0.8577
sR13	53	32220	5.009	0.5085	2.019	0.765
eR13	56	32543	5.293	0.5538	2.229	0.8423
fR13	55	32234	5.202	0.6133	2.458	0.8687
R1Wk2	46	33302	4.321	0.4426	1.695	0.7328
R1Wk4	57	32948	5.383	0.4681	1.892	0.7808
R1Wk6	53	33236	4.995	0.4319	1.715	0.7657
R1Wk8	52	32465	4.91	0.4994	1.973	0.8055

R2Wk2	55	33259	5.186	0.4253	1.704	0.6602
R2Wk4	55	33035	5.19	0.3905	1.565	0.6187
R2Wk6	49	33061	4.613	0.4836	1.882	0.7957
R2Wk8	54	33005	5.094	0.4209	1.679	0.6959
S	57	34199	5.364	0.4763	1.926	0.7558
I	52	32205	4.913	0.5845	2.309	0.8563
S.ASBR	47	32356	4.43	0.2956	1.138	0.5229
I.ASBR	52	33450	4.895	0.4031	1.593	0.6238

Use: S = total species, d = Margalef richness index, J' Pielou evenness index H' Shannon diversity index

DIVERSE

Univariate Diversity indices

Data worksheet

Name: 060220PWmlascomplete-zotus.fa.species.txt

Data type: Abundance

Sample	S	N	d	J'	H'(loge)	1-Lambda'
iR3	31	32270	2.89	0.6178	2.122	0.8352
sR3	34	32593	3.176	0.5885	2.075	0.8349
eR3	28	32613	2.598	0.5822	1.94	0.788
fR3	30	32180	2.794	0.6181	2.102	0.8383
iR4	29	32162	2.698	0.6073	2.045	0.8177
sR4	34	31767	3.183	0.6143	2.166	0.8553
eR4	32	31625	2.992	0.6166	2.137	0.8505
fR4	31	31858	2.893	0.6106	2.097	0.8418
iR6	33	31479	3.09	0.6581	2.301	0.8716
sR6	30	31588	2.799	0.6064	2.062	0.8386
eR6	29	30582	2.711	0.6563	2.21	0.8684
fR6	32	31189	2.996	0.6263	2.171	0.8544
iR9	31	32357	2.889	0.6053	2.079	0.8331
sR9	29	32074	2.699	0.6277	2.114	0.8448
eR9	31	32968	2.884	0.6272	2.154	0.8556
fR9	31	32077	2.891	0.6237	2.142	0.8583
iR11	31	32397	2.889	0.5856	2.011	0.8174
sR11	28	31898	2.604	0.7001	2.333	0.8778
eR11	27	32060	2.506	0.5847	1.927	0.7973
fR11	29	32079	2.699	0.6091	2.051	0.8184

iR12	30	32169	2.794	0.5861	1.993	0.8183
sR12	31	32066	2.891	0.5941	2.04	0.8264
eR12	27	32541	2.502	0.6165	2.032	0.8157
fR12	28	32205	2.601	0.637	2.123	0.842
iR13	27	32218	2.505	0.6815	2.246	0.8646
sR13	29	32940	2.692	0.5318	1.791	0.763
eR13	31	32492	2.888	0.6266	2.152	0.8519
fR13	29	32380	2.696	0.6453	2.173	0.8541
R1Wk2	27	32675	2.501	0.6366	2.098	0.8363
R1Wk4	27	33105	2.498	0.5955	1.963	0.818
R1Wk6	29	32926	2.692	0.6459	2.175	0.8528
R1Wk8	31	32786	2.885	0.6417	2.204	0.8592
R2Wk2	28	32973	2.595	0.6114	2.037	0.8441
R2Wk4	27	33117	2.498	0.5527	1.822	0.7969
R2Wk6	28	32939	2.596	0.6087	2.028	0.8336
R2Wk8	31	32712	2.886	0.5598	1.922	0.8139
S	26	34079	2.395	0.6331	2.063	0.81
I	29	32452	2.696	0.6222	2.095	0.8275
S.ASBR	21	34136	1.916	0.6448	1.963	0.8053
I.ASBR	29	31892	2.7	0.637	2.145	0.8381

Appendix F: Standard curves

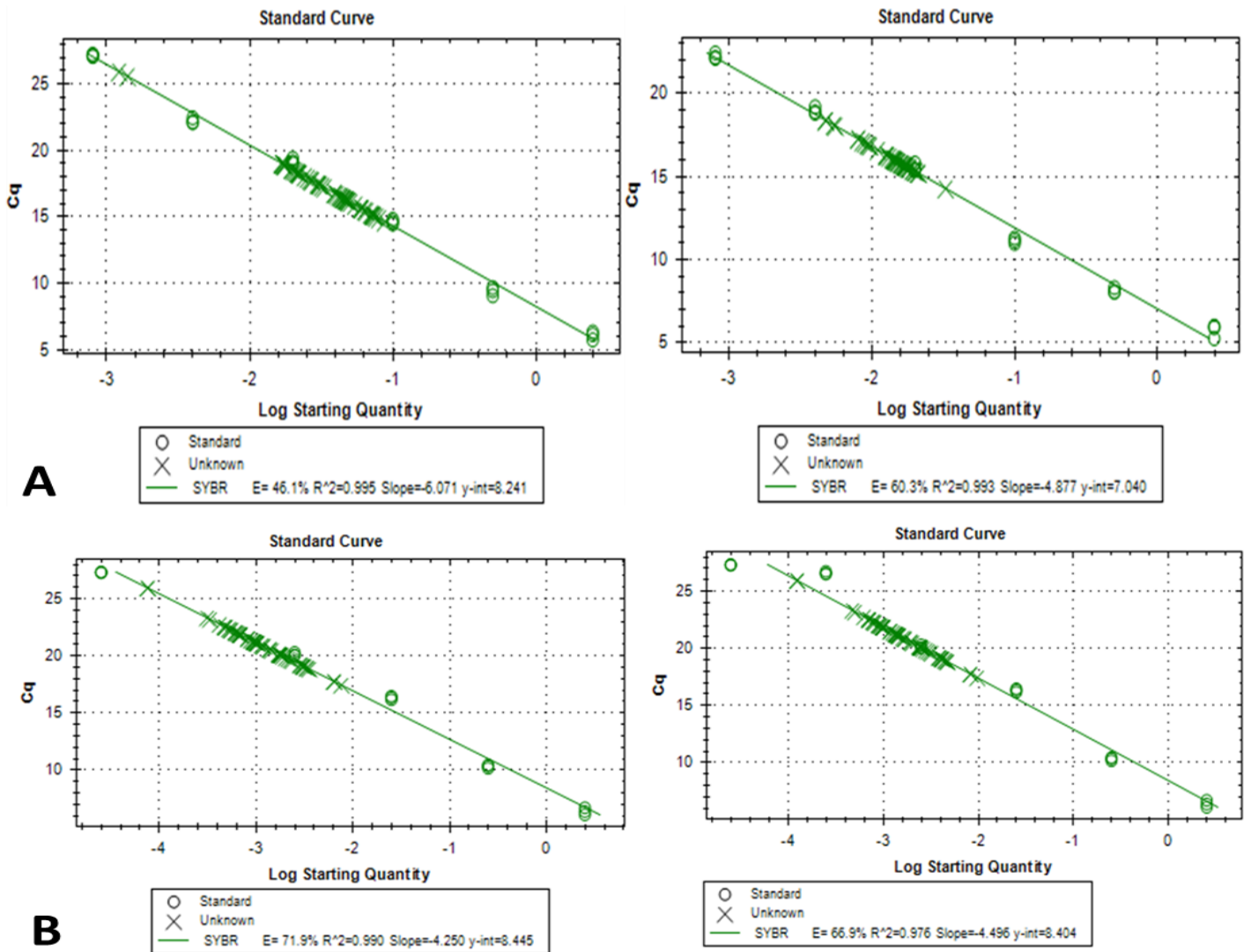


Figure E1: Biochemical methane potential tests standard curves (A) *mcrA* gene (B) *dsrB* gene

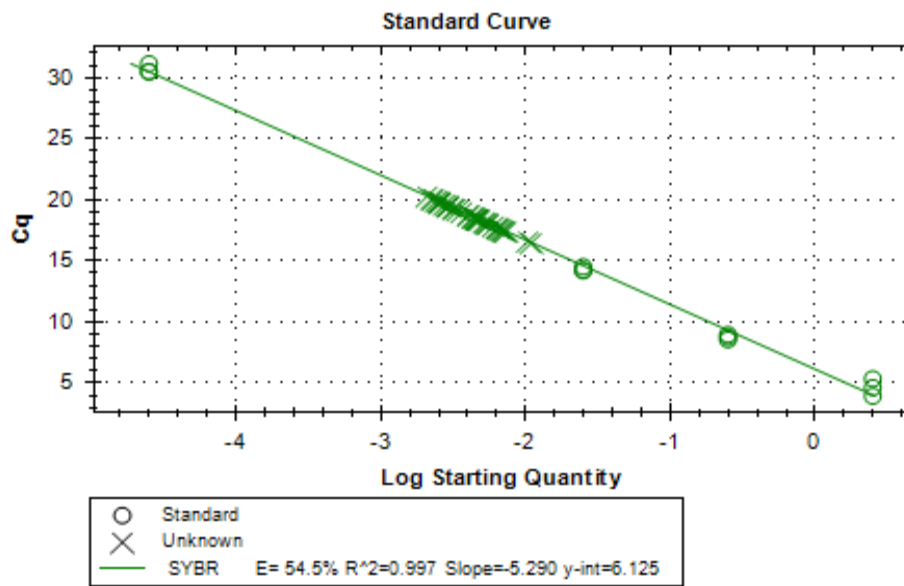


Figure E2: *dsrB* gene anaerobic sequencing batch reactors standard curve

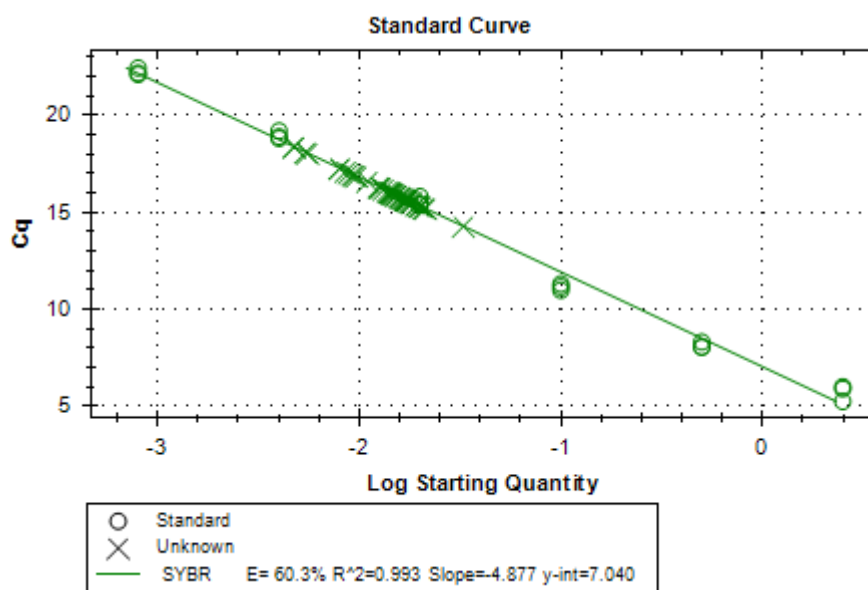


Figure E3: *mcrA* gene anaerobic sequencing batch reactors standard curve

Appendix G: SIMPER

Similarity Percentages - species contributions

One-Way Analysis

Data worksheet

Name: Data1

Data type: Abundance

Sample selection: All

Variable selection: All

Parameters

Resemblance: S17 Bray-Curtis similarity

Cut off for low contributions: 70,00%

Factor Groups

Sample	Sample
I	BMP3
S	BMP3
E	BMP3
F	BMP3
I	BMP4
S	BMP4
E	BMP4
F	BMP4
I	BMP6

S	BMP6
E	BMP6
F	BMP6
I	BMP9
S	BMP9
E	BMP9
F	BMP9
I	BMP11
S	BMP11
E	BMP11
F	BMP11
I	BMP12
S	BMP12
E	BMP12
F	BMP12
I	BMP13
S	BMP13
E	BMP13
F	BMP13
WK2	ASBR1
WK4	ASBR1
WK6	ASBR1
WK8	ASBR1
WK2	ASBR2
WK4	ASBR2

WK6 ASBR2
 WK8 ASBR2
 Substrate BMP substrate
 Inoculum BMP inoculum
 Substrate ASBR substrate
 Inoculum ASBR inoculum

Group BMP3

Average similarity: 83,38

Species	Av.Abund	Av.Sim	Sim/SD	Contrib%	Cum.%
<i>methanobacterium petrolearium</i>	4,12	11,32	11,37	13,57	13,57
<i>methanosaeta sp.</i>	3,91	10,92	17,07	13,09	26,67
<i>methanoculleus bourgensis</i>	4,59	10,09	1,69	12,10	38,77
methanobacterium sp.	2,87	8,03	14,61	9,63	48,39
methanosaeta concilii	2,78	7,49	8,56	8,98	57,37
methanosarcina mazei	3,37	7,05	2,73	8,45	65,83
candidatus methanomassiliicoccus intestinalis	1,74	4,38	6,77	5,25	71,08

Group BMP4

Average similarity: 85,98

Species	Av.Abund	Av.Sim	Sim/SD	Contrib%	Cum.%
methanobacterium petrolearium	4,54	12,52	19,33	14,57	14,57
methanosaeta sp.	3,60	9,98	82,93	11,60	26,17

methanobacterium sp.	3,58	9,01	8,27	10,48	36,65
methanoculleus bourgensis	3,78	8,66	2,32	10,07	46,72
methanosarcina mazei	3,76	7,94	2,71	9,23	55,95
methanosaeta concilii	2,81	7,78	14,16	9,05	65,00
candidatus methanomassiliicoccus intestinalis	1,85	4,98	11,55	5,80	70,79

Group BMP6

Average similarity: 84,81

Species	Av.Abund	Av.Sim	Sim/SD	Contrib%	Cum.%
methanobacterium petrolearium	4,47	11,92	8,21	14,06	14,06
methanosaeta sp.	3,69	10,44	47,95	12,31	26,37
methanosarcina mazei	4,01	9,42	2,58	11,11	37,48
methanobacterium sp.	3,41	8,41	8,43	9,92	47,39
methanoculleus bourgensis	3,12	7,77	4,86	9,16	56,55
methanosaeta concilii	2,81	7,48	10,10	8,83	65,38
candidatus methanomassiliicoccus intestinalis	1,89	4,62	7,36	5,44	70,82

Group BMP9

Average similarity: 86,07

Species	Av.Abund	Av.Sim	Sim/SD	Contrib%	Cum.%
methanobacterium petrolearium	4,30	11,97	17,30	13,91	13,91
methanosaeta sp.	4,24	11,76	14,80	13,67	27,58
methanobacterium sp.	3,35	8,47	4,65	9,84	37,41

methanoculleus bourgensis	3,58	8,46	2,51	9,83	47,24
methanosaeta concilii	3,11	8,23	7,05	9,56	56,80
methanosarcina mazei	3,59	7,39	1,86	8,58	65,38
methanobacterium ferruginis	1,49	4,21	76,43	4,89	70,27

Group BMP11

Average similarity: 83,25

Species	Av.Abund	Av.Sim	Sim/SD	Contrib%	Cum.%
methanobacterium petrolearium	3,96	10,85	9,46	13,03	13,03
methanosaeta sp.	3,90	10,78	11,58	12,95	25,97
methanoculleus bourgensis	4,27	9,31	1,83	11,18	37,16
methanosarcina mazei	4,02	8,92	2,37	10,71	47,87
methanosaeta concilii	2,68	7,32	18,20	8,79	56,66
methanobacterium sp.	2,77	6,77	6,05	8,14	64,79
methanobacterium ferruginis	1,38	3,91	22,06	4,70	69,49
candidatus methanomassiliicoccus intestinalis	1,56	3,87	4,90	4,65	74,14

Group BMP12

Average similarity: 80,66

Species	Av.Abund	Av.Sim	Sim/SD	Contrib%	Cum.%
methanosaeta sp.	4,35	12,03	9,11	14,92	14,92
methanobacterium petrolearium	4,37	11,72	10,05	14,53	29,45
methanosaeta concilii	3,29	8,84	8,94	10,96	40,41

methanobacterium sp.	3,07	8,29	16,91	10,28	50,69
methanoculleus bourgensis	3,69	7,12	1,85	8,82	59,51
methanosarcina mazei	2,97	5,37	2,00	6,66	66,17
methanobacterium ferruginis	1,54	4,15	9,50	5,14	71,31

Group BMP13

Average similarity: 80,41

Species	Av.Abund	Av.Sim	Sim/SD	Contrib%	Cum.%
methanobacterium petrolearium	4,02	10,35	7,21	12,87	12,87
methanosarcina mazei	4,19	10,05	3,27	12,50	25,38
methanosaeta sp.	3,78	9,72	6,37	12,09	37,46
methanoculleus bourgensis	4,10	8,84	2,04	10,99	48,45
methanosaeta concilii	2,82	7,67	16,71	9,54	57,99
methanobacterium sp.	2,70	7,15	6,31	8,90	66,89
candidatus methanomassiliicoccus intestinalis	1,85	4,24	3,02	5,27	72,16

Group ASBR1

Average similarity: 91,93

Species	Av.Abund	Av.Sim	Sim/SD	Contrib%	Cum.%
methanosaeta sp.	5,00	14,57	30,47	15,85	15,85
methanobacterium petrolearium	4,49	12,53	21,60	13,63	29,49
methanosaeta concilii	4,10	11,82	29,02	12,86	42,35
methanobacterium sp.	3,22	8,67	8,65	9,44	51,78

methanosarcina mazei	2,29	6,40	21,10	6,96	58,74
methanoregula formicica	2,50	6,33	5,05	6,88	65,63
candidatus methanomassiliicoccus intestinalis	1,91	5,12	6,00	5,57	71,19

Group ASBR2

Average similarity: 90,62

Species	Av.Abund	Av.Sim	Sim/SD	Contrib%	Cum.%
methanosarcina mazei	4,86	13,84	5,71	15,27	15,27
methanosaeta sp.	4,49	13,49	38,15	14,89	30,16
methanobacterium petrolearium	4,37	13,48	20,86	14,87	45,03
methanosaeta concilii	3,71	11,14	10,28	12,29	57,32
methanobacterium sp.	3,15	8,98	10,33	9,91	67,23
methanobacterium aarhusense	1,83	5,62	24,66	6,20	73,42

Group BMP substrate

Less than 2 samples in group

Group BMP inoculum

Less than 2 samples in group

Group ASBR substrate

Less than 2 samples in group

Group ASBR inoculum

Less than 2 samples in group

Groups ASBR1 & ASBR2

Average dissimilarity = 14,79

Species	Group ASBR1		Group ASBR2		Contrib%	Cum.%
	Av.Abund	Av.Abund	Av.Diss	Diss/SD		
methanosarcina mazei	2,29	4,86	3,97	3,05	26,86	26,86
methanoregula formicica	2,50	1,07	2,20	2,42	14,89	41,75
methanolinea mesophila	1,69	0,63	1,62	2,15	10,92	52,67
methanosaeta sp.	5,00	4,49	0,91	1,82	6,12	58,79
methanobacterium sp.	3,22	3,15	0,79	1,40	5,36	64,15
methanoculleus sp.	0,96	0,54	0,66	2,16	4,47	68,62
methanosaeta concilii	4,10	3,71	0,62	1,10	4,21	72,83

